Application of ecosystem models to preserve endangered species

A Thesis

submitted in partial fulfillment of the requirements for the award of the degree of

Doctor of Philosophy

in

School of Mathematics

by

Sanjoli Jain

Reg no: 901811003

under the supervison of

Dr. Parimita Roy

Assistant Professor

School of Mathematics

THAPAR INSTITUTE OF ENGINEERING AND TECHNOLOGY

PATIALA-147004, Punjab, India

Certificate

I hereby certify that the work, which is being presented in the thesis, entitled **Application of ecosystem models to preserve endangered species**, in partial fulfillment of the requirements for the award of the degree of **Doctor of Philosophy** and submitted to the institution is an authentic record of my own work carried out during the period of degree, under the supervision of **Dr. Parimita Roy**, Assistant Professor, School of Mathematics , Thapar Institute of Engineering and Technology, Patiala.

Date: 12/11/2022

(**Sanjoli Jain**)
Candidate

It is certified that the above statement made by the candidate is correct to the best of my knowledge.

Date: 12/11/2022

Dr. Parimita Roy
Supervisor

...dedicated to my parents

Acknowledgements

I am indebted to my supervisor, Dr. Parimita Roy, for your patience, guidance, and support. I have benefited greatly from your wealth of knowledge and meticulous editing. Your unassuming approach to research and science is a source of inspiration. I am extremely grateful that you took me on as a student and continued to have faith in me over the years.

Thank you to my committee members, Dr. Sharad Saxena, Dr. Sapna Sharma and Dr. Anuj Kumar. Your encouraging words and thoughtful, detailed feedback have been very important to me.

I acknowledge the generous financial support from the Science Engineering Research Board (SERB), Govt. of India and providing the necessary facilities during the course of my research work. I received great experience in serving myself as Project Assistant to Principle Investigator of project, Dr. Parimita Roy, entitled " Extinction risk analysis: An approach to preserve endangered species" (EMR/2016/002092).

Many thanks to all of the members of our research laboratory and staff members of School of Mathematics, Thapar Institute of Engineering and Technologies and to my friends in the university for their kind support during my PhD study. Purnima and Ramneek-thank you for the unsaid support you guys given me. Special thanks to my friends and also lab-mates, Sweta and Shivani, i owe to you guys.

Last, but not least, my warm and heartfelt thanks go to my family, especially my parents, for their tremendous support and hope they had given to me. Without that hope, this thesis would not have been possible. Special thanks to my brother-Archit Jain, husband-Jiten Jain, wing woman-Shipra, you people encouraged me throughout this journey of highs and lows. Thank you all for the strength you gave me. I love you all!

Abstract

This thesis entitled **"Application of ecosystem models to preserve endangered species"** is a study carried out with the objective of understanding the importance of environmental fluctuation and movement of species while predicting the dynamics of species in endanger.

Recently, there has been a growing awareness of the importance of including a spatial aspect when developing realistic models of biological systems, with a consequent development of both approximate and mathematical rigorous methods of analysis. Besides there have been studies of pattern formation in spatial epidemic models, introduced from the pioneer work of A.M. Turing. It is well known that the spatial component of ecological interactions has been identified as an important factor in how ecological communities are functioning and shaped yet; understanding the role of space is challenging both theoretically and empirically. Spatial epidemiology with self-diffusion has become a principal scientific discipline aiming at understanding the causes and consequences of spatial heterogeneity in prey-predator relationship.

Moreover, significant environmental change can push a population near extinction, but in some cases, natural selection can intervene and save the population, allowing it to survive. Population densities of predators, prey, and competitors changes significantly from season to season or year to year.

Also, unusually rapid rates of infectious illnesses are spreading throughout wildlife populations. It is important to look into the assertion that infectious diseases frequently contribute to species extinction in light of the increased interest in both global species loss and newly developing infectious diseases. So, in this work we tried and predict the dynamics for the species that are in danger to extinction due to disease pathogen.

To accomplish the objective choosing a suitable model, fitting the model to the data, and using the fitted model to estimate the risk of extinction are the processes involved in conducting a population viability analysis.

Contents

List of Figures

List of Tables

Chapter 1

INTRODUCTION AND LITERATURE

“ Extinction is the rule,
survival is the expectation.”
-Carl Sagan

1.1 Introduction

A sixth global biological extinction may be on the horizon as life on Earth is vanishing at an unprecedented rate (Dirzo et al. (2014)). Despite being a natural occurrence, extinction only happens to one to five species on average each year. Scientists calculated that the current rate of loss is 1,000–10,000 times that of natural loss (Chivian and Bernstein (2008)). Recent decades have seen a steady reduction in biodiversity status and an increase in extinction rates, which has resulted in a growing international commitment to conservation (Tittensor et al. (2014)). Although the number of extinct and endangered species is rising, our knowledge of the dynamics and causes of extinction is still insufficient. Diamond (1989) suggested four drivers of extinction- habitat loss, species invasion, killing, and coextinction. Disease, however, is rarely mentioned as a possible contributing factor to species extinction or endangerment. Many species can go extinct due to disease, either directly or indirectly. Although it doesn't seem shocking, this wasn't established before today. Significant population losses in wildlife are brought on by infectious illnesses, for example, canine distemper virus in Serengeti lions (Roelke-Parker et al. (1996)), Ebola outbreaks in African apes (Leroy et al. (2004)), and multiple pathogens that affect amphibian populations (Daszak and Cunningham (1999); Pounds et al. (2006); Schloegel et al. (2006)). According to recent studies, viral illnesses are spreading exceptionally quickly in wildlife populations (Harvell et al. (1999); Harvell et al. (2002); Epstein et al. (2003)). Emerging infectious illnesses are those brought on by parasites and pathogens that have lately increased in frequency, number of host species they are infecting, or geographic reach. They can also be brought on by newly discovered parasites and pathogens, or by newly developed agents (Shope and Oaks (1992); Daszak et al. (2000)). The diversity of emerging infectious diseases afflicting wildlife, coupled with the fear that an increased frequency of outbreaks will occur in the future, have raised concern that infectious disease may play a strong role in species extinction (Holmes (1996); Daszak et al. (2000); Harvell et al. (2002)). Despite evidence that diseases can increase extinction risk in wild animals (Woodroffe (1999); Daszak and Cunningham (1999)), few researchers have investigated the factors associated with disease-mediated declines or extinctions. Despite the fact that there are tools and data accessible, there is currently no analytical framework that can be used to accomplish this, and predictive models are not evaluated against historical evidence of the interplay between risk predictors and risk change.

Another important factor responsible for extinction is climate change. For natural systems, the evidence of climate change consequences is strongest and most complete. Recent decades have shown a demonstrable impact of global temperature change on species distribution (Walther et al. (2002); Parmesan and Yohe (2003)). Each species has a defense

mechanism, such as immunizations and disease resistance. Some species are losing their ability to resist disease as a result of the changing temperature and landscape. They are growing more vulnerable to illnesses and epidemics, which could eventually cause them to go extinct. The standard compartmental ecological and eco-epidemiological models are insufficient to adequately understand the spatial spread dynamics of the disease. Finally, to increase the ability to identify infectious diseases of conservation significance, current monitoring programs must be upgraded if a greater understanding of the role of infectious disease in species extinction is to be developed (Aguirre et al. (2002)). By completing these duties, extinctions should be decreased as a result of an understanding of the dynamics of infectious diseases that is based on science. Additionally, it is clear that some species are being over-preyed upon, and invasive mammalian predators are probably the foreign animal species that have the most negative impact on biodiversity worldwide. Thirty invasive predator species are responsible for the extinction or threatened extinction of 738 vertebrate species, accounting for 58% of all bird, mammal, and reptile extinctions. The most extensive consequences come from cats, rodents, dogs, and pigs, and indigenous island faunas are particularly vulnerable to invasion predators. The fact that insular species are most severely damaged suggests that controlling invasive predators on islands should be a top priority for worldwide conservation. For the purpose of slowing the rate of loss of biodiversity worldwide, it is crucial to comprehend and minimize the effects of invading mammalian predators (Doherty et al. (2016)). For instance, quokka is a medium-sized, marsupial who is suffering a significant population decline in south-western Australia (Kitchener (1995); Hayward (2002)), when the red fox arrived there in the early 1930s (King and Smith (1985)).

1.2 Consequences of extinction

Rise to cascading effect

A "trophic cascade" (also known as a "trophic effect cascade") occurs when a species loses its ability to perform a certain role in its ecosystem, which has an influence on both other species and the ecosystem as a whole.

The effect of wolves in Yellowstone Park, who were hunted to almost extinction by 1930, is an often used illustration. Without them, the elk and deer they had eaten prospered, and their grazing damaged the willows and aspens that had protected songbirds from the elk and deer they had eaten. As a result, the stream banks became more prone to erosion, and mosquitoes and other insects that the songbirds would have eaten began to proliferate. In 1995, the wolves were brought back into the park and began to hunt elk once more.

Birds, beavers, fish, and other creatures also returned to the stream banks with the plant growth. (Note: David Bernhardt, the Department of the Interior's acting secretary, just unveiled a plan to remove grey wolves from their endangered designation in the Lower 48 states.)

Kelp forests are another well-known illustration. Because they offer habitat to other species, shield the coastline from storm surges, and absorb carbon dioxide, they are crucial to coastal ecosystems. However, kelp forests are being swiftly decimated by an enormous population of purple sea urchins. Purple sea urchins that feed on giant kelp are eaten by California sea otters. Due to unrestricted hunting in the 19th century and pollution, the population of these otters, which formerly numbered in the hundreds of thousands to millions, has been reduced to about 3,000. Moreover, in 2013 a virus that was probably made worse by warmer temperatures started killing sunflower starfish, which also consumes purple sea urchins. The kelp forests decreased by 93% between 2013 and 2018 due to the purple sea urchins eating on them after the sea otter and sunflower starfish disappeared as predators. (A recent study discovered that ocean heat waves are now posing a hazard to kelp forests.) The red urchin population in Northern California, which is prized for sushi, was severely impacted by the sea urchin explosion, which also seriously harmed the kelp ecology. Red snapper, rock cod, and other fish that depend on kelp forests for breeding may also become susceptible in the future.

Another illustration given by Wooddell was how 10 of the 12 native bird species of Guam went extinct when the invasive brown tree snake was unintentionally introduced to the island in the 1950s. Normally, birds consume seeds and disperse them over the island, but she claimed that this was no longer a healthy environment. As a result, there are far fewer trees and forests. And because there are no birds to consume them, Guam is covered in spiders.

Disappearing of apex predator - a catastrophic effect

According to one study, humans' greatest impact on nature may have been the eradication of the giant predators known as "apex species," which are at the top of the food chain. These huge animals are more susceptible because they have smaller populations, live longer, reproduce more slowly, and require more food, and have a larger habitat. According to scientists, their extinction has contributed to pandemics, fires, the extinction of desirable species and the emergence of invasive ones, a decline in ecosystem services, and a decrease in carbon sequestration.

Elephants are an elite species that, because of tourism, habitat destruction, and ivory poaching, may become extinct in our lifetimes. Ecosystems in Asia and Africa may un-

dergo significant alteration as a result. Elephants disseminate seeds farther than any other mammal through ingestion and digestion, promoting the growth of plants and trees that provide food and shelter for birds, bats, and other species. Elephants also create communal watering holes and enrich the soil with their rich excrement, which gives other animals food.

Wildfires may also be impacted by the decline of apex species. In East Africa in the late 1800s, a contagious virus called rinderpest killed out large numbers of plant-eating wildebeest and buffalo, but plants recovered quickly after that. This excess of flora caused an upsurge in wildfires throughout the dry season. Wildebeest and buffalo were reintroduced in the 1960s after rinderpest was eradicated by vaccination. Wildfires decreased as the environment transitioned back from shrubbery to grasslands, reducing the amount of combustible vegetation.

Disturbs food web

The base of the marine food chain is made up of plankton, which are small plant and animal species that live in freshwater or the ocean. Due to the fact that they utilize carbon dioxide as a carbon source and produce oxygen during photosynthesis, phytoplankton is essential to the health of the seas and the world.

In 2010, scientists discovered that the amount of phytoplankton has fallen by 40% globally since 1950 and blamed the drop on rising sea surface temperatures. According to the scientists, the cooler, deeper waters that are rich in the nutrients that phytoplankton require did not mix well with the warming surface waters. Additionally, zooplankton may not be able to adapt as low-oxygen areas spread owing to climate change since they are extremely sensitive to even small changes in the amount of oxygen in the water.

Additionally, the nutrition of other organisms higher on the food chain is impacted by the quantity and quality of plankton. Sardine and anchovy biomass in the Mediterranean Sea decreased by one-third in just ten years. One scientist hypothesized that this was caused by the disappearance of the sardines' and anchovies' usual plankton, forcing them to switch to a less calorie-dense form of plankton. Scientists are unsure of the exact reason why the plankton composition in some areas is changing, but they speculate that changes in plankton quality could be caused by water temperature changes, pollution, or a shortage of nutrients. Some claim that if it is caused by pollution and global warming, the problem might get worse.

However, Sonya Dyhrman, a professor at the Department of Earth and Environmental Sciences at Columbia University who works with the Lamont-Doherty Earth Observatory to

study phytoplankton, is more upbeat about the future. Microorganisms like phytoplankton have the ability to adapt, acclimate, and evolve, thus Dyhrman said he is more concerned about how the community composition of phytoplankton will change in the future ocean than he is about certain lineages of phytoplankton going extinct.

The structure of the food web may shift if the phytoplankton community changes, but Dyhrman is not very concerned about the fisheries' complete collapse. But she worries that "ocean ecosystems may change, and we don't really know what those changes would entail. What form will that ecosystem's architecture take in the future? The issue is that the ocean is already changing, and we don't yet fully comprehend the ecosystem's architecture to make future predictions."

Losing nature's therapeutic riches

More than 25% of prescription drugs include compounds that were found in plants or animals. The source of penicillin was a fungus. To determine whether one of the components in some tarantulas' venom could aid in the treatment of disorders like Parkinson's, researchers are examining the venom. A single chemical from a rare marine bacterium may serve as the foundation for novel melanoma therapy.

About 1.7 million distinct types of organisms have been identified by scientists to date, but it is estimated that there are between 10 and 50 million species on Earth.

1.3 Importance of diversity for humans

The organization, Intergovernmental Science-Policy Platform on Biodiversity and Ecosystem Services (IPBES), was set to evaluate the alterations in human welfare spawned by alterations in diversity on mother earth. If ecosystems with less biodiversity are less able to offer the ecosystem services—like carbon sequestration, nitrogen cycling, and drought resistance—on which humans rely, then biodiversity losses would be detrimental to human well-being. More recent pieces of evidence suggest that saving wildlife is more self-serving than kindness. Evidently, there are four principal reasons.

Biodiversity gives livelihood

Biodiversity is a very basic component of sustainable food for humans and livelihood in the rural and forest sectors. Humans depend on ecosystem services like fresh water, pollination, soil fertility and stability, food, and medicine, whether they live in a village in the Amazon or a large city like Beijing. Given the demands of a constantly expanding human population, ecosystems that have suffered from the loss of biodiversity are less likely to provide those services. The biggest desert lake in the world, Lake Turkana in Kenya

provides food and income for around 300,000 people as well as a habitat for a variety of species, including birds, Nile crocodiles, and hippos.

Biodiversity and economy

Governments are recognizing the importance of biodiversity not only for conservation but also for a worthwhile economic future. Almost 40% of the world's business cycle depends on Biological resources. There would be a deflation of around US$ 338 billion per year together in food and forest produced for commercial use, like timber if the pace of biodiversity loss remains the same. Insofar as we are aware of the fact that food crops rely on pollinators, like bees, these are declining at a massive rate which might cause a deflation of US$ 235 billion in agronomy. Also, Nature-related tourism is also a significant income generator for many people as well.

Biodiversity regularises climate

Climate change and biodiversity loss are two of the most considerable worldwide perils to human welfare. Bronson, the natural climate researcher at Conservation International, affirms that by 2030 climate ruination can only be curbed if nature can reduce emissions at least by 30 percent or more, and safeguarding biodiversity is of considerable importance in accomplishing such emission reductions.

Biodiverse ecosystem keep humans healthy

Idea that greater biodiversity can indirectly reduce disease in particular focal hosts is not new (e.g. Elton (1958)). In recent studies, researchers asserted that multifariousness shields ecosystems against infectious diseases. Loss of species from the environment can have dangerous consequences for the spread and incidence of infections, including those that affect humans.

"A pattern is emerging which shows that biodiversity loss increases disease transmission," says Keesing (Keesing et al. (2010)); he explained many mechanisms that perhaps say that there would obviously be an increase in disease risk with increasing diversity. Substantiated by few experimental types of research and observations: (a) in some regions of Western United States and also experimentally proven in Panama, fatal lung infection (caused by hantaviruses) in humans prevailed as the diversity of small mammals in the area decreased, (b) again, in some region of United States, researchers observed that areas that have low bird density were more susceptible to West Nile encephalitis, an arthropod-borne virus. Researchers still seek an answer to such observations. The reason that has a lack of conviction is; as infectious diseases are fundamentally ecological systems, involving interactions between at least two or many species, and the loss of species can increase encounter rates between pathogens and hosts. In support of this reason, an experiment examining

the transmission of S. mansoni(parasite that causes human schistosomiasis and alternately infects snails via free-living infectious stages) as a result of community structure (Johnson et al. (2009)) was carried, and it postulated that parasite transmission into snail hosts lessen as the community diversity increases i.e. the loss of species can increase encounter rates between pathogens and hosts.

1.4 Mathematical biology

There is a long history of successful collaboration between mathematicians and biologists, including medical scientists. As a result, it straddles two spheres of study: mathematics and biology (relatively speaking, population ecology). In the life sciences, sophisticated mathematical results have been applied and emerged. For instance, stochastic processes and statistical methods have been developed to solve a variety of population problems in demography, ecology, genetics, and epidemics, and much of the joint work between biologists, physicists, chemists, and engineers involves the synthesis and analysis of mathematical structures. Despite the success of bio-informatics and its widespread acceptance in biology, mathematical biology has had a slower pace of acceptance. A number of notable exceptions exist - in ecology and epidemiology, mathematical models have long been used.

1.4.1 Mathematical modeling in population ecology

An ecological model formalizes dynamic and complex interactions within the ecosystem, which show how organisms interact with one another and with their surroundings. Developing population ecology models is not primarily intended to predict the behavior of specific populations, but rather to provide an understanding of how biological processes, often driven by individual behavior, influence population change over time. In recent years there has been considerable growth and advancements in mathematical tools, which further helps ecologists/environmentalists to take sustainable steps in making some important decisions for mother earth.

History

Despite the use of mathematics for explaining ecological processes since 12th century (Real and Levin (1991)), there was lack of applicable mathematical approaches in ecology. Mathematical modeling has become an integral part of ecological research significantly during the 1970s (EDELSTEIN-KESHET (1988); Hoppensteadt (1982); Jørgensen (1994); Jørgensen (2002)). Mathematical models have largely come up with a qualitative description of patterns in nature. The traditional approach served mankind lesser as mathematicians and

ecologists use dissimilar symbols, terms, and definitions.

Alfred Lotka (1880-1949) and Vito Volterra(1860-1940), pioneered the work independently over forming interaction between prey population and predator population. In 1910, Alfred J. Lotka developed the theory of auto-catalytic chemical reactions, in which he proposed the prey-predator model. Accelerating in the direction of model development which we know today, Lotka extended that model to "organic systems" (Lotka (1920)). Further, utilized the equations to form prey-predator interactions (Lotka (1925)). The pair equations are stated as follows:

$$\frac{dN}{dt} = rN - \lambda NP,$$
$$\frac{dP}{dt} = e\lambda NP - mP.$$

where $N-$density of prey, $P-$density of predator, $r-$per capita prey growth rate in the absence of predators, $m-$per capita death rate of predator in the absence of prey, $\lambda-$scale of predator encounter rate with prey, $e-$efficiency with which consumed prey are transformed into new predators. Also, it only worked with a few assumptions like the rate of change of population is proportional to its size; The prey population has access to plenty of food at all times; There is no limit to the appetite of predators; There are no changes in the environment that favor one species and the genetic adaptation is a slow process.

It was later enhanced and modified innumerable times to fit specific contexts. An alternative to the Lotka-Volterra predator-prey model emerged in the late 1980s, namely the Arditi-Ginzburg ratio-dependent model (Arditi and Ginzburg (1989)). But, ecological interaction is way more than just two species involved. Though it is now possible to form a large number of equations for the interaction of species in an ecosystem, sometimes complexity in the interactions creates difficulty in analyzing. To this, by influencing ecology Austin biologist and philosopher Ludwig von Bertalanffy developed network structures that could be formulated and iterated as well. The two contrasting approaches for the ecological model are (1) developing models which support findings (of theoretically inclined biologists) but are relatively simple (Johnson et al. (2006)), or simulating complex biological systems by using dozens of differential equations (Novák and Tyson (2004)); (2) analytically tractable mathematical models developed by mathematicians who are motivated by biology (Sun and Saker (2005)). In 1995, Kingsland and Kingsland (1995) , wrote about the history of population ecology. In his book, he stated that by the mid-1960s a growing number of ecologists have been interested in computer simulations of ecological interactions traced over several generations and after that computers played a vital role in simulating population dynamics.

Even while mathematical ecological models can't always depict natural processes precisely, they can still be highly helpful in managing ecosystems, especially if all the guiding principles and conditions are taken into account throughout their construction and implementation. They can offer a thorough overview of the environmental issue being studied, first estimates of how anthropogenic or natural factors affect ecosystem functioning, and ultimately, they can highlight existing knowledge gaps and direct future study. Today, we are faced with challenges such as global change and biodiversity loss, in addition to achieving a sustainable future, are complicated in a whole new way.

1.5 Biological systems

Collections of well organised sets of material objects- either molecules, cells, organs, organisms or populations - getting through various(or certain) mechanical, topological, and temporal relations to each other and to their environment, and are associated with activities like material transformations of the biological objects or with information processed by the system, such sets are known as biological systems. These systems further expressed as system of differential or difference equations, which describe how populations change with time, space, or stage of development.

Definition 1.5.1 (Dynamical system) *It is defined as state space V, over time set T, and a function Q over $V \times T$, co-domain V, i.e., $Q : V \times T \to V$. $Q(v, t)$ gives dynamics state at time $t \in T$, with initial state v.*
Here, Q is called the evolution function of the dynamical system, V is called the state space.

Definition 1.5.2 (Autonomous dynamical system) *The system/equation is called autonomous if it is in the form*

$$\frac{dy(t)}{dt} = f(y),$$

i.e. if right hand side function is not explicitly dependent on t.
Otherwise, a non-autonomous equation/system.

In everyday life, dynamical systems include:

Mathematical models of an object or scenario comprises of robustness, logical consideration of connections, least assumptions, and formulas for relations, this will help in understanding object/scenario without its experimental analysis.

1.5.1 Various types of mathematical model for ecology and its significance

1.5.1.1 Model comprises of system of Ordinary Differential Equations-:

In ODE models (Ordinary Differential Equations), functions of only one independent variable with one or more of their derivatives are modelled.

Definition 1.5.3 (System of non-linear ODE) *The mathematical representation is given as follows-*

$$\begin{aligned}
\frac{dx_1}{dt} &= f_1(t, x_1, x_2, ..., x_n), \\
\frac{dx_2}{dt} &= f_2(t, x_1, x_2, ..., x_n), \\
&\cdot \\
&\cdot \\
&\cdot \\
\frac{dx_n}{dt} &= f_n(t, x_1, x_2, ..., x_n).
\end{aligned} \tag{1.5.1}$$

where t is an independent variable and $x_1,\ x_2, ..., x_n$ are the dependent variables.

Example 1.5.1 (Holling Tanner Model)

$$\begin{aligned}
\frac{dn}{dt} &= ru\left(1 - \frac{n}{K}\right) - \frac{mnp}{n + ap}, \\
\frac{dp}{dt} &= sp\left(1 - \frac{hp}{n}\right).
\end{aligned} \tag{1.5.2}$$

where n/p: population of the prey/predator species, r: intrinsic growth rate of the prey, K: environmental carrying capacity of the prey, m: maximal predator per capita comsumption rate, a: handling time of prey by predator, s: intrinsic growth rate of predator and h: conversion rate of prey into predator biomass.
Further, Xiao and Ruan (2001) converted the model by introducing dimensionless variables $u = \frac{n}{K}$ and $v = \frac{mp}{rK}$ and dimensionless parameters $\alpha = \frac{ra}{m}$, $\delta = \frac{sh}{m}$ and $\beta = \frac{m}{hr}$. Hence, the system becomes:

$$\begin{aligned}
\frac{du}{dt} &= u(1 - u) - \frac{uv}{u + \alpha v}, \\
\frac{dv}{dt} &= \delta v\left(\beta - \frac{v}{u}\right)
\end{aligned} \tag{1.5.3}$$

Definition 1.5.4 (Lipschitz Continous) *The function $g(t, y)$ such that $g : \mathbb{R}^{n+1} \to \mathbb{R}^n$*

is called Lipschitz continous in y, if $g(t, y)$ satisfies Lipschitz conditions at y i.e. let us suppose $|t - t_0| \leq u$, $y \in D \subset \mathbb{R}^n$ and if $y_1, y_2 \in D$ s.t.

$$||g(t, y_1) - g(t, y_2)|| \leq L||y_1 - y_2||$$

where L is called Lipschitz constant.

Definition 1.5.5 (Solution of ODE System) *Consider the initial value problem:*

$$\frac{dy}{dt} = g(t, y) \tag{1.5.4}$$

with initial condition $y(t_0) = y_0 \in \mathbb{R}^n$ for some $t_0 \in \mathbb{R}$ and $g : \mathbb{R} \times \mathbb{R}^n \to \mathbb{R}^n$. Then $y(t; t_0, y_0)$ that satisfies the equation and initial condition, is called solution to this problem.

Theorem 1.5.1 (Local Existence and Uniqueness of Solution) *For positive constants u and v such that,*

$$|t - t_0| < u \text{ and } y = \begin{bmatrix} y_1 \\ . \\ . \\ . \\ y_2 \end{bmatrix} \in D := \{y : ||y - y^0|| \leq v\} \subset \mathbb{R}^{\mathrm{n}}$$

the initial value problem 1.5.4 said to have unique solution for:

$$|t - t_0| \leq min\left\{u, \frac{v}{M}\right\} \text{ where } M := \sup_H ||g||,$$

if the function $g(t, y)$ holds the following hypothesis:

- *$g(t, y)$ is continous in $H := [t_0 - u, t_0 + u] \times D$,*
- *$g(t, y)$ is Lipschitz continous in y*

1.5.1.2 Model comprising of system of Partial Differential Equations (Reaction Diffusion model)

Spacial heterogeneity

Ecology is a spatial science, according to Tilman et al. (1997). Spatial heterogeneity is generally defined as the complexity and variability of a system property (e.g., plant biomass, cover) in space. It also describes the uneven distribution of a characteristic, an occasion, or a connection throughout a territory (Anselin (2010)). Spatial heterogene-

ity rather than spatial homogeneity is typically the norm when examining demographic processes. If we consider a different, larger scale, even homogeneous settings are likely to be heterogeneous. For instance, there are pockets of low and high fertility, mortality, and population mobility or migration within the populations that are dispersed across the landscapes. Possingham et al. (2005), tried to answer the question 'To what extent does an understanding of landscape spatial heterogeneity inform conservation decisions?'. The pioneer work by D.G. Kendall who modified the basic Kermack-McKendrick SIR model to include the effects of spatial heterogeneity in an epidemic system was the starting point (Kendall (1957); Kendall (1965)). Allen et al. (2007) suggested a frequency dependent SIS (susceptible-infected-susceptible) reaction-diffusion model for a population in a continuous spatial habitat to better understand the effects of geographical heterogeneity of the environment and individual movement on the persistence and extinction of a disease. Therefore, it is important to be able to model the distribution, movement, and dispersal of species and individuals across a varied and variable landscape (Jørgensen and Fath (2011)).

Furthermore, the majority of food chain models frequently downplay or disregard local spatial dynamics and the spatiotemporal expansion of interdependent species. The main flaw in these models is that they don't account for local random mobility, which can have an impact on species distribution. The reaction-diffusion model is regarded as a key element in identifying population clustering and concentration. The movement of species out from crowded areas caused by population pressure brought on by interspecies interference is referred to as diffusion.

When data are gathered across time and space and have at least one spatial and one temporal attribute, reaction diffusion models emerge.

Definition 1.5.6 (System of PDE) *Suppose the spatial environment is two dimensional, then the mathematical representation is given as follows-*

$$\begin{aligned}
\frac{\partial x_1}{\partial t} &= h_1(x_1, x_2, ..., x_n, z, t) + D_{x_1}\nabla^2 x_1, \\
\frac{\partial x_2}{\partial t} &= h_2(x_1, x_2, ..., x_n, z, t) + D_{x_2}\nabla^2 x_2, \\
&\vdots \\
\frac{\partial x_n}{\partial t} &= h_n(x_1, x_2, ..., x_n, z, t) + D_{x_n}\nabla^2 x_n,
\end{aligned} \tag{1.5.5}$$

for $z = (x, y) \in \Omega = [0, L] \times [0, L]$, $t > 0$, ∇^2 *represents Laplacian operator for 2-D diffusion and* D_{x_1}, $D_{x_2}, ...,$ D_{x_n} *are diffusion coefficients.*

Example 1.5.2 (Holling-Tanner with Spatial Heterogeneity) *Inclusion of diffusion in Holling-Tanner model (1.5.3), assuming animal moves uniformly in all the directions, the model becomes :*

$$\begin{aligned} \frac{\partial u}{\partial t} &= u(1-u) - \frac{uv}{u+\alpha v} + D_u \nabla^2 u, \\ \frac{\partial v}{\partial t} &= \delta v \left(\beta - \frac{v}{u}\right) + D_v \nabla^2 v. \end{aligned} \tag{1.5.6}$$

where spatial domain is $\Omega \in \mathbb{R}$, *wth Neumann boundary conditions i.e.* $u_x = v_x = 0$, *for* $x \in \partial\Omega$ *and some initial conditions.*

1.5.1.3 Model comprising of system of Stochastic Differential Equations (Random system)-:

Uncertainties in the applied inputs can be handled using a stochastic model. Stochastic models include some intrinsic unpredictability; the identical initial conditions and parameter values will result in a variety of outputs.

Deterministic vs Stochastic model: A deterministic model enables precise prediction of future events without the use of randomness. In such models, the model's parameters entirely define the values for the system's dependent variables. Simulation of these models through parameter and input adjustment can provide important insights into the quantitative and qualitative features of epidemics (Sattenspiel (2009)). Product suppliers often employ deterministic models to depict statutory future forecasts of long-term investments (such as pensions). These estimates can then be used to compare various suppliers, particularly with regard to costs, assuming the same projection rates are applied.

Stochastic processes in ecology are unpredictably occurring occurrences that have the potential to influence population and community dynamics. When the environment changes or the population is tiny, many population dynamics seem to be stochastic. Because a small population is more likely to go extinct due to random fluctuations in population size, environmental variation that can diminish population size, for instance, can raise the likelihood of stochastic extinction. Community dynamics can also be influenced by stochastic processes such as chance colonization, random order of immigration/emigration, and random fluctuations of population size. There are various kind of stochastic processes for system based on type of dynamical system. They are as in Table 1.1.

To see the pros and cons of deterministic and stochastic systems, refer Table 1.2.

Table 1.1: Types of stochastic processes.

Stochastic process	Time	Characteristics	Example
Branching process	discrete or continuous	population model where each individual's offspring number is drawn from same distribution	colonization of new habitat, spread of new disease
Markov chain	discrete	switches between different states, with probabilities depending on previous state	nucleotide substitution in DNA sequence evolution
Poisson process	continuous	events that happen independently and with a small probability per unit of time	mutations in lineage of individuals, coalescent process
Wiener process	continuous	random changes in variable but with mean zero	movement of individuals in space

Table 1.2: Pros and cons of deterministic and stochastic modeling.

Type	pros	cons
Deterministic	easy applicability, as rely on only assumption about long-term average	fundamentally flawed, as it doesn't consider unknown variable changes that will affect dynamics
	comprehensive, hence user friendly	inadequate and potentially misleading sometimes
Stochastic	by considering random process various environmental changes or errors are taken into account	immensely complex series of events with a few parameters
	avoids significant shortfalls inherent in deterministic models	systems can not be solved analytically so it is difficult to build an intuitive perspective sometimes
	using many different estimates of future conditions, stochastic models predict a range of possible future	generated random data claims to lie under the estimate 95% confidence interval about 3/4 of the time and hence model fails occasionally

Definition 1.5.7 (System of SDE) *Consider an ODE system*

$$\frac{dy}{dt} = \alpha(t)y(t), \quad y(0) = y_0.$$

Here, $\alpha(t)$ is a deterministic parameter.
Now, suppose $\alpha(t)$ is rather a stochastic parameter, given by

$$\alpha(t) = g(t) + h(t)\xi(t),$$

where $\xi(t)$ is a white noise.
Thus, a stochastic differential equation system is formed

$$\frac{dY}{dt} = g(t)Y(t) + h(t)Y(t)\xi(t).$$

The differential form of Brownian motion is denoted by, $dW(t) = \xi(t)dt$, hence we obtain:

$$dY(t) = g(t)Y(t)dt + h(t)Y(t)dW(t).$$

General form is given by

$$dY(t,\omega) = g(t, Y(t,\omega))dt + g(t, Y(t,\omega))dW(t,\omega), \tag{1.5.7}$$

where ω represents a random variable $Y = Y(t,\omega)$ and initial condition $Y(0,\omega) = Y_0$ with probability 1.

Example 1.5.3 (Holling-Tanner model (with cannibalism) assuming stochasticity) *Basheer et al. (2016) considered the environmental fluctuation in cannibalism (refer to section 1.6, eq. (1.6.2)), the SDE model becomes*

$$\begin{aligned} du &= \left(u(1 + c_1 - u) - \frac{uv}{u + \alpha v} - c\frac{u^2}{u + d}\right) dt + \alpha_1 \frac{u^2}{u + d} dW_t, \\ dv &= \delta v \left(\beta - \frac{v}{u}\right) dt. \end{aligned} \tag{1.5.8}$$

where α_1 as intensity of stochasticity and W_t is standard one-dimensional Browninan motion.

1.6 Biological preliminaries

Here, we will define some of the basic biological terms that are being used throughout the formation of thesis.

Basic Reproduction Number($\mathscr{R}_0$)

One of the most important concepts to emerge from the study of demography is the fundamental reproductive ratio, or $\mathscr{R}_0$, (Sharpe and Lotka (1911); Dublin and Lotka (1925); Kuczynski (1928)). It was later independently investigated for human infectious diseases (Kermack and McKendrick (1927); Dietz (1975)) and vector-borne illnesses like malaria (Ross (1911); Macdonald (1952)). It is acknowledged as the threshold that causes the behaviour of the traditional epidemic model. The predicted quantity of secondary people that an individual will create over the course of its lifetime is known as $\mathscr{R}_0$. Understanding the epidemic and the possible hazard from severe acute respiratory syndrome (SARS) in epidemiology required the estimation of $\mathscr{R}_0$ (Choi and Pak (2003); Lipsitch et al. (2003); Lloyd-Smith et al. (2003); Riley et al. (2003)). $\mathscr{R}_0$ has been likewise used to characterize bovine spongiform encephalitis (Woolhouse and Anderson (1997); Ferguson et al. (1999); De Koeijer et al. (2004)), foot and mouth disease (Ferguson et al. (2001); Matthews et al. (2003)), novel strains of influenza (Mills et al. (2004); Stegeman et al. (2004)) and West Nile virus (Wonham et al. (2004)). The incidence and spread of dengue (Luz et al. (2003)), malaria (Hagmann et al. (2003); Smith et al. (2007)), Ebola (Chowell et al. (2004); Althaus (2014); Khan et al. (2015)), and scrapie (Gravenor et al. (2004)) have also been assessed using $\mathscr{R}_0$ in recent literature. Ongoing theoretical work has extended $\mathscr{R}_0$ for a range of complex models, including stochastic and finite systems (Nasell (1995)), models with spatial structure (Mollison and Denis (1995); Lloyd and May (1996)) or age-structure (Anderson and May (1992); Diekmann and Heesterbeek (2000); Hyman and Li (2000)), and macroparasite models (Anderson and May (1992); Diekmann and Heesterbeek (2000)).Wallinga and Teunis (2004) original network-based method for calculating the reproductive number was extended by White et al. (2013) in a novel way. Their expansion enables us to use a similarity matrix to include spatial and/or demographic data.

However, concept coming from epidemiology, the basic reproduction number '$\mathscr{R}_0$' in population dynamics may be thought as the number of predators one predator gives rise during its life, when introduced in a prey population (Rebelo et al. (2012)- Garrione and Rebelo (2016)); and under acceptable state, we denote it by '$\mathscr{T}_0$', and (say) predators will go extinct if $\mathscr{T}_0 < 1$ and will persist if $\mathscr{T}_0 > 1$.

In autonomus system, $\mathscr{T}_0$ is computed easily, starting from the coefficients involved in system. Regardless, in non autonomous models (Wang and Zhao (2008)), threshold is being defined as the spectral radius of an acceptable operator related to the model. It has been proved as a comprehensive way, allowing to obtain several persistence results for such systems.

Remark 1 (Mathematically) *This threshold parameter represents the asymptotic stability of predator free equilibrium.*

The fundamental reproductive number models can be found using one of two ways. Finding prerequisites for the local stability of the model's predator-free equilibrium is one approach. The other strategy is to use a next-generation operator (Diekmann et al. (1990); Diekmann and Heesterbeek (2000); Van den Driessche and Watmough (2002)), which will be discussed later in this chapter.

Adequate contact or growth rate/functional responses

In ecological groups, predation is a common interaction (Allan (1995)). The functional response is crucial to the dynamics of mathematical models depicting predator-prey relationships (Abrams and Ginzburg (2000); Aldebert et al. (2016)). Few Functional responses are defined in the Table 1.3.

Allee Effect

Allee effect is a biological association between the size or density of a population and its growth. A species suffers from it when its population is really sparse, so it is difficult for them to reproduce or survive. Based on the nature of density at low densities, there are two types of Allee effect: the strong Allee effect and the weak Allee effect. If an Allee effect is weak, a population will have a lower per capita growth rate at a lower population density, but will still exhibit a positive per capita growth rate regardless of population density or size. Under a strong Allee effect, on the other hand, a population's growth rate becomes negative when its population size or density is reached.

Allee (1927) first proposed this phenomenon. In the literature, there are several studies analyzing this effect in different population models and finding it to be important to system dynamics (González-Olivares et al. (2011); Wang et al. (2011)). These models can reveal much about its dynamics and can suggest the appearance of a new equilibrium point that changes the structural stability of the system, in turn altering the stability of other equilibrium points.

Mathematically, the most general representation of this growth function in single species is given by

$$\frac{dx}{dt} = r\left(1 - \frac{x}{K}\right)(x - m)x, \tag{1.6.1}$$

where r: intrinsic growth rate, K: carrying capacity of environment. If $m > 0$ then it is a

Table 1.3: Types functional responses

Functional form	Name	Comments	Reference
$p = aT_sP$	Type I	assumes that the rate of consumption will rise linearly with food density	Holling (1959)
$p = \frac{aT_tP}{1+abP}$	Type II	a predator's rate of prey consumption climbs as prey density rises, but eventually that rate stabilises regardless of prey density growth	Holling (1959)
$p = \frac{aT_tP^k}{1+abP^k}$	Type III	happens in predators who become more active in their search for prey as prey density rises	Holling (1959)
$p = \frac{wP}{P^2/i+P+a}$	Type IV	when prey numbers are high enough, the predator's per-capita rate of predation declines	Andrews (1968)
$f_p(p,A) = \frac{p}{1+T_pp+qT_AA}$	Modified Holling	Predators will switch to alternative food when the density of their preferred prey is low	Van Baalen et al. (2001)
$p = b(1-e^{-aP})$	Ivlev functional response	both consistently constrained and monotonically rising	Ivlev (1975)

strong Allee effect and if $m < 0$ then weak.

Cannibalism

The act of killing and consuming one's conspecifics is referred to as cannibalism. It is common in predator-prey communities that exist naturally, is present in the majority of animal species, including fish, and significantly contributes to controlling population dynamics (Fox (1975)). Because cannibalism is a size-selective form of predation, it affects both the population's abundance and size distribution.

Kohlmeier and Ebenhöh (1995) considered the cannibalism (in predator population) for the first time in the Rosenzweig-McArthur model. Demonstrated that predator cannibalism can stabilize the model's interior equilibrium in unexpected ways. Recently, Basheer et. al. showed how prey cannibalism alters the dynamics of Holling-Tanner-type predator-prey model. This is how they modified no cannibalism Holling-Tanner model presented in Example 1.5.1 to cannibalistic Holling-Tanner model.
Prey cannibalism in Holling-Tanner model:

$$\begin{aligned} \frac{du}{dt} &= u\left(1 + c_1 - u\right) - \frac{uv}{u + \alpha v} - c\frac{u^2}{u + d}, \\ \frac{dv}{dt} &= \delta v\left(\beta - \frac{v}{u}\right). \end{aligned} \tag{1.6.2}$$

As reproduction in the prey population increases, therefore addition of $c_1 u$ term is done to the prey population. Holling type II, with cannibalism rate c has been used as the functional response for cannibalistic prey population and $c_1 < c$.
Predator Cannibalism in Holling-Tanner model:

$$\begin{aligned} \frac{du}{dt} &= u\left(1 - u\right) - \frac{uv}{\alpha v + u}, \\ \frac{dv}{dt} &= \delta v\left(\beta_1 - \frac{v}{\gamma u + \rho v}\right). \end{aligned} \tag{1.6.3}$$

where ρ is cannibalism rate. In this case, even if the predator becomes a cannibal, its food intake remains the same, so the assumption is $\rho + \gamma \leq 1$, with $\gamma < 1,\ \rho < 1$, also, $\beta_1 > \beta$.

1.7 Mathematical tools of analysis

In this section, the mathematical tools, definitions and theorems which are used analytically in this thesis, are over-viewed.

Concepts and tools from dynamical system theory

1.7.1 Phase plane analysis

An abstract space with each of the variables needed to specify the state of a system representing the orthogonal coordinates (Lakshmanan and Rajaseekar (2012)). For second-order autonomous system

$$\begin{aligned} \dot{x} &= g(x, y), \\ \dot{y} &= h(x, y). \end{aligned} \tag{1.7.1}$$

where $x,\ y$ are states of the system. Phase plane is the space having state of the corresponding system. Curve which represents the solution of system, as time varies from zero to infinity, is known as phase plane trajectory and family of such curves is known as phase portrait of the system.

1.7.2 Equilibrium points

An equilibrium point is sometimes called a fixed point, x^*, of the system $\frac{dx}{dt} = f(x(t))$, is a point such that $\frac{dx}{dt} = x^* = f(x^*) = 0$. Intuitively, x^* is a point where the rate of change of x is zero so, if a system is at this point it will not change. This is exactly what it means to be at equilibrium, not changing. A fixed point can be a stable node, an unstable node, a stable focus, an unstable focus, a center, or a saddle point.

- Saddle Point: A saddle point is a fixed position where the trajectory is drawn to it for a while before it becomes too close, at which point it begins to move away from the fixed point.
- Stable Node: A stable node is a fixed point where the trajectories are directly attracted to the node.
- Unstable Node: An unstable node is a fixed point where the trajectories are directly repulsed from the node.
- Stable Focus: The trajectories are drawn to a stable focus, which is a fixed point, but they spiral there rather than being drawn in directly.
- Unstable Focus: The trajectories are repelled from an unstable focus, which is a fixed point, but they spiral away from it rather than being ejected from it.
- Center: A centre is a fixed point that the paths simply orbit. They are neither

attracted to nor repulsed by the fixed point.

Mathematical definitions

Definition 1.7.1 (Local Stability) *If under initial conditions near the equilibrium point, solutions moves closer to the equilibrium point then that equilibrium point is called locally stable.*

Definition 1.7.2 (Global Stability) *If under any initial conditions, solutions approaches an equilibrium point then that equilibrium points called globally stable.*

Definition 1.7.3 (Positive Definite) *For all $y \neq 0$ in D, the function $V(x)$ is defined as positive/negative definite in D if $V(y) > 0 (< 0)$.*

Definition 1.7.4 (Positive Semi Definite) *For all $y \neq 0$ in D, the function $V(x)$ is defined as positive/negative definite in D if $V(y) \geq 0 (\leq 0)$.*

Definition 1.7.5 *Consider the system*

$$\dot{y_i} = g_i(t, y_1, y_2, ..., y_n),\ t \geq t_0,\ x \in D \subset \mathbb{R}^n$$

then the derivative L_t of the function $V(t, y_1, y_2, ..., y_n)$ in the direction of the vector field $g_i(t, x)$ is given by

$$L_t V = \frac{\partial V}{\partial t} + \sum_{i=1}^{n} \frac{\partial V}{\partial y_i} g_i(t, y_1, y_2, ..., y_n).$$

Definition 1.7.6 (ODE Stability)

- ***Lyapunov Stable***- *Consider the system*

  $$\dot{y_i} = g_i(t, y_1, y_2, ..., y_n),$$

  and if there exist a function $V(t, y_1, y_2, ..., y_n)$ in the neighbourhood of $y = 0$ which is positive definite for $t \geq t_0$ and its orbital derivative is negative semi-definite, then the solution $y = 0$ is called stable in Lyapunov sense (or Lyapunov stable).

- ***Asymptotically Stable***- *Consider the system*

  $$\dot{y_i} = g_i(t, y_1, y_2, ..., y_n),$$

  and if there exist a function $V(t, y_1, y_2, ..., y_n)$ in the neighbourhood of $y = 0$ which

is positive definite for $t \geq t_0$ and its orbital derivative is negative definite, then the solution $y = 0$ is called asymptotically stable.

1.7.3 Linearisation

Since, the nature of real physical systems is inherently nonlinear. However, we still require a linear system to continue with some important analysis. To linearise the system near the equilibrium points and hence, identifying the local phase portraits, the method is as follows

Consider, the model (1.7.1), suppose it has equilibrium point (x_0, y_0). Let us define two variables $\epsilon(t) \to 0,\ \delta(t) \to 0$, called deviation variables, s.t. $\epsilon(t) = x(t) - x_0,\ \delta(t) = y(t) - y_0$.

On differentiating both the variables, we get

$$\begin{aligned} \frac{d\epsilon}{dt} &= \frac{dx}{dt} = g(x_0 + \epsilon, y_o + \delta), \\ \frac{d\delta}{dt} &= \frac{dy}{dt} = h(x_0 + \epsilon, y_o + \delta). \end{aligned}$$

By expanding the Taylor series and neglecting higher derivatives

$$\begin{aligned} \frac{d\epsilon}{dt} &= g(x_0, y_0) + \epsilon \frac{\partial g}{\partial x}|_{(x_o, y_o)} + \delta \frac{\partial g}{\partial y}|_{(x_o, y_o)} \\ \frac{d\epsilon}{dt} &= h(x_0, y_0) + \epsilon \frac{\partial h}{\partial x}|_{(x_o, y_o)} + \delta \frac{\partial h}{\partial y}|_{(x_o, y_o)} \end{aligned}$$

As $g(x_0, y_0) \approx h(x_0, y_0) \to 0$ and by writing into the matrix form

$$\begin{bmatrix} \frac{d\epsilon}{dt} \\ \frac{d\delta}{dt} \end{bmatrix} = \begin{bmatrix} \frac{\partial g}{\partial x} & \frac{\partial g}{\partial y} \\ \frac{\partial h}{\partial x} & \frac{\partial h}{\partial y} \end{bmatrix} \begin{bmatrix} \epsilon \\ \delta \end{bmatrix}$$

This how we linearised the non-linear system near equilibrium point (x_0, y_0).

1.7.4 Nullclines

Suppose an autonomous system

$$\begin{aligned} \frac{dx}{dt} &= f(x, y), \\ \frac{dy}{dt} &= g(x, y). \end{aligned} \tag{1.7.2}$$

Then

- $x-$**nullcline:** The collection of phase plane locations where $dx/dt = 0$. The vectors at these positions are vertical in geometry (straight up and down). By figuring out $f(x, y) = 0$, one can locate the $x-$nullclines.
- $y-$**nullcline:** The collection of phase plane locations where $dy/dt = 0$. The vectors at these positions are vertical in geometry (straight up and down). By figuring out $g(x, y) = 0$, one can locate the $y-$nullclines.

1.7.5 Phase portraits

After linearisation of the system near equilibrium point, we can analyze the qualitative feature of phase portraits, resulting in a classification of the various possibilities that may arise.
Let (x_0, y_0) be an equilibrium point of system (1.7.1) and the Jacobian matrix/variational matrix corresponding to (x_0, y_0) be

$$\mathcal{J}(x_0, y_0) = \begin{bmatrix} \frac{\partial g}{\partial x}\big|_{(x_0,y_0)} & \frac{\partial g}{\partial y}\big|_{(x_0,y_0)} \\ \frac{\partial h}{\partial x}\big|_{(x_0,y_0)} & \frac{\partial h}{\partial y}\big|_{(x_0,y_0)} \end{bmatrix}$$

Now, on the basis of eigenvalues of this Jacobian matrix various cases arises. These are as follows:

1. If both the real eigenvalues are negative: trajectories move directly towards and then converges at the critical point, making it asymptotically stable (see Fig. 1.1 (a)). Such type of critical point is also called node.
2. If both the eigenvalues are positive: trajectories move away from the critical point to infinite distant away, making it unstable (see Fig. 1.1(b)). Such type of critical point is called node.
3. If one eigen value is positive and other negative: the trajectories corresponding to the eigenvectors of the positive eigenvalue initially they start at the critical point, after which they diverge infinitely out and the trajectories corresponding to the eigenvector of the negative eigenvalue Starts from infinitely far away, move towards and then convergent at the critical point. So, superimposed result would be that all the trajectories will start from infinitely far away, move towards but rather converging to critical point they change their direction and move back to infinite far away. Such type of unstable critical point is called a saddle point (see Fig. 1.1(c)).

4. If repeated real eigenvalues:

   (a) Two linearly independent eigenvector: the trajectories traces straight lines(either towards critical point if negative real eigenvalue, or away from critical point if positive real eigenvalue), thus a star-point or proper node (see Fig. 1.1(d))

   (b) Only one linearly independent eigenvector: the trajectories are formed by cross between a node and a spiral(either towards critical point if negative real eigenvalue, or away from critical point if positive real eigenvalue), thus an improper node (see Fig. 1.1(e)).

5. If Complex conjugate eigenvalue:

   (a) Real part is zero: the trajectories stay in an orbit forming ellipse i.e. neither approach the critical point nor move to infinity. Such type of critical point is called a center (see Fig. 1.1(f)).

   (b) Real part is nonzero: the trajectories spirally converges to the critical point. Such type of critical point is called a spiral point (see Fig. 1.1(g))

Example 1.7.1 *For a non-linear system:*

$$\frac{dx}{dt} = x - y,$$
$$\frac{dy}{dt} = x^2 + y^2 - 2.$$

The Equilibrium points are $(1,1)$ *and* $(-1,-1)$.
The Jacobian matrix corresponding to $(1,1)$ *becomes*

$$\mathcal{J}(1,1) = \begin{bmatrix} 1 & -1 \\ 2 & 2 \end{bmatrix}$$

The eigenvalues are $\lambda = \dfrac{3 \pm \sqrt{7}i}{2}$. *Hence, the unstable spiral critical point.*

Now, the Jacobian matrix corresponding to $(-1,-1)$ *becomes*

$$\mathcal{J}(-1,-1) = \begin{bmatrix} 1 & -1 \\ -2 & -2 \end{bmatrix}$$

The eigenvalues are $\lambda = \dfrac{-1 \pm \sqrt{17}}{2}$. *Hence, the unstable saddle critical point.*

So, the phase portrait formed is shown in Fig. (1.2).

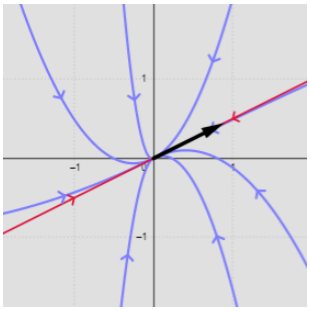

(a) Stable node

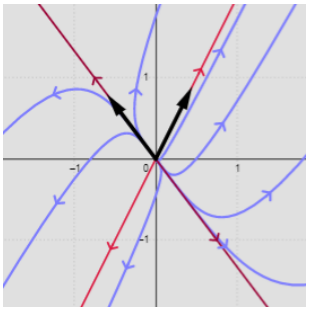

(b) Unstable node

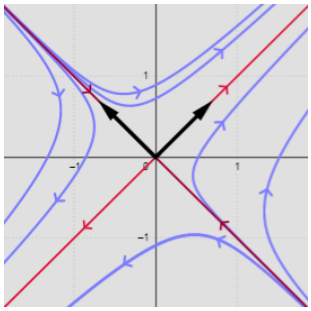

(c) Saddle point

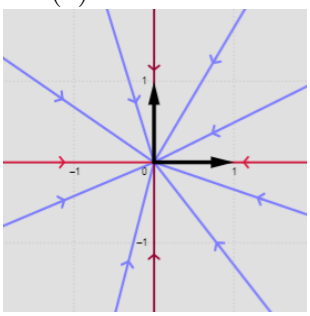

(d) Star point

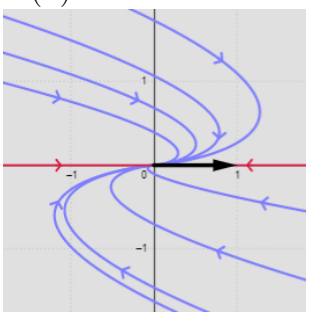

(e) Improper node

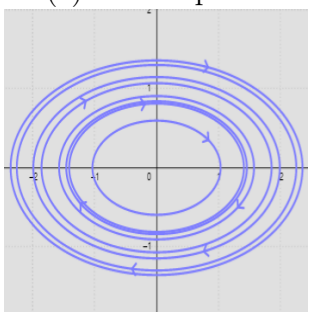

(f) Center

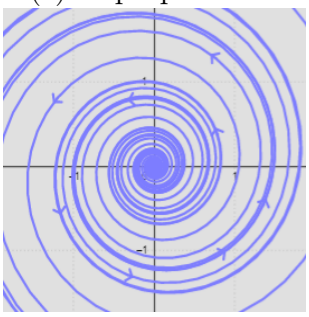

(g) Spiral point

Figure 1.1: Phase portraits with different kind of eigenvalues form.

1.7.6 Local bifurcation

Bifurcation can be defined as a sudden qualitative change in the nature of the dynamics which occur at critical parameter values. Bifurcation often occur in specific ways or routes as control parameter is varied. There are basically four standard types of bifurcations that occur in simple low dimensional non-linear systems namely:

- The saddle node: The saddle-node bifurcation is the basic mechanism by which fixed points are created and destroyed. As parameter is varied, two fixed points move towards each other, collide, and mutually annihilate.

- The pitchfork: The pitchfork bifurcation is common in dynamical system, that is, invariant under the transformation $T = -T$. Fixed points tend to appear and disappear in symmetrical pairs.

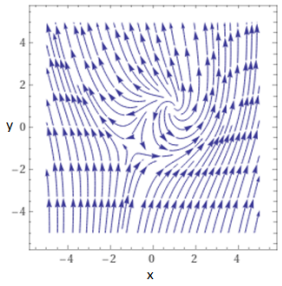

Figure 1.2: Phase portrait of Example 1.7.1

- The transcritical: In transcritical bifurcation, a fixed point must exist for all values of a parameter and can never be destroyed. However, such a point may change its stability when the control parameter passes through the bifurcation point or critical value.
- The Hopf-bifurcation: In this bifurcation, the real part of pair of complex conjugate eigenvalues of the least stable equilibrium point increases through zero as control parameter increases or decreases through a critical value and a time periodic solution arises. Hopf bifurcation can be supercritical and subcritical. In a supercritical Hopf bifurcation, the limit cycle is stable above the bifurcation point. In a subcritical Hopf bifurcation, the bifurcated limit cycle will be unstable.

We mainly got Hopf-bifurcation in our present thesis. Consider the following system

$$\dot{x} = f(x, \mu), \tag{1.7.3}$$

where $\dot{x} = \left(\frac{dx_1}{dt}, \frac{dx_2}{dt}, ..., \frac{dx_n}{dt}\right)$, $f = (f_1, f_2, ..., f_n)^T$ and $\mu \in \mathbb{R}$ is a parameter. We use Df (x,μ) to denote the Jacobian matrix and $f_\mu(x, \mu)$ to denote the vector of partial derivatives of the components of f with respect to parameter μ.

Theorem 1.7.1 *Consider the system (1.7.3) with an equilibrium point x^*. Then, if there exists a parameter $\mu_c \in I$ and $I \in \mathbb{R}$ and $F \in C^\alpha(\mathbb{R}^n X \mathbb{R}^n, \mathbb{R})$ for some $\alpha \geq n$ with $f(x^*, \mu) = 0 \; \forall \; \mu \in \mathbb{R}$, so that the necessary and sufficient condition for system (1.7.3) to have a simple Hopf-bifurcation at $\mu = \mu_c$ are*

- *A simple pair of complex eigenvalues of the Jacobian matrix $\mathcal{J}(x^*)$ of system (1.7.3) at the equilibrium point x^* exists, say $\lambda(\mu) = \eta_1(\mu) \pm i\eta_2(\mu)$ such that they become purely imaginary at $\mu = \mu_c$; whereas all the other eigenvalues remain real and negative.*
- $\left.\frac{dRe(\lambda(\mu))}{d\mu}\right|_{\mu=\mu_c} \neq 0.$

Now using above theorem, we show simple Hopf bifurcation for $n = 3$. Consider the characteristic equation of system (1.7.3) given by

$$P_3(\lambda) = \lambda^3 + A_1\lambda^2 + A_2\lambda + A_3 \tag{1.7.4}$$

where $A_1(\mu) = -tr(\mathcal{J}(x^*))$, $A_2(\mu) = M(\mathcal{J}(x^*))$ and $A_3(\mu) = -det(\mathcal{J}(x^*))$ with $M(J(x^*))$ represents the sum of the principal minors of order two $J(x^*)$. Clearly, the first condition of theorem holds if and only if $A_i > 0$; $i = 1, 2$ and $\Delta = A_1A_2 - A_3 = 0$. So, the characteristic equation at $\mu = \mu_c$, becomes

$$(\lambda^2 + A^2)(\lambda + A_1) = 0 \tag{1.7.5}$$

For all , the roots are generally of the form:

$$\lambda_1(\mu) = \eta_1(\mu) + i\eta_2(\mu), \lambda_2(\mu) = \eta_1(\mu) - i\eta_2(\mu), and \lambda_3(\mu) = A_1(\mu).$$

Now, we shall prove the transversality condition

$$\left.\frac{dRe(\lambda_j(\mu))}{d\mu}\right|_{\mu=\mu_c} \neq 0, j = 1, 2.$$

Substituting $\lambda_1(\mu) = \eta_1(\mu) + i\eta_2(\mu)$ into (1.7.5) and calculating the derivative, we obtain

$$\begin{aligned} K(\mu)\eta_1^{'}(\mu) - L(\mu)\eta_2^{'}(\mu) + M(\mu) &= 0, \\ L(\mu)\eta_1^{'}(\mu) + K(\mu)\eta_2^{'}(\mu) + N(\mu) &= 0, \end{aligned}$$

where

$$\begin{aligned} K(\mu) &= 3\eta_1^2(\mu) + 2A_1(\mu)\eta_1(\mu) + A_2(\mu) - 3\eta_2^2(\mu), \\ L(\mu) &= 6\eta_1(\mu)\eta_2(\mu) + 2A_1(\mu)\eta_2(\mu), \\ M(\mu) &= \eta_1^2(\mu)A_1^{'}(\mu) + A_2^{'}(\mu)\eta_1(\mu) + A_3^{'}(\mu) - A_1^{'}(\mu)\eta_2^2(\mu), \\ N(\mu) &= 2\eta_1(\mu)\eta_2(\mu)A_1^{'}(\mu) + A_2^{'}(\mu)\eta_2(\mu). \end{aligned}$$

We have

$$\left.\frac{dRe(\lambda_j(\mu))}{d\mu}\right|_{\mu=\mu_c} = \left[- \frac{L(\mu)N(\mu) + K(\mu)M(\mu)}{K(\mu)^2 + L(\mu)^2} \right]_{\mu=\mu_c} \neq 0 \text{ and } \lambda_3 = -A_1 \neq 0.$$

Hence, the transversality condition is non-zero if and only if $LN + KM \neq 0$.

1.7.7 Next generation operator method

The reproduction number, $\mathscr{R}_0$, which is defined as the spectral radius of the "next generation operator" is computed using the next generation operator method (Diekmann et al. (1990)). For the model system under consideration, the construction of the operator entails identifying two compartments—infected and non-infected. The procedures for locating the matrix's next-generation operator are described in this section. Diekmann and Heesterbeek (2000) provide a thorough explanation of how the next generation operator is formed.

Assume that there are n compartments of which m are predators. We define the vector $x = x_i,\ i = 1, 2, ...n$ where x_i denotes the number or proportion of individuals in the i_{th} compartment and $X_S = \{x \geq x_i | x_i = 0, i = 1, 2, ..., m\}$ is defined as the predator-free states of the model. Suppose, with non-negative initial conditions, can be written in terms of the following autonomous system:

$$\dot{x_i} = f(x_i) = \mathscr{F}_i(x) - \mathscr{V}_i(x), i = 1, 2, ..., n, \tag{1.7.6}$$

$\mathscr{F}_i(x)$ be the rate of appearance of new predator in compartment i, and let $\mathscr{V}_i(x) = \mathscr{V}_i^-(x) - \mathscr{V}_i^+(x)$ where $\mathscr{V}_i^+(x)$ is the rate of transfer of individuals into compartment i by all other means and $\mathscr{V}_i^-(x)$ is the rate of transfer of individuals out compartment i. The difference $\mathscr{F}_i(x) - \mathscr{V}(x)$ gives the rate of change of x_i. Also, $\mathscr{F}_i(x)$ should include only infections that are newly arising, but does not include terms which describe the transfer of infectious individuals from one infected compartment to another. It is assumed that these functions are at least twice continuously-differentiable in each variable (Van den Driessche and Watmough (2002)). Assume that $\mathscr{F}_i$ and $\mathscr{V}_i$ satisfy the axioms outlined by Diekmann et al. (1990) and Van den Driessche and Watmough (2002) as given below:

$A1$. If $x \geq 0$, then $\mathscr{F}_i,\ \mathscr{V}_i^-,\ \mathscr{V}_i^+ \geq 0$ for $i = 1, 2, ..., m$.

$A2$. $x = 0$, then $\mathscr{V}_i^- = 0$. In particular, if $x \in X_S$ then $\mathscr{V}_i^- = 0$ for $i = 1, 2, ..., m$.

$A3$. $\mathscr{F}_i = 0$, if $i > m$.

$A4$. If $x \in X_S$, then $\mathscr{F}_i(x) = 0$ and $\mathscr{V}_i^+(x) = 0\ for\ i = 1, 2, ..., m$.

$A5$. If $\mathscr{F}(x)$ is set to zero, then all eigenvalues of $\mathscr{D}f(x_0)$ have negative real part.

Now, we can form the next generation matrix (operator) $\mathscr{F}\mathscr{V}^{-1}$ from matrices of partial derivatives of $\mathscr{F}_i$ and $\mathscr{V}_i$. Specifically, $\mathscr{F}$ and $\mathscr{V}$ are the mXm matrices defined by

$$\mathscr{F} = \left[\frac{\partial \mathscr{F}_i}{\partial x_j}(\bar{x})\right] \text{ and } \mathscr{V} = \left[\frac{\partial \mathscr{V}_i}{\partial x_j}(\bar{x})\right] \text{ with } 1 \leq i, j \leq m.$$

where, $\bar{x}$ is the disease-free equilibrium. The entries of $\mathcal{F}\mathcal{V}^{-1}$ give the rate at which infected individuals in x_j produce new infections in x_i, times the average length of time an individual spends in a single visit to compartment j. R_0 is given by the spectral radius (dominent eigenvalue) of the matrix $\mathcal{F}\mathcal{V}^{-1}$.Applications of this method are nicely given in Matthews et al. (1999), Porco and Blower (2000), Castillo-Chavez et al. (2002), and Wonham et al. (2004).

Theorem 1.7.2 *Van den Driessche and Watmough (2002), considered the disease transmission model given by eqn. (1.7.6) with $f(x)$ satisfying axioms (A1)-(A5). If $\bar{x}$ is a DFE of the model, then $\bar{x}$ is LAS if $\mathcal{R}_0 = \rho(\mathcal{F}\mathcal{V}^{-1}) < 1$ (where ρ is the spectral radius), but unstable if $\mathcal{R}_0 > 1$.*

The Next Generation $\mathcal{R}_0$ may not be unique, which would cause it to fail mathematically. Second, the Next Generation $\mathcal{R}_0$ is susceptible to biological failure, just like in models where transmission doesn't just happen through contact. Finally, when a finite amplitude disturbance instead of an infinitesimal perturbation is given, the Next Generation $\mathcal{R}_0$ can fail to forecast persistence.

1.7.8 PRCC for global sensitivity

When building models, we must simplify things and make assumptions about the parameter's values as well as how the model will be put together. The impacts of model parameter values on certain outcome measures are frequently vital to consider because of the ambiguity that may follow selections for parameter values (output). The model's prediction of the ensuing dynamics is subject to variability due to uncertainty in the parameter values used. The magnitude of the induced variability increases as the number of uncertain parameters increases. In order to evaluate this diversity in the prediction, a sensitivity analysis is frequently carried out.

An effective technique used frequently in uncertainty analysis is partial rank correlation coefficient (PRCC) sensitivity analysis, which allows researchers to examine a full parameter space of model with the fewest possible computer simulations. The purpose of the PRCC sensitivity analysis is to determine important factors whose uncertainties contribute to the imprecision of the prediction and to rank these parameters according to the significance of this contribution. A statistical method called correlation is used to assess how closely the parameters in a model are related to the outcome measures. As far as there is hardly any correlation between the inputs, PRCC is a reliable sensitivity measure for nonlinear but monotonic interactions between inputs and output. Strongly monotone yet very nonlinear parameters are thought to respond more sensitively to PRCC than other methods.

As sensitivity analysis determines what factors (inputs) and initial conditions have the greatest impact on the model's outputs. Thus, the researcher will be informed of which parameters require the greatest numerical attention. A highly sensitive parameter should be carefully assessed since even a minor change in that parameter can have a significant impact on the amount of interest in terms of both quantity and quality.

1.7.9 Stability analysis of system

Let $h_i : \mathbb{R} \to \mathbb{R}$ for $i = 1, 2, 3$ be a C^1 function and $h(0) = 0$ such that the system of ordinary differential equations becomes

$$\begin{aligned} \frac{dx_1}{dt} &= h_1(t, x_1, x_2, x_3), \\ \frac{dx_2}{dt} &= h_2(t, x_1, x_2, x_3), \\ \frac{dx_3}{dt} &= h_3(t, x_1, x_2, x_3). \end{aligned} \tag{1.7.7}$$

Consider $\Omega \subset \mathbb{R}^3$ be a bounded domain with smooth boundary and D =diag$(D_{x_1}, D_{x_2}, D_{x_3})$ with $D_{x_i} > 0$. Then, reaction diffusion system with Neumann boundary condition becomes

$$\begin{aligned} \frac{\partial x_1}{\partial t} &= h_1(t, x_1, x_2, x_3) + D_{x_1}\nabla^2 x_1, \\ \frac{\partial x_2}{\partial t} &= h_2(t, x_1, x_2, x_3) + D_{x_2}\nabla^2 x_2, \\ \frac{\partial x_3}{\partial t} &= h_3(t, x_1, x_2, x_3) + D_{x_3}\nabla^2 x_3, && \text{in } \Omega \times (0, \infty), \\ \frac{\partial x_i}{\partial n} &= 0, && \text{on } \partial\Omega \times (0, \infty), \\ x_i(x, 0) &= x_{i0}(x) && \text{in } \Omega, \end{aligned} \tag{1.7.8}$$

where ∇^2 is Laplacian operator and n is the unit outward normal to $\partial\Omega$.

1.7.9.1 Stability analysis without diffusion

Here, we will find the condition for linear stability of the steady state $E^*(x_1^*, x_2^*, x_3^*)$ when the system is non-spatio temporal by using Routh-Hurwitz criteria and, hence, finding conditions for which it becomes unstable in presence of diffusion.

The Jacobian matrix for the system (1.7.7) is given by

$$\mathscr{J}^*(x_1^*, x_2^*, x_3^*) = \begin{pmatrix} b_{11} & b_{12} & b_{13} \\ b_{21} & b_{22} & b_{23} \\ b_{31} & b_{32} & b_{33} \end{pmatrix}, \tag{1.7.9}$$

The characteristic equation becomes

$$\lambda^3 + A_1\lambda^2 + A_2\lambda + A_3 = 0. \tag{1.7.10}$$

Applying Routh-Hurwitz criteria, The steady state $E^*(x_1^*, x_2^*, x_3^*)$ is locally asymptotically stable if $A_1 > 0,\ A_3 > 0$ and $A_1A_2 - A_3 > 0$.

1.7.9.2 Stability analysis with diffusion

Let us consider the spatio-temporal system (1.7.8), if the steady state $E^*(x_!^*, x_2^*, x_3^*)$ is perturbed such that $x_1 = x_1^* + x_1(x, y, t),\ x_2 = x_2^* + x_2(x, y, t)$ and $x_3 = x_3^* + x_3(x, y, t)$. The linearized form of the system is obtained as

$$\begin{aligned} \frac{\partial x_1}{\partial t} &= b_{11}x_1 + b_{12}x_2 + b_{13}x_3 + D_{x_1}\nabla^2 x_1, \\ \frac{\partial x_2}{\partial t} &= b_{21}x_1 + b_{22}x_2 + b_{23}x_3 + D_{x_2}\nabla^2 x_2, \\ \frac{\partial x_3}{\partial t} &= b_{31}x_1 + b_{32}x_2 + b_{33}x_3 + D_{x_3}\nabla^2 x_3, \end{aligned} \tag{1.7.11}$$

where $b'_{ij}s$ are the Jacobian matrix (1.7.9) entries.
Let us assume that the solution to the above system has the following form:

$$\begin{aligned} x_1(x, y, t) &= x_1^0 e^{\lambda t + i(k_x x + k_y y)}, \\ x_2(x, y, t) &= x_2^0 e^{\lambda t + i(k_x x + k_y y)}, \\ x_3(x, y, t) &= x_3^0 e^{\lambda t + i(k_x x + k_y y)}, \end{aligned}$$

where $x_1^0,\ x_2^0$ and x_3^0 are constants. The function $e^{i(k_x x + k_y y)}$ is periodic and bounded ($|e^{i(k_x x + k_y y)}| = 1$), k is the wave number, given by $k^2 = k_x^2 + k_y^2$ and λ is wavelength. Further details concerning linear stability can be found in Segel (1984) and Murray (1993). Substituting these values in system (1.7.11). The homogeneous equation in $x_1,\ x_2$ and x_3

have solution if determinant of the coefficient matrix is zero i.e.

$$\begin{vmatrix} -b_{11}+D_{x_1}k^2 & b_{12} & b_{13} \\ b_{21} & -b_{22}+D_{x_2}k^2 & b_{23} \\ b_{31} & b_{32} & -b_{33}+D_{x_3}k^2 \end{vmatrix} = 0, \tag{1.7.12}$$

or,

$$\lambda^3 + B_1\lambda^2 + B_2\lambda + B_3 = 0, \tag{1.7.13}$$

where,

$$\begin{aligned} B_1(k^2) &= k^2(D_{x_1}+D_{x_2}+D_{x_3}) + A_1, \\ B_2(k^2) &= k^4(D_{x_1}D_{x_2}+D_{x_1}D_{x_3}+D_{x_2}D_{x_3}) - k^2(D_{x_1}(b_{33}+b_{22}) + D_{x_2}(b_{11}+b_{33}) \\ &\quad +D_{x_3}(b_{11}+b_{22})) + A_2, \\ B_3(k^2) &= k^6(D_{x_1}D_{x_2}D_{x_3}) + k^4(-D_{x_1}D_{x_2}b_{33} - b_{22}D_{x_1}D_{x_3} - b_{11}D_{x_2}D_{x_3}) \\ &\quad +k^2(D_{x_1}(b_{33}b_{22}-b_{23}b_{32}) + D_{x_2}(b_{11}b_{33}-b_{13}b_{31}) + D_{x_3}(b_{11}b_{22}-b_{12}b_{21})) + A_3, \end{aligned}$$

where $A_1,\ A_2$ and A_3 are the coefficients of eqn. (1.7.10). For $\mathrm{Re}(\lambda) < 0,\ B_1 > 0,\ B_3 > 0$ and $B_1B_2 - B_3 > 0$ by Routh-Hurwitz criteria,
where, $B_1B_2 - B_3 = C_1k^6 + C_2k^4 + C_3k^2 + A_1A_2 - A_3$,
and,

$$\begin{aligned} C_1 &= (D_{x_1}+D_{x_2})(D_{x_1}+D_{x_3})(D_{x_2}+D_{x_3}) > 0, \\ C_2 &= -b_{11}(D_{x_2}+D_{x_3})(D_{x_2}+2D_{x_1}+D_{x_3}) - b_{22}(D_{x_1}+D_{x_3})(D_{x_1}+2D_{x_2}+D_{x_3}) \\ &\quad -b_{33}(D_{x_2}+D_{x_1})(D_{x_1}+2D_{x_3}+D_{x_2}), \\ C_3 &= (-(b_{22}+b_{33})A_1 + (b_{11}b_{22}-b_{12}b_{21}) - b_{31}b_{13} + b_{33}b_{11})D_{x_1} + (-(b_{11}+b_{33})A_1 \\ &\quad +(b_{11}b_{22}-b_{12}b_{21}) - b_{23}b_{32} + b_{33}b_{22})D_{x_2} + (-(b_{22}+b_{11})A_1 \\ &\quad +(b_{11}+b_{22})b_{33} - b_{23}b_{32} + b_{13}b_{31})D_{x_3}. \end{aligned}$$

1.7.10 Turing instability and pattern formation

A brilliant new idea was put out by Turing (1952) in his famous study, "The Chemical Basis of Morphogenesis." Turing proposed that a spatial pre-pattern in biochemicals, which he called morphogens, causes the patterns we see during embryonic development to emerge. Turing postulated that inhomogeneities in underlying biochemical signalling are what cause the patterns we observe in nature, such as animal colouring, tree branching, and skeletal architecture.

A spatially uniform population distribution that is stable against spatially uniform perturbations (or in the local model without diffusion) can be driven to diffusive instability against spatially heterogeneous perturbations, e.g., a population wave or local outbreak, for sufficient differences of diffusivity. Turing bifurcation occurs when the positive steady state E^* of a system is stable as a solution to the reaction system (without diffusion term) but unstable as a solution of the full reaction-diffusion system. This mechanism, known as diffusion driven instability, leads to pattern appearance. The positive constant E^* is unstable due to Turing instability provided that at least one eigenvalue of characteristic equation is positive.

Example 1.7.2 *Consider the prey-predator model, Huang et al. (2019) :*

$$\begin{aligned} \frac{\partial P_1}{\partial t} &= P_1(1-P_1) - \frac{aP_1P_2}{P_1+e_1} + \nabla^2 P_1, \\ \frac{\partial P_2}{\partial t} &= bP_2\left(1 - \frac{P_2}{P_1+e_2}\right) + \delta\nabla^2 P_1. \end{aligned}$$

where P_1 and P_2 represents the densities of prey and predator, respectively, and (x, y) is the spatial position of species in two dimensional space.

As a varies and other parameters are fixed $e_1 = 0.3,\ e_2 = 0.2,\ b = 0.1781$, and $\delta = 30$. See Fig. 1.3 for pattern evolution with different value of a.

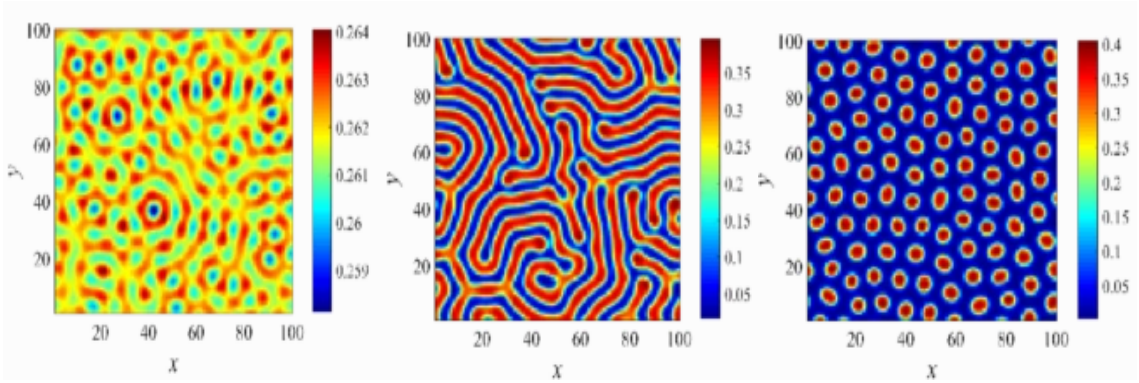

(a) $a = 0.898$ (b) $a = 1.05$ (c) $a = 1.35$

Figure 1.3: For various value of a, we see (a) a homogeneous pattern, (b) stripe pattern, (c) hot spot pattern; in space 100×100 and time $t = 10,000$.

1.7.11 Global stability of predator free equilibrium point

In this section, we give a brief description of the method developed by Castillo-Chavez et al. (2002) for the global stability analysis of the disease-free equilibrium. Now, we state

two conditions which guarantee the global stability of the predator-free state

$$\begin{aligned} \frac{dX_1}{dt} &= G(x_1, X_2), \\ \frac{dX_2}{dt} &= H(X_1, X_2),\ H(X_1, 0) = 0, \end{aligned} \tag{1.7.14}$$

where X_1 denotes the prey population, and X_2 denotes the predator population. The predator-free equilibrium is now denoted by $E(X_1^0, 0)$. The following condition (H1) and (H2) must be met to guarantee a local asymptotic stability:
(H1) For $\frac{dX_1}{dt} = G(X_1, 0)$, $E(X_1^0, 0)$ is globally asymptotically stable,
(H2) $H(X_1, X_2) = BX_2 - \hat{H}(X_1, X_2)$, where $\hat{H}(X_1, X_2) \geq 0,\ \forall (X_1, X_2) \in \Omega$,
where $B = D_Z H(X_1^0, 0)$ is an M-matrix if and only if every off-diagonal entry of B is non-positive and the diagonal entries are all positive and Ω is the region where the model makes biological sense. Then, the following lemma holds:

Lemma 1.7.3 *The fixed point $E(X_1^0, 0)$ is a globally asymptotic stable equilibrium of system (1.7.14) provided that $\mathscr{R}_0 < 1$ and that assumptions (H1) and (H2) are satisfied.*

1.8 Mathematical tool to solve stochastic differential equation

Consider a Stochastic Differential Equation

$$dY(t) = g(t)Y(t)dt + h(t)Y(t)dW(t), \tag{1.8.1}$$

In general,

$$dY(t, \omega) = g(t, Y(t, \omega))dt + h(t, Y(t, \omega))dW(t, \omega), \tag{1.8.2}$$

where $dW(t)$ is defined as differential form of the Brownian motion, and $dW(t) = \xi(t)dt$ and ξ denotes a white noise process. Here, $g(t, Y(t, \omega)),\ h(t, Y(t, \omega)),\ W(t, Y(t, \omega)) \in \mathbb{R}$. The integral form can be written as

$$Y(t, \omega) = Y_0 + \int_0^t g(s, Y(s, \omega))ds + \int_0^t h(s, Y(s, \omega))dW(s, \omega). \tag{1.8.3}$$

where a path-wise Riemann integral makes up the first integral, while an Itô integral makes up the second.
Giving a necessary and sufficient condition for the existence and singularity of strong

solutions is challenging. Usually, we are able to provide sufficient conditions.

1.8.1 Existence and uniqueness of the solution to SDE

1.8.1.1 Itô sufficient condition theorem for existence and uniqueness

Theorem 1.8.1 *Suppose $g : \mathbb{R} \longrightarrow \mathbb{R}$ and $h : \mathbb{R} \longrightarrow \mathbb{R}_+$, are uniformly Lipschitz, then there exist solution of stochastic differential equation (1.8.2). Also, there exists a unique adapted process called $Y(t) = Y(t)^y$ with continuous paths for any acceptable filtration $F = \{\mathcal{F}_t\}_{t\geq 0}$, any initial value $y(0) \in \mathbb{R}$, and any standard Brownian motion $\{W(t)\}_{t\geq 0}$. This unique process is given by*

$$Y(t) = y(0) + \int_0^t g(Y_s)ds + \int_0^t h(Y_s)dW(s) \qquad a.s.$$

Additionally, the two-parameter process $Y(t)^y$ is simultaneously continuous in t and $y(0)$, meaning that the solutions rely constantly on the initial data $y(0)$.

Now, a solution to this equation can be computed by using these three major methods

- **Analytic Approach**-Based on using Itô integral.
- **Numerical techniques**-For computing SDE's path-wise solutions.
- Finding the probability density function of the solution becomes a partial differential equation to be solved.

Talking about the second approach in this thesis, we will proceed further.

1.8.2 Numerical method: Euler-Maruyama scheme

After the name of Leonhard Euler and Gisiro Maruyama, the method known as Euler-Maruyama has been developed for the numerical approximation of a stochastic differential equation (system of stochastic differential equations), which is clearly an extension of the Euler method, used to approximate an ordinary differential equation.
For equation (1.8.2), with initial condition $Y(0) = y(0)$, the solution of SDE over time interval $[0, T]$. The Markov chain X defined below is the Euler-Maruyama approximation to the true solution Y:

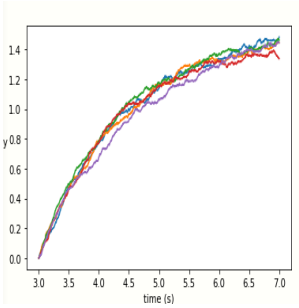

Figure 1.4: Graph showing five runs of Euler-Maruyama method for Ornstein-Uhlenbeck process.

- divide the range $[0, T]$ into N equally sized subranges of width $\Delta t > 0$:
  $0 = \tau_0 < \tau_1 < ... < \tau_N$ and $\Delta t = T/N$,
- declare $X_0 = y_0$,
- define X_n iteratively for $0 \leq n \leq N-1$ by
  $X_{n+1} = X_n + g(X_n, \tau_n)\Delta t + h(X_n, \tau_n)\Delta W_n$
  where, $\Delta W_n = W_{\tau_{n+1}} - W_{\tau_n}$.

The independent, identically distributed normal random variables ΔW_n have an expected value of zero and a variance of Δt.

Example 1.8.1 *Given Ornstein-Uhlenbeck process*

$$dY_t = \theta(\mu - Y_t)dt + \sigma dW_t, \quad Y_o = Y_{init}.$$

where $\theta > 0$ and $\sigma > 0$ are the parameters and μ is a constant. W_t denotes the Wiener process.
Solving it numerically by using Euler-Maruyaama Scheme by forming python code, the following graph(c.f. Fig. 1.4) is obtained.

1.9 Optimal control technique

In order to achieve a given purpose that is optimised over the time horizon under consideration, control theory seeks to construct a time dependent profile of a certain system parameter, referred to as the control variable. The main driving force behind the creation of control theory has been to address performance issues with engineering systems, such as mechanical, electrical, chemical, etc. Ecosystem management issues, for example, present an exciting opportunity to put some of the most cutting-edge control tactics into practise. Kolosov (1997), Kolosov and Sharov (1993), Silvert and Smith (1977), population manage-

ment through harvesting, treatment of water in lakes (Ludwig et al. (2003)), and forest fire management are a few instances of how control theory is used in ecosystem management (Richards et al. (1999); Anderson and Bare (1994)). Numerous species are currently going extinct every day due to the spread of various illnesses and severe competition among biological species. Because a species never regenerates, this represents a significant loss of biological resources. In addition to depriving humanity of a natural resource, the extinction of one species also results in the extinction of other populations via food chains. In order to safeguard population health and biodiversity while minimising the cost of prevention and control, setting up an optimal control problem for an ecological model that includes infection and competition will be beneficial.

The most sophisticated control strategies are those that focus on optimal control. The best control strategy for the specified objective function is theoretically provided by optimal control, which has some advantages above all other advanced control techniques in that it makes no assumptions about the shape of the control rule and can theoretically manage any sort of system. The theory includes the Hamilton-Jacobi-Bellman equation from dynamic programming, the Euler-Lagrange equation from calculus of variation, and Pontryagin's maximum principle as three potential methods for determining the best control law (Kirk (1970); Diwekar (2003)). Pontryagin's maximal principle has been applied in this work.

1.9.0.1 Pontryagin's Maximum Principle

Pontryagin's Maximum Principle (1961) (translated by Semenovich et al. (1962)) identifies a precondition that an optimal trajectory must satisfy. This principle works as follows:

Consider the differential equation system, (called state equations)

$$\dot{y} = g(y, u, t), \tag{1.9.1}$$

where, $y(t) \in \mathbb{R}^n_+$ is the state variable, with initial condition $y(t_0) = y_0$, $y(T)$ are final conditions and vector $u(t) \in \mathbb{R}^m$ is the control variable. Let the performance index which is dependent on time is represented as

$$J(t_0) = \int_{t_0}^{T} G(y(t), u(t), t)dt, \tag{1.9.2}$$

where, function G to be optimised over $[t_0, T]$. Convert this objective function into a

Hamiltonian as

$$H(y,u,t) = G(y,u,t) + \lambda' g(y,u,t), \tag{1.9.3}$$

where, λ is the set of adjoint variables in $\mathbb{R}^n$. Then, the solution of the set of equations: State equations:

$$\dot{y} = \frac{\partial H}{\partial \lambda} = g,\ t \geq t_0 \tag{1.9.4}$$

Adjoint equations:

$$-\dot{\lambda} = \frac{\partial H}{\partial y} = \frac{\partial g'}{\partial y}\lambda + \frac{\partial G}{\partial y},\ t \leq T \tag{1.9.5}$$

Optimality conditions:

$$0 = \frac{\partial H}{\partial u} = \frac{\partial G}{\partial u} + \frac{\partial g'}{\partial u}\lambda. \tag{1.9.6}$$

It is a boundary value problem with $2n$ differential equation and m algebraic equation. At initial time t_0, the state variables are known 'x_0', while at final time T, the adjoint variables are known $\lambda(T)$.

Example 1.9.1 (Optimal control for a prey-predator system) *Sadiq (2017), considered a prey-predator system*

$$\begin{aligned} \frac{dy_1}{dt} &= a_1 y_1^2 (1 - y_1) - b_1 y_1 y_2, \\ \frac{dy_2}{dt} &= -r_2 y_2 + a_2 y_1 y_2. \end{aligned} \tag{1.9.7}$$

where $y_1,\ y_2$ are prey and predator population density, respectively. All parameters $a_1,\ b_1,\ a_2,\ r_2$ are constants.

After imposing control variable for creating optimal control problem, system (1.9.7) becomes

$$\begin{aligned} \frac{dy_1}{dt} &= a_1 y_1^2 (1 - y_1) - b_1 y_1 y_2 + (1 - u(t)) y_2, \\ \frac{dy_2}{dt} &= -r_2 y_2 + a_2 y_1 y_2 - u(t) y_2. \end{aligned} \tag{1.9.8}$$

Here, $u(t)$ is the harvesting amount such that, $0 \leq u(t) \leq M < 1$, where M is the maximum

harvesting. The target functional here is given by

$$J(u(t)) = \int_0^T (c_1 u(t) + c_2 u^2(t))dt \tag{1.9.9}$$

where $c_1,\ c_2$ *are constants with state equations as (1.9.7) and* $y_1(0) = y_{1_0},\ y_2(0) = y_{2_0}$ *are the initial values.*

Objective: *To find the function* $u^*(t)$ *such that it minimize the target function* $J(u(t))$.

Procedure: *Define the Hamiltonian function* H *such that*

$$\begin{aligned} H(t, y_1(t), y_2(t), u(t)) &= c_1 y_2(t) + c_2 u^2(t) + \lambda_1[a_1 y_1^2(t)(1 - y_1(t)) - b_1 y_1(t) y_2(t) \\ &\quad + (1 - u(t)) y_2(t)] + \lambda_2(t)[-r_2 y_2(t) + a_2 y_1(t) y_2(t) - u(t) y_2(t)] \end{aligned}$$

where $\lambda_1,\ \lambda_2$ *are adjoint variables, that satisfy*

$$\begin{aligned} \frac{d\lambda_1(t)}{dt} &= \frac{\partial H(t)}{\partial y_1} = -\lambda_1(t)[2a_1 y_1(t) - 3a_2 y_1^2(t) - b_1 y_2(t)] - \lambda_2(t) a_2 y_2(t) \\ \frac{d\lambda_2(t)}{dt} &= -\frac{\partial H(t)}{\partial y_2} = -c_1 - \lambda_1(t)[-b_1 y_1(t) + (1 - u(t))] - \lambda_2(t)[-r_2 + a_2 y_1(t) - u(t)] \\ \lambda_1(T) &= \lambda_2(T) = 0, \quad \textit{(The Transversality conditions)} \end{aligned}$$

Then, by using the Pontryagin's maximum principle the optimal control $u^*(t)$ *is given by*

$$u^*(t) = \begin{cases} 0 & if \quad \frac{(\lambda_1+\lambda_2)y_2}{2c_2} \leq 0 \\ \frac{(\lambda_1+\lambda_2)y_2}{2c_2} & if \quad 0 < \frac{(\lambda_1+\lambda_2)y_2}{2c_2} < M \\ M & if \quad M < \frac{(\lambda_1+\lambda_2)y_2}{2c_2} \end{cases}$$

As we can see in Fig. 1.5, on introduction with optimal control the prey population increases while the predator population decreases, which is the main aim while forming Lotka-Voltera problem.

1.10 Motivation for research

This thesis is important since we are dealing the extinction problem of wildlife species. Saving endangered species (plants and animals) from becoming extinct and protecting their wild places is crucial for our health and the future of our children. As species are lost so too are our options for future discovery and advancement. The impacts of biodiversity loss include clearly fewer new medicines, greater vulnerability to natural disasters, and greater effects from global warming. The number of extinction and endangered species

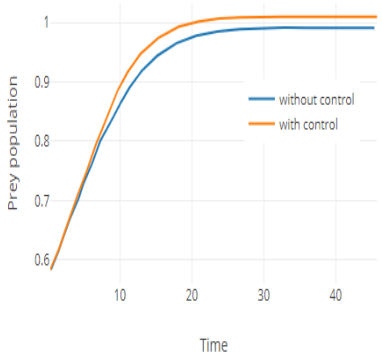

(a) Prey population with time

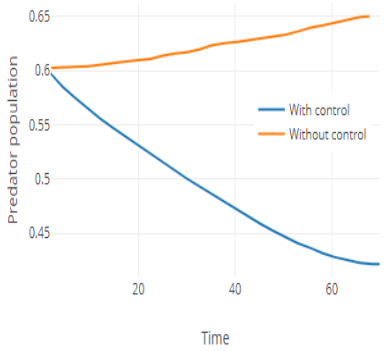

(b) Predator population with time

Figure 1.5: Plot with and without control; with parameters $a_1 = 15,\ r_2 = 0.2,\ a_2 = 0.3,\ b_1 = 0.1,\ c_1 = 0.5$ and $c_2 = 0.07$.

are growing but our understanding of the causes and dynamics of the extinction is still incomplete. This study is a small step towards understanding disease-induced extinction which has rarely been considered. Another important factor responsible for extinction and being ignored from a modeling point of view is climate change.

1.11 Methodology

1.11.1 Descriptive:

To achieve the objectives, firstly, we identified those species most in need and targeted conservation actions towards them. We searched hard for empirical examples of extinctions due to disease and co-extinctions and document them better when found. Next, we gathered biological, environmental, anthropogenic, and evolutionary information for the same species, focusing on variables potentially correlated to extinction risk. We then built a robust model with minimum assumptions and more reality. We have also developed different analytical and numerical schemes to solve mathematical models more accurately. The proposed work would also aim at devising a few new methods which could help researchers in mating a realistic choice of the values of parameters used in simulation experiments.

To investigate the Spatio-temporal dynamics of the proposed model system, we solved the proposed model numerically using the semi-implicit (in time) finite difference method or the finite element method. Through quantitative and qualitative analysis, sensitivity analysis, and numeric simulations, mathematical models have given us a good understanding of how prey-predator dynamics going, and at what rate species depleting, and that hence provides useful prevention and control strategies and guidance. The dissemination of thesis results is particularly directed toward conservation scientists and environmental decision-makers,

to raise awareness of the potential environmental risks associated with alternative policy decisions. By the end of the thesis, a policy piece will be prepared to discuss the relevance of the thesis findings for global biodiversity conservation. For methodology used while forming model and analysing dynamics, see Flow chart Figure 1.6.

1.12 Mathematical software

The numerical simulations in this thesis are done using the following software's:

A. MATLAB

The software MATLAB, which stands for MATrix LABoratory, is based on vectors and matrices. A high-performance language for technical computing is called MATLAB. In a simple-to-use interface, it mixes computation, visualisation, and programming while expressing issues and solutions using well-known mathematical notation. All branches of applied mathematics, academic study, and business all make extensive use of MATLAB. MATLAB offers robust graphic capabilities and can create appealing 2D and 3D images. We have generated space series, time series, two-dimensional snapshots, spatiotemporal patterns, chaotic attractors and bifurcation diagrams using MATLAB 8.1.0.

B. Mathematica

The only completely integrated environment for technical computing is Mathematica. It is a piece of symbolic mathematics-based computational software that is utilised in a variety of scientific, engineering, mathematical, and computing domains. Mathematica's programming language is called the Wolfram Language. Today, Mathematica is employed in all branches of science, including the physical, biological, social, and others, and it enjoys the passionate support of many of the top researchers in the world. Mathematica is currently a common development and production tool in engineering, and a large number of the most significant new products in the world today use it in some capacity during the design phase. Mathematica has been extensively utilised in many types of general planning and analysis as well as playing a vital part in the development of sophisticated financial modelling in commerce. With its language component being widely used as a research, prototyping, and interaction environment, Mathematica has also become a crucial tool in computer science and software development. We have done bifurcation analysis and calculated Jacobian matrix, eigenvalues, Lyapunov sprectrum using Mathematica 7.0.

1.13 Overview of thesis

This thesis consists of five chapters including an introductory chapter, with a particular focus on different assumptions and considering different types of modelling, different species can have. Chapter 2-4 investigate the complexity in designed ecological and eco-epidemiological systems. In chapter 5, summary and conclusions are presented.

In Chapter 2, We looked into the short-tailed scrub wallaby, an endangered species in south-western Australia. Quokkas are most at risk of being predated by certain more harmful species, according to the primary literature on the species (eg.- foxes, dingoes). As a result, we developed an ODE model for a tri-tropical food chain and mathematically examined it. After realising that space is crucial in developing dynamics, we upgraded our first tri-tropic food chain model (ODE) that includes quokka, fox, and dingoes. We then mathematically analysed these models (analytically and numerically).

We studied the Corroboree Frog, a tiny, brightly coloured species, in Chapter 3 on endangered amphibians that live in New South Wales' Kosciuszko National Park. We developed a model in which we discussed how zooplankton predation could lessen the impact of the fungus Batrachochytrium dendrobatidis, which causes Chytridiomycosis infection in frog populations. Also, high temperatures significantly reduce the risk of chytridiomycosis, hence it is important to take environmental stochasticity into account. We use white noise to account for the impact of a randomly fluctuating environment.

As the medium to large marine fish known as Atlantic cod (*Gadus morhua*), which lives in cold water, is thought to pose the greatest danger to biodiversity worldwide. We developed a model in Chapter 4 that takes into account the Allee effect, cannibalism, and overfishing as the main variables affecting cod density.

In Chapter 5, summary and conclusions of the thesis are presented. We also discuss some possible extensions of the present work as future directions.

At the end of the thesis, a detailed bibliography is given with all the references from the chapters.

It is important to remember that this theory is entirely speculative. These models are created with no data or explicit biological system in mind. This was done in an effort to offer general reasons that aid in locating significant and intriguing qualitative results and pinpointing the crucial variables.

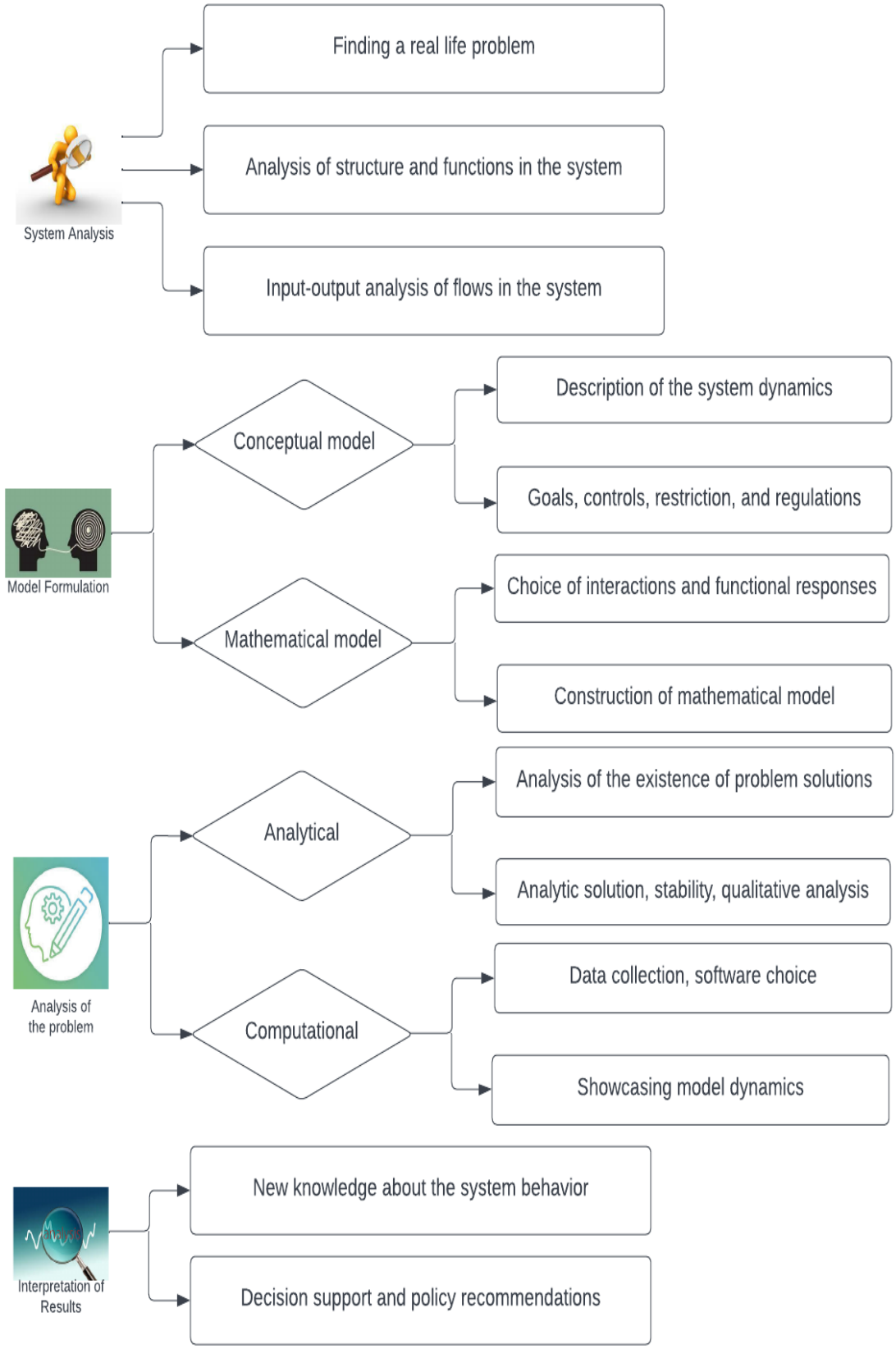

Figure 1.6: Flow chart of methodology adapted.

Chapter 2

UNTANGLING THE ROLE OF TRI-TROPHIC FOOD CHAIN MODEL IN SUSTAINING QUOKKA POPULATION

“ The world’s happiest wild animal is in danger.”

Content of this chapter has been published as:

- P. Roy, S. Jain, and M. Maama. Assessing the viability of tri-trophic food chain model in designing a conservation plan: The case of dwindling quokka population. Ecological Complexity, 41:100811, 2020, (Roy et al. (2020)).
- S. Jain and P. Roy. Investigating the role of zooplankton in sustaining frog population. Mathematical Methods in the Applied Sciences, 45(9):5423–5455, 2022, (Jain and Roy (2022)).

2.1 Introduction

The quokka (*Setonix brachyurus*) is a vulnerable, macropodid marsupial that is native to south-western Australia (Hayward (2002); Hayward et al. (2003); Hayward et al. (2004); Hayward et al. (2005)). On the mainland, quokkas live in smaller colonies. On Rottnest Island, they live in groups of up to 150 individuals. This species mainly feeds at night and rest during the day. They are herbivores and their diet comprises plants including shrubs, succulents, grasses, forbs and sedges. They also eat seeds, berries and other fruit if available. Quokka has a great economic significance for humans and is often referred to as "the happiest animal in the world". Despite the long term knowledge of the decline in the quokka on the mainland (White (1952)), important ecological research has not proceeded. The lack of available resources and the difficulty in locating and capturing animals (Sinclair and Morris (1996)), have hampered research conduction.

According to reports, quokka suffered a dramatic decline in the 1930s, particularly due the introduction of European red fox (*Vulpes vulpes*) (King and Smith (1985)). According to IUCN criteria it is now listed as a vulnerable species (Hayward (2002)). These animals are also predated by domesticated cats, dogs and dingoes. Historical and recent range contractions suggests that, factors other than fox predation have also contributed to the quokka's decline. The most obvious factors includes; change in the environment, the loss of habitat, habitat alteration and possibly by some disease (White (1952); Cook (1960); Hayward (2002)). Habitat loss has been mainly due to timber harvesting, frequent high intensity fires, changes in fire regimes (Burrows et al. (1995)), and urban development. These are likely to have negatively affected the distribution and size of quokka populations (Dickman (1996); Kinnear et al. (2002); May and Norton (1996)).

Mathematical modelling of extinction of wildlife is still a very interesting field of research. Mathematical modelling is a frequently evolving process. Mathematical analysis carried out in a planned way can often lead to better understanding of the food-chain model occurring in nature. In past few years, there has been a steady growth in the designing and studying of mathematical models of population interactions. In nature, when the prey population falls below a certain level, the predator searches for alternative prey and returns only when the prey population rises to the required level. Van Baalen et al. (2001) showed that switching from one prey species to alternative prey is beneficial for the persistence of the predator-prey system. The role of alternative food for biological pest control is examined by many researchers (González-Fernández et al. (2009);Sabelis et al. (2008)). Recently, Sahoo (2012) showed that additional food is very important for survival of consumer species in an ecosystem. In all the above-mentioned work, additional food

is not dynamic but maintained at a specific constant level either by nature or by some superficial factor. In this context, we have proposed a food chain model with one specialist predator and one generalist predator. Exploring in this direction will likely improve our understanding on the consequences of providing additional food, thereby bringing out an explicit link between practical biological control and theoretical studies.

The main objective of this chapter is to develop a realistic food chain model between quokka-fox-dingo and mathematically the system's dynamical properties and behaviors, which can be used to describe the extinction dynamics of the quokka population in Australia. Moreover, most food chain models tend to ignore or downplay local spatial dynamics and spatiotemporal spread of interacting species. The major drawback of these models is that they do not include local random movement, which can also affect the distribution of species. The reaction-diffusion model is considered an important contributing factor in detecting population concentration and clustering. The term diffusion describes the migration of species to avoid crowds produced by the population pressure due to the mutual interference among themselves. More generally, it implies the movement of individuals from a higher concentration region to a lower one. The designed model may or may not be free of all inconsistencies but the analysis of the current model can be expected to reveal important and nontrivial features of the tri-tropic food chain system consisting of a specialist and a generalist predator. This research will make a contribution to science, empowering the development of effective conservation management strategies for securing the quokkas and for assisting biodiversity managers. Some key questions explored in this work are as follows:

- Is it necessary to control foxes for the survival of quokka populations?,
- whether the presence of dingoes is beneficial for quokka populations? and,
- what is the effect of external harvesting on quokka population?.

We have also used the concept of reproduction number to derive threshold parameter ($\mathscr{R}_0$) in our tri-trophic food chain model, to suggest some recovery plans for quokka.

The outline of the chapter is as follows: In Section 2.2, the model is formulated. Section 2.3 contributes to the analysis of the non spatial model system including the boundedness of solutions, characteristics of possible equilibria, conditions under which the equilibria exist and are asymptotically stable. Section 2.4 is devoted to analysis of spatial model systems. Section 2.5 discusses the diffusion driven instability and pattern formation.In Section 2.6, threshold for persistence of species is evaluated. In Section 2.7, the numerical results are reported for both non-spatial and spatial models. In Section 2.8, we interpret our results in terms of their ecological implications.

2.2 Model formulation with and without movement of species

2.2.1 Without prey switching; Without movement of species

Hayward et al. (2007) predicted the occurrence of quokka population control and maintenance of a mosaic at early stage and long unburnt habitat are essential for its conservation. Schroeder et al. (2015) conducted an experimental behavioral study to examine whether foxes attempt to avoid areas with a high number of dingoes. They found that dingoes kill foxes opportunistically rather than through active hunting. Moseby et al. (2012) also performed a field experiment to investigate the interactions between a dingo and exotic mesopredators (cat and red fox) and provided evidence that dingoes may suppress foxes. However, no mathematical model is given so far to model these three species together. Motivated by these studies, we developed a tri-trophic ecological food-chain model with three species similar to Hastings and Powell (1991). The food-chain model includes one prey species (quokka), one mesopredator (red fox), and one apex predator (dingo). The quokka population (Q) is predated by a red fox (F), which in turn is predated by dingoes (D). The quokka population grows logistically. Holling type II responses have been frequently associated with specialist predation (Andersson and Erlinge (1977); Hansson and Henttonen (1985); Leeuwen et al. (2007)). In this research, we consider Holling type II functional response (Holling (1959)), for both quokka and red fox population. Since foxes and dingoes can prosper and grow on other factors too, we consider an additional growth rate which means these species will not completely die in absence of its favourite food (Coman et al. (1991); Fleming et al. (2012)). Dingoes compete aggressively with the red fox (Vulpes vulpes), which is invasive in Australia, and help to control red fox populations where both species overlap. Thus, dingoes may provide refuge areas for small mammals which are not their preferred food (Moseby et al. (2012)). Although, dingoes are large carnivores but our model assumes that they does not eat quokka. This assumption is based on the fact that dingoes mainly consume red fox , rabbits and small rodents (https://www.britannica.com/animal/dingomammal). With the above assumptions, we describe the following set of autonomous non-linear differential equations:

$$\begin{aligned}
\frac{dQ}{dt} &= rQ\left(1-\frac{Q}{K}\right)-\frac{b_1QF}{(Q+a)},\\
\frac{dF}{dt} &= r_2F+\frac{b_2QF}{(Q+a)}-\frac{\omega_1DF}{(F+c)}-d_3F,\\
\frac{dD}{dt} &= r_3D+\frac{\omega_2DF}{(F+c)}-d_3D.
\end{aligned} \tag{2.2.1}$$

Description of parameters are given in Table 2.1 and schematic diagram which explains the dynamics can be seen in Fig. 2.1.

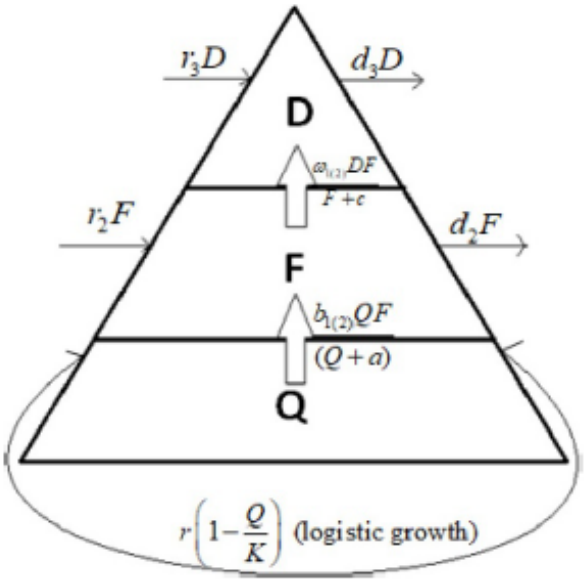

Figure 2.1: Schematic diagram for three species food model system (2.2.1).

Theorem 2.2.1 *If $N(t) = Q(t) + F(t) + D(t)$, then $N(t)$ is non negative and continuous.*

Further, $N < \left[\frac{(r+\eta)^2 K}{4r\eta}\right]$ for all t, where $\eta = min\{d_2 - r_2, d_3 - r_3\}$.

Proof We define a function
$N(t) = Q(t) + D(t) + F(t)$
The time derivative of this equation, along with system (2.2.1) becomes:

$$\begin{aligned}
\frac{dN}{dt} &= \frac{dQ}{dt} + \frac{dF}{dt} + \frac{dD}{dt}, \\
&< rQ\left(1 - \frac{Q}{K}\right) + (r_2 - d_2)F + (r_3 - d_3)D, \\
\frac{dN}{dt} + \eta N &\leq \left[r\left(1 - \frac{Q}{K}\right) + \eta\right]Q + (\eta - (d_2 - r_2))F + (\eta - (d_3 - r_3))D, \\
&\leq -\frac{r}{K}\left[Q - \left(\frac{r+\eta}{2r}K\right)\right]^2 + \frac{(r+\eta)^2 K}{4r}, \\
&\leq \frac{(r+\eta)^2 K}{4r}.
\end{aligned}$$

On integrating, we get

$$\begin{aligned} 0 &< N \leq \frac{(r+\eta)^2 K}{4r} + e^{-\eta t}\left[N(0) - \frac{(r+\eta)^2 K}{4r}\right]. \\ \text{As } t &\to \infty,\ 0 < N \leq \frac{(r+\eta)^2 K}{4r} \end{aligned}$$

Hence, the proof.

2.2.2 With prey switching; Without movement of species

Short et al. (2002) reported that the fox invasion in Australia threatened many native species, further this invasion was controlled by introducing dingoes. This food-chain model is the extension of model (2.2.1) and is more realistic and appropriate for modeling the realistic scenario. Here, we consider the quokka population (Q), is predated by both red fox (F) and dingoes (D), and foxes (F) in turn are predated by dingoes (D). This model takes up some assumptions for its formulation and is described in the following text. We considered dingoes as generalist predators who can switch its prey (quokka or fox) while fox behaves as specialist predator consuming quokka as its favourite food. The quokka population grows logistically. Functional relationship between predator and prey population are the central themes in mathematical ecology. In this model, we consider Holling type II functional response (Holling (1959)), which is associated with specialist predation for interaction between quokka and red fox population. However, dingoes are large carnivores and can eat quokkas when foxes are unavailable. In population dynamical studies, switching is usually modeled as a sigmoid i.e. Holling Type III (Holling (1959)), functional response. Modified Holling type II responses have also been frequently associated with generalist predation (Andersson and Erlinge (1977); Hansson and Henttonen (1985); Leeuwen et al. (2007)). We use the functional response given by Van Baalen et al. (2001), that is, per capita consumption rate of dingoes, with respect to quokka and foxes as $\frac{Q}{1+T_Q Q+pT_F F}$ and $\frac{pF}{1+T_Q Q+pT_F F}$ respectively. This response implies that the densities of prey (Q) and alternative food (F) are scaled with respect to the search rate of the predators. Here, p is the probability with which dingo will consume foxes upon encounter, T_Q is the handling time of a captured quokka and T_F is the time units for handling of alternative food items

i.e. foxes. With the above assumptions, the model can be formulated as follows:

$$\begin{aligned}
\frac{dQ}{dt} &= rQ\left(1-\frac{Q}{K}\right)-\frac{b_1QF}{Q+a}-\frac{e_1QD}{1+T_QQ+pT_FF}=Qh_1(Q,F,D),\\
\frac{dF}{dt} &= \frac{b_2QF}{Q+a}-\frac{\omega_1pDF}{1+T_QQ+pT_FF}-d_2F=Fh_2(Q,F,D),\\
\frac{dD}{dt} &= \frac{e_2QD}{1+T_QQ+pT_FF}+\frac{\omega_2pDF}{1+T_QQ+pT_FF}-d_3D=Dh_3(Q,F,D), \qquad (2.2.2)
\end{aligned}$$

with initial conditions $Q(0)>0, F(0)>0$ and $D(0)>0$. The model parameters $r, K, b_1, a, e_1, T_Q, p, T_F, b_2,\ \omega_1, d_2, e_2, \omega_2, d_3$ are all positive constants. The schematic diagram for model system (2.2.2) is presented in Fig. 2.2. Also, see Table 2.1 for complete description of parameter values for the considered food chain model.

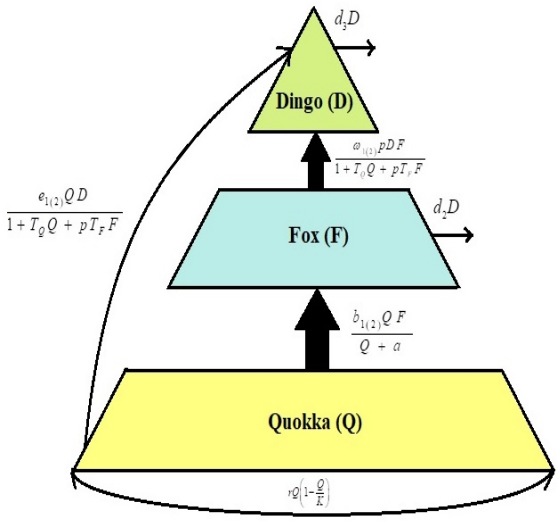

Figure 2.2: Schematic diagram for three species food model system (2.2.2).

Theorem 2.2.2 *If $U(t)=Q(t)+F(t)+D(t)$, then $U(t)$ is non negative and continuous. Further,*

$$U \le \left[\frac{(r+\gamma)^2K}{4r\gamma}\right] \text{ for all } t, \text{ where } \gamma = min\{d_2, d_3\}.$$

Proof As $U(T) = Q(T) + F(T) + D(T)$, taking time derivative we get

$$\begin{aligned}
\frac{dU}{dt} &= \frac{dQ}{dt} + \frac{dF}{dt} + \frac{dD}{dt}, \\
&= rQ\left(1 - \frac{Q}{K}\right) - (b_1 - b_2)\frac{QF}{Q+a} - (\omega_1 - \omega_2)\frac{pDF}{1 + T_Q Q + pT_F F} \\
&\quad -(e_1 - e_2)\frac{QD}{1 + T_Q Q + pT_F F} - d_2 F - d_3 D, \\
&< rQ\left(1 - \frac{Q}{K}\right) - d_2 F - d_3 D. \qquad (\text{as } b_1 > b_2, \omega_1 > \omega_2, e_1 > e_2)
\end{aligned}$$

Further,

$$\frac{dU}{dt} + \gamma U < rQ\left(1 - \frac{Q}{K}\right) + \gamma Q + (\gamma - d_2)F + (\gamma - d_3)D,$$

where, $\gamma = \min\{d_2, d_3\}$.
Proceeding as above theorem we obtain,

$$0 < U \leq \left[\frac{(r+\gamma)^2 K}{4r\gamma}\right] = M, t \to \infty. \tag{2.2.3}$$

Moreover, for a suitable M independent of the initial conditions, we have $\lim_{t\to\infty} sup\, U(t) \leq M$. Thus, $U(T) = Q(T) + F(T) + D(T) \leq M$, hence all the species are uniformly bounded for any initial value in $\mathbb{R}^3_+$.

For a biologically practical system, all population are required to be constrained by a bound in time by their environments.

2.2.3 With prey switching; With movement of species

Spatial component of ecological interactions has been identified as an important factor of how the ecological communities are shaped. Very little attention has been paid so far to study the spatial three species ecological model. We introduce spatial variations to the model system (2.2.2) to proceed further. We assume all populations in the food-chain perform active movement in 2-dimensional space (x and y direction). Animals moves randomly because of various requirements like, finding food, better opportunity for social interactions etc. (Okubo and Levin (2001)). If all are confined to a fixed bounded domain

Ω in $\mathbb{R}^2_+$, we led to consider the following reaction-diffusion system:

$$\begin{aligned}
\frac{\partial Q}{\partial t} - H_Q \nabla^2 Q &= Q(z,t) h_1(Q(z,t), F(z,t), D(z,t)), \\
\frac{\partial F}{\partial t} - H_F \nabla^2 F &= F(z,t) h_2(Q(z,t), F(z,t), D(z,t)), \\
\frac{\partial D}{\partial t} - H_D \nabla^2 D &= D(z,t) h_3(Q(z,t), F(z,t), D(z,t)),
\end{aligned} \tag{2.2.4}$$

for $z = (x, y) \in \Omega = [0, L] \times [0, L]$, $t > 0$, and with boundary conditions:

$$(\mathbf{n}.\nabla)Q = (\mathbf{n}.\nabla)F = (\mathbf{n}.\nabla)D = 0,$$

and initial conditions:

$$\begin{aligned}
Q(z,0) &= Q(0) > 0, \\
F(z,0) &= F(0) > 0, \\
D(z,0) &= D(0) > 0.
\end{aligned}$$

In system (2.2.4), ∇^2 represents Laplacian operator and the functions $h_i (i = 1, 2, 3)$ are continuous interaction functions, having continuous partial derivatives on $\mathbb{R}^3_+$. In the above, the vector $\mathbf{n}$ is an outward unit normal vector to the boundary $(\partial\Omega)$ of the habitat (Ω) and the homogeneous Neumann boundary conditions are considered. The homogeneous Neumann boundary conditions signify that the system is self-contained and there is no population flux across the boundary $(\partial\Omega)$.

Lemma 2.2.3 *Assume $u(z,t)$ is a solution of the problem*

$$\frac{\partial u}{\partial t} = d_1 \Delta u + u\,(a - bu)\,, z \in \Omega, t > 0, a > 0, b > 0$$
$$\frac{\partial u}{\partial \eta} = 0,$$
$$u(z,0) = u_0(z) > 0,$$
then $\lim_{t\to\infty} u(z,t) = \frac{a}{b}$.

Lemma 2.2.4 *If* $b_2 \leq \frac{d_2}{K}$, *the solution of system satisfies*

$$\limsup_{t\to\infty} \max_{z\in\bar{\Omega}} Q(z,t) \leq K =: Q_{max},$$

$$\limsup_{t\to\infty} \max_{z\in\bar{\Omega}} F(z,t) \leq \frac{b_2K + b_2T_QK^2}{pT_F(d_2 - b_2K)} =: F_{max},$$
$$\limsup_{t\to\infty} \max_{z\in\bar{\Omega}} D(z,t) \leq \frac{e_2K + \omega_2 p(b_2K + b_2T_QK^2)}{\omega_1\omega_2 p^2} =: D_{max}.$$

Proof From first equation of (2.2.4), we have,

$$\frac{\partial Q}{\partial t} \leq H_Q\nabla^2 Q + rQ\left(1 - \frac{Q}{K}\right), \tag{2.2.5}$$

on comparing the solution of problem with above lemma. Hence, for an arbitrary $\epsilon > 0$ there exist $T \in (0,\infty)$ such that $Q(z,t) \leq K + \epsilon$ for $(z,t) \in \Omega \times [T,\infty)$.
Now, from second equation of (2.2.4) and using (2.2.5) we have,

$$\begin{aligned}
\frac{\partial F}{\partial t} &\leq H_F\nabla^2 F + \frac{(b_2QF - d_2F)(1 + T_QQ + pT_FF) - \omega_1 pDF}{(1 + T_QQ + pT_FF)},\\
&\leq H_F\nabla^2 F + (b_2QF - d_2F)(1 + T_QQ + pT_FF) - \omega_1 pDF,\\
&\leq H_F\nabla^2 F + F(b_2Q + b_2T_QQ^2 + pb_2T_FQF - pd_2T_FF - \omega_1 pD),\\
&\leq H_F\nabla^2 F + F(b_2K + b_2T_QK^2 - \omega_1 pD + pb_2T_FKF - pd_2T_FF),\\
&= H_F\nabla^2 F + F((b_2K + b_2T_QK^2 - \omega_1 pD) - (pd_2T_F - pb_2T_FK)F).
\end{aligned}$$

Using lemma 2.2.3,

$$\Rightarrow \limsup_{t\to\infty} \max_{z\in\bar{\Omega}} F(z,t) \leq \frac{b_2K + b_2T_QK^2 - \omega_1 pD}{pT_F(d_2 - b_2K)}. \tag{2.2.6}$$

Also,

$$\Rightarrow \limsup_{t\to\infty} \max_{z\in\bar{\Omega}} F(z,t) \leq \frac{b_2K(1 + T_QK)}{pT_F(d_2 - b_2K)}.$$

Finally, from third equation of (2.2.4) and using (2.2.5) and (2.2.6), we have,

$$\begin{aligned}
\frac{\partial D}{\partial t} &\leq H_D\nabla^2 D + e_2QD + \omega_2 pDF,\\
&\leq H_D\nabla^2 D + e_2KD + \omega_2 pD\left(\frac{b_2K + b_2T_QK^2 - \omega_1 pD}{pT_F(d_2 - b_2K)}\right),\\
&\leq H_D\nabla^2 D + D(e_2K + \omega_2 pb_2K(1 + T_QK) - \omega_1\omega_2 p^2 D),
\end{aligned}$$

$$\Rightarrow \limsup_{t\to\infty} \max_{z\in\bar{\Omega}} D(z,t) \leq \frac{e_2K + \omega_2 pb_2K(1 + T_QK)}{\omega_1\omega_2 p^2}. \tag{2.2.7}$$

and hence the proof.

This theorem gives the sufficient conditions for which all the three species are individually bounded i.e. their count can't go beyond certain values if some conditions are satisfied.

Lemma 2.2.5 *The spatio-temporal system persists, if the following conditions hold:*

$$r > D_{max}e_1 + b_1F_{max},\ a < \frac{-D_{max}e_1 - b_1F_{max} + r}{r},\ K < \frac{D_{max}e_1 + b_1F_{max} - r + ar}{D_{max}e_1 + b_1F_{max} - r},$$

$$\frac{d_2(D_{max}e_1K + b_1F_{max}K - (a+K)r)}{K(D_{max}e_1 + b_1F_{max} - r)} < b_2 < \frac{d_2}{K},\ d_3 \leq \frac{e_2K(-D_{max}e_1 - b_1F_{max} + r)}{r(1 + F_{max}pT_F + KT_Q)},$$

$$d \leq \frac{b_2K}{p\omega_1},\ \textit{and}\ \omega_1 < \frac{(b_2 - d_2)(D_{max}e_1 + b_1F_{max})K + (-b_2K + d_2(a+K))r}{D_{max}p(D_{max}e_1K + b_1F_{max}K - (a+K)r)}.$$

Proof From (2.2.4), we have

$$\frac{\partial Q}{\partial t} \geq \left(r\left(1 - \frac{Q}{K}\right) - b_1F_{\max} - e_1D_{\max}\right)Q.$$

Using lemma, we get

$$\Rightarrow \liminf_{t\to\infty} \min_{z\in\Omega} \mathrm{Q(z,t)} \geq \frac{K(r - b_1F_{\max} - e_1D_{\max})}{r} =: Q_{min}.$$

Also from (2.2.4), we have

$$\begin{aligned}
\frac{\partial F}{\partial t} &\geq H_F\nabla^2F + \left(\frac{b_2Q_{\min}}{Q_{\min} + a} - \frac{\omega_1pD}{1 + pT_FF} - d_2\right)F, \\
&\geq H_F\nabla^2F + \left(\frac{(\Lambda - d_2)\,(1 + pT_FF) - \omega_1pD}{(1 + pT_FF)}\right)F,\ \text{where } \Lambda = \frac{b_2Q_{\min}}{Q_{\min} + a} \\
&\geq H_F\nabla^2F + \left(\frac{(\Lambda - d_2 - \omega_1pD) - (d_2 - \Lambda)pT_FF}{1 + pT_FF_{\max}}\right)F, \\
&\quad \text{provided } (\Lambda - d_2 - \omega_1pD) > (d_2 - \Lambda)pT_FF.
\end{aligned}$$

Using lemma, we get

$$\Rightarrow \liminf_{t\to\infty} \min_{z\in\Omega} \mathrm{F(z,t)} \geq \left(\frac{(\Lambda - d_2 - \omega_1pD)}{(d_2 - \Lambda)pT_F}\right) =: F_{\min}. \tag{2.2.8}$$

Also,

$$\Rightarrow \liminf_{t\to\infty} \min_{z\in\Omega} \mathrm{F(z,t)} \geq \left(\frac{(\Lambda - d_2 - \omega_1 p D_{\max})}{(d_2 - \Lambda) p T_F} \right).$$

Now, from (2.2.4) and using (2.2.8), we have

$$\begin{aligned} \frac{\partial D}{\partial t} &\geq H_D \nabla^2 D + \left(\frac{e_2 Q_{\min} + \omega_2 p F_{\min}}{(1 + T_Q Q_{\max} + p T_F F_{\max})} - d_3 \right) D, \\ &\geq H_D \nabla^2 D + \left(\frac{(e_2 Q_{\min} T_F - \omega_2 - d_3 T_F R)}{R T_F} - \frac{\omega_1 \omega_2 p D}{(d_2 - \Lambda) R T_F} \right) D. \\ &\quad \text{where} \quad R = (1 + T_Q Q_{\max} + p T_F F_{\max}) \end{aligned}$$

Using lemma, we get

$$\Rightarrow \liminf_{t\to\infty} \min_{z\in\Omega} \mathrm{D(z,t)} \geq \left(\frac{(e_2 Q_{\min} T_F - \omega_2 - d_3 T_F R)\,(d_2 - \Lambda)}{\omega_1 \omega_2 p} \right) =: D_{min}.$$

Remark 2 *Biologically, if the given conditions hold true then all the three species survive, no matter what the initial population are.*

2.3 Stability analysis of model system

2.3.1 Without prey switching; Without movement of species

2.3.1.1 Existence of equilibrium points

The Jacobian matrix corresponding to model (2.2.1)

$$\mathscr{J}(Q,F,D) = \begin{pmatrix} a_{11} & a_{12} & a_{13} \\ a_{21} & a_{22} & a_{23} \\ a_{31} & a_{32} & a_{33} \end{pmatrix} \tag{2.3.1}$$

The entries of matrix are:

$$\begin{aligned} a_{11} &= \frac{b_1 F Q}{(a+Q)^2} - \frac{b_1 F^*}{a+Q} - \frac{Qr}{K+} + \left(1 - \frac{Q}{K}\right) r, \\ a_{12} &= -\frac{b_1 Q}{a+Q}, \\ a_{13} &= 0, \\ a_{21} &= -\frac{b_2 F Q}{(a+Q)^2} + \frac{b_2 F}{a+Q}, \end{aligned}$$

Table 2.1: Description of parameter values used in model (2.2.2).

Variables/parameters	Unit	Description
Q	Quokka per unit area	Density of quokka population
F	Red fox per unit area	Density of red fox population
D	Dingoes per unit area	Density of dingo population
r	Per day	Intrinsic growth rate of quokka popultion
r_2	Per day	Intrinsic growth rate of red fox
r_3	Per day	Intrinsic growth rate of dingo
K	Quokka per unit area	Carrying capacity of environment
a/c	Per unit area	Measures of the extent to which environment provides refuges to quokka/red fox population,thus decreasing the maximum predation rate
b_1	Per day	Contact rate of quokka and fox
b_2	Per day	Biomass conversion rate of quokka to fox
e_1	Per day	Contact rate of quokka and dingo
e_2	Per day	Biomass conversion rate of quokka to dingo
ω_1	Per day	Contact rate of fox and dingo
ω_2	Per day	Biomass conversion rate of fox to dingo
d_2	Per day	Death rate of fox
d_3	Per day	Death rate of dingo
T_Q	dimensionless	Handling time of a captured quokka by dingo
T_F	dimensionless	Handing time of foxes by dingo
p	dimensionless	Probability that dingo will consumes an alternative food item upon encounter to quokka
H_Q	Per unit area	Diffusion rate of quokka
H_F	Per unit area	Diffusion rate of fox
H_D	Per unit area	Diffusion rate of dingo

$$
\begin{aligned}
a_{22} &= \frac{b_2 Q}{a+Q} + r_2 + \frac{DF\omega_1}{(c+F)^2} - \frac{D\omega_1}{c+F} - d_2, \\
a_{23} &= \frac{F\omega_1}{c+F} \\
a_{31} &= 0, \\
a_{32} &= \frac{DF\omega_2}{(c+F)^2} + \frac{D\omega_2}{c+F}, \\
a_{33} &= r_3 + \frac{F\omega_2}{c+F} - d_3.
\end{aligned}
$$

Lemma 2.3.1 *The formulated model (2.2.2) has following possible equilibrium points:*

- *The equilibrium point,* $E_1 = (0,\ 0,\ 0)$ *, always exists.*
- *The equilibrium point,* $E_2 = (Q_2, 0, 0) = (K, 0, 0)$*, always exists.*
- *The equilibrium* $E_3 = (0, F_3, D_3) = \left(0, \frac{c(r_3 - d_3)}{d_3 - r_3 - \omega_2}, \frac{c(r_2 - d_2)\omega_2}{\omega_1(r_3 + \omega_2 - d_)}\right)$*, exists if* $d_2 < r_2$ *and* $r_3 < d_3 < \omega_2 + r_3$.
- *The equilibrium* $E_4 = (Q_4, F_4, 0) = \left(\frac{a(d_2 - r_3)}{b_2 - d_2 + r_2}, \frac{ab_2 r(b_2 k - (a+K)(d_2 - r_2))}{b_1 K(b_2 - d_@ + r_2)^2}, 0\right)$*, exists if* $d_2 - b_2 < r_2 < d_2$ *and* $a < \frac{K(b_2 - d_2 + r_2)}{d_2 - r_2}$.
- *The equilibrium* $E_5 = (Q_5, F_5, D_5)$

$$
\begin{aligned}
Q_5 &= \frac{1}{2}\left(-a + K + \frac{\sqrt{s}}{r(r_3 + \omega_2 - d_3)}\right), \\
F_5 &= \frac{c(d_3 - r_3)}{r_3 + \omega_2 - d_3}, \\
D_5 &= \frac{\omega_2(-2b_1 cK(b_2 - d_2 + r_2)(d_3 - r_3) + ab_2(-(a+K)r(d_3 - r_3 - \omega_2) - \sqrt{s}))}{2b_1 K(d_3 - r_3)\omega_1(d_3 - r_3 - \omega_2)}, \\
s &= r(4b_1 cK(d_3 - r_3)(d_3 - r_3 - \omega_2) + (a+K)^2 r(r_3 + \omega_2 - d_3)^2),
\end{aligned}
$$

exists if $a < K,\ r_3 < d_3 < \omega_2 + r_3, `b_1 < \frac{a}{2Kc(d_3 - r_3)}$,
$b_2 < \frac{2Kb_1 c(d_3(d_2 - r_2) + r_3(r_2 - d_2))}{2Kb_1 c(d_3 - r_3) - a}$ *and*
$\frac{4b_1 cK(r_3 - d_3)}{(a+K)^2(d_3 - r_3 - \omega_2)} \le r \le \frac{b_1 c(r_3 - d_3)}{a(d_3 - r_3 - \omega_2)}$.

2.3.1.2 Local stability analysis of equilibrium points

Theorem 2.3.2 *The equilibrium point* E_1 *is always unstable.*

Proof Since, the eigenvalues of Jacobian matrix (3.3.2) corresponding to E_1 are $r, r_2 - d_2$ and $r_3 - d_3$. Since, one of the eigenvalue (r) is always positive, thus the equilibrium point E_1 is always unstable. Biologically, it means that system will never settle to species-less in long run.

Theorem 2.3.3 *The equilibrium point E_2 is asymptotically stable if $r_3 < d_3,\ r_2 < d_2$ and $b_2 \leq d_2 - r_2$.*

Proof Since, the eigenvalues of Jacobian matrix (3.3.2) corresponding to E_2 are $-r,\ r_2 - d_2 + \dfrac{b_2 K}{a+K}$ and $r_3 - d_3$. Hence, the equilibrium is asymptotically stable if $r_3 < d_3,\ r_2 < d$ and $b_2 \leq d_2 - r_2$.

Theorem 2.3.4 *The equilibrium point E_3 is unstable always.*

Proof Since, the eigenvalues of Jacobian matrix (3.3.2) corresponding to E_3 are $r - \dfrac{b_1 c(d_3 - r_3)}{a(r_3 + \omega_2 - d_3)}$, $\dfrac{-(d_2 - r_2)(d_3 - r_3) + \sqrt{(d_3 - r_3)(d_2 - r_2)((d_2 - r_2)(d_3 - r_3) + 4(r_3 - d_3)\omega_2 + 4\omega^2)}}{2\omega_2}$ and $\dfrac{-(d_2 - r_2)(d_3 - r_3) - \sqrt{(d_3 - r_3)(d_2 - r_2)((d_2 - r_2)(d_3 - r_3) + 4(r_3 - d_3)\omega_2 + 4\omega^2)}}{2\omega_2}$. It can be verified that whenever equilibrium point E_3 exists, all the eigenvalues cannot be negative simultaneously. Therefore, the equilibrium point E_3 is unstable.

Theorem 2.3.5 *The equilibrium point E_4 is asymptotically stable if*
$d_2 > r_2,\ b_2 > d_2 - r_2,\ \dfrac{K(b_2 - d_2 + r_2)}{b_2 + d_2 - r_2} < a < \dfrac{K(b_2 - d_2 + r_2)}{d_2 - r_2}$,
$r > \dfrac{4b_2 K(b_2 K - (a+K)(d_2 - r_2))(b_2 - d_2 + r_2)^2}{(d_2 - r_2)(a(b_2 + d_2 - r_2) - K(b_2 - d_2 + r_2))^2}$ *and*
$d_3 > \dfrac{-b_1 cK(b_2 - d_2 + r_2)^2 r_3 + ab_2 r((a+K)(d_2 - r_2) - b_2 K)(r_3 + \omega_2)}{ab_2 r((a+K)(d_2 - r_2) - b_2 K) - b_1 cK(b_2 - d_2 + r_2)^2}$

Proof Since, the eigenvalues of Jacobian matrix (3.3.2) corresponding to E_4 are $r_3 + \dfrac{ab_2 r((a+K)(d_2 - r_2) - b_2 K)\omega_2}{ab_2 r((a+K)(d_2 - r_2) - b_2 K) - b_1 cK(b_2 - d_2 + r_2)^2}$, $\dfrac{-p_1 \pm \sqrt{q_1}}{2s_1}$. where, $p_1 = r(d_2 - r_2)(a(b_2 + d_2 - r_2) - K(b_2 - d_2 + r_2)),\ q_1 = r(d_2 - r_2)(4b_2 K(-b_2 K + (a+K)(d_2 - r_2))(b_2 - d_2 + r_2)^2 + r(d_2 - r_2)(a(b_2 + d_2 - r_2) - K(b_2 - d_2 + r_2))^2),\ s_1 = b_2 K(b_2 - d_2 + r_2)$. Hence, the equilibrium point is asymptotically stable if above conditions are satisfied.

Theorem 2.3.6 *The equilibrium point E_5 is asymptotically stable if*

$A_0 > 0,\ A_2 > 0$ *and* $A_2A_1 > A_0$ *where*

$$\begin{aligned}
A_0 &= \frac{1}{K(c+F_5)^2(a+Q_5)^2}(Kb_1F_5(2d_2d_3Q_5(c+F_5)^2 + a(d_3-r_3)((c+F_5)^2(d_2-r_2) \\
&\quad +cD_5\omega_1) - aF_5(c+F_5)(d_2-r_2)\omega_2) - r(K-2Q_5)(a+Q_5)(a(d_3-r_3)((c+F_5)^2 \\
&\quad (d_2-r_2)+cD_5\omega_1) - aF_5(d_2-r_2)\omega_2 + Q_5((d_3-r_3)(cD_5\omega_1 - (c+F_5)^2 \\
&\quad (b_2-d_2+r_2)) + F_5(c+F_5)(b_2-d_2+r_2)\omega_2))), \\
A_1 &= -\frac{b_2d_3Q_5}{a+Q_5} - d_3r + \frac{2d_3Q_5r}{K} + \frac{b_2rQ_5}{a+Q_5} - \frac{2b_2rQ_5^2}{K(a+Q_5)} - d_3r_2 + rr_2 - \frac{2Q_5rr_2}{K} \\
&\quad +\frac{b_2rr_3}{a+Q_5} + rr_3 - \frac{2Q_5rr_3}{K} + r_2r_3 - \frac{d_3\omega_1D_5F_5}{(c+F_5)^2} + \frac{\omega_1d_3D_5}{c+F_5} + \frac{r\omega_1d_3F_5}{(c+F_5)^2} - \frac{r\omega_1D_5}{c+F_5} \\
&\quad -\frac{2r\omega_1Q_5F_5D_5}{(c+F_5)^2K} + \frac{2r\omega_1Q_5D_5}{(c+F_5)K} + \frac{r_3\omega_1D_5F_5}{(c+F_5)^2} - \frac{r_3\omega_1D_5}{c+F_5} + \frac{b_2\omega_2Q_5F_5}{(c+F_5)(a+Q_5)} \\
&\quad +\frac{r\omega_2F_5}{c+F_5} - \frac{2r\omega_2Q_5F_5}{(c+F_5)K} + \frac{r_2\omega_2F_5}{c+F_5} + d_2\left(d_3 + \frac{ab_1F_5}{(a+Q_5)^2} - r + \frac{2rQ_5}{K} - r_3 - \frac{\omega_2F_4}{c+F_4}\right) \\
&\quad +\frac{ab_1F_5(c^2(d_3-r_2-r_3)+F_5^2(d_3-r_2-r_3-\omega_2))}{(c+F_5)^2(a+Q_5)^2} \\
&\quad +\frac{ab_1F_5(c(2d_3F_5+d\omega_1-F_5(2(r_2+r_3)+\omega_2)))}{(c+F_5)^2(a+Q_5)^2},
\end{aligned}$$

and,

$$A_2 = d_2 + d_3 + \frac{ab_1F_5}{(a+Q_5)^2} - \frac{b_2Q_5}{a+Q_5} - r + \frac{2rQ_5}{K} - r_2 - r_3 + \frac{c\omega_1D_5 - \omega_2(c+F_5)F_5}{(c+F_5)^2}$$

Proof Since, the characteristic polynomial of Jacobian matrix (3.3.2), corresponding to E_5 is given by
$P(x) = x^3 + A_2x^2 + A_1x + A_0$ (where $A_0,\ A_1$ and A_2 are defined above)
Now, by Routh-Hurwitz criteria if $A_0 > 0,\ A_2 > 0$ and $A_2A_1 > A_0$, then all the real parts of eigenvalues are negative and hence, E_5 becomes locally asymptotically stable.

2.3.2 With prey switching; Without movement of species

2.3.2.1 Existence of equilibrium points

The Jacobian matrix corresponding to model (2.2.2) is

$$\mathcal{J}(Q,F,D) = \begin{pmatrix} a_{11} & a_{12} & a_{13} \\ a_{21} & a_{22} & a_{23} \\ a_{31} & a_{32} & a_{33} \end{pmatrix} \tag{2.3.2}$$

The entries of matrix are:

$$
\begin{aligned}
a_{11} &= -\frac{a\mathrm{b}_1 F}{(a+Q)^2} + r - \frac{2Qr}{K} - \frac{D\mathrm{e}_1(1+Fp\mathrm{T_F})}{(1+Fp\mathrm{T_F}+Q\mathrm{T_Q})^2},\\
a_{12} &= -\frac{\mathrm{b}_1 Q}{a+Q} + \frac{D\mathrm{e}_1 pQ\mathrm{T_F}}{(1+Fp\mathrm{T_F}+Q\mathrm{T_Q})^2},\\
a_{13} &= -\frac{\mathrm{e}_1 Q}{1+Fp\mathrm{T_F}+Q\mathrm{T_Q}},\\
a_{21} &= F\Big(\frac{a\mathrm{b}_2}{(a+Q)^2} + \frac{Dp\mathrm{T_Q}\omega_1}{(1+Fp\mathrm{T_F}+Q\mathrm{T_Q})^2}\Big),\\
a_{22} &= -\mathrm{d}_2 + \frac{\mathrm{b}_2 Q}{a+Q} - \frac{Dp(1+Q\mathrm{T_Q})\omega_1}{(1+Fp\mathrm{T_F}+Q\mathrm{T_Q})^2},\\
a_{23} &= -\frac{Fp\omega_1}{1+Fp\mathrm{T_F}+Q\mathrm{T_Q}},\\
a_{31} &= \frac{D(\mathrm{e}_2 + \mathrm{e}_2 Fp\mathrm{T_F} - Fp\mathrm{T_Q}\omega_2)}{(1+Fp\mathrm{T_F}+Q\mathrm{T_Q})^2},\\
a_{32} &= \frac{Dp(-\mathrm{e}_2 Q\mathrm{T_F} + \omega_2 + Q\mathrm{T_Q}\omega_2)}{(1+Fp\mathrm{T_F}+Q\mathrm{T_Q})^2},\\
a_{33} &= 0.
\end{aligned}
$$

Lemma 2.3.7 *The formulated model (2.2.2) has following possible equilibrium points:*

- *The equilibrium point,* $E_1 = (0,\ 0,\ 0)$ *, always exists.*
- *The equilibrium point,* $E_2 = (Q_2, 0, 0) = (K, 0, 0)$*, always exists.*
- *The equilibrium* $E_3 = (Q_3, 0, D_3) = \left(\dfrac{d_3}{e_2 - d_3 T_Q}, 0, \dfrac{e_2 r\,(-d_3 + e_2 K - d_3 K T_Q)}{e_1 K\,(e_2 - d_3 T_Q)^2}\right)$*, exists if* $d_3 < \dfrac{e_2}{T_Q}$ *and* $K > \dfrac{d_3}{e_2 - d_3 T_Q}$.
- *The equilibrium* $E_4 = (Q_4, F_4, 0) = \left(\dfrac{ad_2}{b_2 - d_2}, \dfrac{ab_2(-ad_2 + b_2 K - d_2 K)r}{b_1 (b_2 - d_2)^2 K}, 0\right)$*, exists if* $b_2 > d_2$ *and* $a < \dfrac{(b_2 - d_2)K}{d_2}$.
- *To show the existence of equilibrium* $E^* = (Q^*, F^*, D^*)$ *, we will prove two isoclines (of the system) will intersect in the first quadrant. The first isocline is formed by finding the value of* D *from* 1^{st} *equation of system (2.2.2) and then putting in* 2^{nd}*; and the second isocline is formed by putting same* D *in* 3^{rd} *equation of system (2.2.2).*

They are as follows:

$$\begin{aligned} g(Q,F) &= pQ^2r\omega_1 + Q(b_2e_1K - d_2e_1K + apr\omega_1 - Kpr\omega_1) + b_1FKp\omega_1 \\ &\quad -ad_2e_1K - aKpr\omega_1 = 0, \qquad (2.3.3) \\ h(Q,F) &= Q(e_2 - d_3T_Q) + F(p\omega_2 - d_3pT_F) - d_3 = 0. \qquad (2.3.4) \end{aligned}$$

Consider, ***first isocline****:*

It is intersecting F-axis at $\left(\frac{ad_2e_1 + apr\omega_1}{b_1p\omega_1}, 0\right) = (f_1, 0)$ *(in F-Q plane).*

Also, $\left(\frac{dQ}{dF}\right)_1 = \frac{\partial g}{\partial F}\Big/\frac{\partial g}{\partial Q} = \frac{M_1}{N_1}$.

where, $M_1 = b_1Kp\omega_1$,
$N_1 = (b_2 - d_2)e_1K + p(a - K + 2Q)r\omega_1$.

Now, $\left(\frac{dQ}{dF}\right)_1 > 0$ *(if* $b_2 > d_2$ *and* $d_2e_1K + (-a+K)pr\omega_1 < b_2e_1K$*).*

Consider, ***second isocline****:*

It is intersecting F-axis at $\left(\frac{d_3}{p(\omega_2 - d_3T_F)}, 0\right) = (f_2, 0)$ *(in F-Q plane); which is*

on positive F-axis if $\omega_2 > d_3T_F$.

Also, $\left(\frac{dQ}{dF}\right)_2 = \frac{\partial h}{\partial F}\Big/\frac{\partial h}{\partial Q} = \frac{M_2}{N_2}$.

where, $M_2 = p\omega_2 - d_3pT_F > 0$,
$N_2 = e_2 - d_3T_Q$.

Now, $\left(\frac{dQ}{dF}\right)_2 < 0$ *(if* $e_2 < d_3T_Q$ *).*

The two isoclines will surely intersect in first quadrant if first isocline is increasing

$\left(i.e.\ \left(\frac{dQ}{dF}\right)_1 > 0\right)$, *second isocline is decreasing* $\left(i.e.\ \left(\frac{dQ}{dF}\right)_2 < 0\right)$, *and* $f_1 < f_2$,

i.e. if $b_2 > d_2$, $\omega_2 > d_3T_F$, $e_2 < d_3T_Q$,

$r \le \frac{(b_2 - d_2)e_1}{p\omega_1}$, $d_3\omega_1(b_1d_3\omega_1 + a(d_2e_1 + pr\omega_1)(d_3T_F - \omega_2)) > 0$.

Now, by putting above intersecting point (Q^*, F^*) *in system (2.2.2), we can find the*

value of $D^*\left(if\ b_1 < \dfrac{(K-Q^*)(a+Q^*)r}{F^*K}\right)$.

To find number of existing non-trivial equilibrium points, we convert system (2.2.2) in terms of Q *as:*

$$k(Q) = AQ^2 + BQ + C, \tag{2.3.5}$$

where,

$$\begin{aligned}
A &= -d_3prT_f\omega_1 + pr\omega_1\omega_2,\\
B &= -b_2d_3e_1KT_f + d_2d_3e_1KT_f - b_1e_2K\omega_1 - ad_3prT_f\omega_1 + d_3KprT_f\omega_1 + b_1d_3KT_q\omega_1\\
&\quad + b_2e_1K\omega_2 - d_2e_1K\omega_2 + apr\omega_1\omega_2 - Kpr\omega_1\omega_2,\\
C &= ad_2d_3e_1KT_f + b_1d_3K\omega_1 + ad_3KprT_f\omega_1 - ad_2e_1K\omega_2 - aKpr\omega_1\omega_2,
\end{aligned}$$

then the discriminant of quadratic function becomes:

$$\Delta = B^2 - 4AC.$$

- *Case 1: If* $\Delta > 0$*, two simple real roots.*

- *Case 2: If* $\Delta = 0$*, one double real root.*

- *Case 3: If* $\Delta < 0$*, two simple complex roots.*

Example 2.3.1 *If we set the parameters as:* $r = 4.912, K = 200; a = 35; b_1 = 2.191, b_2 = 1.07; e_1 = 1.9; e_2 = 0.16, \omega_1 = 1.09, \omega_2 = 0.781, d_2 = 0.819, d_3 = 1.093, T_Q = 0.27, T_F = 0.25, p = 0.45$*, such that*

$$k(Q) = -1.22334Q^2 + 88.8883Q + 13572.1$$

then, $\Delta = 74314.3 > 0$*; by Case 1, we have two simple real roots* $Q_1^* = -75.0887$ *and* $Q_2^* = 147.749$ *but as we are interested in only positive equilibrium, we get* $Q_2^* = 147.749$ *and hence* $F_2^* = 92.1511$ *and* $D_2^* = 4.81494$ *(i.e.* $E^* = (147.749, 92.1511, 4.81494)$*).*

Hence, the existence of E^* *is shown.*

2.3.2.2 Local stability analysis of equilibrium points

Theorem 2.3.8 *The equilibrium point E_1 is always unstable.*

Proof Since, the eigenvalues of Jacobian matrix (2.3.2) corresponding to E_1 are $r, -d_2$ and $-d_3$. Since, one of the eigenvalue (r) is always positive, thus the equilibrium point E_1 is always unstable. Biologically, it means that system will never settle to zero in long run.

Theorem 2.3.9 *The equilibrium point E_2 is asymptotically stable if $d_2 \geq b_2$ and $d_3 > \dfrac{e_2K}{1+KT_Q}$.*

Proof Since, the eigenvalues of Jacobian matrix (2.3.2) corresponding to E_2 are $-r, -d_2 + \dfrac{b_2K}{a+K}$ and $-d_3 + \dfrac{e_2K}{1+KT_Q}$. Hence, the predator free equilibrium is asymptotically stable if $d_2 \geq b_2$ and $d_3 > \dfrac{e_2K}{1+KT_Q}$.

Theorem 2.3.10 *The equilibrium point E_3 is asymptotically stable if*

$$r \geq \frac{4e_2K(e_2 - d_3T_Q)^2(-d_3 + e_2K - d_3KT_Q)}{d_3(e_2 - e_2KT_Q + d_3T_Q(1+KT_Q))^2}, \frac{d_3}{e_2 - d_3T_Q} < K < \frac{e_2 + d_3T_Q}{e_2T_Q - d_3{T_Q}^2} \quad \text{and,}$$

$$b_2 < \frac{(-ae_2 + d_3(-1+aT_Q))(d_2e_1K(-e_2 + d_3T_Q) + pr(d_3 - e_2K + d_3KT_Q)\omega_1)}{d_3e_1K(e_2 - d_3T_Q)}.$$

Proof Since, the eigenvalues of Jacobian matrix (2.3.2) corresponding to E_3 are

$$\frac{-B_1 \pm \sqrt{B_1^2 - 4A_1C_1}}{2A_1} \quad \text{and} \quad M+N,$$

where, $A_1 = {e_2}^2K - d_3e_2KT_Q$,

$B_1 = d_3e_2r + {d_3}^2rT_Q - d_3e_2KrT_Q + {d_3}^2KrT_Q^2$,

$C_1 = d_3r\left(-e_2 + d_3T_Q\right)\left(d_3 - e_2K + d_3KT_Q\right)$,

$M = -d_2 + \dfrac{b_2d_3}{d_3 + ae_2 - ad_3T_Q}$, and

$N = \dfrac{pr\left(d_3 - e_2K + d_3KT_Q\right)\omega_1}{e_1K\left(e_2 - d_3T_Q\right)}$.

Hence, the equilibrium point is asymptotically stable if above conditions are satisfied.

Theorem 2.3.11 *The equilibrium point E_4 is asymptotically stable if*

$$\frac{b_2K - d_2K}{b_2 + d_2} < a,\ r \geq \frac{4b_2(b_2 - d_2)^2K(b_2K - d_2(a+K))}{d_2(a(b_2+d_2) + (-b_2+d_2)K)^2} \quad \text{and}$$

$$d_3 > \frac{ab_1d_2(-b_2+d_2)e_2K + ab_2(-b_2K + d_2(a+K))pr\omega_2}{ab_2(-b_2K + d_2(a+K))prT_F - b_1(b_2-d_2)K(b_2+d_2(-1+aT_Q))}.$$

Proof Since, the eigenvalues of Jacobian matrix (2.3.2) corresponding to E_4 are

$$\frac{b_1(b_2-d_2)K(b_2d_3 - d_2(d_3+ae_2) + ad_2d_3T_Q) - ab_2(-b_2K + d_2(a+K))pr(d_3T_F - \omega_2)}{ab_2(-b_2K + d_2(a+K))prT_F - b_1(b_2-d_2)K(b_2+d_2(-1+aT_Q))} \text{ and}$$

$$\frac{-B_2 \pm \sqrt{B_2^2 - 4A_2C_2}}{2A_2},$$

where, $A_2 = b_2(b_2-d_2)K,$

$B_2 = d_2(-ab_2r - ad_2r + b_2Kr - d_2Kr),$

$C_2 = d_2r(-ab_2d_2 + ad_2{}^2 + b_2{}^2K - 2b_2d_2K + d_2{}^2K).$

Hence, the equilibrium point is asymptotically stable if above conditions are satisfied.

Theorem 2.3.12 *The equilibrium point E^* is asymptotically stable if*

$$G_1 > 0, G_3 > 0, \quad \text{and} \quad G_1G_2 - G_3 > 0. \tag{2.3.6}$$

where $G_1,\ G_2$ and G_3 are defined in the following proof.

Proof The characteristics equation of $\mathcal{J}(E^*) = \mathcal{J}(Q^*, F^*, D^*)$ is given by

$$\lambda^3 + G_1\lambda^2 + G_2\lambda + G_3 = 0, \tag{2.3.7}$$

where,

$$\begin{aligned}
G_1 &= d_2 + d_3 - r + \frac{ab_1F^*}{(a+Q^*)^2} - \frac{b_2Q^*}{a+Q^*} + \frac{2Q^*r}{K} \\
&\quad - \frac{(D^*e_1Q^*T_Q + D^*F^*p^2T_F\omega_1)}{(1+F^*pT_F+Q^*T_Q)^2} + \frac{(D^*e_1 - e_2Q^* + D^*p\omega_1)}{1+F^*pT_F+Q^*T_Q}, \\
G_2 &= d_3(d_2-r) - rd_2 + \frac{2Q^*r(d_2+d_3)}{K} + \frac{b_2Q^*(r-d_3)}{a+Q^*} - \frac{2b_2Q^{*2}r}{K(a+Q^*)} \\
&\quad + \frac{ab_1F^*d_2}{(a+Q^*)^2} \\
&\quad + \frac{D^*d_3e_1 + e_2Q^*r + D^*d_3p\omega_1 - D^*pr\omega_1 + F^*pr\omega_2 - F^*p\omega_2d_2}{1+F^*pT_F+Q^*T_Q} \\
&\quad + \frac{b_2D^*e_1Q^{*2}T_Q - b_2D^*e_1F^*pQ^*T_F}{(a+Q^*)(1+F^*pT_F+Q^*T_Q)^2}
\end{aligned} \tag{2.3.8}$$

$$
\begin{aligned}
&+\frac{-D^*d_3F^*p^2T_F\omega_1+D^*F^*p^2rT_F\omega_1-D^*d_3e_1Q^*T_Q-D^*e_1F^*p\omega_2}{(1+F^*pT_F+Q^*T_Q)^2}\\
&+\frac{d_2(D^*(e_1+e_1F^*pT_F)-e_2Q^*(1+F^*pT_F+Q^*T_Q))}{(1+F^*pT_F+Q^*T_Q)^2}\\
&-\frac{(D^{*2}e_1F^*p^2T_F\omega_1+D^{*2}e_1pQ^*T_Q\omega_1)}{(1+F^*pT_F+Q^*T_Q)^3}\\
&+\frac{2D^*pQ^*r\omega_1-2F^*pQ^*r\omega_2-2e_2Q^{*2}r}{K(1+F^*pT_F+Q^*T_Q)}\\
&-\frac{2D^*F^*p^2Q^*rT_F\omega_1}{K(1+F^*pT_F+QT_Q)^2}\\
&+\frac{D^{*2}e_1p\omega_1-D^*e_2pQ^*\omega_1+b_2e_2Q^{2*}-b_2D^*e_1Q^*+b_2F^*pQ^*\omega_2}{(a+Q^*)(1+F^*pT_F+Q^*T_Q)}\\
&+\frac{1}{(a+Q^*)^2(1+F^*pT_F+QT_Q)^2}(b_1F^*(D^*pQ^{*2}T_Q\omega_1\\
&+a(-e_2Q^*(1+F^*pT_F+Q^*T_Q)+d_3(1+F^*pT_F+Q^*T_Q)^2\\
&+D^*p(1+2Q^*T_Q)\omega_1-F^*p(1+F^*pT_F+Q^*T_Q)\omega_2))\\
&+b_2D^*e_1F^*pQ^{*2}T_F), \qquad (2.3.9)\\
G_3 \;=\;& \frac{1}{(1+F^*pT_F+Q^*T_Q)^3}\Bigg(D^{*2}d_3e_1p\omega_1-\frac{1}{k(a+Q)^2}\big(d_2(-ab_1F^*K\\
&+(K-2Q^*)(a+Q^*)^2r)(1+F^*pT_F+Q^*T_Q)^2(d_3-e_2Q^*\\
&+d_3F^*pT_F+d_3Q^*T_Q-F^*p\omega_2)\big)+\frac{1}{K(a+Q)^2}\big(d(1+F^*pT_F+Q^*T_Q)\\
&(a^2(-p(K-2Q^*)r(d_3-e_2Q^*+d_3Q^*T_Q)\omega_1+d_2e_1K(d_3+d_3F^*pT_F-F^*p\omega_2))\\
&+Q^{*2}(p(b_1F^*K(-e_2+d_3T_Q)-(K-2Q^*)r(d_3-e_2Q^*+d_3Q^*T_Q))\omega_1\\
&+d_2e_1K(d_3+d_3F^*pT_F-F^*p\omega_2))+a(p(-2(K-2Q^*)Q^*r(d_3-e_2Q^*+d_3Q^*T_Q)\\
&+b_1F^*K(d_3-2e_2Q^*+2d_3Q^*T_Q))\omega_1+2d_2e_1KQ^*(d_3+d_3F^*pT_F-F^*p\omega_2))))\big)\\
&-\frac{1}{K(a+Q^*)^2}(b_2Q^*(1+F^*pT_F+Q^*T_Q)(a(D^*e_1K(d_3+2d_3F^*pT_F-2F^*p\omega_2)\\
&-(K-2Q^*)r(1+F^*pT_F+Q^*T_Q)(d_3-e_2Q^*+d_3F^*pT_F+d_3Q^*T_Q-F^*p\omega_2))\\
&+Q^*(D^*e_1K(d_3+d_3F^*pT_F-F^*p\omega_2)-(K-2Q^*)r(1+F^*pT_F+Q^*T_Q)(d_3\\
&-e_2Q^*+d_3F^*pT_F+d_3Q^*T_Q-F^*p\omega_2))))\Bigg). \qquad (2.3.10)
\end{aligned}
$$

By Routh-Hurwitz criterion (2.3.7) have all roots with negative real parts if (2.3.6) are satisfied. Thus, making equilibrium point E^* is locally asymptotically stable.

Remark 3 *If we take parameters as in Example (2.3.1),* $G_1 = 2.58729 > 0, G_3 = 0.0837404 > 0$ *and* $G_1 * G_2 - G_3 = 0.280056 > 0$, *making* $E^* = (Q^*, F^*, D^*) = (147.7490517, 92.1510996, 4.8149385)$ *a locally asymptotically stable equilibrium point. Biologically, this means that for the given parameter values and small perturbation the population will always settle up*

Table 2.2: Selected set of parameters values used for numerical simulation. We mostly took hypothetical value which are in ecological permissible range due to the lack of knowledge on basic biological parameters.

Parameters	values	Parameters	values
r	4.912	ω_1	1.09
K	200	ω_2	0.781
a	35	d_2	.819
b_1	2.191	d_3	1.093
b_2	1.07	T_Q	0.27
e_1	1.9	T_F	0.25
e_2	0.16	p	0.45

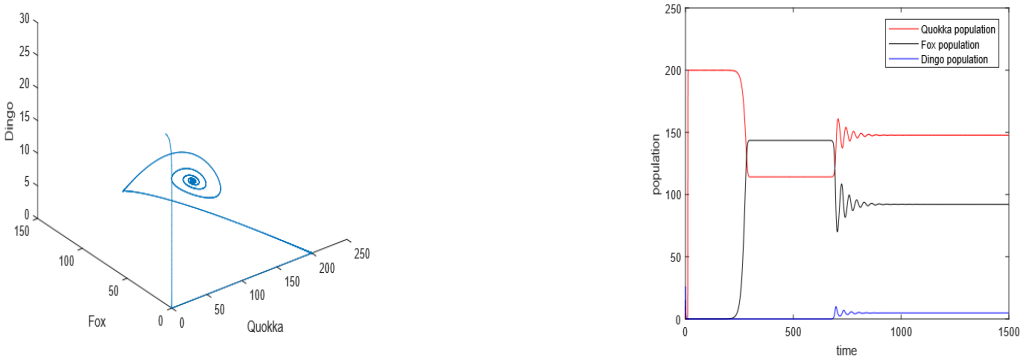

(a) phase portrait (b) time series

Figure 2.3: Stable attractor for the given parameters.

at $E^*(Q^*, F^*, D^*)$ *(c.f. Fig. 2.3).*

2.4 Stability analysis of model system for movement in species

2.4.1 Linear stability analysis

Linear stability analysis of corresponding spatio-temporal model is done by perturbing system with 2-dimensional spatial perturbations of the form:

$$\begin{aligned} Q &= Q^* + \varepsilon_1 \exp(\lambda_k t + i(k_x x + k_y y)) = Q^* + \varepsilon_1 q_1, \\ F &= F^* + \varepsilon_2 \exp(\lambda_k t + i(k_x x + k_y y)) = F^* + \varepsilon_2 f_1, \\ D &= D^* + \varepsilon_3 \exp(\lambda_k t + i(k_x x + k_y y)) = D^* + \varepsilon_3 d_1. \end{aligned} \tag{2.4.1}$$

where $\varepsilon_1, \varepsilon_2$ and ε_3 are sufficiently small constants, λ_k is wavelength, k_x and k_y are the components of the wavenumber k in x and y directions respectively.

Theorem 2.4.1 *Assume that the parameters in model system (2.2.4) satisfy conditions* (2.4.8). *Then the constant positive steady state* $E^*(Q^*, F^*, D^*)$ *of the spatio temporal system is locally asymptotically stable.*

Proof The characteristic equation of the linearized system about the non-trivial equilibrium point $E^*(Q^*,F^*, D^*)$, is given by

$$(\mathcal{J}^* - Hk^2 - \lambda_k I)(q_1, f_1, d_1)^T = 0, \tag{2.4.2}$$

$$\text{where, } \mathcal{J}^* = \begin{pmatrix} a_{11} & a_{12} & a_{13} \\ a_{21} & a_{22} & a_{23} \\ a_{31} & a_{32} & a_{33} \end{pmatrix}, \quad \text{and} \quad H = \begin{pmatrix} H_Q & 0 & 0 \\ 0 & H_F & 0 \\ 0 & 0 & H_D \end{pmatrix}, \tag{2.4.3}$$

where $k^2 = k_x^2 + k_y^2$ and $\mathcal{J}^*$ is same as given in (2.3.2) . From (2.4.2) and (2.4.3), the characteristic polynomial becomes

$$det(\mathcal{J}^* - Hk^2 - \lambda_k I) = \lambda_k^3 + \beta_1(k^2)\lambda_k^2 + \beta_2(k^2)\lambda_k + \beta_3(k^2) = 0,$$

$$\begin{aligned} \text{where, } \beta_1(k^2) &= -tr(\mathcal{J}^* - Hk^2) = k^2(H_Q + H_F + H_D) + G_1, && (2.4.4) \\ \beta_2(k^2) &= k^4(H_Q H_F + H_F H_D + H_Q H_D) - k^2((H_Q(a_{33} + a_{22}) \\ &\quad + H_F(a_{11} + a_{33}) + H_D(a_{11} + a_{22})) + G_2, && (2.4.5) \\ \beta_3(k^2) &= -det(J^* - Hk^2) = k^6(H_Q H_F H_D) - k^4(H_Q H_F a_{33} + H_Q H_D a_{22} \\ &\quad + H_F H_D a_{11}) + k^2(H_Q(a_{33}a_{22} - a_{23}a_{32}) + H_F(a_{11}a_{33} - a_{13}a_{31}) \\ &\quad + H_D(a_{11}a_{22} - a_{12}a_{21})) + G_3. && (2.4.6) \end{aligned}$$

where, G_1, G_2 and G_3 are defined in (2.3.8)-(2.3.10).
Manipulating algebraically one can find $\beta_1(k^2)\beta_2(k^2) - \beta_3(k^2)$ is given by following equation,

$$\beta_1(k^2)\beta_2(k^2) - \beta_3(k^2) = L_1 k^6 + L_2 k^4 + L_3 k^2 + G_1 G_2 - G_3, \tag{2.4.7}$$

where, $L_1 = (H_Q + H_F)(H_Q + H_D)(H_F + H_D)$,
$L_2 = -a_{11}(H_F + H_D)(H_F + 2H_Q + H_D) - a_{22}(H_Q + H_D)(2H_F + H_Q + H_D)$,
$L_3 = (-a_{22}G_1 + a_{11}a_{22} - a_{12}a_{21} - a_{31}a_{13})H_Q + (-a_{11}G_1 + a_{11}a_{22} - a_{12}a_{21}$
$- a_{23}a_{32})H_F + (-(a_{22} + a_{11})G_1 - a_{23}a_{32} + a_{13}a_{31})H_D$.

An application of the Routh-Hurwith criteria gives, $Re(\lambda_k) < 0$ if and only if we have,

$$\beta_1(k^2) > 0, \beta_3(k^2) > 0 \quad and \quad \beta_1(k^2)\beta_2(k^2) - \beta_3(k^2) > 0. \tag{2.4.8}$$

Thus, the constant positive steady state $E^*(Q^*, F^*, D^*)$ of the spatio-temporal system is asymptotically stable.

Remark 4 *Biologically, this means that for the given parameter values and small perturbation the population will always settle up at $E^*(Q^*, F^*, D^*)$ even in the presence of diffusion.*

2.4.2 Global stability analysis of spatial model

The following theorem gives us the sufficient condition for the equilibrium E^* to be globally asymptotically stable even in the presence of diffusion.

Theorem 2.4.2 *If the equilibrium E^* exists, and assume that the following conditions are true:*

$$(i) \quad r > K\left(\frac{b_1F^*}{a+Q^*} + \frac{D^*e_1T_Q}{1+F^*pT_f+Q^*T_Q}\right),$$
$$(ii) \quad b_2 \leq d_2,$$

the equilibrium E^* of model is globally asymptotically stable.

Proof Define a Lyapunov function:

$$V(Q,F,D) = \left[Q - Q^* - Q^*\ln\left(\frac{Q}{Q^*}\right)\right] + \frac{k_1}{2}(F-F^*)^2 + k_2\left[D - D^* - D^*\ln\left(\frac{D}{D^*}\right)\right], \tag{2.4.9}$$

where k_1 and k_2 are positive constants. Also, $V(Q,F,D)$ is non-negative and $V(Q,F,D) = 0$ at only (Q^*, F^*, D^*). Now,

$$\frac{dV}{dt} = \left(\frac{Q-Q^*}{Q}\right)\frac{dQ}{dt} + k_1(F-F^*)\frac{dF}{dt} + k_2\left(\frac{D-D^*}{D}\right)\frac{dD}{dt}.$$

Further,

$$\begin{aligned}
\frac{dV}{dt} &= (Q-Q^*) \\
&\Big(\frac{r}{K}(Q^*-Q)-\frac{b_1F}{Q+a}-\frac{e_1D}{1+T_QQ+pT_FF}+\frac{b_1F^*}{Q^*+a}+\frac{e_1D^*}{1+T_QQ^*+pT_FF^*}\Big) \\
&+k_1(F-F^*) \\
&\Big(\frac{b_2QF}{Q+a}-\frac{\omega_1pDF}{1+T_QQ+pT_FF}-d_2F-\frac{b_2Q^*F^*}{Q^*+a}+\frac{\omega_1pD^*F^*}{1+T_QQ^*+pT_FF^*}+d_2F^*\Big) \\
&+k_2(D-D^*)\Big(\frac{e_2Q+\omega_2pF}{1+T_QQ+pT_FF}-\frac{e_2Q^*+\omega_2pF^*}{1+T_QQ^*+pT_FF^*}\Big), \\
&\leq (Q-Q^*)^2\left(-\frac{r}{K}+\frac{b_1F^*}{(Q^*+a)}+\frac{e_1T_QD^*}{(1+T_QQ^*+pT_FF^*)}\right) \\
&+(F-F^*)^2\left(\frac{b_2k_1Q^*}{(Q^*+a)}-k_1d_2\right) \\
&+(Q-Q^*)(F-F^*)\left(\frac{b_2ak_1F_{max}}{(Q^*+a)}+\frac{e_1pT_FD^*+\omega_1pk_1D^*F^*}{(1+T_QQ^*+pT_FF^*)}\right) \\
&+(Q-Q^*)(D-D^*)\left(\frac{-e_1(1+T_QQ^*+pT_FF^*)+e_2k_2(1+pT_FF^*)}{(1+T_QQ^*+pT_FF^*)}\right) \\
&+(F-F^*)(D-D^*)\left(\frac{-\omega_1pk_1F^*(1+Q^*)+pk_2\omega_2(1+T_QQ^*)}{(1+T_QQ^*+pT_FF^*)}\right).
\end{aligned}$$

If we choose,

$$k_2=\frac{e_1(1+T_QQ^*+pT_FF^*)}{e_2(1+pT_FF^*)} \quad \text{and} \quad k_1=\frac{k_2\omega_2(1+T_QQ^*)}{\omega_1F^*(1+Q^*)}.$$

Then ,

$$\frac{dV}{dt}\leq(Q-Q^*)^2(R_1)+(Q-Q^*)(F-F^*)(R_2)+(F-F^*)^2(R_3),$$

where, $R_1=\dfrac{b_1F^*}{(a+Q^*)}-\dfrac{r}{K}+\dfrac{D^*e_1T_Q}{1+F^*pT_F+Q^*T_Q}$,

$$R_2=\frac{b_2ak_1F_{max}}{(Q^*+a)}+\frac{e_1pT_FD^*+\omega_1pk_1D^*F^*}{(1+T_QQ^*+pT_FF^*)}>0,$$

$$R_3=\frac{b_2k_1Q^*}{(Q^*+a)}-k_1d_2.$$

By condition (i) and (ii) from theorem statement, we have $R_1<0$ and $R_3<0$.
Further, if $(Q-Q^*)(F-F^*)<0$, then $\dfrac{dV}{dt}<0$ always. But, if $(Q-Q^*)(F-F^*)>0$,then $\dfrac{dV}{dt}<0$ if $R_2^2\leq 4R_1R_3$.

Therefore, the sufficient conditions for $\frac{dV}{dt} < 0$ to be negative definite are satisfied and thus the equilibrium E^* of system (2.2.2) is globally asymptotically stable.
For, global stability of a spatial model system (2.2.4) we take Lyapunov function as:

$$S(t) = \iint_{\Omega} V(Q, F, D) dA,$$

where $V(Q, F, D)$ is mentioned in equation (2.4.9). Now,

$$\begin{aligned}
\frac{dS(t)}{dt} &= \iint_{\Omega} \left[\frac{\partial V}{\partial Q}\frac{\partial Q}{\partial t} + \frac{\partial V}{\partial F}\frac{\partial F}{\partial t} + \frac{\partial V}{\partial D}\frac{\partial D}{\partial t} \right] dA, \\
&= \iint_{\Omega} \frac{dV}{dt} dA + \iint_{\Omega} \left[H_Q \frac{\partial V}{\partial Q}\nabla^2 Q + H_F \frac{\partial V}{\partial F}\nabla^2 F + H_D \frac{\partial V}{\partial D}\nabla^2 D \right] dA, \\
&= S_1 + S_2,
\end{aligned}$$

where, $S_1 = \iint_{\Omega} \frac{dV}{dt} dA,$

$$S_2 = \iint_{\Omega} \left[H_Q \frac{\partial V}{\partial Q}\nabla^2 Q + H_F \frac{\partial V}{\partial F}\nabla^2 F + H_D \frac{\partial V}{\partial D}\nabla^2 D \right] dA.$$

By using Green's first identity in the plane,

$$\begin{aligned}
\iint_{\Omega} \frac{\partial V}{\partial Q}\nabla^2 Q dA &= \int \frac{\partial V}{\partial Q}\frac{\partial Q}{\partial n} dS - \iint_{\Omega} \left[\nabla \left(\frac{\partial V}{\partial Q} \right) . \nabla Q \right] dA, \\
&= -\iint_{\Omega} \left[\nabla \left(\frac{\partial V}{\partial Q} \right) . \nabla Q \right] dA.
\end{aligned}$$

Now,

$$\nabla \left(\frac{\partial V}{\partial Q} \right) = \frac{\partial^2 V}{\partial Q^2}\frac{\partial Q}{\partial x}\hat{i} + \frac{\partial^2 V}{\partial Q^2}\frac{\partial Q}{\partial y}\hat{j}.$$

Hence,

$$\iint_{\Omega} \frac{\partial V}{\partial Q}\nabla^2 Q dA = -\iint_{\Omega} \frac{\partial^2 V}{\partial Q^2} \left[\left(\frac{\partial Q}{\partial x} \right)^2 + \left(\frac{\partial Q}{\partial y} \right)^2 \right] dA \leq 0.$$

Similarly,

$$\begin{aligned}
\iint_{\Omega} \frac{\partial V}{\partial F}\nabla^2 F dA &= -\iint_{\Omega} \frac{\partial^2 V}{\partial F^2} \left[\left(\frac{\partial F}{\partial x} \right)^2 + \left(\frac{\partial F}{\partial y} \right)^2 \right] dA \leq 0, \\
\iint_{\Omega} \frac{\partial V}{\partial D}\nabla^2 D dA &= -\iint_{\Omega} \frac{\partial^2 V}{\partial D^2} \left[\left(\frac{\partial D}{\partial x} \right)^2 + \left(\frac{\partial D}{\partial y} \right)^2 \right] dA \leq 0.
\end{aligned}$$

From the above analysis we note that if $S_1 \leq 0$, then $\frac{dS}{dt} < 0$. This implies that if in the absence of diffusion E^* is globally asymptotically stable, then in the presence of diffusion E^* will remain globally asymptotically stable.

2.5 Conditions on diffusion driven instability

Turing instability is a phenomenon that causes certain reaction-diffusion systems to spontaneously give rise to stationary patterns with a characteristic length scale from an arbitrary initial configuration. The key factor in inducing the instability is diffusion and this is why, Turing instability is often called diffusion-driven instability. An unusual feature of Turing systems as compared to many other instabilities in systems out of equilibrium (Cross and Hohenberg (1993); á Ball (2001)) is that the characteristics of the resulting patterns are not determined by externally imposed length scales or constraints, but by the chemical reaction and diffusion rates that are intrinsic to the system. In this section, we will present how Turing instability can be formalized and treated numerically for the given set of parameters in Table 2.2.

Theorem 2.5.1 *The spatial model system* (2.2.4) *will undergo diffusion-driven instability at the homogeneous steady state* E^* *provided the following conditions are satisfied*

$$P_1 < 0 \ \ or\ (P_2 < 0 \ and\ P_2^2 > 3P_1P_3),\ and\ \left(P_3^2 + \frac{27}{2}P_3^2P_0 - \frac{9}{2}P_1P_2P_3\right)^2 < (P_2^2 - 3P_1P_3)^3,$$

where $P_i's$ *are coefficient of the equation* $P(k^2) = P_3k^6 + P_2k^4 + P_1k^2 + P_0$, *such that equation is expressions for* $\beta_3(k^2)$ *and* $\beta_1(k^2)\beta_2(k^2) - \beta_3(k^2)$. *The coefficient* $P_i(i = 0, 1, 2, 3)$ *for expression of* $\beta_3(k^2)$ *and* $\beta_1(k^2)\beta_2(k^2) - \beta_3(k^2)$ *are the same as those given in the (2.4.6)-(2.4.7) .*

Proof The proof directly follows from Theorem 4.2 given in Upadhyay et al. (2016) and hence omitted.

Remark 1. As a consequence of Theorem 2.4.1, under conditions (2.4.8), diffusion cannot destabilize the constant coexistence steady state $E^*(Q^*, F^*, D^*)$ of the system (2.2.4) and Turing instability cannot occur in the proximity of $E^*(Q^*, F^*, D^*)$. However, if condition of Theorem 2.5.1 are satisfied, E^* can loose stability under diffusion, and hence giving rise to Turing instability.

Example 2: If the parameters are chosen as in Table 2.2, then to get the diffusive instability, any of the conditions in (2.4.8) must fail. For diffusive coefficients $H_Q = 0.010$,

$H_F = 10$ and $H_D = 0.015$, we observe that $\beta_3(k^2)$ is negative for the wave number k (s.t. $0.356235 \leq k \leq 1.58218$) and is shown in Fig. 2.4. In this case, Turing instability is possible. Accordingly, the system may eventually go to a non-constant positive steady state giving rise to pattern formation (c.f. Fig. 2.5-2.7). This means diffusion drives system (2.2.4) unstable for some of the values of k.

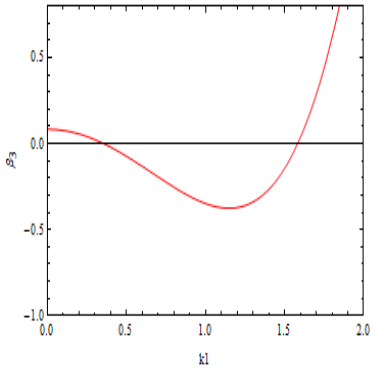

k vs β_3

Figure 2.4: The occurrence of Turing instability as the coefficient (β_3) of the dispersion relation (2.4.6) becomes negative for some range of wavenumber k.

2.5.1 Turing instability

The most important feature of the Turing models is that they generate the pattern with respect to the chemical concentration from any arbitrary initial state and the pattern can be changed from stripes to spots by changing only one parameter of the model. Turing patterns grow due to diffusion-driven instability as a result of infinitesimal perturbations around the stationary state of the model and exist only under non-equilibrium conditions.

In this section, we present Turing patterns for the model system (2.2.4) in two dimensions. These patterns are computed using a finite difference numerical method for the spatial discretization with explicit time-stepping. The initial conditions for all of our calculations are based on small random perturbations of the positive uniform steady state E^* and homogeneous Neumann (zero-flux) boundary conditions are imposed. All of the simulations are carried out on 200×200 square domain using a mesh with $\Delta x = 0.25$, and a time-step of 10^{-3}. Fig. 2.5-2.7 shows the evolution of spatial pattern of all species at iterations 1000, 500000, 1000000.

At time $t = 1$ day, we observe that quokka and dingoes are randomly distributed except foxes which are distributed in small clusters.

As time increases to 500 days we observe strip and spot pattern. A close examination tells

that the number of qoukkas and foxes are lower where dingoes are concentrated. Therefore, we can say that quokka and foxes try to keep away from dingo population. Our simulation result is in agreement with the experiment performed by Moseby et al. (2012). They performed an experiment by introducing dingoes into fox paddock and after 10 months the majority of foxes were captured outside the paddock.

Finally, when time increases to 1000 days we observe that quokka distributes itself to the entire domain leaving some small locations where dingoes and foxes are mostly concentrated. Fox population also avoids the places where dingoes are present and concentrates itself at the upper right corner of the domain. Dingoes show very small area clustering. Moseby et al.(2012), Mitchell and Banks(2005) also supported anecdotal evidence that dingoes may suppress exotic mesopredators, particularly foxes. O'Neill (2002) observed that foxes avoid the places where dingo faeces are found, this is in agreement with our numerical simulation. Thus, we conclude that different patterns can be seen as time evolve and could provide a plausible way to model the mechanisms of biological growth.

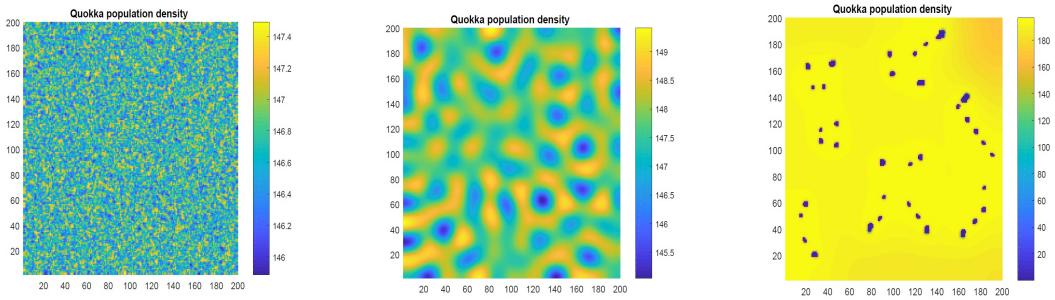

(a) days $t = 1$ (b) days $t = 500$ (c) days $t = 1000$

Figure 2.5: Quokka population density when $H_Q = 0.5$, $H_F = 5$ and $H_D = 0.015$ for days $t = 1$, $t = 500$ and $t = 1000$.

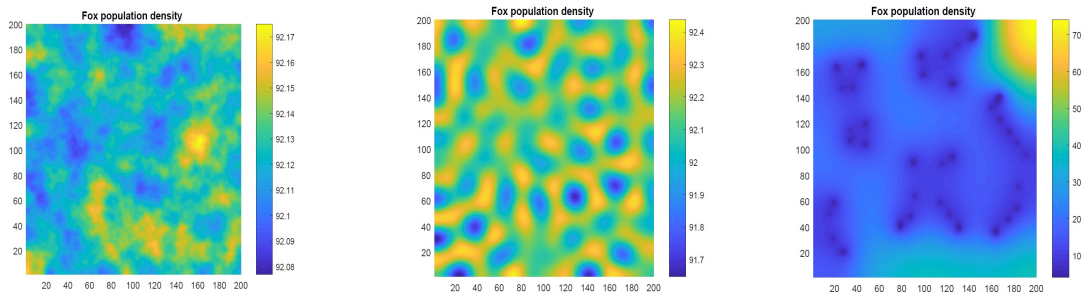

(a) days $t = 1$ (b) days $t = 500$ (c) days $t = 1000$

Figure 2.6: Fox population density when $H_Q = 0.5$, $H_F = 5$ and $H_D = 0.015$ for days $t = 1$, $t = 500$ and $t = 1000$.

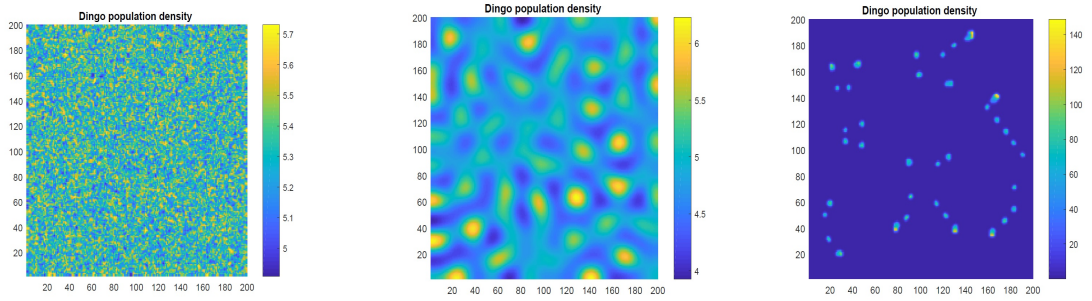

(a) days= 1 (b) days $t = 500$ (c) days $t = 1000$

Figure 2.7: Dingo population density when $H_Q = 0.5$, $H_F = 5$ and $H_D = 0.015$ for days $t = 1$, $t = 500$ and $t = 1000$.

2.6 Threshold for persistence of species

Following, Garrione and Rebelo (2016); Georgescu and Hsieh (2007); Georgescu et al. (2010), we calculated a threshold value $\mathcal{T}_0$ (say), for different cases of predator extinction which may be thought as, the number of predators one predator gives rise during its life, when introduced in a prey population. In food chain model, R_0 can serves as a threshold parameter that predicts whether predator population will uniformly persists or will tend to extinction. In the situation of surplus predator, we can determine which control measures, and at what magnitude and in what combinations, would be most effective in reducing $\mathcal{T}_0$ below one, providing important guidance for designing a policy measures to save predation related extinction. Now, we state the following theorem:

2.6.1 Without prey switching; Without movement of species

Theorem 2.6.1 *Let $\mathcal{T}_0^{D+F}$ be a threshold parameter. Then,*
(a) If $\mathcal{T}_0^{D+F} = \dfrac{b_2 K}{(a+K)(d_2 - r_2)} < 1$, both the predators for system (2.2.1), will tend to extinction that is, $F(t) \to 0, D(t) \to 0$ for $t \to +\infty$.
(b) If $\mathcal{T}_0^{D+F} > 1$, then there is the uniform persistence of $F(t) + D(t)$ for the system.

Proof (a) Following Garrione and Rebelo (2016), we found $\mathcal{F}_1$ and $\mathcal{V}_1$ for the model system (2.2.1), as:

$$\mathcal{F}_1 = \begin{pmatrix} \dfrac{b_2 K}{a+K} & 0 \\ 0 & 0 \end{pmatrix} \text{ and } \mathcal{V}_1 = \begin{pmatrix} d_2 - r_2 & 0 \\ 0 & d_3 - r_3 \end{pmatrix}$$

Then,

$$\mathscr{F}_1\mathscr{V}_1^{-1} = \begin{pmatrix} \dfrac{b_2K}{(a+K)(d_2-r_2)} & 0 \\ 0 & 0 \end{pmatrix}.$$

The threshold value for both predator extinction of the system (2.2.1), denoted by $\mathscr{T}_0^{F+D} = \rho(\mathscr{F}_1\mathscr{V}_1^{-1})$, is given by,

$$\mathscr{T}_0^{F+D} = \frac{b_2K}{(a+K)(d_2-r_2)}.$$

If $\mathscr{T}_0^{D+F} < 1$, then fox and dingo free equilibrium is asymptotically stable and hence they extincts in near future.
(b) If $\mathscr{T}_0^{D+F} > 1$, this ensures the existence and stability of E^*, and hence the persistence of all the three species in the environment. This completes the proof.

2.6.2 With prey switching; Without movement of species

Theorem 2.6.2 *Let $\mathscr{T}_0^{D+F}$ be a threshold parameter. Then,*

(a) If $\mathscr{T}_0^{D+F} = \max\left\{\dfrac{b_2K}{d_2(a+K)}, \dfrac{e_2K}{d_3(1+KT_Q)}\right\} < 1$, both the predators for system (2.2.2), will tend to extinction that is, $F(t) \to 0, D(t) \to 0$ for $t \to +\infty$.
(b) If $\mathscr{T}_0^{D+F} > 1$, then all the three populations of system (2.2.2) persists .

Proof (a) Proceeding same as in Theorem 2.6.1, we have

$$\mathscr{F}_1 = \begin{pmatrix} \frac{b_2K}{a+K} & 0 \\ 0 & \frac{e_2K}{1+KT_Q} \end{pmatrix} \text{ and } \mathscr{V}_1 = \begin{pmatrix} d_2 & 0 \\ 0 & d_3 \end{pmatrix}$$

Then,

$$\mathscr{F}_1\mathscr{V}_1^{-1} = \begin{pmatrix} \frac{b_2K}{d_2(a+K)} & 0 \\ 0 & \frac{e_2K}{d_3(1+KT_Q)} \end{pmatrix}.$$

The threshold value for both predator extinction of the system (2.2.2), denoted by $\mathscr{T}_0^{F+D} = \rho(\mathscr{F}_1\mathscr{V}_1^{-1})$, is given by,

$$\mathscr{T}_0^{F+D} = \max\left\{\frac{b_2K}{d_2(a+K)}, \frac{e_2K}{d_3(1+KT_Q)}\right\}.$$

If $\mathscr{T}_0^{D+F} < 1$, then fox and dingo free equilibrium is asymptotically stable and hence they extincts in near future.
(b) If $\mathscr{T}_0^{D+F} > 1$, this ensures the existence and stability of E^*, and hence the persistence of all the three species in the environment. This completes the proof.

Theorem 2.6.3

(a) If $\mathcal{T}_0^F = \frac{1}{d_2}\left(\frac{b_2 d_3}{d_3 + ae_2 - ad_3T_Q} + \frac{pr(d_3 - e_2K + d_3KT_Q)\omega_1}{e_1K(e_2 - d_3T_Q)}\right) < 1$, *the foxes for system (2.2.2), will tend to extinction that is,* $F(t) \to 0$ *for* $t \to +\infty$.
(b) If $\mathcal{T}_0^F > 1$, *then fox population persists.*

Proof (a) Proceeding same as in Theorem 2.6.2, we have

$$\mathcal{F}_2 = \frac{b_2 d_3}{d_3 + ae_2 - ad_3T_Q} + \frac{pr(d_3 - e_2K + d_3KT_Q)\omega_1}{e_1K(e_2 - d_3T_Q)} \text{ and } \mathcal{V}_2 = d_2.$$

Then,

$$\mathcal{T}_0^F = \mathcal{F}_2\mathcal{V}_2^{-1} = \frac{1}{d_2}\left(\frac{b_2 d_3}{d_3 + ae_2 - ad_3T_Q} + \frac{pr(d_3 - e_2K + d_3KT_Q)\omega_1}{e_1K(e_2 - d_3T_Q)}\right).$$

If $\mathcal{T}_0^F < 1$, then fox free equilibrium is asymptotically stable and hence foxes extincts in near future.
(b) If $\mathcal{T}_0^F > 1$, then fox population will persist. Hence, the proof.

Theorem 2.6.4

(a) If $\mathcal{T}_0^D = \frac{1}{d_3}\left(\frac{a(b_1d_2(d_2 - b_2)e_2K + b_2(ad_2 - b_2K + d_2K)pr\omega_2)}{ab_2(ad_2 - b_2K + d_2K)prT_F - b_1(b_2 - d_2)K)}\right) < 1$, *the dingoes for system (2.2.2), will tend to extinction that is,* $D(t) \to 0$ *for* $t \to +\infty$.
(b) If $\mathcal{T}_0^D > 1$, *then dingo population persists.*

Proof (a) Proceeding same as in Theorem 2.6.2,

$$\mathcal{F}_3 = \frac{a(b_1d_2(d_2 - b_2)e_2K + b_2(ad_2 - b_2K + d_2K)pr\omega_2)}{ab_2(ad_2 - b_2K + d_2K)prT_F - b_1(b_2 - d_2)K)} \text{ and } \mathcal{V}_3 = d_3.$$

Then,

$$\mathcal{T}_0^D = \mathcal{F}_3\mathcal{V}_3^{-1} = \frac{1}{d_3}\left(\frac{a(b_1d_2(d_2 - b_2)e_2K + b_2(ad_2 - b_2K + d_2K)pr\omega_2)}{ab_2(ad_2 - b_2K + d_2K)prT_F - b_1(b_2 - d_2)K)}\right).$$

If $\mathcal{T}_0^D < 1$, then dingo free equilibrium is asymptotically stable and hence dingoes extincts in near future.
(b) If $\mathcal{T}_0^D > 1$, then dingo population will persist. Hence, the proof of Theorem 4.

Using this we may calculate the threshold for default parameters in Table 2.2: (i) varying $e_2 = 0.306$, we find that $\mathcal{T}_0^F = 0.197361 < 1$, and the fox extinction is observed (c.f.

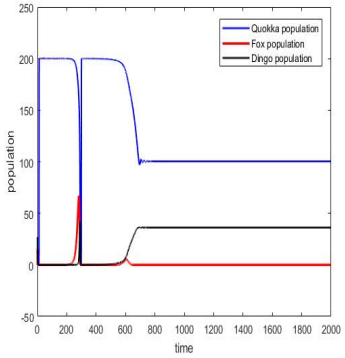

Figure 2.8: Fox population extincts for $e_2 = 0.306$, keeping all the other parameters as same in Table 2.2.

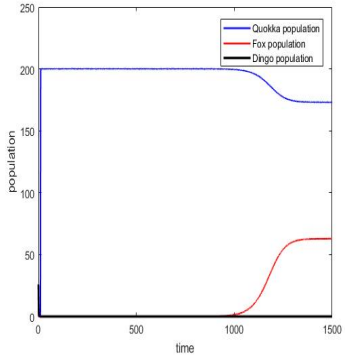

Figure 2.9: Dingo population extincts for $d_2 = 0.89$, keeping all the other parameters as same in Table 2.2.

Fig. 2.8); but (ii) if $d_2 = 0.89$, and all the other parameters are same as in Table 3, we find $\mathcal{T}_0^D = 0.975591 < 1$, the dingo population extinct and the other two persists (c.f. Fig. 2.9), (iii) $d_3 = 1.3$, $d_2 = 1.178$ and other parameter same as in (i), we find $\mathcal{T}_0^{D+F} = max\{0.773038, 0.8559\} = 0.8559 < 1$, we observe both the predator extinct i.e. global stability of E_1 is obtained (c.f. Fig. 2.10). Therefore, we conclude that if foxes act as specialist predator and only depends on quokka population for its growth and dingoes consumes both foxes (more preferable) and quokka, the fox population has high extinction risk while the quokka population has no extinction risk. Hence, the presence of alternative prey (foxes) for dingoes can prevent quokka from extinction. This simulation result is in agreement with the observation of Smith and Quin(1996), Hobbs (2001), Daniels and Corbett (2003), Peterson (1995). They reported that dingo population provide a net benefit to some threatened wildlife species through decreasing predating rates by the red fox. These simulation result is observed to be true for other food chain species also, for eg., the pine marten (*Martes martes*) in Scandinavia was found to increase after declination of the red fox, also removal of grey wolf increased coyote population and removal of coyote increases bobcat (*Lynx rufus*).

2.7 Some important numerical simulation

This section concentrates on numerical viability of the analytical results. Local and global behaviour of both ODE model are performed. Runge-Kutta fourth order method has been used to solve system (2.2.2) and been plotted by MATLAB taking initial condition as $(10, 15, 25)$. We observe that the dynamics of system (2.2.2) ranges from stable equilibrium, limit cycle to chaotic dynamics. Set of parameters used for numerical simulation are given in Table 2.2.

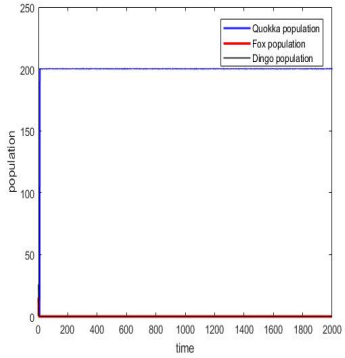

Figure 2.10: Extinction of fox and dingo population for $e_2 = 0.306$, $d_2 = 1.178$, $d_3 = 1.3$, keeping all the other parameters as same in Table 2.2.

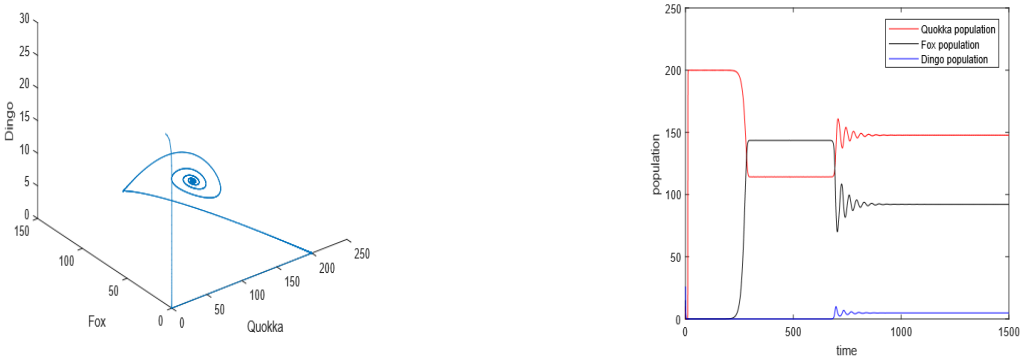

(a) phase portrait (b) time series

Figure 2.11: Stable attractor for the parameters given in Table 2.2.

For parameters as given in Table 2.2 we observe stable non-trivial equilibrium (c.f. Fig. 2.11) but as parameter 'a' being varied from 35 to 22, a limit cycle is observed (c.f. Fig. 2.12). Further, if we reduce $d_3 = 0.8162$ and keeping all the other parameters same; a chaotic behaviour has been seen (c.f. Fig. 2.13). The Lyapunov exponent is used to judge the problem of initial value sensitivity (or chaos phenomenon). If the exponent is positive, it means that the system is sensitive to the initial value and has chaos phenomenon. We calculated chaos indicator i.e. the largest Lyapunov exponent (LLE) for this set of parameters and found that LLE=1.12314. The LLE quantifies the exponential divergence of initially close state-space trajectories and estimates the amount of chaos in a system.

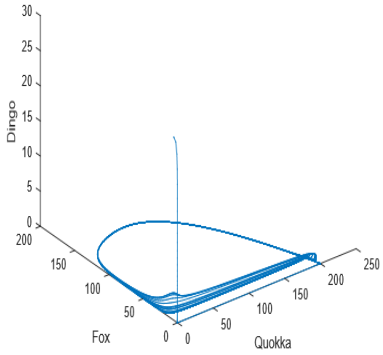

(a) phase portrait

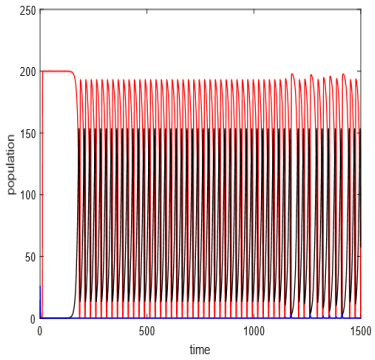

(b) time series

Figure 2.12: Limit cycle for $a = 22$; other parameters are same as in Table 2.2.

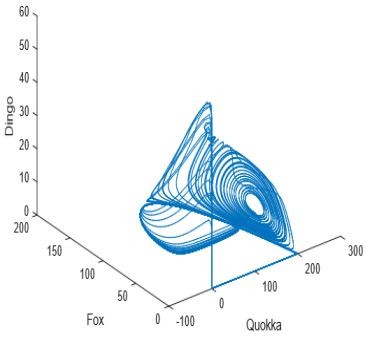

(a) phase portrait

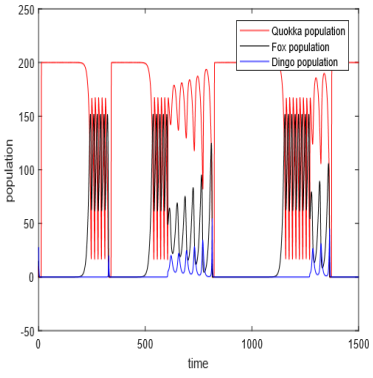

(b) time series

Figure 2.13: Observed chaotic dynamics for $a = 25$ and $d_3 = 0.8162$; other parameters as in Table 2.2.

2.7.1 Bifurcation analysis

We have used MATLAB Matcont toolbox for plotting equilibrium manifold of E^* and is presented in Fig. 2.14. The bifurcation diagram is generated by taking a, the extent to which environment provides refuges to quokka population as bifurcation parameter. A branch of equilibria E^* of system (2.2.2) is presented in Fig. 2.14. Considering other values of parameters as given in Table 3, and varying 'a' our model undergoes Hopf bifurcation at $a = a_c = 22.686843$ giving rise to a limit cycle. Hopf bifurcation is a point where the equilibrium changes its stability via a pair of purely imaginary eigenvalues, giving rise to a limit cycle from an equilibrium. Stable limit cycle are important biologically as it guarantees that the system oscillates even in absence of external periodic forcing.
When $a < a_c$ the unstable branch (not all eigen values has negative real part) is observed, as $a > a_c$, the branch becomes stable as a result of Hopf bifurcation.

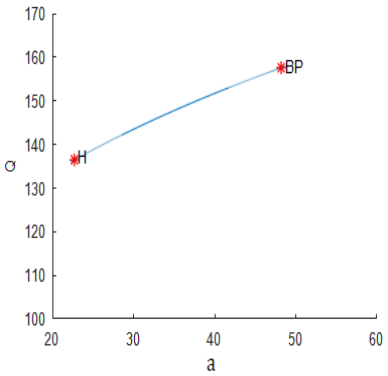

Figure 2.14: A branch of equilibria displaying the occurrence of Hopf bifurcation at $a = a_c = 22.686843$ in (a, Q) plane. H: denote a Hopf point, BP: denotes branch point. Other parameters are same as in Table 2.2

Remark 5 *This analysis shows that maintaining quokkas natural environment can allow all three species to coexists in a oscillatory way.*

2.8 Discussions and conclusions

Protecting biodiversity and nature conservation problem is an increasing public demand. The quokka population provides an excellent opportunity to improve our understanding about extinction dynamics in a changing world. The study of food-chain model can act as important tool for designing conservation policy of endangered species. In this research, we have proposed and analyzed a three species food-chain model consisting quokka, fox and dingo populations. The system has five equilibrium points. The non trivial equilibrium E^* is locally as well as globally asymptotically stable when certain conditions are

satisfied. Other equilibrium states are also determined and analysed for their stability. The existence of a Hopf bifurcation is established numerically. The result of computation and theoretical analysis shows that the model exhibits rich dynamics. We have also studied the reaction-diffusion model in two-dimensions and investigated its stability as well as established conditions for diffusion-driven instability. From our study it is clear that alternative prey source for top predator population can give us a stable predator-prey food chain model, opposite to the research article by Kumari (2013). From the analysis of this model we conclude that, if foxes depends only on quokka population for its survival, and further they are controlled by dingoes, the fox population has high extinction risk while the quokka population has no extinction risk. Glen et al. (2007) also verified this result experimentally that if dingoes can limit population of foxes, this might lead to expanded distribution of vulnerable prey species. Hence, the presence of dingoes can prevent quokka from extinction. Moreover, if the harvesting rate of quokka is greater than its intrinsic rate all the species of the food chain will eventually go to extinction. Hence, our study can open a new window of study in future. Our study shows that the quokka population will never get extinct, unless the external harvesting factors are too high.

Our numerical simulation suggests that to solve quokka conservation problem, we found that two predator species (foxes and dingoes) can survive in the same locality. Our numerical simulation for reaction-diffusion model suggest that areas where foxes and dingoes population are not present could be considered for quokka reintroduction. Human and spatial variables like hunting *Setonix brachyurus*, habitat destruction also plays a significant role in restricting the quokka number rather than the predation. Climate change could also be a factor in the decline of quokkas. It is hypothesized that all species range will be lost by the year 2070 in the most severe climate change scenario. Our main focus should be in learning how to restore the ecological conditions that allow quokka settlement and reproduction. We hope that our results will enhance the understanding of spatial food chain and tackle conservation problem. As the meta population is unlikely to restore itself given its low population sizes and recruitment rates; we emphasis that necessary administrative management is required. Clearly for this to occur, all threatening processes must be identified and removed to the possible extent. A proper surveillance should be carried out to ensure and detect changes in population size and structure. Our model and theory of quokka interaction with foxes and dingoes motivates us for long-term monitoring to show increasing population densities followed by a measure to increase environmental protection rate of quokka from foxes in order to maintain the oscillatory behaviour of three species.

Chapter 3

INVESTIGATING THE ROLE OF ZOOPLANKTON IN SUSTAINING FROG POPULATION

" What is there to life if a man cannot hear the lonely cry of a whippoorwill or the arguments of the frogs around a pond at night. "

-Chief Seattle

Content of this chapter has been published as:

- S. Jain and P. Roy. Investigating the role of zooplankton in sustaining frog population. Mathematical Methods in the Applied Sciences, 45(9):5423–5455, 2022, (Jain and Roy (2022)).

3.1 Introduction

One of the greatest evolution stories in Earth's history is owned by amphibians. Amphibians were evolved from lobe-finned fish named sarcopterygians around 395 million years ago. Amphibia is a cold blooded vertebrate species, characterized by four well-developed limbs for locomotion and are classified into three different clades; salamanders (Urodela), caecilians (Apoda) and frogs (Anura). Amphibians oxidate themselves both through buccal pumping and cutaneous respiration. Irrespective of their great survival history, an infectious disease called chytridiomycosis caused by an aquatic fungal pathogen is recently responsible for declination of several species of amphibian globally (Skerratt et al. (2007)). In Australia since 1970's, a sudden demise of amphibian species was observed. It leaded to the theory that some pathogen is wrecking Australian frogs (Laurance et al. (1996)). Later, it was found that infection through chytrid fungus effected approximately $6,000$ amphibian species and is linked to devastating population declines and species extinctions (Skerratt et al. (2007); Berger and Udell (1998); Fisher et al. (2009)). *Batrachochytrium dendrobatidis* and *Ichthyochytrium vulgare* are two species of chytrid fungus known to parasitize water species (Červinka et al. (1974); Plehn (1916); Schäperclaus (1992)), but B_d appears to be primarily responsible for amphibian extinction (Berger et al. (1998); Longcore et al. (1999)). Remarkably just over the past 30 years, B_d has caused the catastrophic decline of at least 200 species of frog. It is now widespread throughout the world leaving only few countries (Berger et al. (1998, 2009); Longcore et al. (1999); Skerratt et al. (2007)). The escalation of chytrid fungus in the population is further increased by human activities (like, the international pet trade), through environment (i.e., like windswept, etc.), direct contact between infected frogs and tadpoles, and also through exposure to infected water. Some frog species are not that sensitive to die from chytridiomycosis and may act as carriers (Daszak et al. (2004)). This tosses the idea that the execution of adverted translocation of infected frogs must be put to end.

In this research, consider Corroboree Frog (*Pseudophryne corroboree*); a small, vividly-coloured species that is restricted to Kosciuszko National Park, in the south-east of New South Wales. Chytridiomycosis has been implicated as reason of disappearance of this species as well and for that reason it is listed on the IUCN Red List as critically endangered. Because of rapid declination and loss of very important frog species; urgent efforts are needed to preserve frog species. Just like other amphibians mops water, they also absorbs various essential electrolytes (sodium, potassium, magnesium and chloride) by way of their thin, permeable skin. As B_d is keratinophilic, infecting the superficial layers of amphibian dermis containing keratin (Berger et al. (1998)), they have abnormally low level of these electrolytes in blood (suppresses their reflex); resulting in early death (Voyles et al.

(2007, 2009)). Also with chytridiomycosis, the infection leads to hyperkeratosis (thickening of keratinized layer of skin), which leads to scraping of considerable amount skin. Other amphibians like the lungless salamanders, breathe through the skin and due to chytridiomycosis over the skin obstruct respiration and hence cause suffocation. Its impact on amphibians has displayed "the most spectacular destruction of vertebrate biodiversity" in history.

Despite its severity no vaccines are currently available to mitigate the disease from all frog species. A study found that amphibians can acquire resistance to the fungus and can be immunised by contact with dead fungi, and can even learn to avoid exposing themselves to infectious fungi (McMahon et al. (2014)). Their survival is hoped from the vaccination programs which are still under trial. An experiment (on yellow legged frogs) was performed in University of California at Santa Barbara. The healthy frogs were vaccinated by spraying the fungus into their habitats and then treating them with anti-fungal before they die. When they were healthy again, they reinfected them by *Batrachochytrium dendrobatids*. Scientists found that all frogs that were immunized survived. Once immunization is induced, the hoppers are reintroduced to the wild and potentially reduce the spread of the fungus to the point that it goes locally extinct. Another possibility is to dump enough vaccine into ponds to induce an acquired immune response in the field. However, all frogs don't seem to be able to build immunity to chytrid like the yellow-legged frogs can. Therefore, there is a need to obtain other feasible cure for curbing the disease in the wild populations (Stice and Briggs (2010)). In captivity, different treatments have been attempted to diminish the infection like: rising temperature, making surrounded water briny (salty), by using various fungicides, and by coating skin with cultured bacteria that have anti-fungal properties (Garner et al. (2009); Young et al. (2007)). Thermal treatment is regarded as most functional for captive species (Young et al. (2007)). Chytridiomycosis can also be successfully treated with antifungal medications and by disinfection of contaminated enclosures (Pessier et al. (2010)); like the drug itraconazole has been used to medicate B_d-infected amphibians, by giving infected amphibians a shallow bath of itraconazole (Forzán et al. (2008); Garner et al. (2009); Nichols and Lamirande (2000)), or by introducing it orally (Young et al. (2007)). Another promising area of research is looking at the possibility of introducing symbiotic bacteria that inhibit the growth of B_d into wild amphibian populations (Harris et al. (2009)). Other methodology used for disease mitigation includes habitat modification and bio-augmentation.

Unfortunately, there are no satisfactory methods for the treatment of wild animals in the natural environment. It is very difficult or impossible to get enough of the antifungal medications into the environment to be able to successfully rid infected frogs from B_d.

Interestingly, researchers also discovered that zooplankton can act as biological control for this deadly fungus disease which is devastating for amphibian populations around the world (Buck et al. (2011)). Some evidences have been found that zooplankton can eat the zoospore, the free-swimming stage of the fungus. This biological control offers the best option to control this fungal disease. To the best of our knowledge, no one has attempted to mathematically validate this hypothesis so far. The aim of this chapter is to get a better understanding on how predation by zooplankton can act as biological control for the deadly chytrid fungus by developing a realistic mathematical model (deterministic, stochastic and reaction-diffusion), which can be used to describe the extinction dynamics of frog population in Australia. This research will make an original contribution to science, empowering the development of effective conservation management strategies for securing the frog population and for assisting biodiversity managers. Here we explore three key factors affecting the ongoing threatening processes of frog:

- How zooplankton can act as biological control?,
- Whether the presence of zooplankton is crucial for maintaining frog populations?, and
- What is the affect of fluctuating environments on such relationships?

This chapter is organised as follows: In Section 3.2, we formulated our model system. In Section 3.3, we studied the existence and stability of the equilibrium points for the formulated model. In Section 3.4, we will show existence and uniqueness of solution for stochastic model and asymptotic behaviour of our stochastic model around the endemic equilibrium (B_d, F_S, F_I, Z). In Section 3.5 , we consider a spatially explicit extension of our model. Section 3.6 evaluates the threshold for persistence of disease in frog population. Numerical simulation and comparison is provided in Section 3.7. Finally, conclusion is presented in Section 3.8.

3.2 Model formulation

3.2.1 Model without randomness

To start with, let us consider a simple model with only frog and B_d population. Our model takes up some assumptions for its formulation and is described in the following text. We considered all population grows logistically. Unlike some authors (Das and Chattopadhyay (2015)), we assumed infected frogs don't contribute to reproduction, nor do they compete with susceptible frogs for resources. This assumption is made on the fact that chytrid is a deadly disease and kills most frogs. Same assumptions were considered by Nandi et al.

(2015) and Cojocaru et al. (2020). The disease is transmitted by the contact between B_d and susceptible frog (F_S), and contact in between susceptible frog (F_S) and infected frog (F_I). We considered simple mass action for describing the transmission of disease among frogs from its population and through B_d. With the above assumptions, the model can be formulated as follows:

$$\begin{aligned}
\frac{dB_d}{dt} &= r_1 B_d \left(1 - \frac{B_d}{K_1}\right) - \beta_1 B_d, \\
\frac{dF_S}{dt} &= r_2 F_S \left(1 - \frac{F_S}{K_2}\right) - \lambda F_I F_S - \nu_{F_S} F_S B_d - h_1 F_S, \\
\frac{dF_I}{dt} &= \nu_{F_S} B_d F_S + \lambda F_I F_S - \mu_{F_I} F_I.
\end{aligned} \tag{3.2.1}$$

See Table 3.2 for complete description of parameter values.

However, chytrid fungus is not eliminated automatically from the environment. Zooplankton plays a vital role in naturally reducing chytrid fungus. The motive of this research is to give a safe and effective way to minimize chytrid fungus. Zooplankton can be considered a biological agent to remove *Batrachochytrium dendrobatidis* as there are no effective treatments available to reduce chytrid fungus. Itraconazole has proven efficacious in eliminating the infection, but using this antifungal causes skin depigmentation in tadpoles. Also, the water-soluble formulation of itraconazole is not widely available. Parker et al. (2002) proposed that treatment with formaldehyde and malachite green might be of use, but its adoption is questionable since formaldehyde is toxic, especially to tadpoles. Increasing the environmental temperature to 37° C (Woodhams et al. (2003)), although possibly effective for clearing infection in some host species, can not be tolerated by many amphibians. This research proposes safe and effective treatment against chytrid fungus by introducing zooplankton that does not harm other organisms in the aquatic environment.

To our knowledge no mathematical model has been proposed to validate the hypothesis of "reducing *Batrachochytrium dendrobatidis* infection among frog populations through predation by zooplankton". However, few experimental work has been done in this direction. Buck et al. (2011) performed an experiment and showed that B_d are consumed by zooplankton and supported his claim that zooplankton can act as potential biological control in mitigating the disease. Harris et al. (2009) placed frogs into a solution with J. lividum leading to the successful colonization of the skin. Nichols et al. (2000) performed a series of three experiments during March–October, 1998, on two species of captive bred poison dart frogs (*Dendrobates tinctorius* and *D. auratus*). Their experiments demonstrated that *Batrachochytrium dendrobatidis* can be a fatal pathogen in frogs. Woodhams et al. (2011) gave population level treatments based on three steps: (i) identifying mechanisms

of disease suppression; (ii) parameterizing epizootiological models of disease and population dynamics for testing under semi-natural conditions; and (iii) beginning a process of adaptive management in field trials with natural populations. They found that recognizing the opportunistic nature of *Bd* and combining this knowledge with epizootiological models, mitigation strategies can be designed to control disease without the need to completely eliminate the pathogen from the environment. Ackleh et al. (2016) developed a mathematical model of a frog population infected with chytridiomycosis, to investigate how the inoculation of *Janthinobacterium lividum* could reduce the impact of B_d disease on frogs. Motivated by these studies, we extended our model. In the extended model, we consider the *Batrachochytrium dendrobatidis* population (B_d), is predated by zooplankton (Z). Functional relationship between population are the central themes in mathematical ecology. In this chapter, we consider Holling type II functional response (Holling (1959)), which is associated with specialist predation for interaction between zooplankton and B_d population. Disease transmission occurs via zoospore that invades skin and grows into the parasitic zoosporangium. With this assumption, the model (3.2.1) becomes:

$$\begin{aligned}
\frac{dB_d}{dt} &= r_1 B_d \left(1 - \frac{B_d}{K_1}\right) - \frac{\beta_1 B_d Z}{\theta + B_d}, \\
\frac{dF_S}{dt} &= r_2 F_S \left(1 - \frac{F_S}{K_2}\right) - \lambda F_I F_S - \nu_{F_S} F_S B_d - h_1 F_S, \\
\frac{dF_I}{dt} &= \nu_{F_S} B_d F_S + \lambda F_I F_S - \mu_{F_I} F_I, \\
\frac{dZ}{dt} &= r_3 Z \left(1 - \frac{Z}{K_3}\right) + \frac{\beta_2 B_d Z}{\theta + B_d} - h_2 Z.
\end{aligned} \tag{3.2.2}$$

Letting $b_1 = \dfrac{r_1}{K_1}$, $b_2 = \dfrac{r_2}{K_2}$, $b_3 = \dfrac{r_3}{K_3}$, we have the following system of differential equation,

$$\begin{aligned}
\frac{dB_d}{dt} &= B_d \left(r_1 - b_1 B_d\right) - \frac{\beta_1 B_d Z}{\theta + B_d}, \\
\frac{dF_S}{dt} &= F_S \left(r_2 - b_2 F_S\right) - \lambda F_I F_S - \nu_{F_S} F_S B_d - h_1 F_S, \\
\frac{dF_I}{dt} &= \nu_{F_S} B_d F_S + \lambda F_I F_S - \mu_{F_I} F_I, \\
\frac{dZ}{dt} &= Z \left(r_3 - b_3 Z\right) + \frac{\beta_2 B_d Z}{\theta + B_d} - h_2 Z.
\end{aligned} \tag{3.2.3}$$

The schematic diagram for model system (3.2.3) is presented in Fig. 3.1. Also see Table 3.2 for complete description of parameter values for the considered model.

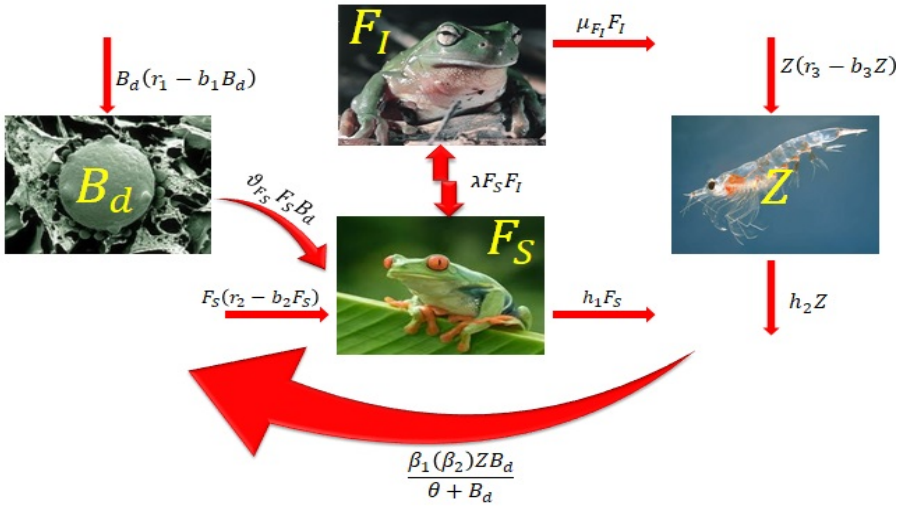

Figure 3.1: Schematic diagram for three species food model system (3.2.3).

3.2.2 Model with randomness

As water bodies are more vulnerable to be affected by environmental change by depleting the level of dissolved oxygen due to various interaction processes (Misra et al. (2006)), water temperature rise due to rising global warming, etc.. Here, an additional threat to the Southern Corroboree Frog is climate change. Chytridiomycosis is strongly mitigated by high temperatures (Berger et al. (2004); Piotrowski et al. (2004); Skerratt et al. (2007)). However, reduced precipitation and warmer temperatures ultimately affect breeding pools and vegetation around them. Drought results in egg and tadpole deaths, and as the frequency of drought increases with climate change, the ability for the Southern Corroboree Frog to recovery reduces greatly. Therefore, it is relevant and crucial to consider environmental stochasticity, which will have strong effect on the dynamics, and also, such systems behave in ways that are difficult for its deterministic equivalent to predict (Sharma et al. (2015)).

To take into account the effect of randomly fluctuating environment, we incorporate white noise. We assume fluctuations in the growth rate of frog, zooplankton and in contact rate of infected frogs with susceptible frogs.

$$r_1 \to r_1 + \sigma_1 dW_1(t),\ \lambda \to \lambda + \sigma_2 dW_2(t),\ r_3 \to r_3 + \sigma_3 dW_3(t),$$

where W_1, W_2, W_3 are mutually independent Brownian motions. σ_1, σ_2 and σ_3 represent the intensities of the white noise. Thus, the deterministic model (3.2.2) take the following

stochastic form,

$$\begin{aligned} dB_d &= \left(B_d\left(r_1 - b_1 B_d\right) - \frac{\beta_1 B_d Z}{\theta + B_d}\right) dt + \sigma_1 B_d dW_1(t), \\ dF_S &= \left(F_S\left(r_2 - b_2 F_S\right) - \lambda F_I F_S - \nu_{F_S} F_S B_d - h_1 F_S\right) dt - \sigma_2 F_S F_I dW_2(t), \\ dF_I &= (\nu_{F_S} B_d F_S + \lambda F_I F_S - \mu_{F_I} F_I)dt + \sigma_2 F_S F_I dW_2(t), \\ dZ &= \left(Z\left(r_3 - b_3 Z\right) + \frac{\beta_2 B_d Z}{\theta + B_d} - h_2 Z\right) dt + \sigma_3 Z dW_3(t), \end{aligned} \tag{3.2.4}$$

with $(B_d(0), F_S(0), F_I(0), Z(0)) \in \mathbb{R}^4_+$. Here $w = \{W_1(t), W_2(t), W_3(t) : t \geq 0\}$ represents the three dimensional standard Brownian motion defined on a complete probability space $\{\Omega, F, P\}$ with a filtration $\{F_t\}_{t\geq 0}$ satisfying the usual conditions. All parameters involved are assumed to be positive throughout this chapter.

3.2.3 Spatial dynamics via Reaction-diffusion model

One factor that makes the ecosystem dynamics spatial is the movement of organisms. In the marine environment, activity occurs because organisms either are attuned with the turbulent water flows or possess the ability to self-motion or because of the combined action of the two mechanisms (Sekerci and Petrovskii (2015)). Correspondingly, for this study, we consider an idealized reaction-diffusion system. The reaction-diffusion model describes the emergence of periodic patterns such as spots, stripes, and mazes on the surface of animal coats through chemical interaction among cells. However, it can also be used to understand the distribution of the species. To do this, we consider the following reaction-diffusion system:

$$\begin{aligned} \frac{\partial B_d}{\partial t} - H_{B_d}\nabla^2 B_d &= B_d\left(r_1 - b_1 B_d\right) - \frac{\beta_1 B_d Z}{\theta + B_d}, \\ \frac{\partial F_S}{\partial t} - H_{F_S}\nabla^2 F_S &= F_S\left(r_2 - b_2 F_S\right) - \lambda F_I F_S - \nu_{F_S} F_S B_d - h_1 F_S, \\ \frac{\partial F_I}{\partial t} - H_{F_I}\nabla^2 F_S &= \nu_{F_S} B_d F_S + \lambda F_I F_S - \mu_{F_I} F_I, \\ \frac{\partial Z}{\partial t} - H_Z\nabla^2 Z &= Z\left(r_3 - b_3 Z\right) + \frac{\beta_2 B_d Z}{\theta + B_d} - h_2 Z. \end{aligned} \tag{3.2.5}$$

for $(x, y) \in \Omega = [0, L] \times [0, L]$, $t > 0$, and with boundary conditions:

$$(\mathbf{n}.\nabla)B_d = (\mathbf{n}.\nabla)F_S = (\mathbf{n}.\nabla)F_I = (\mathbf{n}.\nabla)Z = 0,$$

Table 3.1: Description of parameter values used in model.

Variables/ parameters	Unit	Description
B_d	*Batrachochytrium dendrobatidis* per unit area	Density of *Batrachochytrium dendrobatidis population*
F_S	Susceptible frog per unit area	Density of Susceptible frog population
F_I	Infected frog per unit area	Density of Infected frog population
Z	Zooplankton per unit area	Density of Zooplankton population
r_1	Per day	Intrinsic growth rate of B_d population
r_2	Per day	Intrinsic growth rate of frog population
r_3	Per day	Intrinsic growth rate of zooplankton population
K_1	B_d per unit area	Carrying capacity of environment for B_d population
K_2	Frog per unit area	Carrying capacity of environment for the frog population
K_3	Zooplankton per unit area	Carrying capacity of environment for the zooplankton
θ	Per unit area	Measures of the extent to which environment provides refuges to B_d population, thus decreasing the maximum predation rate
λ	Per day	Contact rate of F_S and F_I
ν_{F_S}	Per day	Contact rate of F_S and B_d
μ_{F_I}	Per day	Death rate of infected frog, including all factors like natural death, death due to disease, harvesting etc.
β_1	Per day	Predation rate of Zooplankton
β_2	Per day	Biomass conversion rates of B_d to Z
h_1	Per day	Harvesting rate of frog
h_2	Per day	Harvesting rate of Zooplankton
σ_1	Per unit area	Intensities of the white noise in Bd
σ_2	Per unit area	Intensities of the white noise in frog
σ_3	Per unit area	Intensities of the white noise in zooplankton

and initial conditions:

$$\begin{aligned} B_d(x,y,0) &= B_d(0) > 0, \\ F_S(x,y,0) &= F_S(0) > 0, \\ F_I(x,y,0) &= F_I(0) > 0, \\ Z(x,y,0) &= Z(0) > 0, \end{aligned}$$

In system (3.2.5), ∇^2 represents Laplacian operator. In the above, the vector $\mathbf{n}$ is an outward unit normal vector to the boundary ($\partial\Omega$) of the habitat (Ω) and the homogeneous Neumann boundary conditions are considered. The homogeneous Neumann boundary conditions signify that the system is self-contained and there is no population flux across the boundary ($\partial\Omega$). This model is realistic as animals moves from one place to another in search of food and mate.

3.3 Stability analysis of model without randomness

3.3.1 Existence of equilibrium points

The Jacobian matrix corresponding to model (3.2.3) is given by:

$$\mathcal{J}(B_d, F_S, F_I, Z) = \begin{pmatrix} b_{11} & 0 & 0 & b_{14} \\ b_{21} & b_{22} & b_{23} & 0 \\ b_{31} & b_{32} & b_{33} & 0 \\ b_{41} & 0 & 0 & b_{44} \end{pmatrix} \tag{3.3.1}$$

where,

$$\begin{aligned}
b_{11} &= -2b_1 B_d + r_1 - \frac{\beta_1 \theta Z}{\left(B_d + \theta\right)^2}, \\
b_{14} &= -\frac{B_d \beta_1}{B_d + \theta}, \\
b_{21} &= -F_S \nu_{F_S}, \\
b_{22} &= -2b_2 F_S - h_1 - F_I \lambda - B_d \nu_{F_S} + r_2, \\
b_{23} &= -F_S \lambda, \\
b_{31} &= F_S \nu_{F_S}, \\
b_{32} &= F_I \lambda + B_d \nu_{F_S}, \\
b_{33} &= F_S \lambda - \mu_{F_I}, \\
b_{41} &= \frac{\beta_2 \theta Z}{\left(B_d + \theta\right)^2}, \\
b_{44} &= -h_2 + r_3 + \frac{B_d \beta_2}{B_d + \theta} - 2b_3 Z.
\end{aligned}$$

Lemma 3.3.1 *The formulated model* (2.3.8) *has following possible equilibrium points:*

- *The trivial equilibrium point, E_0 = (0,0,0,0), always exists.*
- *The infection free equilibrium, $E_1 = \left(0, 0, 0, \frac{r_3 - h_2}{b_3}\right)$, exists if $h_2 < r_3$.*
- *The B_d persisting equilibrium, $E_2 = \left(\frac{r_1}{b_1}, 0, 0, 0\right)$, always exists.*
- *Susceptible frogs persisting equilibrium, $E_3 = \left(0, \frac{r_2 - h_1}{b_2}, 0, 0\right)$, exists if $h_1 < r_2$.*
- *Frog persisting equilibrium, $E_4 = \left(0, \frac{\mu_{F_I}}{\lambda}, \frac{\lambda r_2 - h_1\lambda - b_2\mu_{F_I}}{\lambda^2}, 0\right)$, which exists if $h_1 < r_2$ and $b_2 < \frac{\lambda(r_2 - h_1)}{\mu_{F_I}}$.*
- *The disease free equilibrium, $E_5 = \left(0, \frac{r_2 - h_1}{b_2}, 0, \frac{r_3 - h_2}{b_3}\right)$, exists if $h_1 < r_2$ and $h_2 < r_3$.*
- *The B_d free equilibrium, $E_6 = \left(0, \frac{\mu_{F_I}}{\lambda}, \frac{\lambda r_2 - h_1\lambda - b_2\mu_{F_I}}{\lambda^2}, \frac{r_3 - h_2}{b_3}\right)$, which exists if $h_2 < r_3$, $h_1 < r_2$ and$b_2 < \frac{\lambda(r_2 - h_1)}{\mu_{F_I}}$.*
- *The zooplankton free equilibrium, $E_7 = (B_d^7, F_S^7, F_I^7, 0)$, exists if $h_1 < r_2$ and $b_1 > \frac{\nu_{F_S} r_1}{r_2 - h_1}$,*

  where, $B_d^7 = \frac{r_1}{b_1}$, $F_S^7 = \frac{b_1(-h_1\lambda + r_2\lambda + b_2\mu_{F_I}) - p}{2b_1 b_2 \lambda}$,

  $$F_I^7 = \frac{-b_1(h_1\lambda - r_2\lambda + b_2\mu_{F_I}) - 2r_1\lambda\nu_{F_S} + p}{2b_1\lambda^2} \text{ and}$$

  $$p = \sqrt{b_1(b_1(h_1\lambda - r_2\lambda + b_2\mu_{F_I})^2 + 4b_2 r_1 \lambda \mu_{F_I}\nu_{F_S})}.$$

- *The zooplankton free equilibrium, $E_8 = (B_d^8, F_S^8, F_I^8, 0)$, exists if $b_2 < \frac{(r_2 - h_1)\lambda}{\mu_{F_I}}$ and $b_1 \geq \frac{4b_2 r_1 \lambda \mu_{F_I}\nu_{F_S}}{(r_2\lambda - h_1\lambda - b_2\mu_{F_I})^2}$*

  where, $B_d^8 = \frac{r_1}{b_1}$, $F_S^8 = \frac{b_1(-h_1\lambda + r_2\lambda + b_2\mu_{F_I}) + p}{2b_1 b_2 \lambda}$,

$$F_I^8 = \frac{-b_1(h_1\lambda - r_2\lambda + b_2\mu_{F_I}) - 2r_1\lambda\nu_{F_S} - p}{2b_1\lambda^2}.$$

- *The equilibrium $E^* = (B_d^*, F_S^*, F_I^*, Z^*)$, which exist if all of the components are positive.*

3.3.2 Local stability analysis of equilibrium points

Theorem 3.3.2 *The equilibrium point E_0 is always unstable.*

Proof The corresponding eigenvalues to Jacobian matrix (3.3.1) are r_1, $r_2 - h_1$, $-\mu_{F_I}$ and $r_3 - h_2$. Thus, the trivial equilibrium is always unstable. Suggesting that, extinction of infection, frogs and zooplankton, all together is never possible in real world scenario.

Theorem 3.3.3 *The Equilibrium point $E_1 = \left(0, 0, 0, \frac{r_3 - h_2}{b_3}\right)$, is locally asymptotically stable if*

$$h_1 > r_2 \quad \text{and} \quad b_3 < \frac{\beta_1 (r_3 - h_2)}{r_1\theta}. \tag{3.3.2}$$

Proof The corresponding eigenvalues to Jacobian matrix (3.3.1) are $-\mu_{F_I}$, $h_3 - r_3$, $-h_1 + r_2$ and $r_1 + \frac{\beta_1(h_2 - r_3)}{b_3\theta}$. Thus, under (3.3.2) E_1 is stable. Biologically it says that, if harvesting rate of frog is greater than its growth rate and, $b_3 = \frac{r_3}{K_3}$ is less than certain value, then infection and frog population extincts.

Theorem 3.3.4 *The Equilibrium point $E_2 = \left(\frac{r_1}{b_1}, 0, 0, 0\right)$, is locally asymptotically stable if*

$$r_2 < h_1 \text{ and } r_3 + \frac{\beta_2 r_1}{r_1 + b_1\theta} < h_2. \tag{3.3.3}$$

Proof The corresponding eigenvalues to Jacobian matrix (3.3.1) are $-r_1$, $-\mu_{F_I}$, $-h_1 - \frac{\nu_{F_S} r_1}{b_1} + r_2$ and $r_3 + \frac{\beta_2 r_1}{r_1 + b_1\theta} - h_2$. Thus, under (3.3.3) E_2 is stable. Biologically, it means if growth rate of both frog and zooplankton are less than its harvesting rate respectively both the population will extinct leaving B_d to grow logistically till its carrying capacity.

Theorem 3.3.5 *The Equilibrium point $E_3 = \left(0, \frac{r_2 - h_1}{b_2}, 0, 0\right)$, is always unstable.*

Proof The corresponding eigenvalues to variational matrix (3.3.1) are r_1, $h_1 - r_2$, $-h_2 + r_3$ and $-\mu_{F_I} + \frac{\lambda(r_2 - h_1)}{b_2}$. Thus, E_3 is always unstable. Biologically, it means only

susceptible frog cannot survive in the long run.

Theorem 3.3.6 *The Equilibrium point* $E_4 = \left(0, \frac{\mu_{F_I}}{\lambda}, \frac{-h_1\lambda - b_2\mu_{F_I} + \lambda r_2}{\lambda^2}, 0\right)$, *is always unstable.*

Proof The corresponding eigenvalues to Jacobian matrix (3.3.1) are r_1, $\frac{-b_2\mu_{F_I} \pm \sqrt{\mu_{F_I}}\sqrt{4h_1\lambda^2 + {b_2}^2\mu_{F_I} + 4b_2\lambda\mu_{F_I} - 4\lambda^2 r_2}}{2\lambda}$ and $r_3 - h_2$. Thus, E_4 is unstable. Biologically, frog population cannot survive alone in the long run.

Theorem 3.3.7 *The Equilibrium point* $E_5 = \left(0, \frac{r_2 - h_1}{b_2}, 0, \frac{r_3 - h_2}{b_3}\right)$, *is locally asymptotically stable if*

$$h_2 < r_3, \quad h_1 < r_2, \quad b_3 < \frac{\beta_1 (r_3 - h_2)}{r_1\theta} \quad \text{and} \quad b_2 > \frac{\lambda (r_2 - h_1)}{\mu_{F_I}}. \tag{3.3.4}$$

Proof The corresponding eigenvalues to Jacobian matrix (3.3.1) are $h_1 - r_2$, $h_2 - r_3$, $r_1 + \frac{\beta_1\left(h_2 - r_3\right)}{b_3\theta}$ and $-\mu_{F_I} + \frac{\lambda\left(r_2 - h_1\right)}{b_2}$. Thus, under (3.3.4) E_5 is stable. Biologically it means, if we keep harvesting rate lower than the species growth rate, disease free situation may prevail.

Theorem 3.3.8 *The Equilibrium point* $E_6 = \left(0, \frac{\mu_{F_I}}{\lambda}, \frac{-h_1\lambda - b_2\mu_{F_I} + \lambda r_2}{\lambda^2}, \frac{-h_2 + r_3}{b_3}\right)$, *is locally asymptotically stable if*

$$h_2 < r_3, \quad b_3 < \frac{\beta_1 (-h_2 + r_3)}{r_1\theta}, \quad \text{and} \quad \frac{4\lambda^2 (-h_1 + r_2)}{b_2 (b_2 + 4\lambda)} \leq \mu_{F_I}. \tag{3.3.5}$$

Proof The corresponding eigenvalues to variational matrix (3.3.1) are $h_2 - r_3$, $r_1 + \frac{\beta_1\left(h_2 - r_3\right)}{b_3\theta}$ and $\frac{-b_2\mu_{F_I} \pm \sqrt{\mu_{F_I}}\sqrt{4h_1\lambda^2 + {b_2}^2\mu_{F_I} + 4b_2\lambda\mu_{F_I} - 4\lambda^2 r_2}}{2\lambda}$. Thus, under (3.3.5) E_6 is stable.

Theorem 3.3.9 *The Equilibrium point* $E_7 = (B_d^7, F_S^7, F_I^7, 0)$, *is locally asymptotically stable if eigenvalues of variational matrix* V_7 *are negative.*

Proof The corresponding eigenvalues to Jacobian matrix (3.3.1) are $-r_1$, $r_3 - h_2 + \frac{\beta_2 r_1}{r_1 + b_1\theta}$ and $\frac{b_1 p(-b_2 + \lambda) + b_1^2((h_1 - r_2)(b_2 - \lambda)\lambda - b_2(b_2 + \lambda)\mu_{F_I}) \pm s}{4b_1^2 b_2\lambda}$, where,
$s = \sqrt{b_1^2(((-b_2 + \lambda)(p + b_1(h_1 - r_2)\lambda) + b_1 b_2(b_2 + \lambda)\mu_{F_I})^2 + 8b_2 p\lambda(p + b_1(h_1\lambda - r_2\lambda - b_2\mu_{F_I})))}$.
Thus, E_7 is asymptotically stable if all the eigenvalues are negative.

Theorem 3.3.10 *The Equilibrium point* $E_8 = (B_d^8, F_S^8, F_I^8, 0)$, *is locally asymptotically*

stable if eigenvalues of variational matrix are negative.

Proof The corresponding eigenvalues to variational matrix (3.3.1) are $-r_1,\ -h_2+r_3+\dfrac{\beta_2 r_1}{r_1+b_1\theta}$ and $\dfrac{b_1p(-b_2+\lambda)+b_1^2((h_1-r_2)(b_2-\lambda)\lambda-b_2(b_2+\lambda)\mu_{F_I})\pm q}{4b_1^2b_2\lambda}$, where,
$q=\sqrt{b_1^2(((b_2-\lambda)(p+b_1(-h_1+r_2)\lambda)+b_1b_2(b_2+\lambda)\mu_{F_I})^2+8b_2p\lambda(p+b_1(-h_1\lambda+r_2\lambda+b_2\mu_{F_I})))}$.
Thus, E_8 is asymptotically stable if all the eigenvalues are negative.

Theorem 3.3.11 *The equilibrium $E^*=(B_d^*,F_S^*,F_I^*,Z^*)$, is asymptotically stable if*
(i) $r_1\le\dfrac{Z^*\beta_1\theta}{(B_d{}^*+\theta)^2},\ r_2\le 2b_2F_S{}^*+F_I{}^*\lambda+B_d{}^*\nu,\ F_S{}^*\lambda<\mu,\ h_3\ge r_3+\dfrac{B_d{}^*\beta_2}{B_d{}^*+\theta}$,
(ii) $A_1A_2A_3>A_3^2+A_1^2A_4$,
where,

$$\begin{aligned}
A_1 &= -(b_{11}+b_{22}+b_{33}+b_{44}),\\
A_2 &= -b_{23}b_{32}+b_{22}b_{33}-b_{14}b_{41}+(b_{22}+b_{33})b_{44}+b_{11}(b_{22}+b_{33}+b_{44}),\\
A_3 &= b_{14}(b_{22}+b_{33})b_{41}+b_{23}b_{32}b_{44}-b_{22}b_{33}b_{44}+b_{11}(b_{23}b_{32}-b_{22}b_{33}-(b_{22}+b_{33})b_{44}),\\
A_4 &= (b_{23}b_{32}-b_{22}b_{33})(b_{14}b_{41}-b_{11}b_{44}).
\end{aligned}$$

Proof The characteristic equation corresponding to variational matrix (3.3.1) around $E^*(B_d^*,F_S^*,F_I^*,Z^*)$ is given by

$$\Lambda^4+A_1\Lambda^3+A_2\Lambda^2+A_3\Lambda+A_4=0,$$

By Routh–Hurwitz conditions, E^* is locally asymptotically stable if $A_1>0,\ A_2>0,\ A_3>0,\ A_4>0$ and $A_1A_2A_3-A_3^2-A_1^2A_4>0$.

For our model, $A_1>0,\ A_2>0,\ A_3>0$ and $A_4>0$ if conditions (i) of theorem are satisfied. So, E^* is locally asymptotically stable if conditions (i) and (ii) holds true.
Hence, the proof.

Example 3.3.1 *If we set the parameter of model (2.2.2) as* $r_1=2.5, r_2=1.911, r_3=1.2361, K_1=350, K_2=500, K_3=200, \beta_1=2.512, \beta_2=1.932, \theta=10, \lambda=0.31, \mu_{F_I}=0.891, \nu_{F_S}=2.291, h_1=0.431, h_2=1.199$*, we see that the hurwitz conditions are satisfied (as* $A_1=0.2227>0, A_2=1.1088>0, A_3=0.0435>0, A_4=0.0627>0$*, and* $A_1A_2A_3-A_3^2-A_1^2A_4=0.0057>0$*). Hence, the equilibrium point* $(B_d^*,F_S^*,F_I^*,Z^*)=(0.1321,2.2827,3.7693,10.0799)$ *is locally asymptotically stable, can be seen in Fig. 3.2.*

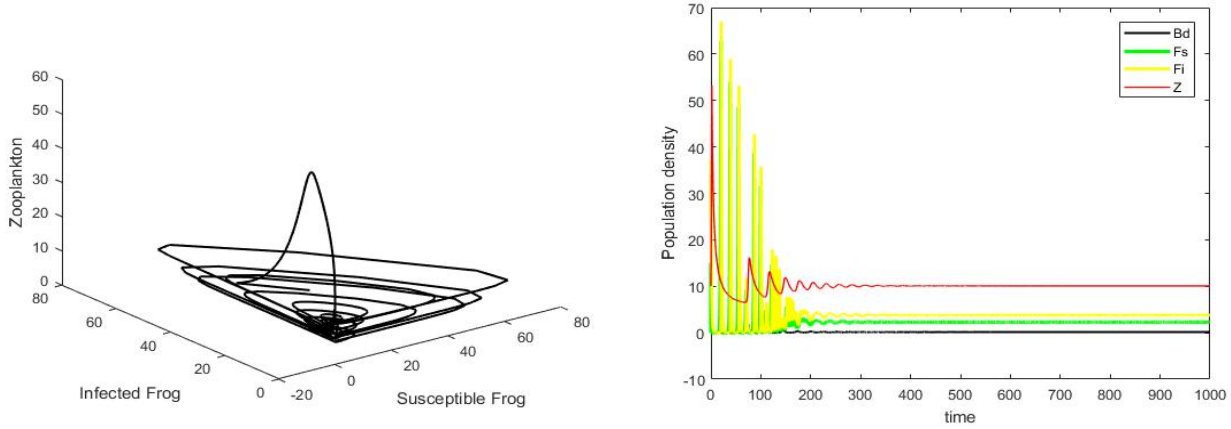

(a) phase portrait (b) time series

Figure 3.2: Stable attractor for the parameters given in Table 2.

3.4 Existence and uniqueness of positive solution for stochastic system

When we analyze deterministic system, we seek the constant equilibrium population and then investigate its stability. While for stochastic system (3.2.4), there is no positive time independent equilibrium point as a solution of corresponding equation. In this chapter, we explore the stability in time average.

Since, (3.2.4) represents a population system, it is necessary to prove that the solution does not explode at a finite time. To prove the solution is positive and does not explode at finite time, we use the stochastic comparison theorem. Let $X(t) = (B_d(t), F_S(t), F_I(t), Z)^T$ and $\mathbb{R}^4 = \{X(t) \in \mathbb{R}^4 : 0 < B_d(t), F_S(t), F_I(t), Z(t),\ t \geq 0\}$.

Theorem 3.4.1 *For any given initial value* $(B_{d0}, F_{S0}, F_{I0}, Z_0) \in \mathbb{R}^4_+$ *model (3.2.4) has unique global positive solution* $(B_d(t), F_S(t), F_I(t), Z(t))$ *for* $t \geq 0$*, that is,* $(B_d(t), F_S(t), F_I(t), Z(t)) \in \mathbb{R}^4_+$ *with probability one for* $t \in [0, \infty)$.

Proof Consider the following system:

$$du_1 = \left(\left(r_1 - b_1 e^{u_1(t)}\right) - \frac{\beta_1 e^{u_4(t)}}{\theta + e^{u_1(t)}} - \frac{\sigma_1^2}{2}\right) dt + \sigma_1 dW_1(t), \tag{3.4.1}$$

$$du_2 = \left(\left(r_2 - b_2 e^{u_2(t)}\right) - \lambda e^{u_3(t)} - \nu_{F_S} e^{u_1(t)} - h_1 + \frac{\sigma_2^2}{2}\right) dt - \sigma_2 e^{u_3(t)} dW_2(t), \tag{3.4.2}$$

$$du_3 = \left(\frac{\nu_{F_S} e^{u_1(t)} e^{u_2(t)}}{e^{u_3(t)}} + \lambda e^{u_2(t)} - \mu_{F_I} - \frac{\sigma_2^2}{2}\right) dt + \sigma_2 e^{u_2(t)} dW_2(t), \tag{3.4.3}$$

$$du_4 = \left(\left(r_3 - b_3 e^{u_4(t)}\right) + \frac{\beta_2 e^{u_1(t)}}{\theta + e^{u_1(t)}} - h_2 - \frac{\sigma_3^2}{2}\right) dt + \sigma_3 dW_3(t), \tag{3.4.4}$$

with initial value $(u_1(0), u_2(0), u_3(0), u_4(0)) = (lnB_{d0}, lnF_{S0}, lnF_{I0}, lnZ_0)$. Obviously, the coefficients of system (3.4.1)-(3.4.4) are locally Lipschitz continuous. Thus, there is a unique maximal local solution $(u_1(t), u_2(t), u_3(t), u_4(t))$ of system (3.4.1)-(3.4.4) for $t\epsilon[0, \tau_e)$, where τ_e denotes the explosion time. Let $B_d(t) = e^{u_1(t)}, F_S(t) = e^{u_2(t)}, F_I(t) = e^{u_3(t)}, Z(t) = e^{u_4(t)}$. Using Itô formula, it follows that $(B_d(t), F_S(t), F_I(t), Z(t)) = (e^{u_1(t)}, e^{u_2(t)}, e^{u_3(t)}, e^{u_4(t)})$ is the unique positive local solution of system (3.2.4) with initial value $(B_{d0}, F_{S0}, F_{I0}, Z_0)$ for $t \in [0, \tau_e)$. Next, we show $(u_1(t), u_2(t), u_3(t), u_4(t))$ is a global solution of (3.4.1)-(3.4.4), i.e. $\tau_e = \infty$. Since the solution is positive, we have

$$dB_d \leq B_d(r_1 - b_1 B_d)dt + \sigma_1 B_d dW_1(t),$$

Let

$$\phi_1(t) = \frac{e^{\left(r_1 - \frac{\sigma_1^2}{2}\right)t + \sigma_1 W_1(t)}}{\frac{1}{B_{d0}} + b_1 \int_0^t e^{\left(r_1 - \frac{\sigma_1^2}{2}\right)s + \sigma_1 W_1(s)} ds}$$

then $\phi_1(t)$ is the unique solution of the equation

$$\begin{aligned} d\phi_1(t) &= \phi_1(t)(r_1 - b_1\phi_1(t))dt + \sigma_1\phi_1(t)dW_1(t), \\ \phi(0) &= B_{d0}, \end{aligned}$$

and by the comparison theorem for stochastic equations, we have $B_d(t) \leq \phi_1(t), t \in [0, \tau_e)$, a.s.

Now, adding 2nd and 3rd equation of system (3.2.4) and considering, $F = F_S + F_I$ we have

$$\begin{aligned} d(F_S + F_I) &= F_S(r_2 - b_2 F_S) - h_1 F_S - \mu_{F_I} F_I, \\ dF &\leq F(r_2 - b_2 F). \end{aligned}$$

By the arguments as above,

$$F(t) \leq \phi_2(t), \quad t \in [0, \tau_e), \quad a.s.$$

This implies,

$$F_S(t) \leq \phi_2(t), \tag{3.4.5}$$

$$F_I(t) \leq \phi_2(t), \quad t \in [0, \tau_e), \quad a.s. \tag{3.4.6}$$

where

$$\phi_2(t) = \frac{r_2}{b_2 + F(0)r_2 e^{-r_2 t}},$$

Now, we have

$$dZ(t) \leq Z(r_3 - h_2 - b_3 Z + \beta_2 \phi_1)dt + \sigma_3 Z(t) dW_3.$$

Similarly, we can get

$$Z(t) \leq \phi_3(t), \quad t \in [0, \tau_e), \quad a.s.$$

where

$$\phi_3(t) = \frac{e^{\left(r_3 - h_2 - \frac{\sigma_3^2}{2}\right)t + \beta_2 \int_0^t \phi_1(s)ds + \sigma_3 W_3(t)}}{\frac{1}{Z_0} + b_3 \int_0^t e^{\left(r_3 - h_2 - \frac{\sigma_1^2}{2}\right)s + \beta_2 \int_0^t \phi_1(s)ds + \sigma_3 W_3(s)} ds},$$

Now, consider the following

$$dB_d \geq B_d \left(r_1 - b_1 B_d - \frac{\beta_1 \phi_3}{\theta}\right) dt + \sigma_1 B_d dW_1(t).$$

Obviously,

$$\xi_1(t) = \frac{e^{\left(r_1 - \frac{\sigma_1^2}{2}\right)t - \frac{\beta_1}{\theta}\int_0^t \phi_3(s)ds + \sigma_1 W_1(t)}}{\frac{1}{B_{d0}} + b_1 \int_0^t e^{\left(r_1 - \frac{\sigma_1^2}{2}\right)s - \frac{\beta_1}{\theta}\int_0^s \phi_3(u)du + \sigma_1 W_1(s)} ds},$$

is the solution of

$$\begin{aligned} d\xi_1(t) &= \xi_1 \left(r_1 - b_1 \xi_1 - \frac{\beta_1 \phi_3}{\theta}\right) dt + \sigma_1 \xi_1 dW_1(t), \\ \xi_1(0) &= B_d(0), \end{aligned}$$

Then, from the comparison theorem of stochastic differential equation, it follows that $B_d(t) \geq \xi_1(t)$ for $t \in [0, \tau_e)$. Also,

$$dF_S \geq F_S \left(r_2 - b_2 F_S - \lambda \phi_2 - \nu_{F_S} \phi_1 - h_1\right) dt - \sigma_2 F_S F_I dW_2(t).$$

Then, from the comparison theorem of stochastic differential equation, it follows that $F_S(t) \geq \xi_2(t)$ for $t \in [0, \tau_e)$,

where

$$\xi_2(t) = \frac{e^{\left(r_2 - h_1 - \frac{\sigma_2^2}{2}\right)t - \int_0^t \lambda\phi_2(s) - \nu_{F_S}\phi_1(s)ds + \sigma_1 W_1(t)}}{\frac{1}{F_{S_0}} + b_2 \int_0^t e^{\left(r_2 - h_1 - \frac{\sigma_2^2}{2}\right)t - \int_0^s (\lambda\phi_2(u) - \nu_{F_S}\phi_1(u))du + \sigma_1 W_1(s)} ds}.$$

Similarly,

$$dF_I \geq F_I\left(\lambda\xi_2 - F_I - \mu_{F_I}\right)dt + \sigma_2 F_S F_I dW_2(t).$$

Then, from the comparison theorem of stochastic differential equation, it follows that $F_I(t) \geq \xi_3(t)$ for $t \in [0, \tau_e)$,
where,

$$\xi_3(t) = \frac{e^{\left(-\frac{\sigma_2^2}{2} - \mu_{F_I}\right)t + \int_0^t \lambda\xi_2(s)ds + \sigma_2 W_2(t)}}{\frac{1}{F_{I_0}} + \int_0^t e^{\left(-\frac{\sigma_2^2}{2} - \mu_{F_I}\right)t + \int_0^s (\lambda\xi_2(u))du + \sigma_2 W_2(s)} ds}$$

Similarly,

$$dZ \geq Z\left(r_3 - b_3 Z - h_2\right)dt + \sigma_3 Z dW_3(t).$$

By argument as above, we get $Z(t) > \xi_4(t)$,
where,

$$\xi_4(t) = \frac{e^{\left(r_3 - h_2 - \frac{\sigma_3^2}{2}\right)t + \sigma_3 W_3(t)}}{\frac{1}{Z_0} + b_3 \int_0^t e^{\left(r_3 - h_2 - \frac{\sigma_3^2}{2}\right)s + \sigma_3 W_3(s)} ds}.$$

Thus, for $t \in [0, \tau_e)$

$$\begin{aligned} 0 &< \xi_1(t) \leq B_d \leq \phi_1(t), \\ 0 &< \xi_2(t) \leq F_S \leq \phi_2(t), \\ 0 &< \xi_3(t) \leq F_I \leq \phi_2(t), \end{aligned}$$

$$0 \;<\; \xi_4(t) \leq Z \leq \phi_4(t).$$

Since, $ln\xi_i(t)$ $(i = 1, 2, 3, 4)$ and $ln\phi_j(t)$ $(i = 1, 2, 3)$ exist for every $t \geq 0$, it follows that $\tau_e = \infty$. Thus, for any initial value $(u_1(0), u_2(0), u_3(0), u_4(0)) = (lnB_{d0}, lnF_{S0}, lnF_{I0}, lnZ_0) \in \mathbb{R}^4$, and (3.4.1)-(3.4.4) has a unique global solution $(u_1(t), u_2(t), u_3(t), u_4(t))$ on $[0, \infty)$ a.s. Note that the coefficients of (3.4.1)-(3.4.4) are local Lipschitz continuous. Therefore, for any initial value $(B_{d0}, F_{S0}, F_{I0}, Z_0) \in \mathbb{R}^4_+$, model has a unique global positive solution $(B_d, F_S, F_I, Z) = (e^{u_1(t)}, e^{u_2(t)}, e^{u_3(t)}, e^{u_4(t)})$ on $[0, \infty)$ a.s. The proof is therefore complete.

The following theorem shows the existence of a B_d and zooplankton-free equilibrium point E_4.

Theorem 3.4.2 *If* $r_1 - \dfrac{\sigma_1^2}{2} < 0, r_3 - h_2 + \beta_2 < 0$, *then the system* (3.2.4) *is globally asymptotically stable, in the sense that for any initial value* $X_0 \in \Omega$, *the solution* $X(t)$ *will tend to the equilibrium point* E_4 *asymptotically with probability one.*

Proof We consider the first equation of system (3.2.4). Thus, for $B_d(t)$, if $B_d(0) > 0$, we can use the function $V_1(t) = ln(B_d(t))$, with $B_d(t) \in (0, 1)$. Applying Itô's formula, one obtains that

$$\begin{aligned} dV_1(t) &= dB_d - \frac{1}{2}\sigma_1^2 dt, \\ &= \left((r_1 - b_1 B_d) - \frac{\beta_1 Z}{(\theta + B_d)} - \frac{1}{2}\sigma_1^2\right) dt + \sigma_1 dW_1(t). \end{aligned}$$

Then,

$$\int_0^t dV_1(t) = \int_0^t \left(r_1 - b_1 B_d - \frac{\beta_1 Z}{(\theta + B_d)} - \frac{1}{2}\sigma_1^2\right) ds + \int_0^t \sigma_1 dW_1(s),$$

Using the fact that $\lim_{t\to\infty} \dfrac{W_1(t)}{t} = 0$ a.s., one gets $\lim_{t\to\infty} \dfrac{1}{t} lnB_d(t) = \theta_1 < 0$ a.s., where $\theta_1 = r_1 - \dfrac{\sigma_1^2}{2}$. Then one obtains that $B_d(t) \leq e^{\theta_1 t}$, for all $t \geq 0$, a.s. Since, $B_d(t) > 0$, for all $t \geq 0$ a.s., we get

$$\lim_{t\to\infty} B_d = 0,$$

a.s.

Now, from adding adding 2^{nd} and 3^{rd} equation of system (3.2.4) and considering $F =$

$F_S + F_I$, it follows that

$$\begin{aligned} \frac{dF_s + dF_I}{dt} &= F_S(r_2 - b_2 F_S) - h_1 F_S - \mu_{F_I} F_I, \\ \frac{dF}{dt} &\leq F(r_2 - b_2 F). \end{aligned}$$

Thus,

$$F(t) \leq \frac{r_2}{b_2 + F(0) r_2 e^{-r_2 t}},$$

for all $t \geq 0$, a.s. Since, $F > 0$, for all $t \geq 0$ a.s., we get $lim_{t\to\infty} F = \frac{r_2}{b_2}$, a.s.
Now, we can use the function $V_3(t) = ln(Z(t))$, with $Z(t) \in (0, 1)$. Applying Itô formula, one obtains that,

$$\begin{aligned} dV_3(t) &= dZ - \frac{1}{2}\sigma_3^2 dt, \\ &= \left((r_3 - b_3 Z) + \frac{\beta_2 B_d}{(\theta + B_d)} - h_2 - \frac{1}{2}\sigma_3^2 \right) dt + \sigma_3 dW_3(t), \end{aligned}$$

then,

$$\begin{aligned} \int_0^t dV_3(t) &= \int_0^t \left(r_3 - b_3 Z + \frac{\beta_2 B_d}{(\theta + B_d)} - h_2 - \frac{1}{2}\sigma_3^2 \right) ds + \int_0^t \sigma_3 dW_3(s), \\ &\leq \int_0^t (r_3 - h_2 + \beta_2)\, ds + \int_0^t \sigma_3 dW_3(s). \end{aligned}$$

Simplifying and dividing the above inequality by $t > 0$, it follows that

$$\frac{1}{t} V_3(t) < \frac{1}{t} V_3(0) + \frac{1}{t} \int_0^t (r_3 - h_2 + \beta_2)\, ds + \int_0^t \sigma_3 dW_3(s),$$

i.e.,

$$\frac{1}{t} ln(Z(t)) < \frac{1}{t} ln(Z(0)) + \frac{1}{t} \int_0^t (r_3 - h_2 + \beta_2)\, ds + \int_0^t \sigma_3 dW_3(s).$$

Using the fact that $\lim_{t\to\infty} \frac{W_3(t)}{t} = 0$ a.s., one gets $\lim_{t\to\infty} \frac{1}{t} lnZ = \theta_3 < 0$ a.s., where $\theta_3 = r_3 - h_2 + \beta_2$. Then one obtains that $Z(t) \leq e^{\theta_3 t}$, for all $t \geq 0$, a.s. Since, $Z(t) > 0$, for all $t \geq 0$ a.s., we get $\lim_{t\to\infty} Z = 0$, a.s. Thus, the proof of the theorem is completed.

Theorem 3.4.3 *If $h_1 > r_2$ and $b_1 > \beta_1 Z^*/\theta(\theta + B_d^*)$, then for any given initial value the*

solution of model (3.2.4) *satisfies*

$$\int_0^t \Bigg[\left(b_1 - \frac{\beta_1 Z^*}{\theta(\theta + {B_d}^*)}\right)(B_d - {B_d}^*)^2 + (h_1 - r_2)(F_S - {F_S}^*)^2 \quad + \quad \mu_{F_I}(F_I - {F_I}^*)^2 - (r_2 - h_1 - \mu_{F_I} - b_2(F_S + {F_S}^*)(F_S - {F_S}^*)(F_I - {F_I}^*)\Bigg] du \quad \leq \quad \frac{{\sigma_1}^2 {B_d}^*}{2} + \left(\frac{\beta_1 {B_d}^*}{\beta_2 \theta}\right)\frac{{\sigma_3}^2 Z^*}{2}.$$

Proof Define the Lyapunov function as

$$V(B_d, F_S, F_I, Z) = V_1(B_d) + V_2(F_S, F_I) + \left(\frac{\beta_1 {B_d}^*}{\beta_2 \theta}\right) V_3(Z),$$

where

$$\begin{aligned} V_1 &= B_d - {B_d}^* - {B_d}^* \ln \frac{B_d}{{B_d}^*}, \\ V_2 &= \frac{1}{2}(F_S + F_I - {F_S}^* - {F_I}^*)^2, \\ V_3 &= Z - Z^* - Z^* \ln \frac{Z}{Z^*}. \end{aligned}$$

By computing, we have

$$\begin{aligned} LV_1 &= \left(1 - \frac{{B_d}^*}{B_d}\right)\left((r_1 - b_1 B_d)B_d - \frac{\beta_1 B_d Z}{\theta + B_d}\right) + \frac{1}{2}{\sigma_1}^2 {B_d}^*, \\ &= (B_d - {B_d}^*)\left(-b_1(B_d - {B_d}^*) - \frac{\beta_1 {B_d}^*(Z - Z^*)}{(\theta + B_d)(\theta + {B_d}^*)} + \frac{\beta_1 Z^*(B_d - {B_d}^*)}{(\theta + B_d)(\theta + {B_d}^*)}\right) + \frac{1}{2}{\sigma_1}^2 {B_d}^*, \\ &\leq \left(-b_1 + \frac{\beta_1 Z^*}{\theta(\theta + {B_d}^*)}\right)(B_d - {B_d}^*)^2 - \frac{\beta_1 {B_d}^*(Z - Z^*)(B_d - {B_d}^*)}{(\theta + B_d)(\theta + {B_d}^*)} + \frac{1}{2}{\sigma_1}^2 {B_d}^*, \\ LV_2 &= (F_S + F_I - {F_S}^* - {F_I}^*)\left(F_S(r_2 - b_2 F_S) - h_1 F_S - \mu_{F_I} F_I\right), \\ &= ((F_S - {F_S}^*) + (F_I - {F_I}^*))\big((r_2 - h_1)(F_S - {F_S}^*) - b_2(F_S - {F_S}^*)(F_S + {F_S}^*) \\ &- \mu_{F_I}(F_I - {F_I}^*)\big), \\ &\leq (r_2 - h_1)(F_S - {F_S}^*)^2 - \mu_{F_I}(F_I - {F_I}^*)^2 + (r_2 - h_1 - \mu_{F_I})(F_S - {F_S}^*)(F_I - {F_I}^*) \\ &- b_2(F_S + {F_S}^*)(F_S - {F_S}^*)(F_I - {F_I}^*), \\ LV_3 &= \left(1 - \frac{Z^*}{Z}\right)\left(Z(r_3 - b_3 Z) + \frac{\beta_2 B_d Z}{\theta + B_d} - h_2 Z\right) + \frac{1}{2}{\sigma_3}^2 Z^*, \\ &= (Z - Z^*)\left(-b_3(Z - Z^*) + \frac{\beta_2 \theta(B_d - {B_d}^*)}{(\theta + B_d)(\theta + {B_d}^*)}\right) + \frac{1}{2}{\sigma_3}^2 Z^*, \\ &\leq \frac{\beta_2 \theta(B_d - {B_d}^*)(Z - Z^*)}{(\theta + B_d)(\theta + {B_d}^*)} + \frac{1}{2}{\sigma_3}^2 Z^*. \end{aligned}$$

We obtain

$$\begin{aligned} LV &\leq \left(-b_1 + \frac{\beta_1 Z^*}{\theta(\theta + {B_d}^*)}\right)(B_d - {B_d}^*)^2 + (r_2 - h_1)(F_S - {F_S}^*)^2 \\ &- \mu_{F_I}(F_I - {F_I}^*)^2 + (r_2 - h_1 - \mu_{F_I} - b_2(F_S + {F_S}^*))(F_S - {F_S}^*)(F_I - {F_I}^*) \\ &+ \frac{{\sigma_1}^2 {B_d}^*}{2} + \left(\frac{\beta_1 {B_d}^*}{\beta_2 \theta}\right)\frac{{\sigma_3}^2 Z^*}{2}. \end{aligned}$$

Then

$$\begin{aligned} dV &= LVdt + \sigma_1(B_d - B_d^*)dW(t) + \sigma_3(Z - Z^*)\left(\frac{\beta_1 B_d^*}{\beta_2\theta}\right)dW(t), \\ &\leq \left(\left(-b_1 + \frac{\beta_1 Z^*}{\theta(\theta + {B_d}^*)}\right)(B_d - {B_d}^*)^2 + (r_2 - h_1)(F_S - {F_S}^*)^2\right. \\ &- \mu_{F_I}(F_I - {F_I}^*)^2 + (r_2 - h_1 - \mu_{F_I} - b_2(F_S + {F_S}^*))(F_S - {F_S}^*)(F_I - {F_I}^*) \\ &+ \left.\frac{{\sigma_1}^2 {B_d}^*}{2} + \left(\frac{\beta_1 {B_d}^*}{\beta_2\theta}\right)\frac{{\sigma_3}^2 Z^*}{2}\right)dt + \sigma_1(B_d - B_d^*)dW(t) + \sigma_3(Z - Z^*)\left(\frac{\beta_1 B_d^*}{\beta_2\theta}\right)dW(t). \end{aligned}$$

Integrating both the sides from 0 to t yields

$$\begin{aligned} V(t) - V(0) &\leq \int_0^t \left[-\left(b_1 - \frac{\beta_1 Z^*}{\theta(\theta + {B_d}^*)}\right)(B_d - {B_d}^*)^2 - (h_1 - r_2)(F_S - {F_S}^*)^2 \right. \\ &- \mu_{F_I}(F_I - {F_I}^*)^2 + (r_2 - h_1 - \mu_{F_I} - b_2(F_S + {F_S}^*))(F_S - {F_S}^*)(F_I - {F_I}^*) \\ &+ \left.\frac{{\sigma_1}^2 {B_d}^*}{2} + \left(\frac{\beta_1 {B_d}^*}{\beta_2\theta}\right)\frac{\sigma_3^* Z^*}{2}\right]du - \int_0^t \left[\sigma_1(B_d - B_d^*)\right. \\ &+ \left.\sigma_3(Z - Z^*)\left(\frac{\beta_1 B_d^*}{\beta_2\theta}\right)\right]dW(u). \end{aligned}$$

Further,

$$\begin{aligned} &\frac{1}{t}\int_0^t \left[\left(b_1 - \frac{\beta_1 Z^*}{\theta(\theta + {B_d}^*)}\right)(B_d - {B_d}^*)^2 + (h_1 - r_2)(F_S - {F_S}^*)^2 + \mu_{F_I}(F_I - {F_I}^*)^2\right. \\ &\left. - (r_2 - h_1 - \mu_{F_I} - b_2(F_S + {F_S}^*))(F_S - {F_S}^*)(F_I - {F_I}^*)\right]du \leq \frac{{\sigma_1}^2 {B_d}^*}{2} + \left(\frac{\beta_1 {B_d}^*}{\beta_2\theta}\right)\frac{{\sigma_3}^2 Z^*}{2} \\ &- \frac{V(t) - V(0)}{t} - \frac{1}{t}\int_0^t \left(\sigma_1(B_d - B_d^*) + \sigma_3(Z - Z^*)\left(\frac{\beta_1 B_d^*}{\beta_2\theta}\right)\right)dW(u). \end{aligned}$$

Following, lemma 3.1 from Zhang et al. (2019), we have

$$\lim_{t\to\infty}\frac{1}{t}\int_0^t \left(\sigma_1(B_d - B_d^*) + \sigma_3(Z - Z^*)\left(\frac{\beta_1 B_d^*}{\beta_2\theta}\right)\right)dW(u) = 0,$$

implies

$$\int_0^t \Bigg[\left(b_1 - \frac{\beta_1 Z^*}{\theta(\theta + {B_d}^*)} \right) (B_d - {B_d}^*)^2 + (h_1 - r_2)\,(F_S - {F_S}^*)^2 + \mu_{F_I}(F_I - {F_I}^*)^2$$
$$- (r_2 - h_1 - \mu_{F_I} - b_2\,(F_S + {F_S}^*))\,(F_S - {F_S}^*)\,(F_I - {F_I}^*) \Bigg] du \leq \frac{{\sigma_1}^2 {B_d}^*}{2} + \left(\frac{\beta_1 {B_d}^*}{\beta_2 \theta} \right) \frac{{\sigma_3}^2 Z^*}{2}.$$

Remark 6 *From above, we can see that* $\frac{{\sigma_1}^2 {B_d}^*}{2} + \left(\frac{\beta_1 {B_d}^*}{\beta_2 \theta} \right) \frac{{\sigma_3}^2 Z^*}{2} \to 0$ *as* $\sigma_1 \to 0$ *and* $\sigma_3 \to 0$. *This asserts that endemic equilibrium* $(B_d^*, F_S^*, F_I^*, Z^*)$ *of model* (3.2.2) *is the point where the solution of model* (3.2.4) *fluctuates. Further, as* σ_3 *decreases, the difference in models also decreases.*

3.5 Analysis of reaction-diffusion model

In this section, we will analyze the linear stability of the corresponding spatio-temporal model by perturbing it with two-dimensional spatial perturbations of a form:

$$\begin{aligned} B_d &= {B_d}^* + \varepsilon_1 \exp(\lambda_k t + i(k_x x + k_y y)), \\ F_S &= {F_S}^* + \varepsilon_2 \exp(\lambda_k t + i(k_x x + k_y y)), \\ F_I &= {F_I}^* + \varepsilon_2 \exp(\lambda_k t + i(k_x x + k_y y)), \\ Z &= Z^* + \varepsilon_3 \exp(\lambda_k t + i(k_x x + k_y y)). \end{aligned} \tag{3.5.1}$$

where ε_1, ε_2 and ε_3 are sufficiently small constants, λ_k is wavelength, k_x and k_y are the components of the wavenumber k in x and y directions, respectively.

Theorem 3.5.1 *Assume that the parameters of the model (3.2.5) satisfies the conditions (3.5.5)-(3.5.6). Then, the steady state* $E^* = (B_d^*, F_S^*, F_I^*, Z^*)$ *is locally asymptotically stable even in the presence of diffusion.*

Proof About the nontrivial equilibrium point $E^* = (B_d^*, F_S^*, F_I^*, Z^*)$, the characteristic equation of a linearized system is given as

$$|V - Hk^2 - \lambda_k I| = 0, \tag{3.5.2}$$

$$\text{where, } V = \begin{pmatrix} b_{11} & 0 & 0 & b_{14} \\ b_{21} & b_{22} & b_{23} & 0 \\ b_{31} & b_{32} & b_{33} & 0 \\ b_{41} & 0 & 0 & b_{44} \end{pmatrix}, \quad \text{and} \quad H = \begin{pmatrix} H_{B_d} & 0 & 0 & 0 \\ 0 & H_{F_S} & 0 & 0 \\ 0 & 0 & H_{F_I} & 0 \\ 0 & 0 & 0 & H_Z \end{pmatrix}, \tag{3.5.3}$$

where $k^2 = k_x^2 + k_y^2$ and V is the variational matrix for E^*. Now we write the four degree characteristic polynomial as

$$det(V - Hk^2 - \lambda_k I) = \lambda_k^4 + \beta_1(k^2)\lambda_k^3 + \beta_2(k^2)\lambda_k^2 + \beta_3(k^2)\lambda_k + \beta_4(k^2) \tag{3.5.4}$$

where,

$$\begin{aligned}
\beta_1(k^2) &= -tr(V - Hk^2) = k^2(H_{B_d} + H_{F_S} + H_{F_I} + H_Z) + A_1, \\
\beta_2(k^2) &= k^4(H_{B_d}H_{F_I} + H_{B_d}H_{F_S} + H_{F_I}H_{F_S} + H_{B_d}H_Z + H_{F_I}H_Z + H_{F_S}H_Z) \\
&\quad -k^2(b_{11}(H_{F_I} + H_{F_I} + H_Z) + b_{22}(H_{B_d} + H_{F_I} + H_Z) + b_{33}(H_{B_d} + H_{F_S} \\
&\quad +H_Z) + b_{44}(H_{B_d} + H_{F_S} + H_{F_I})) + A_2 \\
\beta_3(k^2) &= k^6(H_{B_d}H_{F_I}H_{F_S} + H_{F_I}H_{F_S}H_Z + H_{B_d}H_{F_I}H_Z + H_{B_d}H_{F_S}H_Z) \\
&\quad -k^4(b_{11}(H_{F_S}H_Z + H_{F_I}H_Z + H_{F_I}H_{F_S}) + b_{22}(H_{B_d}H_{F_I} + H_{B_d}H_Z + H_{F_I}H_Z) \\
&\quad +b_{33}(H_{B_d}H_{F_S} + H_{B_d}H_Z + H_{F_S}H_Z) + b_{44}(H_{B_d}H_{F_I} + H_{B_d}H_{F_S} + H_{F_I}H_{F_S})) \\
&\quad +k^2(H_{B_d}(b_{22}b_{44} + b_{22}b_{33} + b_{33}b_{44} - b_{23}b_{32}) + H_{F_S}(b_{11}b_{33} + b_{11}b_{44} + b_{33}b_{44} \\
&\quad -b_{14}b_{41}) + H_{F_I}(b_{11}b_{44} + b_{22}b_{44} + b_{22}b_{11} - b_{14}b_{41}) + H_Z(b_{11}b_{33} + b_{22}b_{33} + b_{22}b_{11} \\
&\quad -b_{23}b_{32})) + A_3 \\
\beta_4(k^2) &= k^8(H_{B_d}H_{F_S}H_{F_I}H_Z) - k^6(b_{11}H_{F_I}H_{F_S}H_Z + b_{22}H_{B_d}H_{F_I}H_Z + b_{33}H_{B_d}H_{F_S}H_Z \\
&\quad +b_{44}H_{B_d}H_{F_I}H_{F_S}) + k^4(b_{11}(b_{44}H_{F_S} + b_{22}H_Z)H_{F_I} + b_{33}(b_{22}H_{B_d} + b_{11}H_{F_S})H_Z \\
&\quad +b_{44}(b_{22}H_{F_I} + b_{33}H_{F_S})H_{B_d} - b_{14}b_{41}H_{F_S}H_{F_I} - b_{23}b_{32}H_{B_d}H_Z) \\
&\quad +k^2((H_{B_d}b_{44} + H_Z b_{11})(b_{23}b_{32} - b_{22}b_{33}) + (H_{F_I}b_{22} + H_{F_S}b_{33})(b_{14}b_{41} - b_{11}b_{44})) \\
&\quad +A_4.
\end{aligned}$$

where $A_1,\ A_2,\ A_3$ and A_4 are as defined in Theorem 10.
To prove the stability of the system, we need to show roots of (20) will have negative real part i.e., $Re(\lambda_k) < 0$. An application of the Routh-Hurwitz criteria says that roots of (20)

will have negative real parts if and only if,

$$\beta_1(k^2) > 0,\ \beta_2(k^2) > 0,\ \beta_3(k^2) > 0,\ \beta_4(k^2) > 0 \ \text{ and} \tag{3.5.5}$$

$$(\beta_1(k^2)\beta_2(k^2) - \beta_3(k^2))\beta_3(k^2) - \beta_4((k^2))\beta_1^2((k^2)) = \rho_1 k^6 + \rho_2 k^5 + \rho_3 k^4 + \rho_4 k^3 + \rho_5 k^2$$
$$+\rho_6 + A_1A_2A_3 - A_3^2 - A_1^2A_4 > 0. \tag{3.5.6}$$

where, ρ_1, ρ_2, ρ_3 and ρ_4 are given in Appendix A.

A constant positive steady state $E^* = (B_d^*, F_S^*, F_I^*, Z^*)$ of the spatio-temporal system is, therefore, asymptotically stable. For a given set of parameter values, this means that even in the presence of diffusion, the population will always settle at $E^* = (B_d^*, F_S^*, F_I^*, Z^*)$ regardless of perturbation.

3.5.1 Turing instability

Turing instability deals with the patchiness in dynamics that occurs due movement of species. Following Dubey et al. (2009), in which they, formed a simple model of an aquatic ecosystem with fish, zooplankton, phytoplankton, and nutrient levels that includes an analytical explanation for the reason why plankton patches appear.

Turing bifurcation occurs when the positive steady state $E^* = (B_d^*, F_S^*, F_I^*, Z^*)$ for the non-spatial system (3.2.2) is stable and it is unstable for the diffusive system (3.2.5). For a system to be Turing unstable, at least one eigenvalue of the characteristic equation (3.5.4) must be positive. The condition for steady state $E^* = (B_d^*, F_S^*, F_I^*, Z^*)$ of system (3.2.2) to be stable is discussed in Theorem 10. However, due to diffusion, it will become unstable if any of the conditions

$$\beta_1(k^2) > 0,\ \beta_4(k^2) > 0 \text{ and } (\beta_1(k^2)\beta_2(k^2) - \beta_3(k^2))\beta_3(k^2) - \beta_4(k^2)\beta_1^2(k^2) > 0, \tag{3.5.7}$$

are not satisfied.
We will illustrate this by taking appropriate parameter values:

Example 3.5.1 *Setting the parameters as in Table 2.2, it can be easily verified that the non-spatial system (3.2.2) is stable. However, to get the diffusive instability any of the conditions in (3.5.5)-(3.5.6) must fail. For diffusive coefficients* $H_{B_d} = 0.00004$, $H_{F_S} = 0.10$, $H_{F_I} = 0.03$, *and* $H_Z = 0.09$, *we observe that* $\beta_4(k^2)$ *is negative for the wave number* k *between* $4.6631 < k < 27.7215$, *as shown in Fig. 3.3. For these values of diffusion Turing instability is observed. Consequently, the system may eventually reach a non-constant*

positive steady state, giving rise to patterns (c.f. Fig. 3.18-3.21).

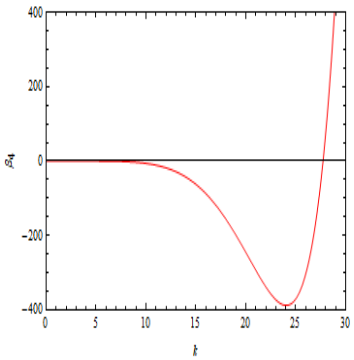

k vs β_4

Figure 3.3: The occurrence of Turing instability as the coefficient (β_4) of the dispersion relation becomes negative for some range of wavenumber k.

3.6 Threshold for persistence of disease

Since we are interested in disease-free state, we now work out the threshold $\mathcal{T}_0$ for our eco-epidemic model and is a good measure for local asymptotic stability of E_5 as well as long term prediction of the epidemics. Following the work of Diekmann et al. (1990), we found matrices $\mathscr{F}$ and $\mathscr{V}^{-1}$ as follows,

$$\mathscr{F} = \begin{pmatrix} -\dfrac{\beta_1(r_3 - h_2)}{\theta b_3} & 0 \\ \dfrac{\nu_{F_S}(r_3 - h_2)}{b_3} & \dfrac{\lambda(r_3 - h_2)}{b_3} \end{pmatrix}, \quad \mathscr{V}^{-} = \begin{pmatrix} -\dfrac{1}{r_1} & 0 \\ 0 & \dfrac{1}{\mu_{F_I}} \end{pmatrix}.$$

The spectral radius of $\mathscr{F}\mathscr{V}^{-1}$ is the required basic reproduction number. $\mathcal{T}_0$ for the model (3.2.3) is given as follows:

$$\mathcal{T}_0 = \rho(\mathscr{F}\mathscr{V}^{-1}) = \rho \begin{pmatrix} \dfrac{1}{r_1}\left(\dfrac{\beta_1(r_3 - h_2)}{\theta b_3}\right) & 0 \\ \dfrac{-\nu_{F_S}(r_2 - h_1)}{b_2 r_1} & \dfrac{\lambda(-h_1 + r_2)}{\mu_{F_I} b_2} \end{pmatrix}.$$

Hence, threshold is given by $\mathcal{T}_0 = \max\left\{\dfrac{1}{r_1}\left(\dfrac{\beta_1(r_3 - h_2)}{\theta b_3}\right), \dfrac{\lambda(-h_1 + r_2)}{\mu_{F_I} b_2}\right\}$.

For the values of parameters as in example 3.3.1, the reproduction number,
$\mathcal{T}_0 = \max\left\{0.603156, 134.727\right\} = 134.727 > 1$ implying disease will persist in all future.
Now, we set parameters as $r_1 = 2.5, r_2 = 1.911, r_3 = 1.2361, K_1 = 350, K_2 = 150, K_3 = 322, \beta_1 = 2.58, \beta_2 = 1.932, \theta = 10, \lambda = 0.15, \mu_{F_I} = 4.9, \nu_{F_S} = 2.291, h_1 = 1.5, h_2 = 1.199$

and found that $\mathcal{T}_0 = 0.99758 < 1$ and extinction of infected frog B_d was observed (c.f. Fig. 3.4). This situation is favourable to save the frog population.

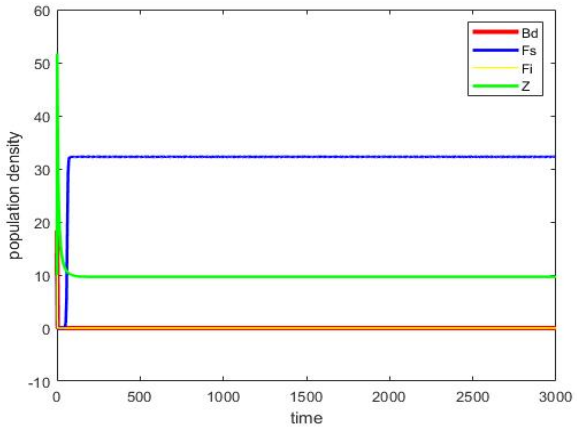

Figure 3.4: Extinction of infected frog and B_d when $K_1 = 350, K_2 = 150, K_3 = 322, \beta_1 = 2.58, \lambda = 0.15, \mu_{F_I} = 4.9, \nu_{F_S} = 2.291, h_1 = 1.5, h_2 = 1.199$. Other parameters are same as in example 1. Observe that, $\mathcal{T}_0 = 0.99758 < 1$.

3.6.1 Global sensitivity analysis of $\mathcal{T}_0$

In order to figure out how best we can reduce the prevalence of chytridiomycosis disease; it is necessary to know the comparative importance of the different parameters. In this section, we calculate the global sensitivity indices of the threshold parameter $\mathcal{T}_0$ to the parameters in the model. These indices can direct us how targeting a specific parameter can impact the accomplishment of a desired goal. Since the association between parameters and output is not known beforehand; using both Extended Fourier amplitude sensitivity test (eFAST) and PRCC is ideal. In this work, we use the PRCC method to find parameters that have foremost influence on $\mathcal{T}_0$ and should be focused for efficient and effective intervention. We initiated uncertainty analysis by selecting ranges for each parameter value. When parameter estimation is uncertain, we can treat each parameter as a random variable with a corresponding probability density function (PDF). In a situation when there is no prior knowledge, the uniform distribution can be a better choice Marino et al. (2008). Therefore, a uniform probability distribution function is designated to each parameter (c.f. Table 3.2). The PRCC sensitivity results for $\mathcal{T}_0$ to the eleven different parameters are calculated and are listed in Table 3.2 and also illustrated using bar charts in Fig. 3.5. The sign of PRCC indicates the direction of the association between input and output factors. A value of +1 signifies a perfect positive linear relationship, a value of -1 indicates a perfect negative linear relationship, and a value near to 0 foreshadows no relationship. From the results given in Table 3.2, we found that that $\mathcal{T}_0$ is the increasing function of $\lambda,\ r_2,\ \beta_1, r_3$ while

Table 3.2: The PRCC sensitivity indices of the threshold ($\mathcal{T}_0$) with the distributions and ranges of input parameters.

Parameters	Distribution	Ranges	PRCC values
r_1	Uniform	$[0.1, 2]$	-0.119662416371917
r_2	Uniform	$[1, 5]$	0.495476127814423
r_3	Uniform	$[1.5, 5]$	0.058317887170955
b_2	Uniform	$[0.00001, 0.5]$	-0.687127855253438
b_3	Uniform	$[0.00001, 0.2]$	-0.259828220509122
θ	Uniform	$[1, 50]$	-0.090120983043229
λ	Uniform	$[0.001, 1]$	0.698049581653010
β_1	Uniform	$[0.01, 0.8]$	0.138093965573370
h_1	Uniform	$[0.01, 1]$	0.698049581653010
h_2	Uniform	$[0.009, 1.3]$	-0.017265122559312
μ_{F_I}	Uniform	$[0.001, 1.5]$	-0.666718988633706

decreasing function of $h_1,\ b_2,\ \mu_{F_I},\ h_2,\ b_3,\ \theta$. The parameters exerting maximum influence on $\mathcal{T}_0$ is λ followed by b_2, and μ_{F_I}. The most influential parameter is the rate λ. Since, the sensitivity index of 0.698049, increasing (decreasing) λ by 10% increases (or decreases) the value of $\mathcal{T}_0$ by approximately 6.98%. Since, there is no vaccine till date it is recommended to establish long term captive assurance colonies. This could ensure the long term survival of the species. Secondly, we found that increasing the growth rate of frog (r_2) would be quite effective in achieving disease free situation. Another parameter with equal importance is the death rate of infected frogs. Simulation suggests that infected frogs must be detected, humanely euthanized and discarded in a safe manner or buried.

The identification of these parameters is vital in formulating control strategies effective for controlling chytridiomycosis. In summary, the result of sensitivity analysis suggests that a strategy that reduces the contact rate (λ) and, the strategy which increases the growth rate of frog (r_2) and the death rate of infected frog (μ_{F_I}) would be quite effective in restricting the ongoing mitigation.

3.7 Some important numerical simulations

In this section, we focus on numerical viability of the analytical results. Local behaviour and global behaviour of both ODE and stochastic models are performed.

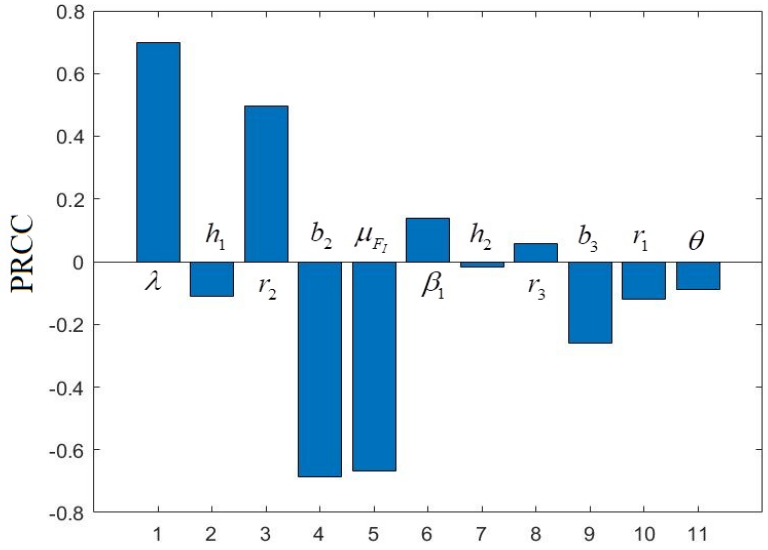

Figure 3.5: Partial rank correlation coefficient (PRCC) results for significance of parameters involved in $\mathcal{T}_0$

3.7.1 Numerical simulation for ODE model

Runge-Kutta fourth order has been used to solve ODE system (3.2.1) and (3.2.2) with initial condition $(10, 15, 25, 10)$. Simulating model (3.2.1) we observe that for the parameters $r_1 = 1.3;\ r_2 = 1.911;\ K_1 = 350;\ K_2 = 500;\ \lambda = 0.09;\ \nu_{F_S} = 0.291;\ \theta = 50;\ \beta_1 = 2.12;\ h_1 = 0.1;\ \mu_{F_S} = 0.891$, extinction of B_d is observed (c.f. Fig. 3.6). If the growth rate of B_d is increased to $r_1 = 2.3$, extinction of frog populations is observed and is illustrated in the Fig. 3.7. This model suggests that the only way to save the frog population is to reduce the growth rate, r_1, or increase the removal rate, β_1, of B_d. However, chytrid fungus is not eliminated automatically from the environment. Therefore, it is necessary to investigate the interaction between *B. dendrobatidis* and zooplankton i.e model (2.3.8) to provide a safe and effective way to save frog population.

Now, we perform the simulation experiment for model (3.2.3) considering parameters as given in Table 3.3, we observe that the eigenvalues of variational matrix V^* are negative as all the Routh-Hurwitz conditions are satisfied as $A_1 = 0.2227 > 0, A_2 = 1.1088 > 0, A_3 = 0.0435 > 0, A_4 = 0.0627 > 0$, and $A_1A_2A_3 - A_3^2 - A_1^2A_4 = 0.0057 > 0$ (see theorem 10). Hence, the equilibrium point $(B_d^*, F_S^*, F_I^*, Z^*) = (0.1321, 2.2827, 3.7693, 10.0799)$ is stable (c.f. Fig. 3.8). Limit cycle was also observed by increasing $h_2 = 1.399$ (c.f. Fig. 3.9). Irrespective of the plenteous literature on Chytridiomycosis, knowledge on basic biological parameters from natural populations are still missing. However, all our numerical simulations are executed utilizing ecologically acceptable parameter values as reported by

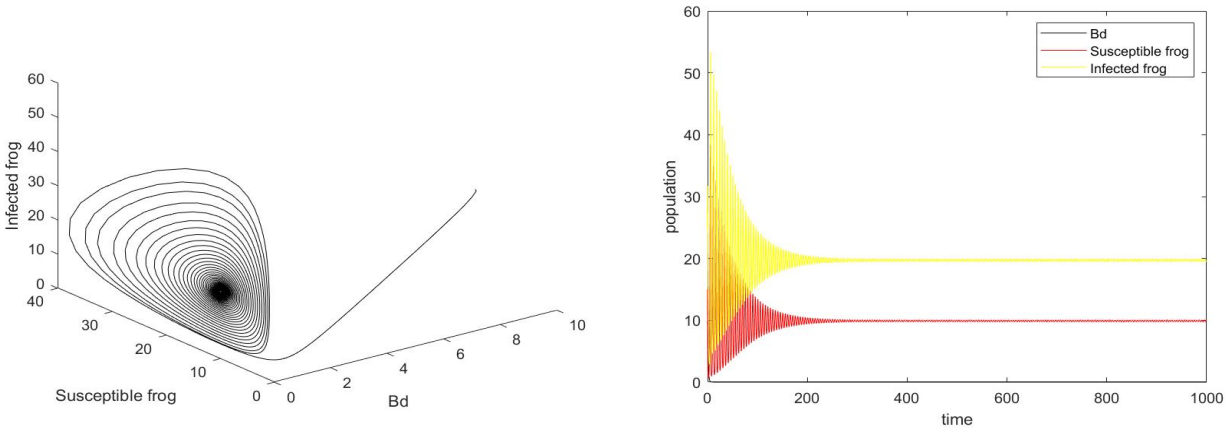

(a) phase portrait (b) time series

Figure 3.6: Extinction of B_d in model (3.2.1) for the parameters $r_1 = 1.3$; $r_2 = 1.911$; $K_1 = 350$; $K_2 = 500$; $\lambda = 0.09$; $\nu_{F_S} = 0.291$; $\theta = 50$; $\beta_1 = 2.12$; $h_1 = 0.1$; $\mu_{F_S} = 0.891$.

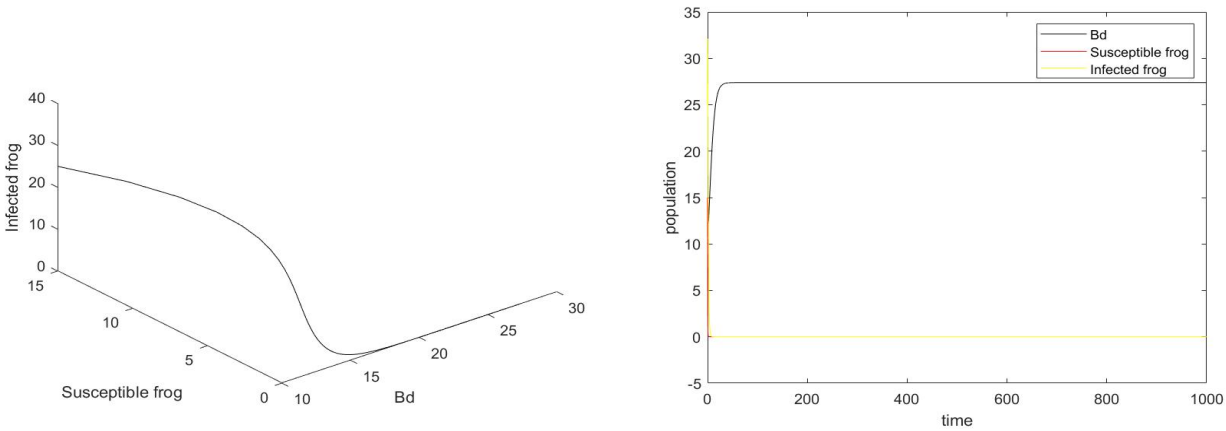

(a) phase portrait (b) time series

Figure 3.7: Extinction of frog population in model (3.2.1) for the parameters $r_1 = 2.25$; $r_2 = 1.911$; $K_1 = 350$; $K_2 = 500$; $\lambda = 0.09$; $\nu_{F_S} = 0.291$; $\theta = 50$; $\beta_1 = 2.12$; $h_1 = 0.1$; $\mu_{F_S} = 0.891$.

Jorgensen (1995). We have also performed PRCC analysis to take into account these random parameters and get an overall view on the effect of these parameters.

3.7.1.1 Effect of zooplankton harvesting

We took the parameter as given in Table 3.3 and varied parameter h_2 and found that on decreasing h_2 from 1.309 where all species coexists (c.f. Fig. 3.10) to 1.099, B_d gets extinct and frog gets better place to survive (c.f. Fig. 3.11). Conversely, when we increase the harvesting rate of zooplankton to 1.9 we observe the frog population extincts (c.f. Fig. 3.12). From this section, we conclude that as we increase the value of h_2, frog

Table 3.3: Parameter values used for simulating model (3.2.2)

Parameters	Values	References
r_1	2.5	Ackleh et al. (2016)
r_2	1.911	Tobler et al. (2012)
r_3	1.2361	Hopcroft and Roff (1998)
b_1	2.5/350	Assumed
b_2	1.911/500	Assumed
b_3	1.2361/200	Assumed
θ	10	Assumed
λ	0.31	Ackleh et al. (2016)
ν_{F_S}	2.291	Vredenburg et al. (2010)
β_1	2.512	Assumed
β_2	1.932	Assumed
h_1	0.431	Assumed
h_2	1.199	Assumed
μ_{F_I}	0.891	Ackleh et al. (2016)

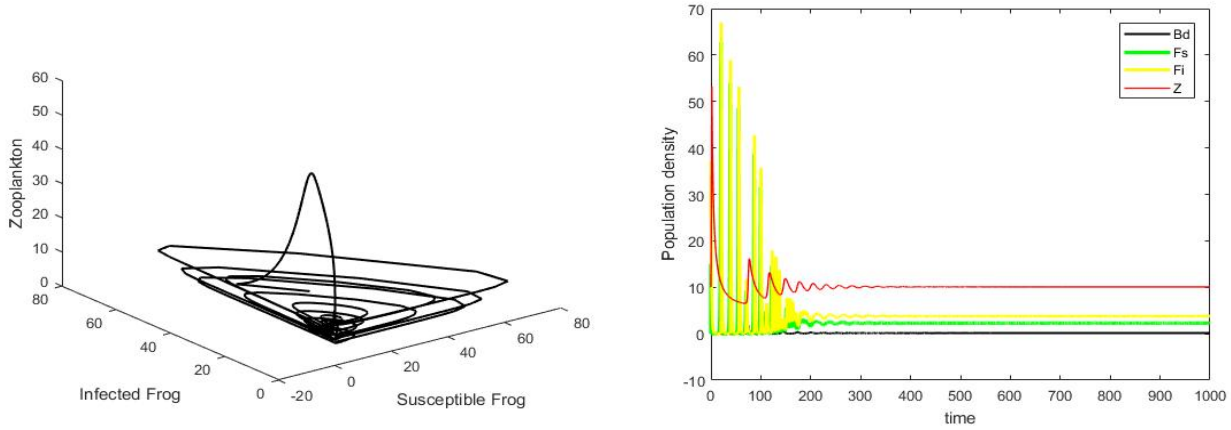

(a) phase portrait (b) time series

Figure 3.8: Stable attractor for model (3.2.3) and parameters given in Table 3.3.

extincts permanently after a threshold value. Therefore, for saving the frog from completely getting extinct it is suggested to control the parameter h_2. We also note that presence of zooplankton can be a measure to control the rapid growth of Chytridiomycosis disease in frog population and preserving remnant population in Australia.

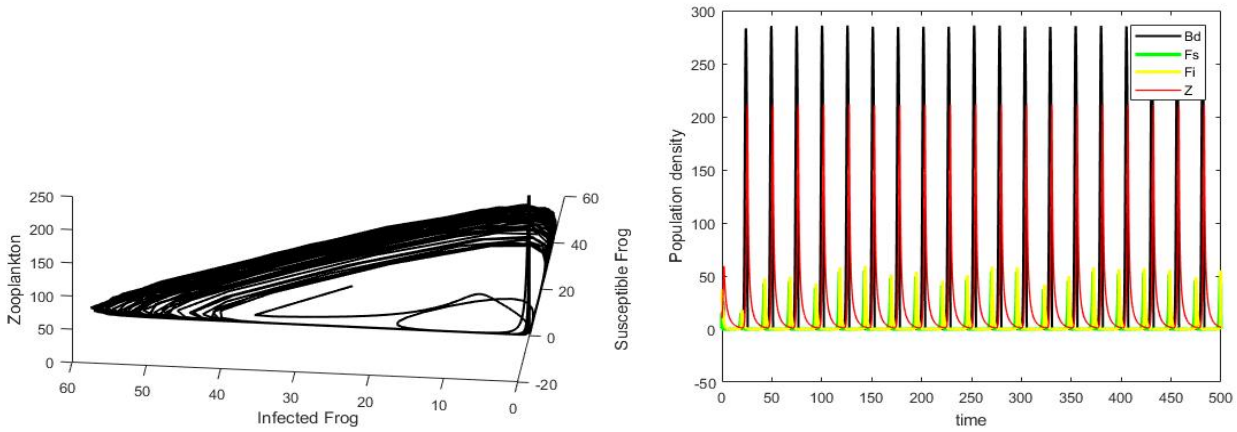

(a) phase portrait (b) time series

Figure 3.9: Limit cycle for model (3.2.3) with $h = 1.399$; other parameters are same as in Table 3.3.

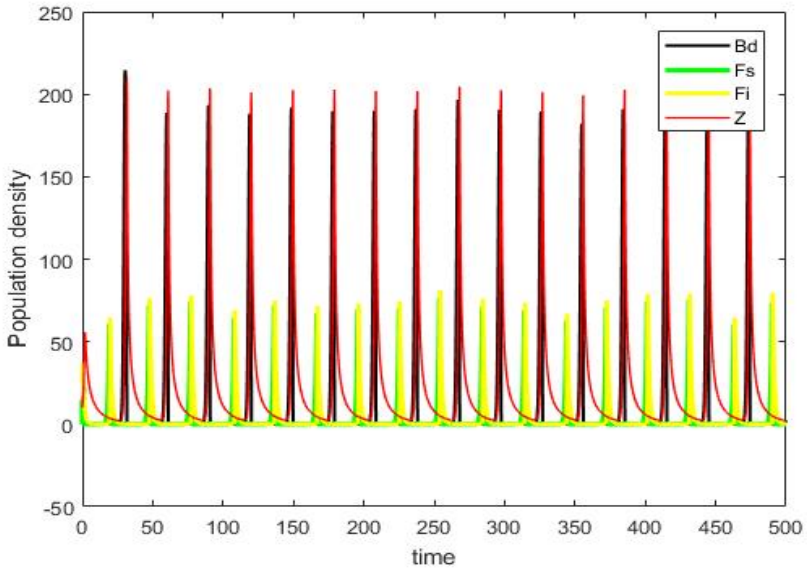

Figure 3.10: Co-existence of all three species for $h_2 = 1.309$. Other parameters as same as Table 3.3.

3.7.2 Bifurcation analysis

In this section, we will focus on detecting the presence of Hopf bifurcation of E^*.

Theorem 3.7.1 *When $h_2 = h_{2_c}$ i.e. the harvesting rate of zooplankton crosses a critical value, the system (3.2.3) undergoes Hopf bifurcation around the non-trivial equilibrium point.*

Proof The proof can be followed from Theorem 8 of Roy et al. (2020) and hence omitted.

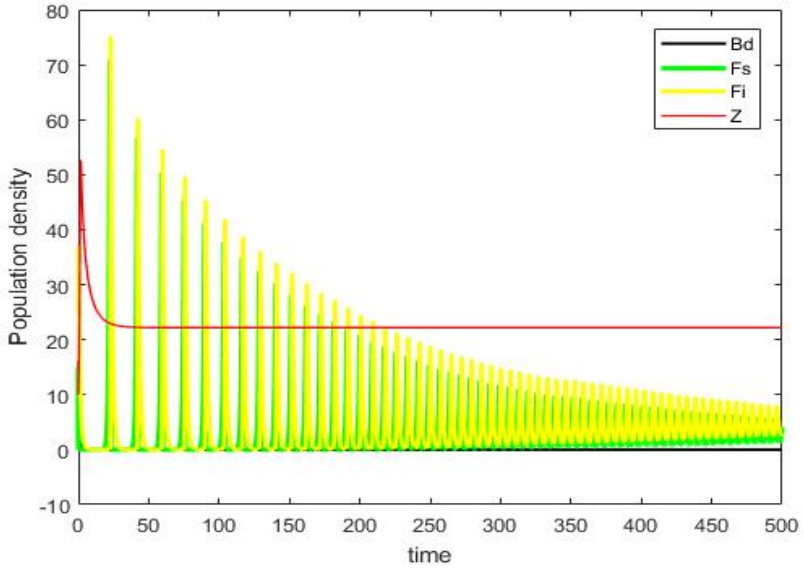

Figure 3.11: Extinction of B_d for $h_2 = 1.099$. Other parameters as same as Table 3.3.

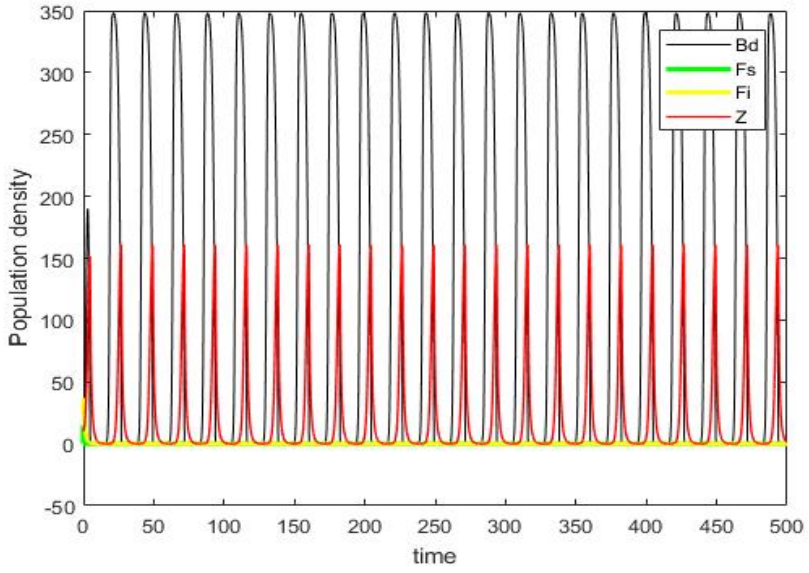

Figure 3.12: Extinction of frog population for $h_2 = 1.9$. Other parameters as same as Table 3.3.

We now show it numerically using MATLAB Matcont toolbox for plotting equilibrium manifold of E^* and are presented in Fig. 3.13. This bifurcation diagram is generated by taking h_2, the zooplankton harvesting rate as bifurcation parameter. A branch of equilibria E^* of system (3.2.3) is presented in Fig. 3.13. Considering other values of parameters as given in Table 3.3, and varying 'h_2' our model undergoes Hopf-bifurcation at $h_2 = h_{2_c} = 1.2232254$ giving rise to a limit cycle from the state of stable equilibrium. Hopf bifurcation is a point where the equilibrium changes its stability via a pair of purely

imaginary eigenvalues, giving rise to a limit cycle from an equilibrium. Stable limit cycle are biologically significant as it assures that the system oscillates even in absence of external periodic forcing. When $h_2 < h_{2_c}$ the stable branch (all eigenvalues has negative real part) is observed, as $h_2 > h_{2_c}$, the branch becomes unstable as a result of Hopf bifurcation. This analysis shows that maintaining zooplankton in its natural environment with low harvesting rate ($h_2 < h_{2_c}$), can permit all three species to coexists in a oscillatory way.

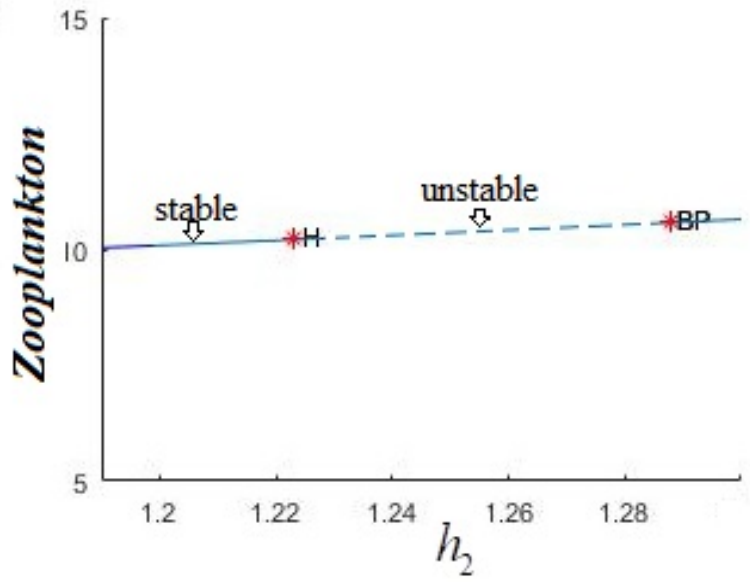

Figure 3.13: A branch of equilibria displaying the occurrence of Hopf bifurcation at $h_2 = h_{2_c} = 1.2232254$ in $(h_2; Z)$ plane. H: denote a Hopf point, BP: denotes branch point.

3.7.3 Numerical simulation for stochastic model

We used Euler's Maruyama method (Higham (2001)) to numerically show the effect of the environmental stochasticity at all trophic level. We took parameters from Table 3.3 for which all population coexists in deterministic case. From Fig. 3.14, we observed that when the environmental stochasticity experienced by zooplankton is too high, all species tend to extinction except B_d. If environmental stochasticity experienced by zooplankton is low while the frog population experiences too much environmental stochasticity, then zooplankton and B_d will persist but frog itself will tend to extinction (Fig. 3.15). If environmental stochasticity experienced by both zooplankton and frog are low while B_d experience too much environmental stochasticity, then only B_d will tend to extinction, else both will persist in mean (Fig. 3.16). These result shows that persistence and extinction of B_d and Z species depends on the demographic impacts of environmental stochasticity

Table 3.4: Effects of stochasticity on the extinction of the species.

	σ_1(increase)	σ_2(increase)	σ_3(increase)
Batrachochytrium dendrobatidis	Tends to extinction	None	None
Frog	None	Tends to extinction	Tends to extinction
Zooplankton	None	None	Tends to extinction

on its own population. However, persistence and extinction of frog depends on the demographic impacts of environmental stochasticity on its own population and of zooplankton. From the biological point of view this is reasonable, as Zooplankton predates B_d, and with increasing of σ_3, zooplankton are likely to be extinct, hence B_d can persist better which will cause more disease and death of frog population. Similarly, with increasing of σ_1, the B_d population will decline and hence zooplankton will also decline in mean abundance, while frog gets a better environment to persist. Table 3.4 recapitulate the results.

We now compare the result of stochastic model and the corresponding deterministic model. The main results are given as follows: (i) Taking parameter as in Fig. 3.8 and for small environmental stochasticity $\sigma_1 = 0.000001, \sigma_2 = 0.000001, \sigma_3 = 0.000001$ we found stable point in deterministic case does not become chaos in stochastic case rather it fluctuates randomly around some average value which is trivial (c.f. Fig. 3.17). It is well known that most of natural phenomena does not strictly follow deterministic laws but rather oscillate randomly around some average value so that the deterministic equilibrium is no longer an absolutely fixed state (Arditi and Ginzburg (1989); Bandyopadhyay and Chakrabarti (2003); Bandyopadhyay and Chattopadhyay (2005)).

3.7.4 Numerical simulation for Reaction-Diffusion model

Here, we present Turing patterns for the two-dimensional spatial system (3.2.5). We compute these patterns by using the finite difference numerical method with explicit time-stepping. In all of our calculations, we use small random perturbations around the positive uniform steady state E^* as initial conditions and homogeneous Neumann (zero-flux) boundary conditions as boundary conditions with the system size of $[L \times L]$, with $L = 200$ for Fig. 3.18–3.22. All the parameter values are chosen from Turing space as discussed in Example 2 (Section 5.2). In the present study, we set $\Delta h = 0.25$, $\Delta t = 0.001$.

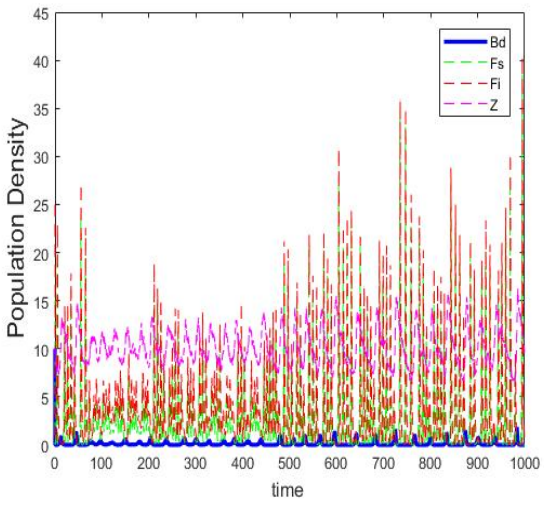

(a) $\sigma_3 = 0.000001$

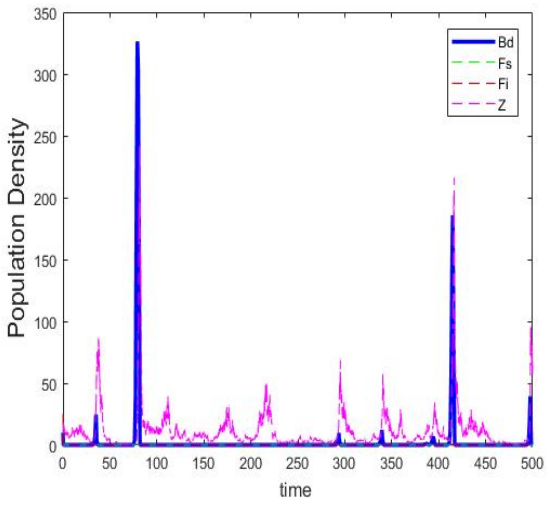

(b) $\sigma_3 = 0.0001$

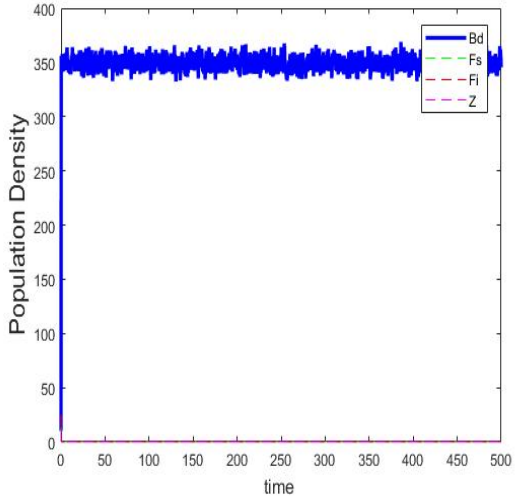

(c) $\sigma_3 = 0.01$

Figure 3.14: Time series of model (3.2.4) for the parameters given in Table 3.3 and $\sigma_1 = 0.000001$, $\sigma_2 = 0.000001$ (a) $\sigma_3 = 0.000001$, (b) $\sigma_3 = 0.0001$, (c) $\sigma_3 = 0.01$ with x-axis as time interval (in days) and y-axis as the population sizes of each species.

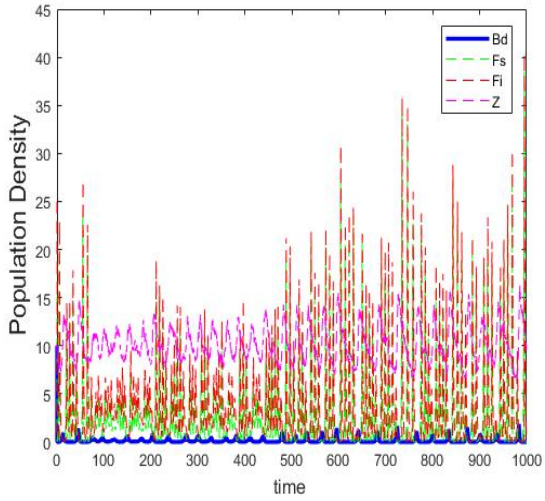

(a) $\sigma_2 = 0.0000001$

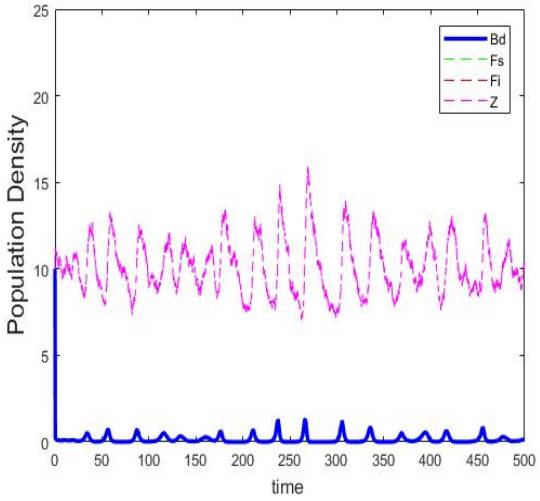

(b) $\sigma_2 = 0.0001$

Figure 3.15: Time series of model (2.3.10) for the parameters given in Table 3.3 and $\sigma_1 = 0.000001$, $\sigma_3 = 0.000001$ (a) $\sigma_2 = 0.0000001$, (b) $\sigma_2 = 0.0001$ with x-axis as time interval (in days) and y-axis as the population sizes of each species.

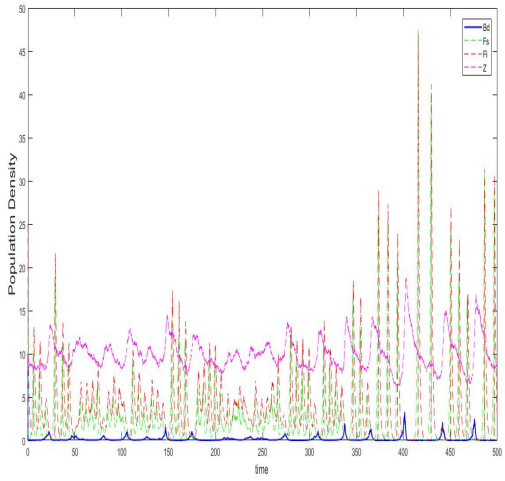

(a) $\sigma_1 = 0.000001$

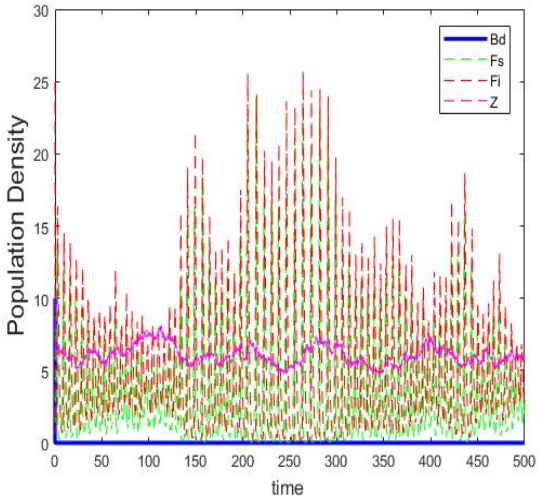

(b) $\sigma_1 = 0.0001$

Figure 3.16: Time series of model (3.2.4) for the parameters given in Table 3.3 and $\sigma_2 = 0.000001$, $\sigma_3 = 0.000001$ (a) $\sigma_1 = 0.0001$, (b) $\sigma_1 = 0.01$ with x-axis as time interval (in days) and y-axis as the population sizes of each species.

From Fig. 3.18, we observe that as time increases from $t = 1$ to $t = 10$ density of B_d decreases. This shows that the spatial system may provide some early warning signals for the approaching ecological disaster. However, it increases in the long run ($t = 100$) and spreads out in the entire domain. A closer examination of the susceptible and infected frog density distribution at $t = 100$ days shows that susceptible frogs are not present at places with a high density of B_d because the presence of B_d infects the frog (c.f. Fig.

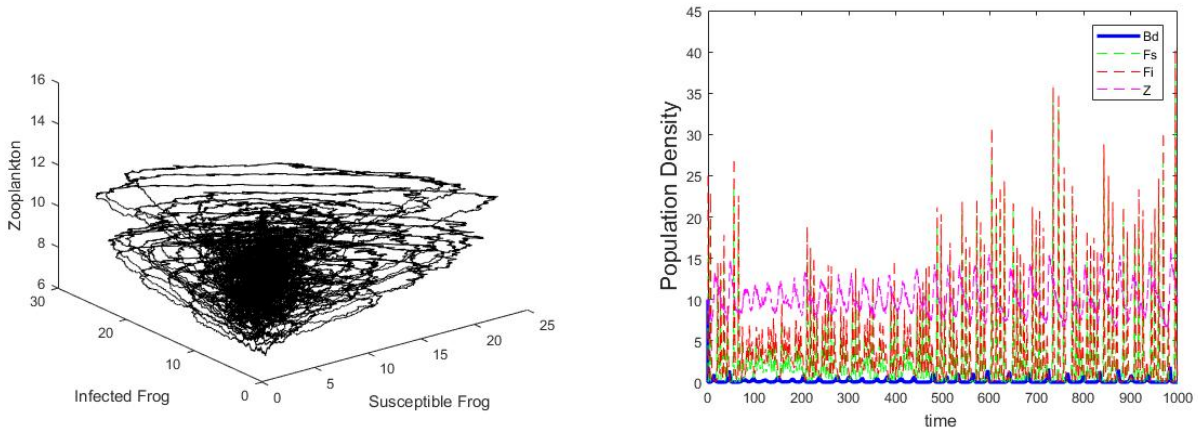

(a) phase portrait (b) time series

Figure 3.17: (a) Phase portrait of model (3.2.4) for parameters as in Fig. 3.8 and $\sigma_1 = 0.000001$, $\sigma_2 = 0.000001$, $\sigma_3 = 0.000001$; (b) Time series of model (3.2.4) where x-axis represents time interval (in days) and y-axis as the population sizes of each species.

3.19-3.20). Hence, they come into the infected frog category. As t increases from 1 to 100, zooplankton cluster themselves, giving rise to a beautiful pattern formation (c.f. Fig. 3.21).

To decipher the effect of diffusion among species, we have also simulated the reaction-diffusion model (3.2.5) by increasing the diffusion coefficient of infected frog and zooplankton. We observe that as H_{F_I} increases from 0.001 to 1, the scattered distribution of both infected and susceptible populations seems to get closer and closer (c.f. Fig. 3.22). However, they are not localized to a particular region but spread in the entire domain.

As the diffusion coefficient of zooplankton, H_Z increases from 0.0001 to 0.1; infected frog distribution is lowered while density and distribution of susceptible frog increases. This result strengthens the validation of our hypothesis that "zooplankton may act as biological control" to control defaunation among Corroboree frog population due to *Batrachochytrium dendrobatidis* (c.f. Fig. 3.22).

3.8 Discussions and conclusion

One of the most dramatic examples of fungal impacts on vertebrate populations is the effect of the amphibian disease chytridiomycosis, caused by the chytrid fungus *Batrachochytrium dendrobatidis* (B_d). The sudden and dramatic die-offs of frogs have prompted a large-scale research effort to pinpoint the source of the deadly fungus. Only a little amount of information is available on the impact of the fungus on individuals. Furthermore, little has been published on the prevalence of infection among frog populations as a whole, as distinct

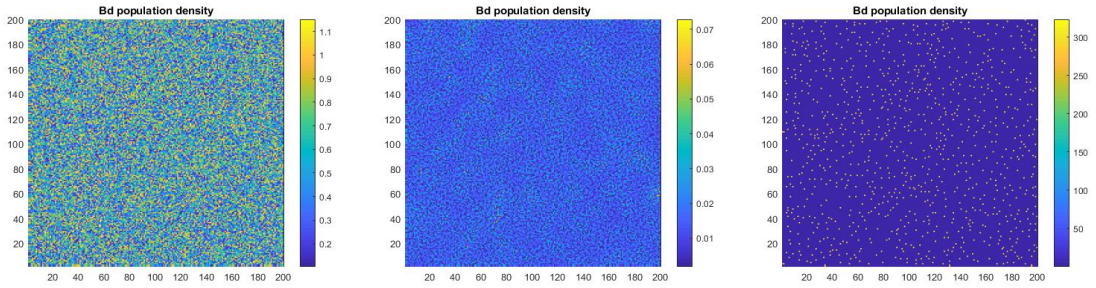

(a) days $t = 1$ (b) days $t = 10$ (c) days $t = 100$

Figure 3.18: B_d population density when $H_{B_d} = 0.00004$, $H_{F_S} = 0.10$, $H_{F_I} = 0.03$, and $H_Z = 0.09$ for days $t = 1,\ t = 10$ and $t = 100$.

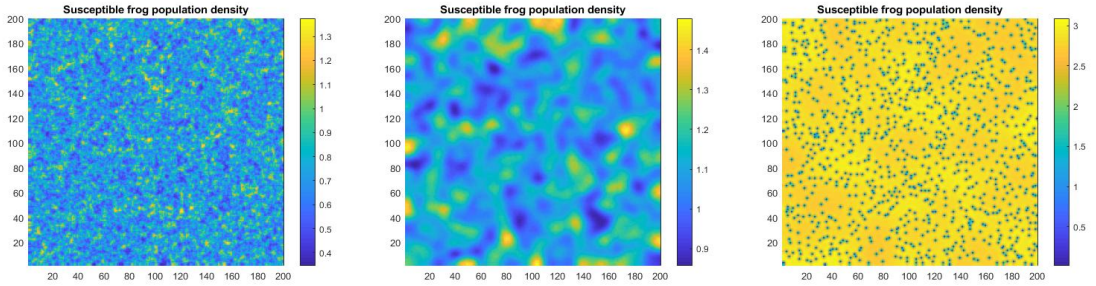

(a) days $t = 1$ (b) days $t = 10$ (c) days $t = 100$

Figure 3.19: Susceptible frog population density distribution when $H_{B_d} = 0.00004$, $H_{F_S} = 0.10$, $H_{F_I} = 0.03$, and $H_Z = 0.09$ for days $t = 1,\ t = 10$ and $t = 100$.

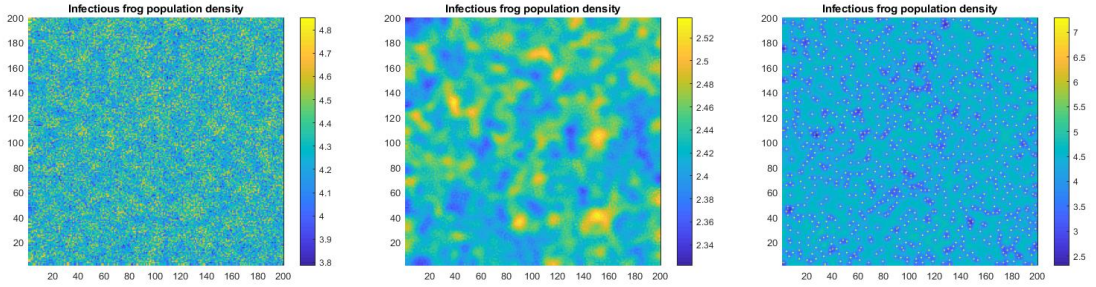

(a) days $t = 1$ (b) days $t = 10$ (c) days $t = 100$

Figure 3.20: Infected frog population density distribution when $H_{B_d} = 0.00004$, $H_{F_S} = 0.10$, $H_{F_I} = 0.03$, and $H_Z = 0.09$ for days $t = 1,\ t = 10$ and $t = 100$.

from the prevalence among morbid frogs only. Most of the researchers are not interested in looking for an infectious disease as the cause of the declines. Despite many gaps in our understanding of chytridiomycosis, we tried to unravel important elements of this lethal disease through mathematical modelling and made progression towards amphibian conservation. Vaccination programs are also under the trial and so it is important to look for some alternative strategies to halt the extinction. Multiple conservation strategies have been proposed in this work and if implemented it might help to mitigate the threat

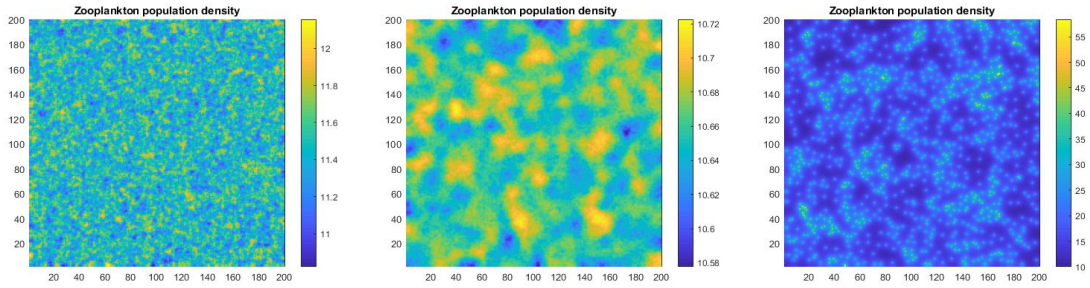

(a) days $t = 1$ (b) days $t = 10$ (c) days $t = 100$

Figure 3.21: Zooplankton population density distribution when $H_{B_d} = 0.00004$, $H_{F_S} = 0.10$, $H_{F_I} = 0.03$, and $H_Z = 0.09$ for days $t = 1,\ t = 10$ and $t = 100$.

of chytridiomycosis. In this research, we examined both stochastic and reaction-diffusion eco-epidemiological system that demonstrates the interaction between B_d-the susceptible frog-infected frog-Zooplankton. The model shows spectacular dynamics such as stable focus and limit cycles. We analytically obtained the parametric condition for existence and stability of the system equilibria for the ODE model. We have also found the conditions for the boundedness of the solutions for stochastic models. Modeling the eco-epidemiological system with stochasticity can help us to grasp the concept of extinction and persistence of species thoroughly. Our simulation results show that the increasing harvesting rate of zooplankton (h_2), reduces the frog population with the threat of extinction. It has been found that B_d population density decreases with the increase of zooplankton.

Our study demonstrates the reduction of *Batrachochytrium zoospores* by the zooplankton and supports its role as a potential biological control (Woodhams et al. (2011)), in saving frog population. Briggs et al. (2010) suggested that Batrachochytrium infection is responsible for host mortality, which implies that controlling Batrachochytrium zoospores may save frog population. We suggest that zooplankton can limit the number of infective Batrachochytrium zoospores in an effective manner and may be a useful means for biological control of chytridiomycosis. Numerical simulation of reaction diffusion model reveals that increasing diffusion of zooplankton can lower the infectious frog density. It also interesting to note that all the population tends to cluster themselves in the long run. These analysis confirms that the threat of Batrachochytrium to amphibians would be lower in systems containing dense populations of zooplankton.

The result of global sensitivity analysis shows that increasing the growth rate r_2 and decreasing the contact rate λ can result in controlling the deadly disease. It is only possible by captive breeding of frogs and then releasing into the wild to maximise recruitment potential. The government should also focus on eliminating the infected frog population. Our study also demonstrates that zooplankton availability, type of interaction among species

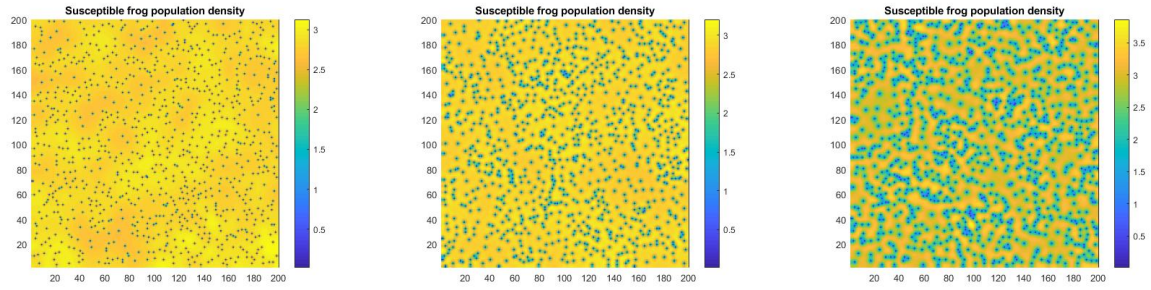

(a) $H_{F_I} = 0.001$ $H_{F_I} = 0.10$ $H_{F_I} = 1$

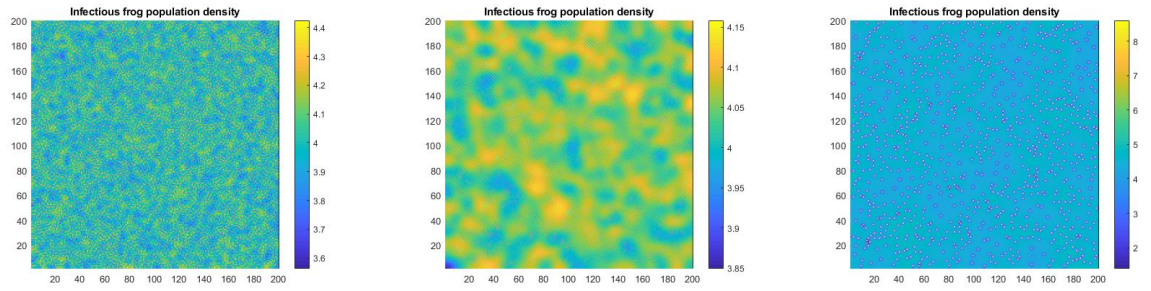

(b) $H_{F_I} = 0.001$ $H_{F_I} = 0.10$ $H_{F_I} = 1$

Figure 3.22: (a) Susceptible frog distribution; (b) Infectious frog distribution; with diffusion coefficients $H_{B_d} = 0.00004, H_{F_S} = 0.10$, $H_Z = 0.09$ and different infectious frog diffusion as shown in figure, for $t = 100$ days.

and role of environmental stochasticity plays an important role in designing the future policy to save the biodiversity loss. Our results shows that if zooplankton is subjected to harvesting and environmental stochasticity, frog population will be affected adversely. Current management strategies must focus on (i) zooplankton introduction, (ii) treating and captivating frogs in a disease free colonies, (iii) improving frog population abundance via re introductions and translocation, (iv) quarantine, surveillance and moment control of diseased frogs. However, we further encourage in depth study to find the effects of zooplankton on B_d populations. A public awareness campaign is essential to control and mitigate the impact of chitridiomycosis. The feasibility of controlling an outbreak of chytrimiomycosis depends on the nature and location of the outbreak and the management strategy adopted. To conserve the biodiversity and to minimize the decline of frog population and their distribution active research is required on this fungal disease. Interventions should be conducted and the generated reports should contain urgently needed actions for improved management. Its time to think about bio-security and we utter these results can help in securing our future (Banerjee et al. (2020)).

Chapter 4

THE ROLE OF ALLEE EFFECT IN CANNIBALISTIC SPECIES:AN ACTION PLAN TO SUSTAIN DECLINING COD POPULATION

"If we wipe out the fish, the oceans are going to die. If the oceans die, we die."

-Paul Watson

Content of this chapter is under the review as:

- "Role of food chain model in designing an action plan to sustain the declining cod population" in Journal of **Mathematical Methods in the Applied Sciences**.

4.1 Introduction

The world's biodiversity is deteriorating at an unprecedented rate. The list of declining species is long. In this list, the Atlantic cod (*Gadus morhua*) is perceived as the greatest threat to global biodiversity. The Atlantic cod is a medium to large size marine fish inhabiting in cold water ($0^o - 15^o$ C). The habitat requirement of cod is not known clearly. They inhabit all water overlying the continental shelves of the Northwest and Northeast Atlantic oceans. Cod are also found in abundance in the Skaggerak and Kattegat and the southern parts of the Baltic sea (on the Status of Endangered Wildlife in Canada) (2010)). Cod was once considered as world's most fertile fish. Since 1990's this fishing suffered depletion and has not recovered till now. The major reason for declination is considered to be a combination of over-fishing, climate change combined with its cannibalistic nature. The productivity of the stock is much lower than it was in the 1970's when a similar decline occurred (Shelton et al. (2006)). The Atlantic cod is an important species in many of the world's ocean systems from an economic, ecological and cultural perspective (Akveld (1974); Garcia et al. (1995); Kurlansky and Davidson (2006); of the United Nations. Fisheries Department (1999)).

This species is now facing notable changes within the ecosystems in which it resides due to over-fishing as well as larval and juvenile mortalities due to cannibalism (Brown et al. (2003); Rosenlund and Halldórsson (2007)). Cannibalism is defined as the act of killing and consuming its conspecifics. It is prevalent in natural predator-prey communities and is ubiquitous in the majority of animal groups, including fishes, and has a significant contribution in regulating population dynamics (Fox (1975)). Cannibalism is a size-selective form of predation and therefore has consequences on both the abundance and size structure of the entire population. Cannibalism in Atlantic cod is a frequent phenomenon in both aquaculture and wild fish stocks and if it is not managed properly, the losses can be devastating (Folkvord (1991); Bogstad et al. (1994)). Due to this, cannibalism in Atlantic cod has received considerable attention in field and aquaculture studies and is assumed to significantly affect recruitment of the cod fishery as well as contribute to high economic losses in the aquaculture industry (Bogstad et al. (1994); Blom and Folkvord (1997)). Past observations suggest that environmental heterogeneity is beneficial for juveniles because it reduces the possibility of predation. Thus, to make juvenile survival and production as much as possible, it is crucial to estimate the possible influences of the size distribution of juveniles on cannibalism and growth (Folkvord and Otterå (1993)).

Another important factor known as the Allee effect, interpreted as the difficulty in finding mates at low-density (Stephens et al. (1999)), can influence cod population density. The

theory underlying Allee effects is well established, and empirical evidence has been detected in various systems (Kramer et al. (2018); Gregory et al. (2010)). Despite this knowledge, implications of Allee effects for recovery plans, practical conservation decisions, and harvesting strategies have been barely implemented (Stephens and Sutherland (1999)). A primary reason for this is that it can be difficult to document an Allee effect in populations that have declined, or for which there are little data. Conservation biologists and managers are usually more interested in demographic Allee effects because they ultimately govern extinction or recovery of species at low population. In most of the articles, the Allee effect is considered to have a negative impact on the population. In this chapter, we will validate the hypothesis that whether the Allee effect is beneficial for the cannibalistic population or not.

The declination of the population is expected to continue even in the absence of fishing unless productivity improves. In this research, we investigate whether cod harvesting or increasing grey seal abundance are the main factors responsible for cod declination. This study aims to get a better understanding of how predation of juvenile cod by adult cod can act as a threat for its population. The annihilation of the cod population in the southern Gulf of St. Lawrence is so significant, and our proposed model will describe the dynamics. Hence, an original benefaction to science, uplifting the conservation management strategies for holding up the cod population and assisting the biodiversity managers. Here we explore four key factors affecting the ongoing threatening processes of cod:

- To mathematically observe cannibalistic behaviour with Allee effect of cod,
- How restocking and proper management can act as biological control?,
- Whether the absence of grey seal is crucial for maintaining adult cod populations?, and
- What is the effect of control measures on cod survival?

To the best of our knowledge, no one has attempted to mathematically validate this hypothesis so far.

This chapter is organised as follows: In Section 4.2, we formulated our model system with and without Allee effect. In Section 4.3, we have shown the existence and stability of equilibrium points of formulated model without Allee effect. In Section 4.4, we discussed the threshold for persistence of species in model having Allee effect. In Section 4.5, we discuss optimal control analysis of our model around the endemic equilibrium (J, A, G). Numerical simulation and comparison are done in Section 4.6. Finally, the conclusion is presented in Section 4.7.

4.2 Model formulation

4.2.1 Model without Allee Effect

Atlantic cod failed to recover since 1990's mainly due to its cannibalistic nature, a demographic Allee effect and an emergent effect resulting from increasing grey seal abundance. We proposed a mathematical model consisting of cod and grey seals. We further divided the cod population into two classes Juvenile (J-(0-7)y) and Adult cod ($A >$ 7y). We assume that the cod population grows logistically and only juvenile cod is predated by a grey seal(G) (Chouinard et al. (2005)). We incorporated a Holling type II functional response (Holling (1959)), for grey seals preying on the 0-7 age-group of Atlantic cod (Neuenhoff et al. (2019)). The grey seal is a highly mobile species. They forage in waters from Georges Bank to the northern Gulf of St. Lawrence and eat a varied diet that includes cod as 50% in their diet. Many researcher detected cannibalism to be the main mortality factor in cod after metamorphosis (Puvanendran et al. (2008); Blom and Folkvord (1997) ; Folkvord (1991)). We have also included this fact by incorporating the cannibalism term $\omega_1 AJ$ to our model. Over the last century, humans emerged as a globally dominant predator of wild marine fish, primarily due to large advances in fishing technology. Therefore, incorporating harvesting terms h_1 and h_2 in adult cod and grey seal populations respectively are also reasonable in the model formation. The model, with the considered assumption, will be formulated as:

$$\begin{aligned}
\frac{dJ}{dt} &= r_1 A\left(1-\frac{A}{K_1}\right) - \omega_1 AJ - \frac{\omega_3 GJ}{\theta + J} - \rho J, \\
\frac{dA}{dt} &= \rho J + \omega_2 AJ - h_1 A, \\
\frac{dG}{dt} &= r_2 G\left(1-\frac{G}{K_2}\right) + \frac{\omega_4 GJ}{\theta + J} - h_2 G.
\end{aligned} \tag{4.2.1}$$

with $J(0) = J_0 > 0, A(0) = A_0 > 0$ and $G(0) = G_0 > 0$. All the parameters used in system (4.2.1) are positive. Fig. 4.1 is the schematic representation of the model system. To see the description of parameter values of formulated model refer to Table 4.1 .

we shall discuss the positivity and boundedness of the system (4.2.1) to ensure that the model is well-posed.

Theorem 4.2.1 *All solutions of system* (4.2.1) *starting from* $\mathbb{R}^3_+$ *remains positive for all*

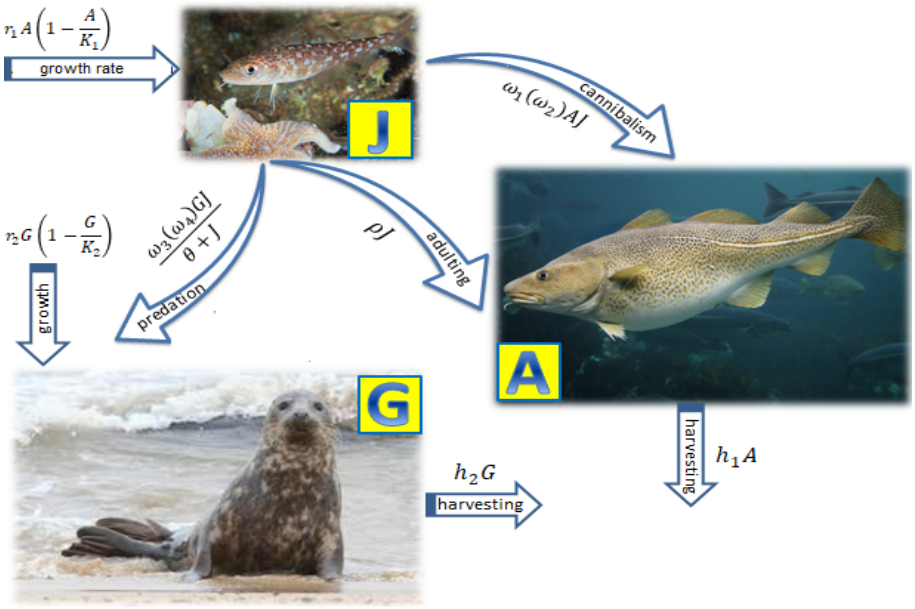

Figure 4.1: Schematic diagram for three species food model system (4.2.1)

time. Furthermore,

$$\limsup P(t)_{t\to\infty} \leq \left(\frac{r_1K_1}{4}+\frac{r_2K_2}{4}+\gamma K_1\right),$$

where, $P(t)=J(t)+A(t)+G(t)$ *and* $\gamma=\min\{h_1,h_2\}$.

Proof As $P(t)=J(t)+A(t)+G(t)$, taking time derivative on both the sides we get

$$\frac{dP}{dt}=\frac{dJ}{dt}+\frac{dA}{dt}+\frac{dG}{dt},$$

Now, from model (4.2.1), we get

$$\begin{aligned}
\frac{dP}{dt} &= r_1A\left(1-\frac{A}{K_1}\right)+(\omega_2-\omega_1)AJ+(\omega_4-\omega_3)\frac{GJ}{\theta+J}+r_2G\left(1-\frac{G}{K_2}\right)\\
&\quad -h_1A-h_2G,\\
&< r_1A\left(1-\frac{A}{K_1}\right)+r_2G\left(1-\frac{G}{K_2}\right)-h_1A-h_2G,\\
\frac{dP}{dt}+\gamma P &< r_1A\left(1-\frac{A}{K_1}\right)+r_2G\left(1-\frac{G}{K_2}\right)+\gamma J+(\gamma-h_1)A+(\gamma-h_2)G,
\end{aligned}$$

Table 4.1: Description of parameter values used in model (4.2.1).

Variables/ parameters	Unit	Description
J	Juvenile cod per unit area	Density of juvenile Atlantic cod population
A	Adult cod per unit area	Density of adult Atlantic cod population
G	Grey seal per unit area	Density of grey seal population
r_1	Per day	Intrinsic growth rate of adult cod population
r_2	Per day	Intrinsic growth rate of grey seal population
K_1	Cod per unit area	Cod's carrying capacity
K_2	Grey seal per unit area	Grey seal's carrying capacity
ω_1	Per day	Rate of cannibalism in cod
ω_2	Per day	Biomass conversion rates of juvenile cod to adult cod
ω_3	Per day	Predation rate of juvenile cod by grey seal
ω_4	Per day	Biomass conversion rates of juvenile cod to grey seal
ρ	Per day	Conversion rate of juvenile cod to adult cod
θ	Per unit area	Protection measure, served by the environment to juvenile cod thus diminishing the predation rates
h_1	Per unit area	Harvesting rate of adult Atlantic cod
h_2	Per unit area	Harvesting rate of grey seal

since, $\gamma = \min\{h_1, h_2\}$,

$$\begin{aligned}
\frac{dP}{dt} + \gamma P &< r_1 A\left(1 - \frac{A}{K_1}\right) + r_2 G\left(1 - \frac{G}{K_2}\right) + \gamma J, \\
&< r_1\left(A - \frac{A^2}{K_1}\right) - r_2\left(\frac{G^2}{K_2} - G\right) + \gamma K_1, && (\because J \le K_1) \\
&< -r_1\left(\frac{A}{\sqrt{K_1}} - \frac{\sqrt{K_1}}{2}\right)^2 + \frac{r_1 K_1}{4} - r_2\left(\frac{G}{\sqrt{K_2}} - \frac{\sqrt{K_2}}{2}\right)^2 + \frac{r_2 K_2}{4} + \gamma K_1, \\
&< \frac{r_1 K_1}{4} + \frac{r_2 K_2}{4} + \gamma K_1, && (\because A \le K_1 \text{ and } G \le K_2) \\
0 < P(t) &\le \left(\frac{r_1 K_1}{4} + \frac{r_2 K_2}{4} + \gamma K_1\right) + e^{-\gamma t}\left(P(0) - \frac{r_1 K_1}{4} - \frac{r_2 K_2}{4} - \gamma K_1\right).
\end{aligned}$$

As $t \to \infty$,

$$0 < P \le \left(\frac{r_1 K_1}{4} + \frac{r_2 K_2}{4} + \gamma K_1\right).$$

This theorem indicates that all the populations are within a close bound through out the time span, which is necessary for system to hold its biological significance.

4.2.1.1 Dissipative and persistence

Biologically, persistence of a system means long term survival of each component no matter what the initial populations are. Mathematically, it means strictly positive solutions not having omega limit points on the boundary of the non-negative cone (Craciun et al. (2013)). We first state the well known conclusion as Lemma 4.2.2.

Lemma 4.2.2 *If* $m > 0,\ n > 0$ *and* $\dot{y}(t) \leq (\geq) y(t)\big(n - my^{\beta}(t)\big)$, *where* $\beta > 0$*(constant),* $t \geq 0$ *and* $y(0) > 0$, *then we have* $\dot{y}(t) \leq (\geq) \frac{n}{m}^{\frac{1}{\beta}} \Big[1 + \Big(\frac{ny^{-\beta}(0)}{m} - 1\Big)e^{-nmt}\Big]^{\frac{-1}{\beta}}$.

Theorem 4.2.3 *The non-negative solution of system* (4.2.1) *satisfies*

$$\begin{aligned} \lim_{t\to\infty} J(t) &\leq K_1, \\ \lim_{t\to\infty} A(t) &\leq \frac{\rho K_1}{h_1 - \omega_2 K_1}, \\ \lim_{t\to\infty} G(t) &\leq \frac{K_2(r_2 + \omega_2 K_1 - h_2)}{r_2}, \end{aligned}$$

if $\omega_2 K_1 - h_1 < 0$ *and* $r_2 + \omega_2 K_1 - h_2 > 0$.

Proof We will show that the solution stays positive. From the system (4.2.1) we can see that-

$$\begin{aligned} J(t) &\leq K_1, && (4.2.2) \\ \frac{dA}{dt} &\leq \rho K_1 + (\omega_2 K_1 - h_1)A, && (4.2.3) \\ \frac{dG}{dt} &\leq r_2 G\left(1 - \frac{G}{K_2}\right) + \omega_2 G K_1 - h_2 G, \\ &= G\big(r_2 + \omega_2 K_1 - h_2 - \frac{r_2 G}{K_2}\big). && (4.2.4) \end{aligned}$$

By integrating (4.2.3) and taking limit $(t \to \infty)$ we see that,

$$\lim_{t\to\infty} A(t) \leq \frac{\rho K_1}{h_1 - \omega_2 K_1}.$$

By integrating (4.2.4), taking limit $(t \to \infty)$ and using lemma 1 we see that,

$$\lim_{t\to\infty} G(t) \leq \frac{K_2(r_2 + \omega_2 K_1 - h_2)}{r_2}.$$

Hence, we get the proof.

Biologically, this theorem indicates the sufficient conditions for which all the these species have their individual bounds i.e. their number can't surpass some definite value if some conditions hold. Hence, a dissipative system (Smith and Thieme (2011)).

Theorem 4.2.4 *Assume that upper bound conditions hold and in addition $r_2 > h_2$, then the system persists.*

Proof From system (4.2.1), we get

$$\begin{aligned}\frac{dJ}{dt} &> J\Big[-\frac{\omega_1\rho K_1}{h_1-\omega_2K_1}-\frac{\omega_3K_2(r_2+\omega_2K_1-h_2)}{r_2}-\rho\Big]\\ &\quad +r_1\frac{\rho K_1}{h_1-\omega_2K_1}\Big(1-\frac{\rho K_1}{K_1(h_1-\omega_2K_1)}\Big),\\ \frac{dJ}{dt} &> (-C_1)J+C_2\end{aligned}$$

where, $C_1=\dfrac{\omega_1\rho K_1}{h_1-\omega_2K_1}+\dfrac{\omega_3K_2(r_2+\omega_2K_1-h_2)}{r_2}+\rho,$

$$C_2=r_1\frac{\rho K_1}{h_1-\omega_2K_1}\Big(1-\frac{\rho K_1}{K_1(h_1-\omega_2K_1)}\Big).$$

by integrating, we get

$$J(t)>\frac{C_2}{C_1}+C_3\exp\left(-C_1t\right)\quad\Big\{C_3 \text{ is a constant, and } C_3<J(0)-\frac{C_2}{C_1}\Big\}$$

taking limit $(t\to\infty)$,

$$\lim_{t\to\infty}J>\frac{C_2}{C_1}. \tag{4.2.5}$$

Now, using (2)

$$\frac{dA}{dt}>(-h_1)A+\rho\frac{C_2}{C_1}\quad\{\text{Using eqn (4.2.5)}\}$$

By integrating, we get

$$A(t)>\frac{\rho C_2}{C_1h_1}+C_4\exp\left(-h_1t\right)\quad\Big\{C_4 \text{ is a constant, and } C_4<A(0)-\frac{\rho C_2}{C_1h_1}\Big\}$$

taking limit $(t\to\infty)$,

$$\lim_{t\to\infty}A>\frac{\rho C_2}{C_1h_1}. \tag{4.2.6}$$

Lastly,

$$\frac{dG}{dt} > G\Big[r_2 - h_2 - \frac{r_2 G}{K_2}\Big].$$

Using Lemma 1 and taking limit ($t \to \infty$),

$$\lim_{t\to\infty} G > \frac{K_2(r_2 - h_2)}{r_2}. \tag{4.2.7}$$

From (4.2.5), (4.2.6) and (4.2.7), we say system persists.

Biologically, all the species will survive if the indicated conditions hold true, even we have the different initial populations.

4.2.2 Model with Allee Effect

Atlantic cod has experienced relatively greater and deeper population depletion than any other species. Beside from its relevance to marine conservation and fisheries, Atlantic cod also provides an excellent basis for investigating the influence of Allee effect on population recovery. A demographic Allee effect has been observed in cods through extensive analyses of several populations in past literature. In this research, we will investigate whether the Allee effect has a positive or negative role in the survival of cod populations. The population growth rate is generally assumed to be relatively faster at low abundance, because of low competition (i.e., negative density dependence). But population growth can be limited in small populations as the result of the Allee effect. Now, we investigate how an Allee effect can influence the dynamics of recovery in cannibalistic species. In this section, we modify the system (4.2.1) to illustrate the impact of strong Allee effect in the cod population. With the above assumptions, the model (4.2.1) can be formulated as follows:

$$\begin{aligned}
\frac{dJ}{dt} &= r_1 A\left(1 - \frac{A}{K_1}\right)(A - \beta) - \omega_1 AJ - \frac{\omega_3 GJ}{\theta + J} - \rho J, \\
\frac{dA}{dt} &= \rho J + \omega_2 AJ - h_1 A, \\
\frac{dG}{dt} &= r_2 G\left(1 - \frac{G}{K}\right) + \frac{\omega_4 GJ}{\theta + J} - h_2 G.
\end{aligned} \tag{4.2.8}$$

with $J(0) = J_0 > 0, A(0) = A_0 > 0$ and $G(0) = G_0 > 0$. Here, the parameter β represents a strong Allee effect.

4.3 Stability analysis of model without Allee Effect

4.3.1 Existence of equilibrium points

The Jacobian matrix corresponding to model (4.2.1) is given by:

$$\mathcal{J}(J,A,G) = \begin{pmatrix} c_{11} & c_{12} & c_{13} \\ c_{21} & c_{22} & c_{23} \\ c_{31} & c_{32} & c_{33} \end{pmatrix} \tag{4.3.1}$$

The entries of matrix are:

$$\begin{aligned}
c_{11} &= -\rho - A\omega_1 + \frac{GJ\omega_3}{(J+\theta)^2} - \frac{G\omega_3}{J+\theta} \\
c_{12} &= (1 - \frac{A}{K_1})r_1 - \frac{Ar_1}{K_1} - J\omega_1, \\
c_{13} &= -\frac{J\omega_3}{J+\theta}, \\
c_{21} &= \rho + A\omega_2, \\
c_{22} &= -h_1 + J\omega_2, \\
c_{23} &= 0 \\
c_{31} &= -\frac{GJ\omega_4}{(J+\theta)^2} + \frac{G\omega_4}{J+\theta}, \\
c_{32} &= 0, \\
c_{33} &= -h_2 + (1 - \frac{G}{K_2})r_2 - \frac{Gr_2}{K_2} + \frac{J\omega_4}{J+\theta}.
\end{aligned}$$

Lemma 4.3.1 *The formulated model (4.2.1) has following possible equilibrium points:*

- *The equilibrium* $E_0 = (0,0,0)$*, exists always.*
- *The cod (juvenile and adult) free equilibrium* $E_1 = \left(0, 0, \frac{K_2(r_2-h_2)}{r_2}\right)$*, exists if* $h_2 < r_2$*.*
- *The equilibrium* $E_2 = \left(\frac{-R+P}{Q}, \frac{S+P}{T}, 0\right)$*, always exists*
  where, $R = h_1K_1(\omega_1 - 2\omega_2) + r_1(\rho + K_1\omega_2)$*,*
  $P = \sqrt{(r_1\rho + h_1K_1\omega_1)^2 - 2K_1r_1(2h_1\rho - r_1\rho + h_1K_1\omega_1)\omega_2 + {K_1}^2{r_1}^2{\omega_2}^2}$*,*
  $Q = 2K_1(\omega_1 - \omega_2)\omega_2$*,*
  $S = -r_1\rho - h_1K_1\omega_1 + K_1r_1\omega_2$*,*
  $T = 2r_1\omega_2$*.*

- *For establishing the existence of non-trivial equilibrium, $E^* = (J^*,\ A^*,\ G^*)$, we form two isoclines (first one by finding A from (2) and then putting in (1); second one by putting the same A in (3)) as follows,*

$$\begin{aligned} f(A,G) &= A^3(h_1 r_1 \omega_2 + r_1 \theta {\omega_2}^2) \\ &\quad + A^2(h_1 r_1 \rho + {h_1}^2 K_1 \omega_1 - h_1 K_1 r_1 \omega_2 + 2 r_1 \theta \rho \omega_2 + h_1 K_1 \theta \omega_1 \omega_2 - K_1 r_1 \theta {\omega_2}^2) \\ &\quad + A(-h_1 K_1 r_1 \rho + r_1 \theta \rho^2 + h_1 K_1 \theta \rho(\omega_1 + \omega_2) - 2 K_1 r_1 \theta \rho \omega_2 + G h_1 K_1 \omega_2 \omega_3) \\ &\quad + G h_1 K_1 \rho \omega_3 - K_1(r_1 - h_1)\theta \rho^2 = 0, \qquad (4.3.2) \\ h(A,G) &= A K_2 \left((h_2 - r_2)(h_1 + \theta \omega_2) - h_1 \omega_4\right) \\ &\quad + G\left(A^* r_2 (h_1 + \theta \omega_2) + r_2 \rho \theta\right) + K_2 \rho \theta (h_2 - r_2). \qquad (4.3.3) \end{aligned}$$

Case 1: For first isocline,

From (4.3.2) when $G \to 0$,

then $A \to \dfrac{S + \sqrt{4 r_1 K_1 \rho (r_1 - h_1)\omega_2 + (-r_1 \rho - h_1 K_1 \omega_1 + K_1 r_1 \omega_2)^2}}{T} (= A_{1a})$;

A_{1a} is positive when $h_1 < \dfrac{r_1 \omega_2}{\omega_1}, K_1 > \dfrac{r_1 \rho}{\omega_2 r_1 - h_1 \omega_1}$.

Consider, $\dfrac{dA}{dG} = \dfrac{M_1}{N_1}$,

where,

$$\begin{aligned} M_1 &= (\rho + A\omega_2) K_1 h_1 \omega_3, \\ N_1 &= 3A^2 r_1 \omega_2 (h_1 + \theta \omega_2) \\ &\quad + 2A({h_1}^2 K_1 \omega_1 + r_1 \theta \omega_2 (2\rho - K_1 \omega_2) + h_1 (r_1 \rho - K_1 r_1 \omega_2 + K_1 \theta \omega_1 \omega_2)) \\ &\quad + h_1 K_1 (-r_1 \rho + \theta \rho(\omega_1 + \omega_2) + G \omega_2 \omega_3) + r_1 \theta \rho (\rho - 2 K_1 \omega_2) + h_1^2 K_1 \rho. \end{aligned}$$

Further, $\dfrac{dA}{dG} > 0$ *if* $N_1 > 0$ ($M_1 > 0$, *already*)

Case 2: For second isocline,

Similarly, from (4.3.3) when $G \to 0$,

then $A \to \dfrac{(-h_2 + r_2)\theta \rho}{(h_2 - r_2)(h_1 + \theta \omega_2) - h_1 \omega_4} (= A_{2a})$;

A_{2a} is positive when $\omega_4 > h_2 - r_2, h_2 > r_2$ *and* $\theta < \dfrac{h_1(-h_2 + r_2 + \omega_4)}{(h_2 - r_2)\omega_2}$.

Now, consider $\frac{dA}{dG} = \frac{M_2}{N_2}$,

where,

$$\begin{aligned} M_2 &= r_2(\theta\rho + A(h_1 + \theta\omega_2)), \\ N_2 &= (h_2K_2 + (G - K_2)r_2)(h_1 + \theta\omega_2) - h_1K_2\omega_4. \end{aligned}$$

Further, $\frac{dA}{dG} < 0$ *if* $N_2 < 0$ ($M_2 > 0$, *already)*

From case 1 and case 2, we assert that the two isoclines intersect at some point in first quadrant (both positive)

if $h_1 < \frac{r_1\omega_2}{\omega_1}, K_1 > \frac{r_1\rho}{\omega_2 r_1 - h_1\omega_1}, \omega_4 > h_2 - r_2, h_2 > r_2,$ *and* $\frac{(h_1(-h_2 + r_2 + \omega_4))}{((h_2 - r_2)\omega_2)}$

$> \theta > \frac{r_2 - h_2 + \omega_4}{(h_2 - r_2)Q}\Big[-K_1(\omega_1 - \omega_2)\omega_2\Big\{\frac{2P}{Q}\Big\} + (h_1K_1(\omega_1 - 2\omega_2) + r_1(\rho + K_1\omega_2))\Big],$

(so that $A_{1a} < A_{2a}$*). Knowing the intersection point, we find the values of* A^* *and* G^**; and hence, the value of* J^**. This shows the existence of* E^* .
Now, we reduce system (4.2.1) into an equation in terms of J *(by finding* A *in terms of* J *from (2) and finding* G *in terms of* J *from (3) and then putting both in (1)), becomes*

$$k(J) = aJ^4 + bJ^3 + cJ^2 + dJ + e, \tag{4.3.4}$$

where,

$$\begin{aligned} a &= K_1r_2\rho\omega_1\omega_2 - K_1r_2\rho{\omega_2}^2, \\ b &= -r_1r_2\rho(\rho + K_1\omega_2) - K_1(h_1r_2\rho(\omega_1 - 2\omega_2) + \omega_2(r_2(2\theta\rho(-\omega_1 + \omega_2) \\ &\quad + K_2\omega_2\omega_3) + K_2\omega_2\omega_3(-h_2 + \omega_4))), \\ c &= -{h_1}^2K_1r_2\rho - 2r_1r_2\theta\rho(\rho + K_1\omega_2) + K_1\theta\omega_2(r_2\theta\rho(\omega_1 - \omega_2) + K_2(h_2 - r_2)\omega_2\omega_3) \\ &\quad + h_1K_1(r_1r_2\rho + r_2(-2\theta\rho\omega_1 + 4\theta\rho\omega_2 + 2K_2\omega_2\omega_3) + 2K_2\omega_2\omega_3(-h_2 + \omega_4)), \\ d &= -r_1r_2\theta^2\rho(\rho + K_1\omega_2) + h_1K_1\theta(r_2\rho(2r_1 - \theta\omega_1 + 2\theta\omega_2) + 2K_2(-h_2 + r_2)\omega_2\omega_3) \\ &\quad - {h_1}^2K_1(r_2(2\theta\rho + K_2\omega_3) + K_2\omega_3(-h_2 + \omega_4)), \\ e &= h_1K_1\theta((-h_1 + r_1)r_2\theta\rho + h_1K_2(h_2 - r_2)\omega_3), \end{aligned}$$

then the discriminant of quartic function becomes
$\Delta = 256a^3e^3 - 192a^2bde^2 - 128a^2c^2e^2 + 144a^2cd^2e - 27a^2d^4 + 144ab^2ce - 6ab^2d^2e -$

$80abc^2de + 18abcd^3 + 16ac^4e - 4ac^3d^2 - 27b^4e^2 + 18b^3cde - 4b^3d^3 - 4b^2c^3e + b^2c^2d^2$
Also, $\mathcal{T} = 8ac - 3b^2, \mathcal{U} = b^3 + 8da^2 - 4abc, \mathcal{V} = c^2 - 3bd + 12ae, \mathcal{W} = 64a^3e - 16a^2c^2 + 16ab^2c - 16a^2bd - 3b^4$.
Now,

- *Case 1: If* $\Delta < 0$ *then there will be 2 real distinct and 2 complex conjugates roots.*

- *Case 2: If* $\Delta > 0$ *then*
  - *(a) If* $\mathcal{T} < 0$ *and* $\mathcal{W} < 0$ *then there will be 4 real and distinct roots.*

  - *(b) If* $\mathcal{T} > 0$ *and* $\mathcal{W} > 0$ *then there will be 2 pairs of complex conjugate roots.*

- *Case 3: If* $\Delta = 0$ *then*
  - *(a) If* $\mathcal{T} < 0$ *and* $\mathcal{W} < 0$ *and* $\mathcal{V} \neq 0$ *then there will be 2 real simple and 1 real double roots.*

  - *(b) If* $\mathcal{W} > 0$ *or* $\mathcal{T} > 0(\mathcal{W} \neq 0$ *or* $\mathcal{U} \neq 0)$ *then there will be 1 real double and a pair of complex conjugate roots.*

  - *(c) If* $\mathcal{V} = 0$ *and* $\mathcal{W} \neq 0$ *then there will be 1 real triple and 1 real simple roots.*

  - *(d) If* $\mathcal{W} = 0$ *then*
    - *(i) If* $\mathcal{T} < 0$ *then there will be 2 real double roots.*

    - *(ii) If* $\mathcal{T} > 0$ *and* $\mathcal{U} = 0$ *then there will be 2 double complex conjugate roots.*

    - *(iii) iIf* $\mathcal{V} = 0$ *then there will be 4 equal roots.*

Example 4.3.1 *Let us set* $r_1 = 0.49,\ h_1 = 0.12,\ r_2 = 1.2,\ h_2 = 0.7,\ \omega_1 = 0.9,\ \omega_2 = 0.25,\ \omega_3 = 1.1, \omega_4 = 0.95, \theta = 25, \rho = 1/(7 * 365), K_1 = 1000$ *and* $K_2 = 100$ *the eqn*

(4.3.4) becomes

$$k(J) = 0.0763209J^4 - 9965.01J^3 - 76323.8J^2 + 80154.2J - 19787. \qquad (4.3.5)$$

For these parameters: $\Delta = 7.65037X10^{18} > 0$, $\mathcal{T} = -2.97951X10^8 < 0$ *and* $\mathcal{W} = -2.95916X10^{16} < 0$. *Hence, from Case 2 (a) there will be 4 real and distinct roots. Since, we are interested in positive values of all three species* (J, A, G), *calculating mathematically we get two positive equilibriums, (i)* $E_1^* = (0.479992, 100.154, 43.158)$ *and (ii)* $E_2^* = (0.479959, 18.2116, 43.1579)$.

4.3.2 Local stability analysis of equilibrium points

Theorem 4.3.2 *The equilibrium point* E_0 *is locally asymptotically stable if* $r_2 < h_2$ *and* $r_1 < h_1$.

Proof Since, the eigenvalues of Jacobian matrix (4.3.1) corresponding to E_0 are $-h_2 + r_2$, $\frac{1}{2}(-h_1 - \rho \pm \sqrt{{h_1}^2 - 2h_1\rho + 4r_1\rho + \rho^2})$. All the eigenvalues are negative if $r_2 < h_2$ and $r_1 < h_1$. Hence, the proof.

Theorem 4.3.3 *The Equilibrium point* E_1 *is locally asymptotically stable if*

$$r_1 < h_1 + \frac{h_1K_2(-h_2 + r_2)\omega_3}{r_2\theta\rho}. \qquad (4.3.6)$$

Proof The corresponding eigenvalues to variational matrix (4.3.1) are $h_2 - r_2$, $\dfrac{M \pm \sqrt{N}}{L}$
where, $M = -h_1r_2\theta - r_2\theta\rho + h_2K_2\omega_3 - K_2r_2\omega_3$,
$N = (h_1r_2\theta + r_2\theta\rho - h_2K_2\omega_3 + K_2r_2\omega_3)^2 - 4r_2\theta(h_1r_2\theta\rho - r_1r_2\theta\rho$
$-h_1h_2K_2\omega_3 + h_1K_2r_2\omega_3)$,
$L = 2r_2\theta$.
Thus, under (4.3.6) E_1 is stable.

Theorem 4.3.4 *The Equilibrium point* E_2 *is locally asymptotically stable if all the eigenvalues are negative.*

Proof The corresponding eigenvalues to Jacobian matrix (4.3.1) are $-h_2 + r_2 + \dfrac{(P-R)\omega_4}{P - R - Q\theta}$,
$\dfrac{1}{2K_1QT^2}\Big(-K_1TW \pm V\Big)$
where, $W = \big(QT(h_1 + \rho) + Q(P+S)\omega_1 + (P-R)T\omega_2\big)$,
$V = \sqrt{K_1T^2(K_1W)^2 - 4Q(T(Q(2r_1(P+S) + K_1(h_1 - r_1)T)\rho + K_1(h_1Q(P+S)}$
$+(-P+R)T\rho)\omega_1) + (Qr_1(P+S)(2(P+S) - K_1T) + K_1(P-R)T^2\rho)\omega_2))$.

Thus, E_2 is locally asymptotically stable if all these eigenvalues are negative.

Theorem 4.3.5 *The equilibrium $E^* = (J^*,\ A^*,\ G^*)$, is asymptotically stable if $B_1 > 0, B_3 > 0$ and $B_1B_2 - B_3 > 0$ where $B_1,\ B_2,\ B_3$ are defined in the proof.*

Proof The characteristic equation of Jacobian matrix (4.3.1) corresponding to E^* becomes:

$$\lambda^3 + B_1\lambda^2 + B_2\lambda + B_3 = 0,$$

where,

$$\begin{aligned}
B_1 &= h_1 + h_2 - r_2 + \rho + A^*\omega_1 - J^*\omega_2 + \frac{2G^*r_2}{K_2} - \frac{G^*J^*\omega_3}{(J^*+\theta)^2} - \frac{-G^*\omega_3 + J^*\omega_4}{J^*+\theta},\\
B_2 &= h_1(h_2 - r_2) + \frac{2G^*h_1r_2}{K_2} + \rho(h_1 - r_1 - r_2) + h_2\rho + A^*h_1\omega_1 + A^*h_2\omega_1\\
&\quad -A^*r_2\omega_1 + J^*\rho\omega_1 - (A^*r_1 + J^*(h_2 - r_2 + \rho))\omega_2\\
&\quad +\frac{2(A^*(K_2r_1\rho + G^*K_1r_2\omega_1) + A^{*2}K_2r_1\omega_2 + G^*K_1r_2(\rho - J^*\omega_2))}{K_1K_2}\\
&\quad -\frac{G^*\theta(-2G^*r_2 + K_2(-h_1 - h_2 + r_2 + J^*\omega_2))\omega_3}{K_2(J^*+\theta)^2}\\
&\quad +\frac{J^*K_2(J^*+\theta)(h_1 + \rho + A^*\omega_1 - J^*\omega_2)\omega_4}{K_2(J^*+\theta)^2},\\
B_3 &= -\frac{1}{K_1K_2(J^*+\theta)^2}\\
&\quad \Big(2A^{*2}r_1(J^*+\theta)\omega_2\big(-(h_2k_2 + 2G^*r_2 - K_2r_2)(J^*+\theta) + J^*K_2\omega_4\big)\\
&\quad +A^*r_1(J^*+\theta)(2\rho - K_1\omega_2)\big(-(h_2K_2 + 2G^*r_2 - K_2r_2)(J^*+\theta) + J^*K_2\omega_4\big)\\
&\quad +h_1K_1\big(h_2K_2(-(J^*+\theta)^2(\rho + A^*\omega_1) - G^*\theta\omega_3) + (2G^* - K_2)r_2(-(J^*+\theta)^2\\
&\quad (\rho + A^*\omega_1) - G^*\theta\omega_3) + J^*K_2(J^*+\theta)(\rho + A^*\omega_1)\omega_4\big)\\
&\quad +K_1\big(G^*J^*\theta\omega_2\omega_3(1 + 2G^*r_2) + h_2K_2(-(J^*+\theta)^2\rho)(-r_1 + J^*(\omega_1 - \omega_2))\big)\\
&\quad +G^*r_2\big(-2(J^*+\theta)^2\rho(-r_1 + J^*\omega_1 - J^*\omega_2) - J^*K_2\theta\omega_2\omega_3\big)\\
&\quad +K_2(J^*+\theta)\rho(-r_1 + J^*\omega_1 - J^*\omega_2)(r_2(J^*+\theta) + J\omega_4))\Big).
\end{aligned}$$

By Routh-hurwitz criterion, we can say that E^* is locally asymptotically stable if $B_1 > 0, B_3 > 0$ and $B_1B_2 - B_3 > 0$.

Remark 7 *Setting the parameters as in Example 4.3.1; we find that*

- *For $E_1^* = (0.479959, 100.154, 43.1579)$, $B_1 = 92.485 > 0, B_3 = 0.520667 > 0$ and $B_1B_2 - B_3 = 4500.48 > 0$, and*

- *For* $E_2^* = (0.479959, 18.2116, 43.1579)$, $B_1 = 18.7368 > 0, B_3 = -0.0946749 \not> 0$ *and* $B_1B_2 - B_3 = 174.073 > 0$

Hence, for this set of parameters positive equilibrium E_1^* *is locally asymptotically stable and* E_2^* *is unstable.*

4.3.3 Global stability analysis

By rewriting the model (4.2.1) in the autonomous dynamical form:

$$\dot{x} = g(x), \tag{4.3.7}$$

where g: $\Omega_1 \to \mathbb{R}^3_+$, $\Omega_1 \subset \mathbb{R}^3$ and h $\in C^1(\Omega)$, $x = (J, A, G)^T$.
To prove global stability the following conditions must hold:
(C_1) Ω_1 is simply connected.
(C_2) there exists a compact absorbing set(K) in the interior of Ω_1,
(C_3) E^* is the unique equilibrium point of system (4.3.7) in Ω_1.
Further, we give some definitions and preliminary notations as follows:
The Lozinskii measure $\bar{\mu}(B)$ (where B is any square matrix), is defined as:

$$\bar{\mu}(B) = \lim_{h \to 0^+} \frac{|I + hB| - 1}{h}.$$

Let H be a matrix-valued function and H_g be matrix with entries of H replaced by its directional derivative in the direction of g i.e.

$$(h_{ij}(x))_g = (\nabla h_{ij}(x).g(x)).$$

Further, we define $B = H_g H^{-1} + H\mathcal{V}^{[2]}H^{-1}$, where $\mathcal{V}^{[2]}$ is the second additive matrix of Jacobian matirx of the system.

Lemma 4.3.6 *E^* is globally asymptotically stable in Ω_1 if it satisfies stated conditions $(C_1) - (C_3)$ along with condition:*

$$\bar{q_2} = \limsup_{t \to \infty} \sup_{x_0 \in K} \frac{1}{t} \int_0^t \bar{\mu}(B(x(s, x_0)))ds < 0,$$

where $x(t, x_0)$ is the solution of (4.3.7) with $x_0 \in K$ be initial condition at $t = 0$.

Theorem 4.3.7 *The unique E^* is globally asymptotically stable in Ω_1 under assumption (C_1)-(C_3) and conditions*

$$K_1 > 2A^*,\ \omega_1 < \frac{(-2A^*r_1 + K_1r_1)}{J^*K_1}, \omega_4 < \frac{G^*r_2 - K_2r_2 + K_2Y}{J^*K_2 + G^*K_2\theta} \text{ and}$$

$$h_1 > max\Big\{\frac{-2A^*r_1 + K_1r_1 - J^*K_1\omega_1 + J^*K_1\omega_2}{K_1}, \omega_1(K_1 - A^*) + J^*\omega_2 + \frac{(-2G^* + J^*)\omega_3}{J^* + \theta} + K_2\omega_3 + G^*J^*\omega_3\Big\},$$

(where Y is defined in the proof) if there exist a function $H(x)$ and a Lozinskii measure $\bar{\mu}(B)$ such that $\bar{q_2} < 0$.

Proof The Jacobian matrix $\mathscr{J}(E^*)$ corresponding to equilibrium point E^* of the model is given by:

$$\mathscr{J}(E^*) = \begin{pmatrix} -\rho - A^*\omega_1 + \frac{G^*J^*\omega_3}{(J^*+\theta)^2} - \frac{G\omega_3}{J^*+\theta} & (1 - \frac{A^*}{K_1})r_1 - \frac{A^*r_1}{K_1} - J^*\omega_1 & -\frac{J^*\omega_3}{J^*+\theta} \\ \rho + A^*\omega_2 & -h_1 + J^*\omega_2 & 0 \\ -\frac{G^*J^*\omega_4}{(J^*+\theta)^2} + \frac{G^*\omega_4}{J^*+\theta} & 0 & -h_2 + (1 - \frac{G^*}{K_2})r_2 - \frac{G^*r_2}{K_2} + \frac{J^*\omega_4}{J^*+\theta} \end{pmatrix}.$$

The second additive matrix $\mathscr{J}^{[2]}(E^*)$ is given by:

$$\mathscr{J}^{[2]}(E^*) = \begin{pmatrix} \bar{B}_{11} & B_{12} \\ B_{21} & \bar{B}_{22} \end{pmatrix},$$

where, $\bar{B}_{11} = -h_1 - \rho + J^*\omega_2 - A^*\omega_1 - \frac{G^*\theta\omega_3}{(J^*+\theta)^2} - \frac{G^*\omega_3}{J^*+\theta}$,

$$B_{12} = \Big(0, \frac{J^*\omega_3}{J^*+\theta}\Big), B_{21} = \Big(0, \frac{G^*J^*\omega_4}{(J^*+\theta)^2} - \frac{G^*\omega_4}{J^*+\theta}\Big)^T,$$

$$\bar{B}_{22} = \begin{pmatrix} -h_2 + r_2 - \rho - A^*\omega_1 - \frac{2G^*r_2}{K_2} + \frac{-G^*\theta\omega_3 + J^*(J^*+\theta)\omega_4}{(J^*+\theta)^2} & (1 - \frac{A^*}{K_1})r_1 - \frac{A^*r_1}{K_1} - J^*\omega_1 \\ \rho + A^*\omega_2 & -h_1 - h_2 + r_2 + J^*\omega_2 - \frac{2G^*r_2}{K_2} + \frac{J^*\omega_4}{J^*+\theta} \end{pmatrix}.$$

Choosing

$$H = H(J, A, G) = diag\Big\{1, \frac{J}{G}, \frac{J}{G}\Big\}, H^{-1} = diag\Big\{1, \frac{G}{J}, \frac{G}{J}\Big\},$$

$$H_g = diag\Big\{0, \frac{\dot{J}}{G} - \frac{J}{G^2}\dot{G}, \frac{\dot{J}}{G} - \frac{J}{G^2}\dot{G}\Big\}, H_gH^{-1} = diag\Big\{0, \frac{\dot{J}}{J} - \frac{\dot{G}}{G}, \frac{\dot{J}}{J} - \frac{\dot{G}}{G}\Big\}.$$

Now, $B = H_gH^{-1} + H\mathscr{V}^{[2]}H^{-1} = \begin{pmatrix} B_{11} & B_{12} \\ B_{21} & B_{22} \end{pmatrix}$,

where,

$$B_{11} = -h_1 - \rho - A^*\omega_1 + J^*\omega_2 - \frac{G^*\theta\omega_3}{(J^*+\theta)^2} - \frac{G^*\omega_3}{J^*+\theta}, B_{22} = \begin{pmatrix} \frac{\dot{J}}{J} - \frac{\dot{G}}{G} & 0 \\ 0 & \frac{\dot{J}}{J} - \frac{\dot{G}}{G} \end{pmatrix} + \bar{B}_{22}.$$

If (a, b, c) be a vector in $\mathbb{R}^3$,then norm can be defined as $|(a, b, c)| = max\{|a|, |b| + |c|\}$.Calculating $\bar{\mu}$ Martin Jr (1974) if $g_1 = B_{11} + |B_{12}|$ and $g_2 = \bar{\mu}_1(B_{22}) + |B_{21}|$,

$$\bar{\mu}(B) \leq sup\{g_1, g_2\}, \tag{4.3.8}$$

where $|B_{12}|, |B_{21}|$ are matrix norms with respect to the l_1 vector norm and $\bar{\mu}_1(B_{22})$ be the Lozinskii measure,we get

$$\begin{aligned} |B_{12}| &= \frac{J^*\omega_3}{J^*+\theta}, \\ |B_{21}| &= \frac{G^*\theta\omega_4}{(J^*+\theta)^2}, \end{aligned}$$

$$\begin{aligned} \bar{\mu}_1(B_{22}) &= max\Big\{ -\frac{\dot{G}}{G} - h_2 + \frac{\dot{J}}{J} + r_2 - \frac{2G^*r_2}{K_2} - A\omega_1 + \frac{-G^*\theta\omega_3 + J^*(J^*+\theta)\omega_4}{(J^*+\theta)^2} \\ &\quad + A^*\omega_2, -\frac{\dot{G}}{G} - h_1 - h_2 + \frac{\dot{J}}{J} + r_2 - \frac{2G^*r_2}{K_2} + J^*\omega_2 + \frac{J^*\omega_4}{J^*+\theta} \\ &\quad + \Big|\Big(1 - \frac{A^*}{K_1}\Big)r_1 - \frac{A^*r_1}{K_1} - J^*\omega_1\Big|\Big\}, \\ &= \frac{\dot{J}}{J} - \frac{\dot{G}}{G} - h_2 - \frac{2G^*r_2}{K_2} + \frac{J^*\omega_4}{J^*+\theta} + r_2 + max\Big\{A^*(\omega_2 - \omega_1) - \frac{G^*\theta\omega_3}{(J^*+\theta)^2}, \\ &\quad J^*\omega_2 - h_1 + \Big|\Big(1 - \frac{A^*}{K_1}\Big)r_1 - \frac{A^*r_1}{K_1} - J^*\omega_1\Big|\Big\}. \end{aligned}$$

Then,

$$\begin{aligned} g_1 &= -h_1 - \rho - A^*\omega_1 + J^*\omega_2 - \frac{G^*\theta\omega_3}{(J^*+\theta)^2} - \frac{G^*\omega_3}{J^*+\theta} + \frac{J^*\omega_3}{J^*+\theta}, \\ g_2 &= \frac{\dot{J}}{J} - \frac{\dot{G}}{G} - h_2 - \frac{2G^*r_2}{K_2} + \frac{J^*\omega_4}{J^*+\theta} + r_2 + \frac{G^*\theta\omega_4}{(J^*+\theta)^2} \\ &\quad + max\Big\{A^*(\omega_2 - \omega_1) - \frac{G^*\theta\omega_3}{(J^*+\theta)^2}, J^*\omega_2 - h_1 + \Big|\Big(1 - \frac{A^*}{K_1}\Big)r_1 - \frac{A^*r_1}{K_1} - J^*\omega_1\Big|\Big\}. \end{aligned}$$

From (4.2.1), we can rewrite g_1 and g_2 as,

$$\begin{aligned} g_1 &= \frac{\dot{J}}{J} - \frac{r_1 A}{J}\Big(1 - \frac{A}{K_1}\Big) + A\omega_1 + \frac{\omega_3 G}{\theta + J} - h_1 - A^*\omega_1 + J^*\omega_2 - \frac{G^*\theta\omega_3}{(J^* + \theta)^2} \\ &\quad - \frac{G^*\omega_3}{J^* + \theta} + \frac{J^*\omega_3}{J^* + \theta}, \end{aligned}$$

$$\begin{aligned} g_2 &= \frac{\dot{J}}{J} + \frac{r_2 G}{K_2} - \frac{\omega_4 J}{\theta + J} - \frac{2G^* r_2}{K_2} + \frac{J^*\omega_4}{J^* + \theta} + \frac{G^*\theta\omega_4}{(J^* + \theta)^2} + max\Big\{A^*(\omega_2 - \omega_1) \\ &\quad - \frac{G^*\theta\omega_3}{(J^* + \theta)^2}, J^*\omega_2 - h_1 + \Big|\Big(1 - \frac{A^*}{K_1}\Big)r_1 - \frac{A^* r_1}{K_1} - J^*\omega_1\Big|\Big\}. \end{aligned}$$

$$\begin{aligned} \bar{\mu}(B) &\leq sup\{g_1, g_2\}, \\ &= \frac{\dot{J}}{J} + max\Big\{ - \frac{r_1 A}{J}\Big(1 - \frac{A}{K_1}\Big) - h_1 + \omega_1(A - A^*) + J^*\omega_2 + \frac{G\omega_3}{J + \theta} + \frac{G^* J^*\omega_3}{(J^* + \theta)^2} \\ &\quad + \frac{(-2G^* + J^*)\omega_3}{J^* + \theta}, \frac{(G - G^*)r_2}{K_2} - \frac{J\omega_4}{J + \theta} + \frac{G^*\omega_4\theta}{(J^* + \theta)^2} + \frac{J^*\omega_4}{J^* + \theta} \\ &\quad + max\Big\{A^*(\omega_2 - \omega_1) - \frac{G^*\theta\omega_3}{(J^* + \theta)^2}, J^*\omega_2 - h_1 + \Big|\Big(1 - \frac{2A^*}{K_1}\Big)r_1 - J^*\omega_1\Big|\Big\}\Big\}, \\ &= \frac{\dot{J}}{J} + max\Big\{ - \frac{r_1 A}{J}\Big(1 - \frac{A}{K_1}\Big) - h_1 + \omega_1(A - A^*) + J^*\omega_2 + \frac{G\omega_3}{J + \theta} + \frac{G^* J^*\omega_3}{(J^* + \theta)^2} \\ &\quad + \frac{(-2G^* + J^*)\omega_3}{J^* + \theta}, \frac{(G - G^*)r_2}{K_2} - \frac{J\omega_4}{J + \theta} + \frac{G^*\omega_4\theta}{(J^* + \theta)^2} + \frac{J^*\omega_4}{J^* + \theta} + Y\Big\}, \end{aligned}$$

where, $Y = max\Big\{A^*(\omega_2 - \omega_1) - \frac{G^*\theta\omega_3}{(J^* + \theta)^2}, J^*\omega_2 - h_1 + \Big|\Big(1 - \frac{A^*}{K_1}\Big)r_1 - \frac{A^* r_1}{K_1} - J^*\omega_1\Big|\Big\}$,

and let $A^* < \frac{K_1}{2}, \omega_1 < \frac{(-2A^* r_1 + K_1 r_1)}{J^* K_1}, h_1 > \frac{-2A^* r_1 + K_1 r_1 - J^* K_1\omega_1 + J^* K_1\omega_2}{K_1}$

such that $Y < 0$,

then,

$$\begin{aligned} \bar{\mu}(B) &< \frac{\dot{J}}{J} + max\Big\{ - h_1 + \omega_1(K_1 - A^*) + J^*\omega_2 + K_2\omega_3 + G^* J^*\omega_3 + \frac{(-2G^* + J^*)\omega_3}{J^* + \theta}, \\ &\quad \frac{(K_2 - G^*)r_2}{K_2} + G^*\omega_4\theta + J^*\omega_4 + Y\Big\}, \\ &< \frac{\dot{J}}{J} + W,\ W < 0\ \Big(\text{if } h_1 - \frac{(-2G^* + J^*)\omega_3}{J^* + \theta} > \omega_1(K_1 - A^*) + J^*\omega_2 + K_2\omega_3 \\ &\quad + G^* J^*\omega_3,\ \text{and } Y > \frac{(K_2 - G^*)r_2}{K_2} + G^*\omega_4\theta + J^*\omega_4\Big) \end{aligned}$$

where,

$$W = max\Big\{-h_1+\omega_1(K_1-A^*)+J^*\omega_2+K_2\omega_3+G^*J^*\omega_3+\frac{(-2G^*+J^*)\omega_3}{J^*+\theta}, \frac{(K_2-G^*)r_2}{K_2}$$

$$+G^*\omega_4\theta + J^*\omega_4 + Y\Big\} < 0.$$

On integrating and taking limit $t \to \infty$,

$$\lim_{t\to\infty} sup\frac{1}{t}\int_0^t \bar{\mu}(B)ds < W < 0.$$

By lemma 4.3.6, we say that E^* is globally asymptotically stable.

Ecologically this means, the system is capable of returning to its equilibrium state $E^* = (J^*, A^*, G^*)$ after any perturbation, (i) if harvesting rate of cod h_1 cod population is greater that a threshold value, (ii) if the cannibalism rate ω_1 is less than some threshold value, and (iii) if conversion rate of biomass ω_4 and eventually the predation rate of juvenile cod by grey seal is less than some threshold value.

4.4 Threshold for persistence of species

Now, since we are interested to explore the effect of Allee in cod survival and extinction we will now find a threshold $\mathcal{T}_0^{J+A}$ (Roy et al. (2020)). For this model, $\mathcal{T}_0^{J+A}$ represents threshold parameter that is helpful in predicting whether cod population will persist uniformly or tend to extinction. In the situation of surplus predators, we can establish which control measures, at what magnitude, and in what combinations, would be most effective in increasing $\mathcal{T}_0^{J+A}$ greater than 1, which further provides important guidance in developing policy measures to safeguard cod population. Further, we state the following theorem:

Theorem 4.4.1 *Let* $\mathcal{T}_0^{J+A} = \left|\frac{h_1K_2(h_2-r_2)\omega_3}{r_2\theta\rho(\beta r_1+h_1)}\right|$ *be a threshold. Then, if*

– $\mathcal{T}_0^{J+A} > 1$ *and* $r_2 < h_2$ *cod population (juvenile and adult) persists as* $t \to \infty$.

– $\mathcal{T}_0^{J+A} < 1$, *cod population may extinct or persists uniformly.*

Proof As by Garrione and Rebelo (2016), we found $\mathcal{F}$ and V

$$\mathcal{F} = \begin{pmatrix} \frac{(h_2K_2-K_2r_2)\omega_3}{r_2\theta} & 0 \\ 0 & 0 \end{pmatrix} \text{ and } \mathcal{V} = \begin{pmatrix} \rho & r_1\beta \\ -\rho & h_1 \end{pmatrix}.$$

Then the basic reproduction number for cod (juvenile and adult), $\mathcal{T}_0^{J+A}$ is spectral radius

of matrix $\mathcal{F}\mathcal{V}^{-1}$ i.e.,

$$\mathcal{T}_0^{J+A} = \Big|\frac{h_1 K_2(h_2 - r_2)\omega_3}{r_2\theta\rho(\beta r_1 + h_1)}\Big|.$$

Example 4.4.1 *For* $r_1 = 0.49,\ r_2 = 1.2,\ h_1 = 0.12,\ h_2 = 1.1994,\ \omega_1 = 0.9,\ \omega_2 = 0.25, \omega_3 = 1.1,\ \omega_4 = 0.95,\ \theta = 25,\ \rho = 0.00039,\ K_1 = 1000,\ K_2 = 100,\ \beta = 1.5$*, we have* $\mathcal{T}_0^{J+A} = 0.791723 < 1$*. Here, we observe the existence and stability of two equilibrium points, (i)* $E_1 = (0, 0, 0.05)$*, extinction equilibrium, which is attained as we set initial condition as [0.001, 0.000001, 0.04] (c.f. Fig. 4.2(a)), and (ii)* $E^* = (0.4799, 999.116, 1.5413)$*, positive equilibrium, which is attained as we set initial condition as [0.1, 10, 0.1] (c.f. Fig. 4.2(b)). Hence the two stable equilibrium can exist at* $\mathcal{T}_0^{A+J} < 1$*. This means, survival is possible for a cannibalistic population even if* $\mathcal{T}_0^{J+A} < 1$*. This analysis is in agreement with Veprauskas and Cushing (2017). They showed that under strong Allee effect a cannibalistic population can survive when* $\mathcal{T}_0 < 1$*.*
Now, if we take $h_2 = 1.21 > r_2$ *and all the parameters as the same as above then we observe that* $\mathcal{T}_0^{J+A} = 13.1954 > 1$*. In this case, the equilibrium* E_1 *does not exist and* E^* *is locally asymptotically stable. Therefore, for any initial condition in basin of attraction of* E^* *will be attracted to* E^* *and the dynamics goes to non extinction of cod (c.f. Fig.4.3). This situation is favourable as it guarantees persistence of all species.*

Allee effect has tremendous potential on population survival and extinction that remains unexplored in most marine species. We believe that this limits both our ecological understanding and probable success for conserving marine species. This analysis shows that, both adult and juvenile survival can be benefited by the Allee effect and can provide survival even when $\mathcal{T}_0^{J+A} < 1$. This is due to the fact that as adult cod decline due to Allee effect, in turn juvenile gets a better place to survive due to less cannibalism and eventually becomes a fully grown adult. This is an interesting phenomenon which suggests that if an initial threshold is maintained in a restrictive domain, the population has a chance to survive indefinitely even if $\mathcal{T}_0^{J+A} < 1$.

4.4.1 Global sensitivity analysis of $\mathcal{T}_0^{J+A}$

In order to determine how best we can reduce Atlantic cod morbidity and mortality due to cannibalism and Allee effect, it is necessary to know the relative importance of different parameters responsible for its death. Cod extinction and persistence can be related to the threshold $\mathcal{T}_0^{J+A}$. We calculate the sensitivity indices of the reproductive number, $\mathcal{T}_0^{J+A}$, to the parameters in the model. Here, we use partial rank correlation coefficient (PRCC) method to find the parameters that have high impact on $\mathcal{T}_0^{J+A}$, and should be targeted by

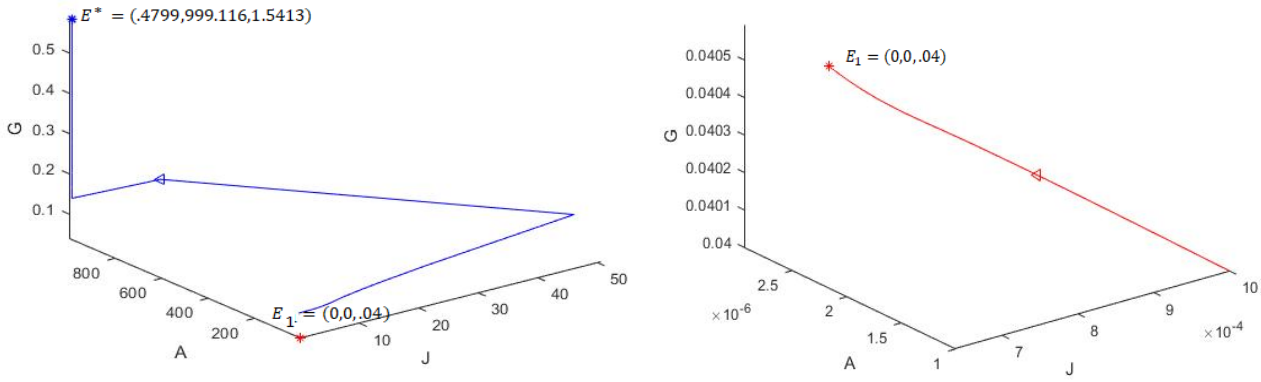

(a) (b)

Figure 4.2: (a) Stability of equilibrium E^* for $\mathcal{T}_0^{J+A} < 1$ with initial condition [0.1, 10, 0.1]. (b) Stability of equilibrium E_1 for $\mathcal{T}_0^{J+A} < 1$ with initial condition [0.001, 0.000001, 0.04].

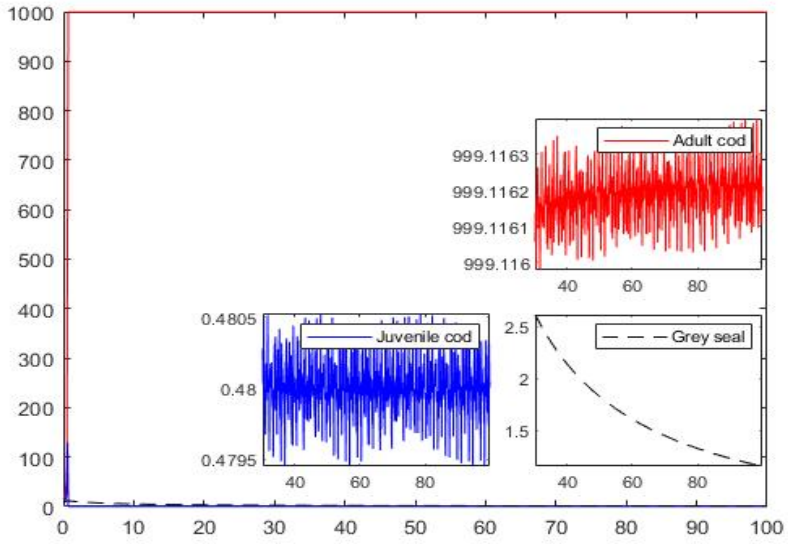

Figure 4.3: Existence and Stability of equilibrium E^* equilibrium for $\mathcal{T}_0^{J+A} > 1$ with any initial condition.

intervention strategies.

For assessing the monotonicity amongst input and output variables while accounting correlation between input parameters,the PRCC sensitivity technique has been widely utilized (Crick and Hill (1987); Iman and Helton (1988); Iman and Helton (1991)). Downing et al. (1985) delineated that the PRCC is more functional for stipulating the sensitivity of parameters holding nonlinear but monotonic relationship. PRCC as a great mathematical work, comes up with the answers to questions such as how the output acts on if we increase (or decrease) a certain parameter. Thus,by calculating PRCC we can assert

that what parameters we can take as basis to get the desired value of output. We begin the uncertainty inspection by initiating the values of parameters as well as their ranges. Parameters behave as random variables with corresponding probability density function (PDF) if the estimation is undetermined . If no prior(or specific) information about the distribution(of parameters) is given, we proceed by assigning each parameter with some uniform probability function as(cf. Table 4.2).

The PRCC sensitivity results are calculated for $\mathcal{T}_0^{J+A}$, they are listed in Table 4.3 and also illustrated using bar charts in Fig. 4.4. The sign of PRCC indicates the direction of association between the input and output factors. PRCCs for all the parameters are significantly different from zero. A value of +1 indicates a perfect positive linear relationship, a value of -1 indicates a perfect negative linear relationship and a value of 0 indicates no relationship. The resulting sensitivity indices of $\mathcal{T}_0^{J+A}$ to the 9 different parameters in the model (see Fig.(4.4)). From the results given in Table 5 we found that for the most influential parameter for $\mathcal{T}_0^{J+A}$ is h_2 followed by r_2. The most influential parameter is the harvesting rate of seals, h_2. Since, the sensitivity index of h_2 is 0.7455, increasing (decreasing) h_2 by 10% increases (or increases) the value of $\mathcal{T}_0^{J+A}$ by approximately 7.45%. The most negatively influential parameter is the growth rate of seals, r_2. Since, the sensitivity index of r_2 is -0.6999, increasing (decreasing) r_2 by 10% decreases (or increases) the value of $\mathcal{T}_0^{J+A}$ by approximately 6.99%. We also found that other parameters are less sensitive for $\mathcal{T}_0^{J+A}$.

The identification of these parameters is vital in formulating control strategies effective for saving the cod population. The result of sensitivity analysis suggest that a strategy which reduces the grey seal birth rate (r_2) and increasing its harvesting rate (h_2) would be quite effective in restricting the declination of cod population in Gulf of St. Lawrence, Canada.

Table 4.2: Distributions and ranges of the input parameters.

Parameters	Distribution	Range
h_1	Uniform	[0.001,0.49]
K_2	Uniform	[1,500]
r_2	Uniform	[0.01,0.7]
h_2	Uniform	[0.001,0.9]
ω_3	Uniform	[0.8,1.2]
θ	Uniform	[1,40]
ρ	Uniform	$[10^{-5}, 0.1]$
r_1	Uniform	[0.24, 0.5]
β	Uniform	$[10^{-5}, 2]$

Table 4.3: The PRCC sensitivity indices of the threshold ($\mathcal{T}_0^{J+A}$), to the system parameters, p_j.

Parameters (p_j)	PRCC Index
h_1	0.0105
K_2	0.1462
r_2	-0.6999
h_2	0.7455
ω_3	0.0306
θ	-0.1216
ρ	-0.0746
r_1	-0.0328
β	-0.0402

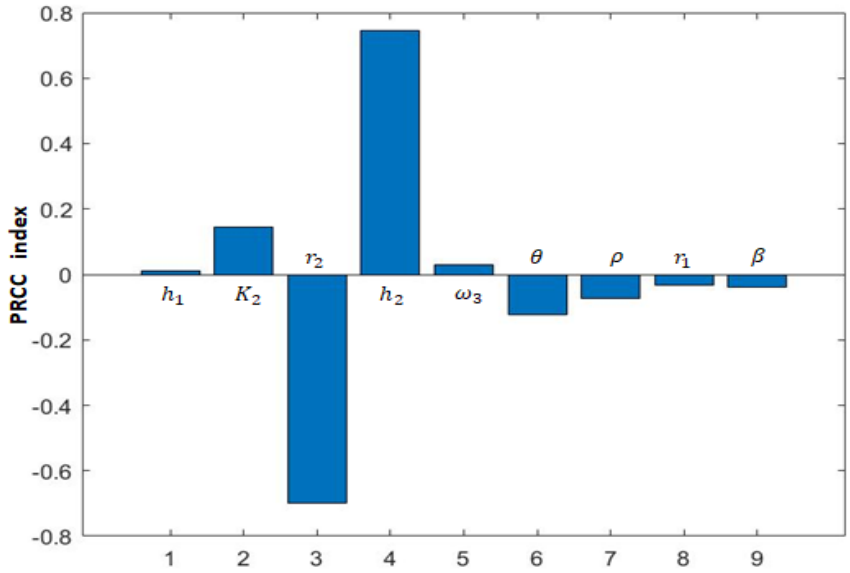

Figure 4.4: Graphical representation of PRCC index for $\mathcal{T}_0^{J+A}$.

4.5 Optimal control analysis

As predicted by few scientists, Atlantic cod will essentially go extinct within 20 years, despite best attempts to manage it (https://www.sciencemag.org/news/2008/11/no-recovery-atlantic-cod-population). For this reason, more possible efforts are needed to reduce the risk of population extinction. Our aim is to minimize the reduction of Atlantic cod, while keeping the cost of the control strategy implementation low. For this purpose, we include the control function $u_j's$ in our model. Control functions for such models are mostly functions of time appearing as coefficients in the model. An important decision while formulating an optimal control problem is to decide how and where to introduce the control in the system. A planned strategy is required to reduce the declination of Atlantic cod.

Therefore, we include controls (i) u_1, which represent efforts to increase artificial breeding, (ii) u_2, which represents the effort to isolate juvenile and adult cod population and (iii) u_3, which represents the effort to increase grey seal harvesting. The dynamics of the system (4.2.8) with control components is governed by the system of differential equations as follows:

$$\begin{aligned}
\frac{dJ}{dt} &= (r_1+u_1)A\left(1-\frac{A}{K_1}\right)(A-\beta)-(u_2+\omega_1)AJ-\frac{\omega_3 GJ}{\theta+J}-\rho J, && (4.5.1)\\
\frac{dA}{dt} &= \rho J+\omega_2 AJ-h_1 A, && (4.5.2)\\
\frac{dG}{dt} &= r_2 G\left(1-\frac{G}{K_2}\right)+\frac{\omega_4 GJ}{\theta+J}-(h_2+u_3)G. && (4.5.3)
\end{aligned}$$

sujected to the initial conditions $J(0)=J_0, A(0)=A_0, G(0)=G_0$. Next, by using bounded measurable control we define our objective function as,

$$\mathcal{J}(u_1,u_2,u_3)=\int_0^T (C_1G(t)+C_2u_1^2+C_3u_2^2+C_4u_3^2)dt,$$

subject to the state system (4.5.1)-(4.5.3). To find an optimal solution, the Lagrangian and Hamiltonian are calculated for the optimal control problem. The Langrangian of the control problem is given by,
$L=(C_1G(t)+C_2u_1^2+C_3u_2^2+C_4u_3^2)dt$, where the coefficients C_1, C_2, C_3, C_4 represents the balancing cost factors for grey seals and control strategies respectively. The optimal control problem involves in finding u_1^*, u_2^*, u_3^* such that the associated state trajectories (J^*, A^*, G^*) is solution of the controlled system of equation in the interval $[0,T]$ with the initial conditions and minimizing the cost functional $\mathcal{J}$. $\mathcal{J}(u_1,u_2,u_3)=min_{u_1,u_2,u_3\in\Delta}\{\mathcal{J}(u_1,u_2,u_3)|u_1,$ $u_2,u_3\in U\}$, where Δ is the set of admissible controls given by $\Delta=\{(u_1,u_2,u_3)\in L^1[0,T]|0\le u_1\le 1, 0\le u_2\le 1, 0\le u_3\le 1\}, t\in[0,T]$. Pontryagin's Maximum Principle converts system into a problem of minimizing a Hamiltonian function (H), defined as

$$\begin{aligned}
H &= C_1G+C_2u_1^2+C_3u_2^2+C_4u_3^2\\
&\quad +\lambda_J\left((r_1+u_1)A\left(1-\frac{A}{K_1}\right)(A-\beta)-(u_2+\omega_1)AJ-\rho J-\frac{\omega_3 GJ}{\theta+J}\right)\\
&\quad +\lambda_A(\rho J+\omega_2 AJ-h_1A)\\
&\quad +\lambda_G\left(r_2G\left(1-\frac{G}{K}\right)+\frac{\omega_4 GJ}{\theta+J}-(h_2+u_3)G\right),
\end{aligned}$$

where $\lambda_J, \lambda_A, \lambda_G$ are adjoint variables. Hence, minimization function becomes:

$$H(J^*,A^*,G^*,\lambda_J(t),\lambda_A(t),\lambda_G(t),u_1,u_2,u_3),$$

where J^*, A^*, G^* be optimal state solution.
By corollary 4.1 of Fleming and Rishel (2012), we say that optimal control exists and by applying Pontryagin's Maximum Principle (Pontryagin (2018)), we obtain the following result:

Theorem 4.5.1 *For optimal control $(u_1^*,\ u_2^*,\ u_3^*)$ and solution $J^*,\ A^*$ and G^* of state system (4.5.1)-(4.5.3), adjoint variable $\prod = (\lambda_J, \lambda_A, \lambda_G)$ exists and satisfies,*

$$\begin{aligned}
\frac{d\lambda_J}{dt} &= A\left(u_2+\omega_1\right)\lambda_J - \omega_2 A\lambda_A + \frac{G\theta}{\left(\theta+J\right)^2}\left(\omega_3\lambda_J - \omega_4\lambda_G\right) + \rho\left(\lambda_J - \lambda_A\right), \\
\frac{d\lambda_A}{dt} &= \frac{\left(3A^2 + \beta K_1 - 2A\left(\beta + K_1\right)\right)\left(r_1+u_1\right)}{K_1}\lambda_J + h_1\lambda_A + J\left(\left(u_2+\omega_1\right)\lambda_J - \omega_2\lambda_A\right), \\
\frac{d\lambda_G}{dt} &= -C_1 + \left(h_2 - r_2 + u_3\right)\lambda_G + \frac{2Gr_2}{K_2}\lambda_G + \frac{J}{\theta+J}\left(\omega_3\lambda_J - \omega_4\lambda_G\right), \qquad (4.5.4)
\end{aligned}$$

with transversality conditions: $\lambda_J(T) = 0, \lambda_A(T) = 0, \lambda_G(T) = 0$, and, $\lambda_J^*, \lambda_A^*, \lambda_G^*$ be the solution of system (4.5.4).
Further,

$$\begin{aligned}
u_1^*(t) &= \max\left\{0, \min\left\{1, \frac{A^*\left(\frac{A^*}{K_1} - 1\right)\left(A^* - \beta\right)\lambda_J^*}{2C_2}\right\}\right\}, \\
u_2^*(t) &= \max\left\{0, \min\left\{1, \frac{A^*J^*\lambda_J^*}{2C_3}\right\}\right\}, \\
u_3^*(t) &= \max\left\{0, \min\left\{1, \frac{G^*\lambda_G^*}{2C_4}\right\}\right\}. \qquad (4.5.5)
\end{aligned}$$

Proof The adjoint system can be obtained by

$$\frac{d\lambda_J}{dt} = -\frac{\partial H}{\partial J}, \frac{d\lambda_A}{dt} = -\frac{\partial H}{\partial A}, \frac{d\lambda_G}{dt} = -\frac{\partial H}{\partial G}.$$

For optimality conditions, we differentiate H with respect to optimal controls u_1, u_2, u_3 and equate it to 0. On solving, we get (4.5.5) in $\Delta = \{(u_1, u_2, u_3) \in L^1[0,T] |\ 0 \le u_1 \le 1, 0 \le u_2 \le 1, 0 \le u_3 \le 1\},\ t \in [0,T]$. Hence, the proof.

The state system (4.5.1)-(4.5.3), adjoint system (4.5.4) and optimal control (4.5.5) are simulated using MATLAB program. As in optimality we have initial condition of state system as $J(0),\ A(0)$ and $G(0)$ and terminal condition for adjoint variable $\prod(T) = 0$ in interval $[0,T]$.

Initially we postulate controls $u_1,\ u_2$ and u_3. Then, we solve the state system by using

Runge-Kutta method forward in time. After that, we solve adjoint system backward in time taking terminal conditions and state system solution at time T which we just calculated. Through the ongoing process, $u_i's, i = 1, 2, 3$ are updated at each iteration by using (4.5.5). We will continue the above given steps until convergence of successive iteration is attained. The effect of control in-comparison to the model without control have been are shown in Fig.4.5. Clearly, we observe that the cod population increases on implementing control. Thus, if we maintain optimal value of three discussed controls, (i) efforts to increase artificial breeding, (ii) the effort to isolate juvenile and adult cod population and (iii) the effort to increase grey seal harvesting, we can effectively decelerate adult cod death at an unusually high rates.

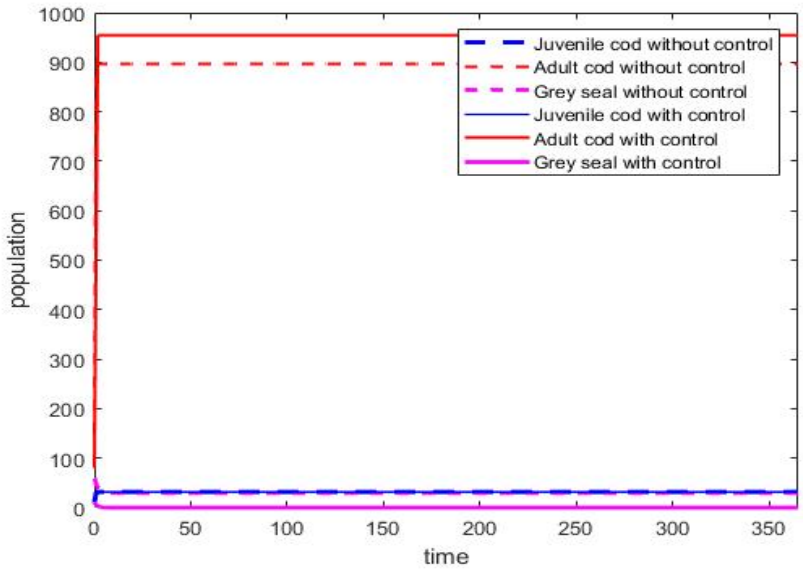

Figure 4.5: The evolution and comparison (with and without control measure) of all species.

4.6 Some important numerical simulations

4.6.1 Without Allee effect

Runge-Kutta fourth order has been used to solve ODE system (4.2.1) with non-zero positive initial condition. We observe that for the following set of parameters given in Table 4.4, stable dynamics is observed (c.f. Fig. 4.6(a)). There is enough literature on Atlantic cod, despite of that basic biological parameters are still missing. However, all our numerical simulations are executed utilizing parameter values that are taken from literature. References and ranges are given in Table 4.4.

4.6.1.1 Dynamical behaviour for the equilibrium points

For the parameter values given in Example 4.3.1, we found the existence of two positive equilibrium $E_1^* = (0.48,\ 100.1547,\ 43.1580)$ and $E_2^* = (0.4799,\ 18.2116,\ 43.1579)$ as shown previously. Here, we numerically illustrate the local stability of two equilibrium E_1^* and E_2^*. For this, we took several initial values $I_1 = (10, 80, 10),\ I_2 = (50, 80, 50),\ I_3 = (50, 150, 5)$ and $I_4 = (10, 150, 60)$. We observe that all the solution converges to the equilibrium E_1^* but not to E_2^* because of its unstable nature at these parametric values (the eigenvalues of variational matrix corresponding to E_1^* are $-91.9559, -0.519,\ -0.0109$ (all negative) and E_2^* are $-18.2271, -0.5197, 0.0099$ (not all negative). The equilibrium points, $E_0,\ E_1$, and E_2 also exists but are not stable (c.f. Fig. 4.7). From this analysis it is clear that even though many equilibrium point exists for given set of parameter values only E_1^* is acting as a point attractor. Simulation results are compatible with the analysis done in previous section.

4.6.1.2 Persistence and extinction dynamics

We also perform the simulation experiments and demonstrated the global stability of the model system (4.2.1) about three equilibrium point E_1, E_2 and E^*. There is a cod-free equilibrium point E_1, which is most undesirable as the juvenile and adult cod population both are absent. By numerical simulation, we observe that with the parameter values given in Table 4.4 and with initial condition as [10,8,60], Atlantic cod (juvenile and adult) population extincts (see Fig. 4.8(a)). While if we just slightly vary r_1 from 0.49 to 0.6, we see that cod population persists (see Fig. 4.8(b)). Now, taking the same parameters, while increasing the cannibalism rate from 0.9 to 1.1 can again lead juvenile cod to extinction. We illustrated this numerically (see Fig. 4.8(c)). Now, taking the same initial population and parameters as in Table 4.4, while increasing the culling/harvesting rate h_2 from 0.4 to 1.22, the grey seal extincts (see Fig.4.8(d)) permanently providing cod a better place to survive.

From this section, we conclude that increasing the value of r_1 beyond a threshold value cod population will persistence forever. Therefore, for saving the cod population from completely getting extinct it is suggested to increase the parameter r_1, by artificial and captive breeding. On the other hand, it is also noteworthy that harvesting grey seal (h_2) above a threshold value can be a measure to control the rapid decline of cod population and thus preserving remnant population in Gulf of St. Lawrence.

Table 4.4: Parameter values used for simulating model .

Parameters	values	range	references
r_1	0.49	0.24-0.50	*
r_2	1.2	1.1-2.1	**
h_1	.12	$0.1 - 5.479$	Chouinard et al. (2000)
h_2	0.4		assumed
K_1	1000		assumed
K_2	100		assumed
β	.9	0-1	
ω_1	0.9		assumed
ω_2	0.25	$< \omega_1$	
ω_3	1.1	0.8-1.2	Cook and Trijoulet (2016)
ω_4	0.95	$< \omega_3$	
θ	25		assumed
ρ	0.00039	adult age 7year	Chouinard et al. (2000)

* - (https://www.sararegistry.gc.ca/virtual$_sara/files/cosewic/sr$ $_Atlantic\%20Cod\_0810\_e1.pdf$)
$** - (https://www.dfo-mpo.gc.ca/species-especes/profiles$ $-profils/greyseal-phoquesgris-eng.html$)

4.6.1.3 Effect of initial condition on persistence

In this section, we used two different initial condition to illustrate the fact that a threshold number of adult cod are required to main its population forever. Taking parameters as in Table 4.4 and initial conditions as (i) [10, 150, 60] and (ii) [10, 8, 60]. We see that with former initial condition cod population persists, while with later initial condition cod population extincts (see Fig. 4.9).

4.6.2 With Allee Effect

We simulated our model (4.2.8) with same parameter as given in Table 4.4 and then compared our result with simulation of model (4.2.1). Although most of the researcher believes Allee effect creates a threshold density below which a population cannot survive making species more extinction prone (Zu and Mimura (2010)). However, our finding shows that an Allee effect greatly increased the cod population. In Fig. 4.8(a) we observe that, in absence of the Allee effect the cod population tends to extinction. However, with the same set of parameters but under the influence of strong Allee effect (c.f. Fig. 4.10) cod species comes into picture. The tabular comparison have been summarised in Table. 4.5. Parameter values are taken as given in Table 4.4 and for Allee parameter β is set to $\beta = 0.9$. Above simulation agrees with Veprauskas and Cushing (2017). They showed that under strong Allee effect a cannibalistic population can survive when a non-cannibalistic popu-

lation cannot.

Table 4.5: Comparison with/without Allee effect

	Without Allee effect	With Allee effect
J	≈ 0	≈ 0.479
A	≈ 0	≈ 1000
G	≈ 66.6	≈ 68.15

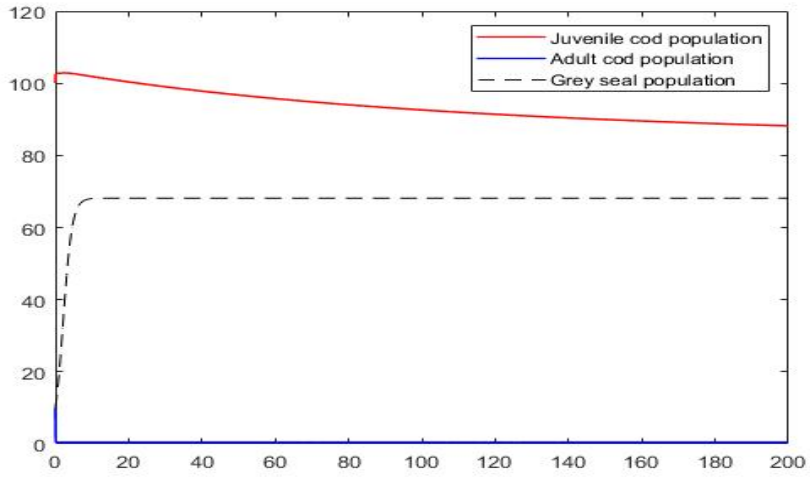

Figure 4.6: Time series solution of system (4.2.1) taking parameters given in Table 4.4 and with initial conditions [10, 8, 60].

4.7 Discussions and conclusion

The demand for safeguarding biodiversity and conserving nature has blown up majorly, as different species serve nature differently. The Atlantic cod population contributes to our understanding of extinction in a technologically evolving world. In designing the conservation policy of an endangered species, a depth study of the food hierarchy model of that particular species is essential. This research has lodged and inspected a food-chain model comprised of juvenile cod, adult cod, and grey seal populations. The system without the Allee effect has four equilibrium points. All the equilibrium states are determined and analyzed for their local stabilities. Computational and theoretical analysis results manifest that the model demonstrates rich dynamics. We calculated the value of the reproduction

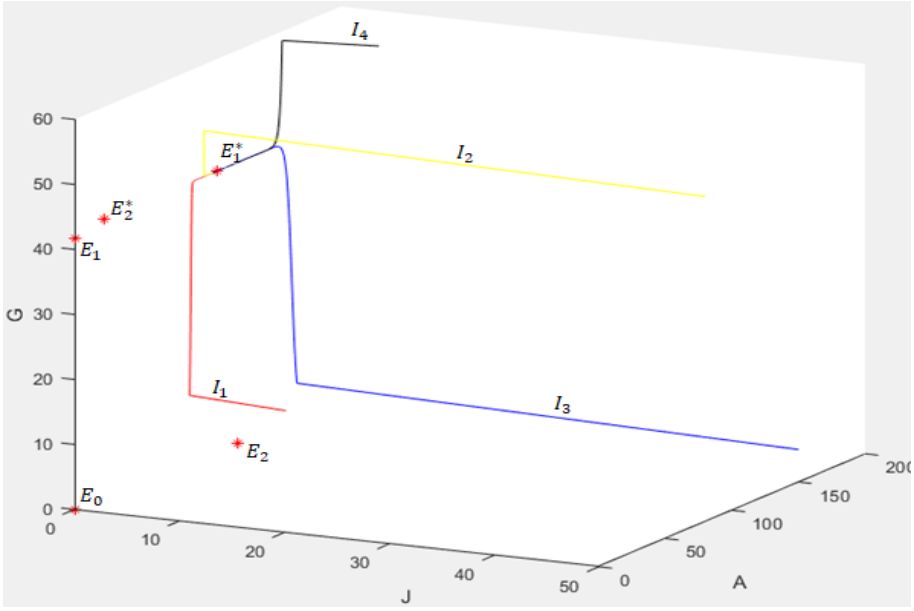

Figure 4.7: Dynamical behaviour of the solution of system (4.2.1) taking different initial conditions.

number for our proposed food chain model. It is found that cod survival is possible even when $\mathcal{T}_0^{J+A} < 1$. We have also studied and numerically simulated the Optimal Control model.

From our study, it is clear that cannibalism and grey seals are a significant threat to Atlantic cod. Hence, the presence of controlled harvesting and captive reproduction can prevent cod from extinction. Moreover, the ideal possibility for survival of cod species is when the harvesting rate of the grey seal is more significant than its intrinsic growth rate. Hence, our study can open a new window of study in the future. Depth examination of the model demonstrates that the Atlantic cod population will never vanish unless excessive external harvesting factor. The presence of a strong Allee effect is added to the model to detect the possibility of population extinction due to it. Our extended models are based on biological observation and previously published work. Most of the studies reported that Allee effects make the species extinction prone. However, our investigation suggests that the Allee effect among the cod population may benefit its long-term survival because of its cannibalistic nature.

The overall objective should be to reduce the impacts of grey seals on the threatened cod population and not on the seal's density. The key point of this study is to provide feedback on the response of Allee to cod persistence, thereby providing long-term justification for cod persistence. A plan of action intended towards preventing the introduction and displacement of grey seals in the area resided by Atlantic cod must be implemented. Educating the public on cod extinction issues, assessing cod population densities and distribution,

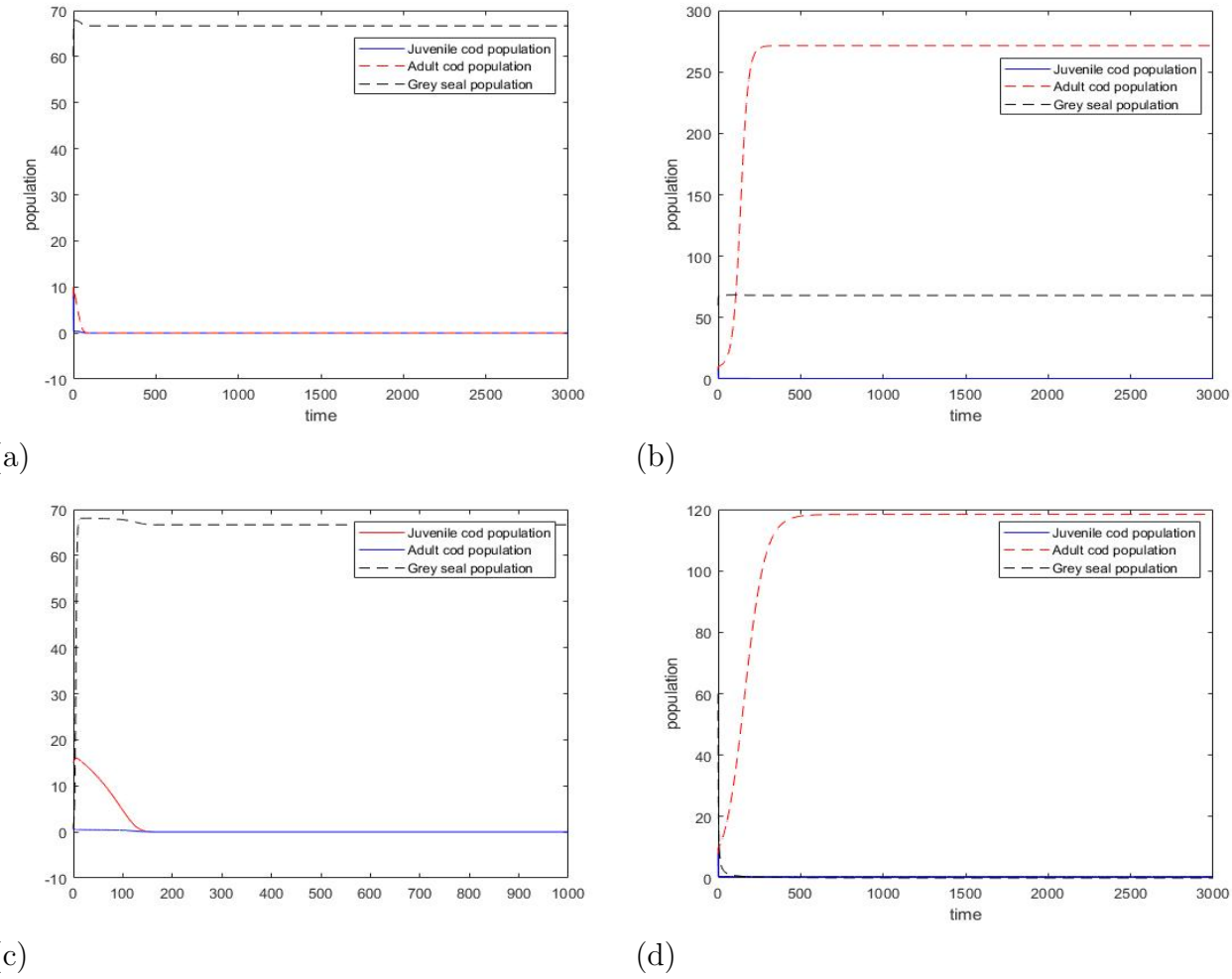

Figure 4.8: (a) Extinction of cod for $r_1 = 0.49$, (b) Persistance of cod for $r_1 = 0.6$, (c) Extinction of Juvenile at $\omega_1 = 1.1$, and (d) Extinction of greay seal at $h_2 = 1.22$. Other parameter are same as given in Table 4.4

and developing alternatives trap to control grey seals can be other measures to save cod in St. Lawrence. However, further work should be encouraged to study cannibalism with the Allee effect exhibited by cod populations.

Some other control measures that can be used to preserve cod population and to promote recovery of native wildlife species under threat include (i) artificial breeding, (ii) habitat restoration, (iii) harvesting grey seals, (iv) separating adult and juvenile cod.

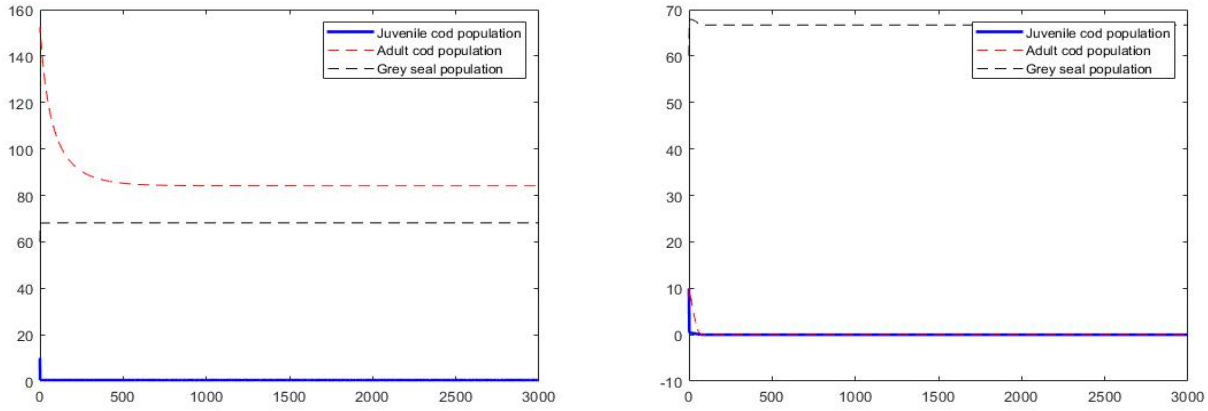

(a) (b)

Figure 4.9: (a) The initial condition $[10, 150, 60]$ leads to population persistence, (b) The initial condition $[10, 8, 60]$ leads to cod population collapse.

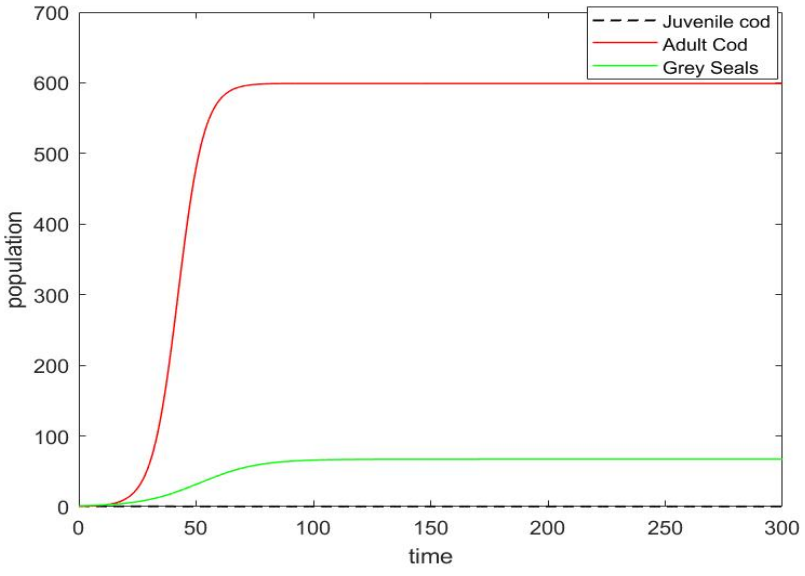

Figure 4.10: Time series solution for the system (4.2.8). Parameters are given Table 4.4

Chapter 5

RESULTS AND CONCLUSION

“ The study of origins is the art of drawing sufficient conclusions from insufficient evidence.”

-Allan Sandage

According to a study for the U.N., the continued loss of species could cost the world 18 percent of global economic output by 2050. Already, a number of industries have been economically impacted by species loss. Example like- the collapse of bee populations has hurt many in the $50 billion-a-year global honey industry. A 2019 United Nations study found that agriculture has suffered as a result of the rising extinction rate. 20% of the earth's vegetated surface has lost productivity since the year 2000. Interdisciplinary participation is crucial due to the biological sciences' complexity and the ongoing strength of mathematics. Mathematicians now have access to an intriguing new world of difficult problems thanks to the mathematical biology research that has been conducted over the past several decades. Therefore, this research has merit and, in a mathematical sense, will be a pioneering effort for some species. Each chapter has its own course of discussion, where each chapter's results have put into context. Here, we combine all those results.

For mathematical convenience and tractability of the model, several assumptions are made. To better understand how non-linearity, complexity interact in spatially extended eco-epidemiological systems, environmental fluctuation and various biological interactions (like Allee effect, cannibalism) effects the dynamics of a population, we have conducted this study. Five chapters make up the thesis. The significance of species variety has been covered in Chapter 1, along with the definition of mathematical terminologies and the many mathematical techniques employed. Chapter 2-4 considers different species in danger of extinction. In Chapter 2, we took into account quokka species, a vulnerable macropodid marsupial notably as a result of the introduction of the European red fox, experienced a catastrophic fall in the 1930s. While in Chapter 3, we discussed how chytridiomycosis, an infectious illness caused by an aquatic fungus infection, kills amphibians. Lastly, we examined how cannibalism, overfishing, and grey seal predation are all contributing factors to the atlantic cod population's rapid decline in Chapter 4. All the three models are analyzed using different tools of dynamical system theory, namely, Routh-Hurwitz criteria, next-generation operator theory, geometric approach for global stability, persistence analysis etc. We have studied the reaction-diffusion model in two dimensional case and investigated its stability conditions. It has been shown that the instability observed in the model systems is diffusion-driven. The expression for critical wave number has been obtained. In reaction diffusion systems, two basic types of symmetry-breaking bifurcations are responsible for emergence of spatiotemporal patterns (i) Hopf bifurcation that breaks the temporal symmetry and give rise to oscillations that are uniform in space and periodic in time, (ii) Turing bifurcation that breaks spatial symmetry, leading to the formation of patterns that are stationary in time and oscillatory in space. Predator free threshold ($\mathcal{T}_0$), are calculated for each model. It is observed that in all the systems, the predator-free equilibrium is locally asymptotically stable if $\mathcal{T}_0$ is less than unity. We have formulated

spatial models with different transmission rate such as mass action and asymptotic type. Functional responses are also selected in accordance with the field observation. Type II responses are typical of specialist predator. Interaction between B_d and Zooplankton show a Type II functional response in frog extinction model. Type III response is associated with predator switching by generalist consumer. Thus, we have used Holling Type III functional response to model Quokka-Fox-Dingo dynamics. The spatio-temporal patterns were obtained by computer simulation driven by forces of diffusion. The following summarises the study's main findings and contributions:

Although the system dynamics approach is a powerful tool for representing and understanding changing behaviours over time, it is insufficient for representing spatial processes. Modelling tri-tropic food chain for an endangered species "Quokka", by performing various analytic and numeric methodologies we concluded that deduction of an apex predator leads to 'release' of mesopredators, which are otherwise suppressed (competition, direct killing, fear-induced behavioural changes) by the larger predator. Even if both predators target the same prey, the total intensity of predation is reduced in the presence of the apex predator. We have extended to a spatio-temporal food chain model for this situation that includes one specialist predator and one generalist predator in Chapter 2, we perform extensive numerical simulations of spatially extended model in two dimensional space. All our numerical simulations employ non-zero initial conditions and zero-flux boundary conditions with a system size of 200×200. Simulations suggest that a stable predator-prey food chain model may be obtained by using an alternative prey source for the apex predator population. As suggested by Glen et al. (2007), our study also demonstrates the same that dingoes may spread more fragile prey species if they can keep fox populations in check. According to our research, the quokka population won't go extinct unless external variables that contribute to harvesting have become too greater.

Management decisions require an improved understanding of the drivers and processes that influence ecosystem services. Our study contributes to the evolution of terrestrial as well as marine ecosystem models. Activity occurs in the marine environment either as a result of organism's sensitivity to the turbulent water flows, their capacity for self-motion, or a combination of the two mechanisms. In accordance with this, we take into account an idealised reaction-diffusion system while studying about the species, like, amphibians (Chapter 3). From amphibians model, we concluded that increasing zooplankton diffusion can reduce the density of infectious frogs, according to a numerical simulation of the response diffusion model. It is also fascinating to note that over time, the entire population tends to group together. These analysis support the hypothesis that Batrachochytrium would provide a reduced threat to amphibians in zooplankton-rich settings.

Further, every year, gigatonnes of carbon are released into the atmosphere by human activity. Increasing global temperatures, altered regional weather patterns, rising sea levels, ocean acidification, increased nutrient loads, and altered ocean circulation are only a few of the direct effects of cumulative post-industrial emissions. These and other physical effects are having an impact on ecosystem services, human food security, and marine biological processes ranging from genes to ecosystems and over scales from rock pools to ocean basins. For studying and analysing the dynamics of marine life as influenced by environmental factors, stochastic ecology model are used. We developed a stochastic model in Chapters 3 and 4, examined the existence and uniqueness of the solution, and numerically assessed the dynamics using the Euler-Maruyama method. From Chapter 3 stochastic simulations we get that as the harvesting rate of zooplankton (h_2) increasing, the frog population reduces with the threat of extinction.

There are still many other evolutionary questions that can be addressed. Finally, it is important that we maintain the creativity needed to continue to take advantage of technological advances and integrate advances in other fields if we are devoted to reach at the highly optimized research in the field of spatial eco-epidemiology.

5.1 Limitation and future extensions

A good model needs to be both sophisticated enough to reflect a system authentically and basic enough to be mathematically solvable. Simplicity frequently comes at the expense of realism, and the Lotka-Volterra model suffers from this as a result of its dependence on unreasonable presumptions. For instance, prey populations are constrained by food availability as well as predation, and no predator can consume an endless supply of prey.

According to Jørgensen (2008), the many ecological models that are now available can be divided into the following categories: Bio-geo-chemical and bio-energetic dynamic models, static models, population dynamics models, population dynamics models, structural dynamic models, Fuzzy models, artificial neural networks, individual based models, spatial models, ecotoxicological models, stochastic models and hybrid models. Talking about this work, it uses a variety of mathematical techniques to analyse the dynamics of diverse, consequently, distinctive environmental situations, endangered species. And, population dynamics models and bio-geo-chemical, bio-energetic models that comes with short comings, like, it considers static population, thus not giving any clue about ecological reactions; flaws in parameter estimation; an improper portrayal of the true attributes of ecosystems due to lack of available data and ignorance of the significant randomness, hence this type of modelling is insufficient for the formulation of chosen species and its behaviour. Conse-

quently, investigating upon spatial distribution of the state variables while forming spacial patterns of species allocation, also, considering randomness of forcing processes in population dynamic models are the primary goals of this thesis.

As the right ecological model must be chosen based on the type of dataset that is available and the nature of the problem that needs to be solved, that's why, it is plausible that a number of limitations might have influenced the results obtained. For instance:

- In Chapter 2, quokkas are also found to be susceptible to infection like: Toxoplasma parasites (Gibb et al. (1966)), and Salmonella bacteria (Iveson and Hart (1983); Hart et al. (1986)), which haven't been considered in formulating the model.
- In Chapter 3, other multiple causes for the global decline of amphibians includes, habitat destruction, pollution, increases in ultraviolet light due to ozone depletion, invasive species and other issues which have not been considered individually.
- Model described in chapter 4 also suffers from certain limitations. It does not show the effect of diseases such as Vibriosis, Viral hemorrhagic septicemia virus, Infectious pancreatic necrosis virus, etc., which may also be a significant cause of death in cod populations (Samuelsen et al. (2006)). Additionally, our model doesn't include seasonal effects on cod demography (Castonguay et al. (1999); Hermansen and Dreyer (2010)). In the interest to relate dynamical models to reality, more mathematical complications are needed to be implemented. The spatial effect is also not included while the formulation. Some recent papers investigated complex dynamics in the reaction-diffusion model with strong Allee effect (Petrovskii et al. (2002)). Our future work will be intended to address this issue. It can assist us in understanding the spatial spread of cod population more accurately when the population migrates from one location to another randomly.

Over and above these, spacial models and stochastic models both have their own limitations for the evaluation of the dynamics. Given that spatial relationships are frequently extremely complicated, it takes an extensive knowledge to compute them using numerical method over the residing land. And, in stochastic models we generally use normal distribution of enduring dataset, this is due to our limited understanding of the precise values of the enforcing functions. Also, they require much computer time and are really complex. In a stochastic model, the cause and effect relationship are chosen randomly or stochastically. As a result, stochastic systems are typically not solved analytically, making it challenging to develop an intuitive perspective in a number of situations.

Also, the population dynamics are affected by various environmental parameters, like-temperature, fertility season, etc., which are ignored and the mean values of environmental

elements (such as- growth rate, predation rate and many more) are considered. In many biological systems, seasonality is a common environmental trait caused by cyclical climate conditions. The seasonality which is vastly underappreciated and includes not only the temperature but, rainfall, wind, human activity, etc., should be incorporated in the type of models we choose.

In recent years, it has become clear that a large number of biological, medical, and other processes—both natural and artificial—involve temporal delays. To disregard time delays is to deny reality because they happen so frequently and in practically every circumstance. According to Kuang (1993), any model of species dynamics without delays is at best an approximation because animals must wait for a period of time after eating before engaging in other activities and responding to stimuli. In many biological dynamical systems, time delay is crucial. This is especially true in ecology, where time delays have been shown to have a significant effect in determining whether prey densities as a result of predation are stable or unstable (Nindjin et al. (2006)). Now there is no question that a better analysis must take into consideration the influence of time-delay caused by the time needed to transition from the egg stage to the adult stage, gestation period, and other factors. In epidemiology, the delayed model is more accurate since it considers the lag between a factor's release, absorption, and effect (Jackson and Chen-Charpentier (2017)). The classic volumes by MacDonald (2013), Gopalsamy (2013), and Kuang (1993) contain in-depth justifications for the necessity and value of time delays in realistic models.

Our results are encouraging and should be validated by a larger sample size. We propose that further research should be undertaken in the stated areas.

Bibliography

[1] P. á Ball. The self-made tapestry, 2001.

[2] P. A. Abrams and L. R. Ginzburg. The nature of predation: prey dependent, ratio dependent or neither? *Trends in Ecology & Evolution*, 15(8):337–341, 2000.

[3] A. S. Ackleh, J. Carter, V. K. Chellamuthu, and B. Ma. A model for the interaction of frog population dynamics with batrachochytrium dendrobatidis, janthinobacterium lividum and temperature and its implication for chytridiomycosis management. *Ecological Modelling*, 320:158–169, 2016.

[4] A. A. Aguirre, R. S. Ostfeld, G. M. Tabor, C. House, and M. C. Pearl. *Conservation medicine: ecological health in practice*. Oxford University Press, 2002.

[5] L. Akveld. The cod: Ac jensen. crowell, new york, ny, 1972, 182 pp., us 7.95, 1974.

[6] C. Aldebert, D. Nerini, M. Gauduchon, and J. Poggiale. Structural sensitivity and resilience in a predator–prey model with density-dependent mortality. *Ecological complexity*, 28:163–173, 2016.

[7] J. D. Allan. Predation and its consequences. In *Stream Ecology*, pages 163–185. Springer, 1995.

[8] W. C. Allee. Animal aggregations. *The Quarterly Review of Biology*, 2(3):367–398, 1927.

[9] L. J. Allen, B. M. Bolker, Y. Lou, and A. L. Nevai. Asymptotic profiles of the steady states for an sis epidemic patch model. *SIAM Journal on Applied Mathematics*, 67 (5):1283–1309, 2007.

[10] C. L. Althaus. Estimating the reproduction number of ebola virus (ebov) during the 2014 outbreak in west africa. *PLoS currents*, 6, 2014.

[11] D. J. Anderson and B. B. Bare. A dynamic programming algorithm for optimization of uneven-aged forest stands. *Canadian journal of forest research*, 24(9):1758–1765, 1994.

[12] R. M. Anderson and R. M. May. *Infectious diseases of humans: dynamics and control*. Oxford university press, 1992.

[13] M. Andersson and S. Erlinge. Influence of predation on rodent populations. *Oikos*, pages 591–597, 1977.

[14] J. F. Andrews. A mathematical model for the continuous culture of microorganisms utilizing inhibitory substrates. *Biotechnology and bioengineering*, 10(6):707–723, 1968.

[15] L. Anselin. Thirty years of spatial econometrics. *Papers in regional science*, 89(1): 3–25, 2010.

[16] R. Arditi and L. R. Ginzburg. Coupling in predator-prey dynamics: ratio-dependence. *Journal of theoretical biology*, 139(3):311–326, 1989.

[17] M. Bandyopadhyay and C. Chakrabarti. Deterministic and stochastic analysis of a nonlinear prey-predator system. *Journal of Biological Systems*, 11(02):161–172, 2003.

[18] M. Bandyopadhyay and J. Chattopadhyay. Ratio-dependent predator–prey model: effect of environmental fluctuation and stability. *Nonlinearity*, 18(2):913, 2005.

[19] M. Banerjee, B. W. Kooi, and E. Venturino. A safe harbor can protect an endangered species from its predators. *Ricerche di Matematica*, pages 1–24, 2020.

[20] A. Basheer, E. Quansah, S. Bhowmick, and R. D. Parshad. Prey cannibalism alters the dynamics of holling–tanner-type predator–prey models. *Nonlinear Dynamics*, 85 (4):2549–2567, 2016.

[21] A. N. Berger and G. F. Udell. The economics of small business finance: The roles of private equity and debt markets in the financial growth cycle. *Journal of banking & finance*, 22(6-8):613–673, 1998.

[22] L. Berger, R. Speare, P. Daszak, D. E. Green, A. A. Cunningham, C. L. Goggin, R. Slocombe, M. A. Ragan, A. D. Hyatt, K. R. McDonald, et al. Chytridiomycosis causes amphibian mortality associated with population declines in the rain forests of australia and central america. *Proceedings of the National Academy of Sciences*, 95 (15):9031–9036, 1998.

[23] L. Berger, R. Speare, H. Hines, G. Marantelli, A. Hyatt, K. McDonald, L. Skerratt, V. Olsen, J. Clarke, G. Gillespie, et al. Effect of season and temperature on mortality in amphibians due to chytridiomycosis. *Australian Veterinary Journal*, 82(7):434–439, 2004.

[24] L. Berger, J. E. Longcore, R. Speare, A. Hyatt, and L. F. Skerratt. Fungal diseases in amphibians. *Amphibian biology*, 8:2986–3052, 2009.

[25] G. Blom and A. Folkvord. A snapshot of cannibalism in 0-group atlantic cod (gadus morhua) in a marine pond. *Journal of Applied Ichthyology*, 13(4):177–181, 1997.

[26] B. Bogstad, G. R. Lilly, S. Mehl, O. K. Palsson, and G. Stefánsson. Cannibalism and year-class strength in atlantic cod (gadus morhua l.) in arcto-boreal ecosystems (barents sea, iceland, and eastern newfoundland). 1994.

[27] C. J. Briggs, R. A. Knapp, and V. T. Vredenburg. Enzootic and epizootic dynamics of the chytrid fungal pathogen of amphibians. *Proceedings of the National Academy of Sciences*, 107(21):9695–9700, 2010.

[28] J. A. Brown, G. Minkoff, and V. Puvanendran. Larviculture of atlantic cod (gadus morhua): progress, protocols and problems. *Aquaculture*, 227(1-4):357–372, 2003.

[29] J. C. Buck, L. Truong, and A. R. Blaustein. Predation by zooplankton on batrachochytrium dendrobatidis: biological control of the deadly amphibian chytrid fungus? *Biodiversity and conservation*, 20(14):3549–3553, 2011.

[30] R. Burrows, H. Hofer, and M. L. East. Population dynamics, intervention and survival in african wild dogs (lycaon pictus). *Proceedings of the Royal Society of London. Series B: Biological Sciences*, 262(1364):235–245, 1995.

[31] C. Castillo-Chavez, S. Blower, P. Van den Driessche, D. Kirschner, and A.-A. Yakubu. *Mathematical approaches for emerging and reemerging infectious diseases: models, methods, and theory*, volume 126. Springer Science & Business Media, 2002.

[32] C. Castillo-Chavez, Z. Feng, W. Huang, et al. On the computation of ro and its role on. *Mathematical approaches for emerging and reemerging infectious diseases: an introduction*, 1:229, 2002.

[33] M. Castonguay, C. Rollet, A. Fréchet, P. Gagnon, D. Gilbert, and J.-C. Brêthes. Distribution changes of atlantic cod (gadus morhua l.) in the northern gulf of st lawrence in relation to an oceanic cooling. *ICES Journal of Marine Science*, 56(3): 333–344, 1999.

[34] S. Červinka, J. Vitovec, J. Lom, J. Hoška, and F. Kub. Dermocystidiosis–a gill disease of the carp due to dermocystidium cyprini n. sp. *Journal of Fish Biology*, 6 (6):689–699, 1974.

[35] E. Chivian and A. Bernstein. *Sustaining life: how human health depends on biodiversity*. Oxford University Press, 2008.

[36] B. Choi and A. Pak. A simple approximate mathematical model to predict the number of severe acute respiratory syndrome cases and deaths. *Journal of Epidemiology & Community Health*, 57(10):831–835, 2003.

[37] G. Chouinard, D. Swain, M. Hammill, and G. Poirier. Covariation between grey seal (halichoerus grypus) abundance and natural mortality of cod (gadus morhua) in the southern gulf of st. lawrence. *Canadian Journal of Fisheries and Aquatic Sciences*, 62(9):1991–2000, 2005.

[38] G. A. Chouinard, L. G. Currie, and G. A. Poirier. *Assessment of Cod in the Southern Gulf of St. Lawrence, February 2000*. Fisheries & Oceans, Science, Canadian Stock Assessment Secretariat, 2000.

[39] G. Chowell, N. W. Hengartner, C. Castillo-Chavez, P. W. Fenimore, and J. M. Hyman. The basic reproductive number of ebola and the effects of public health measures: the cases of congo and uganda. *Journal of theoretical biology*, 229(1): 119–126, 2004.

[40] M.-G. Cojocaru, T. Migot, and A. Jaber. Controlling infection in predator-prey systems with transmission dynamics. *Infectious Disease Modelling*, 5:1–11, 2020.

[41] B. Coman, J. Robinson, and C. Beaumont. Home range, dispersal and density of red foxes (vulpes vulpes l.) in central victoria. *Wildlife Research*, 18(2):215–223, 1991.

[42] D. Cook. Some mammal remains found in caves near margaret river. *Western Australian Naturalist*, 7:107–108, 1960.

[43] R. M. Cook and V. Trijoulet. The effects of grey seal predation and commercial fishing on the recovery of a depleted cod stock. *Canadian Journal of Fisheries and Aquatic Sciences*, 73(9):1319–1329, 2016.

[44] G. Craciun, F. Nazarov, and C. Pantea. Persistence and permanence of mass-action and power-law dynamical systems. *SIAM Journal on Applied Mathematics*, 73(1): 305–329, 2013.

[45] M. Crick and M. Hill. The role of sensitivity analysis in assessing uncertainty. In *Uncertainty analysis for performance assessments of radioactive waste disposal systems*. 1987.

[46] M. C. Cross and P. C. Hohenberg. Pattern formation outside of equilibrium. *Reviews of modern physics*, 65(3):851, 1993.

[47] M. J. Daniels and L. Corbett. Redefining introgressed protected mammals: when is a wildcat a wild cat and a dingo a wild dog? *Wildlife Research*, 30(3):213–218, 2003.

[48] K. P. Das and J. Chattopadhyay. A mathematical study of a predator–prey model with disease circulating in the both populations. *International Journal of Biomathematics*, 8(02):1550015, 2015.

[49] P. Daszak and A. Cunningham. Extinction by infection. *Trends in Ecology & Evolution*, 14(7):279, 1999.

[50] P. Daszak, A. A. Cunningham, and A. D. Hyatt. Emerging infectious diseases of wildlife–threats to biodiversity and human health. *science*, 287(5452):443–449, 2000.

[51] P. Daszak, A. Strieby, A. A. Cunningham, J. Longcore, C. Brown, and D. Porter. Experimental evidence that the bullfrog (rana catesbeiana) is a potential carrier of chytridiomycosis, an emerging fungal disease of amphibians. *Herpetological Journal*, 14:201–208, 2004.

[52] A. De Koeijer, H. Heesterbeek, B. Schreuder, R. Oberthür, J. Wilesmith, H. Van Roermund, and M. De Jong. Quantifying bse control by calculating the basic reproduction ratio r 0 for the infection among cattle. *Journal of mathematical biology*, 48(1):1–22, 2004.

[53] J. Diamond. Overview of recent extinctions. *Conservation for the twenty-first century*, 1989.

[54] C. R. Dickman. Impact of exotic generalist predators on the native fauna of australia. *Wildlife Biology*, 2(3):185–195, 1996.

[55] O. Diekmann and J. A. P. Heesterbeek. *Mathematical epidemiology of infectious diseases: model building, analysis and interpretation*, volume 5. John Wiley & Sons, 2000.

[56] O. Diekmann, J. A. P. Heesterbeek, and J. A. Metz. On the definition and the computation of the basic reproduction ratio r 0 in models for infectious diseases in heterogeneous populations. *Journal of mathematical biology*, 28(4):365–382, 1990.

[57] K. Dietz. Transmission and control of arbovirus diseases. *Epidemiology*, 104:104–121, 1975.

[58] R. Dirzo, H. S. Young, M. Galetti, G. Ceballos, N. J. Isaac, and B. Collen. Defaunation in the anthropocene. *science*, 345(6195):401–406, 2014.

[59] U. M. Diwekar. A novel sampling approach to combinatorial optimization under uncertainty. *Computational Optimization and Applications*, 24(2):335–371, 2003.

[60] T. S. Doherty, A. S. Glen, D. G. Nimmo, E. G. Ritchie, and C. R. Dickman. Invasive predators and global biodiversity loss. *Proceedings of the National Academy of Sciences*, 113(40):11261–11265, 2016.

[61] D. J. Downing, R. Gardner, and F. Hoffman. An examination of response-surface methodologies for uncertainty analysis in assessment models. *Technometrics*, 27(2): 151–163, 1985.

[62] B. Dubey, N. Kumari, and R. K. Upadhyay. Spatiotemporal pattern formation in a diffusive predator-prey system: an analytical approach. *Journal of Applied Mathematics and Computing*, 31(1):413–432, 2009.

[63] L. I. Dublin and A. J. Lotka. On the true rate of natural increase: As exemplified by the population of the united states, 1920. *Journal of the American statistical association*, 20(151):305–339, 1925.

[64] L. EDELSTEIN-KESHET. Applications of nonlinear difference equations to population biology. *EDELSTEIN-KESHET, L. Mathematical models in biology. New York: Random House*, pages 72–111, 1988.

[65] C. S. Elton. The reasons for conservation. In *The ecology of invasions by animals and plants*, pages 143–153. Springer, 1958.

[66] P. R. Epstein, E. Chivian, and K. Frith. Emerging diseases threaten conservation. *Environmental Health Perspectives*, 111(10):A506–A507, 2003.

[67] N. Ferguson, C. Donnelly, M. Woolhouse, and R. Anderson. Estimation of the basic reproduction number of bse: the intensity of transmission in british cattle. *Proceedings of the Royal Society of London. Series B: Biological Sciences*, 266(1414):23–32, 1999.

[68] N. M. Ferguson, C. A. Donnelly, and R. M. Anderson. The foot-and-mouth epidemic in great britain: pattern of spread and impact of interventions. *Science*, 292(5519): 1155–1160, 2001.

[69] M. C. Fisher, T. W. Garner, and S. F. Walker. Global emergence of batrachochytrium dendrobatidis and amphibian chytridiomycosis in space, time, and host. *Annual review of microbiology*, 63:291–310, 2009.

[70] P. J. Fleming, B. L. Allen, and G.-A. Ballard. Cautionary considerations for positive dingo management: a response to the johnson and ritchie critique of fleming et al.(2012). *Australian Mammalogy*, 35(1):15–22, 2012.

[71] W. H. Fleming and R. W. Rishel. *Deterministic and stochastic optimal control*, volume 1. Springer Science & Business Media, 2012.

[72] A. Folkvord. Growth, survival and cannibalism of cod juveniles (gadus morhua): effects of feed type, starvation and fish size. *Aquaculture*, 97(1):41–59, 1991.

[73] A. Folkvord and H. Otterå. Effects of initial size distribution, day length, and feeding frequency on growth, survival, and cannibalism in juvenile atlantic cod (gadus morhua l.). *Aquaculture*, 114(3-4):243–260, 1993.

[74] M. J. Forzán, H. Gunn, and P. Scott. Chytridiomycosis in an aquarium collection of frogs: diagnosis, treatment, and control. *Journal of Zoo and Wildlife Medicine*, 39 (3):406–411, 2008.

[75] L. R. Fox. Cannibalism in natural populations. *Annual review of ecology and systematics*, 6(1):87–106, 1975.

[76] S. M. Garcia, C. Newton, et al. *Current situation, trends and prospects in world capture fisheries*. FAO, Fisheries Department, 1995.

[77] T. Garner, G. Garcia, B. Carroll, and M. Fisher. Using itraconazole to clear batrachochytrium dendrobatidis infection, and subsequent depigmentation of alytes muletensis tadpoles. *Diseases of aquatic organisms*, 83(3):257–260, 2009.

[78] M. Garrione and C. Rebelo. Persistence in seasonally varying predator–prey systems via the basic reproduction number. *Nonlinear Analysis: Real World Applications*, 30:73–98, 2016.

[79] P. Georgescu and Y.-H. Hsieh. Global dynamics of a predator-prey model with stage structure for the predator. *SIAM Journal on Applied Mathematics*, 67(5):1379–1395, 2007.

[80] P. Georgescu, Y.-H. Hsieh, and H. Zhang. A lyapunov functional for a stage-structured predator–prey model with nonlinear predation rate. *Nonlinear Analysis: Real World Applications*, 11(5):3653–3665, 2010.

[81] D. Gibb, B. Kakulas, D. H. Perret, and D. J. Jenkyn. Toxoplasmosis in the rottnest quokka (setonix brachyurus). *Australian Journal of Experimental Biology and Medical Science*, 44(6):665–672, 1966.

[82] A. S. Glen, C. R. Dickman, M. E. Soule, and B. Mackey. Evaluating the role of the dingo as a trophic regulator in australian ecosystems. *Austral Ecology*, 32(5): 492–501, 2007.

[83] J. González-Fernández, F. De la Peña, J. Hormaza, J. Boyero, J. Vela, E. Wong, M. Trigo, and M. Montserrat. Alternative food improves the combined effect of an omnivore and a predator on biological pest control. a case study in avocado orchards. *Bulletin of entomological research*, 99(5):433–444, 2009.

[84] E. González-Olivares, J. Mena-Lorca, A. Rojas-Palma, and J. D. Flores. Dynamical complexities in the leslie–gower predator–prey model as consequences of the allee effect on prey. *Applied Mathematical Modelling*, 35(1):366–381, 2011.

[85] K. Gopalsamy. *Stability and oscillations in delay differential equations of population dynamics*, volume 74. Springer Science & Business Media, 2013.

[86] M. Gravenor, P. Papasozomenos, A. McLean, and G. Neophytou. A scrapie epidemic in cyprus. *Epidemiology & Infection*, 132(4):751–760, 2004.

[87] S. D. Gregory, C. J. Bradshaw, B. W. Brook, and F. Courchamp. Limited evidence for the demographic allee effect from numerous species across taxa. *Ecology*, 91(7): 2151–2161, 2010.

[88] R. Hagmann, J. D. Charlwood, V. Gil, C. Ferreira, V. Do Rosário, and T. A. Smith. Malaria and its possible control on the island of príncipe. *Malaria journal*, 2(1):1–9, 2003.

[89] L. Hansson and H. Henttonen. Gradients in density variations of small rodents: the importance of latitude and snow cover. *Oecologia*, 67(3):394–402, 1985.

[90] R. N. Harris, R. M. Brucker, J. B. Walke, M. H. Becker, C. R. Schwantes, D. C. Flaherty, B. A. Lam, D. C. Woodhams, C. J. Briggs, V. T. Vredenburg, et al. Skin microbes on frogs prevent morbidity and mortality caused by a lethal skin fungus. *The ISME journal*, 3(7):818–824, 2009.

[91] R. N. Harris, A. Lauer, M. A. Simon, J. L. Banning, and R. A. Alford. Addition of antifungal skin bacteria to salamanders ameliorates the effects of chytridiomycosis. *Diseases of aquatic organisms*, 83(1):11–16, 2009.

[92] P. Hart, L. Spencer, A. Nikoloutsopoulos, A. Lopez, M. Vadas, P. McDonald, and J. Finlay-Jones. Role of cell surface receptors in the regulation of intracellular killing of bacteria by murine peritoneal exudate neutrophils. *Infection and immunity*, 52 (1):245–251, 1986.

[93] C. D. Harvell, K. Kim, J. Burkholder, R. R. Colwell, P. R. Epstein, D. J. Grimes, E. E. Hofmann, E. Lipp, A. Osterhaus, R. M. Overstreet, et al. Emerging marine diseases–climate links and anthropogenic factors. *Science*, 285(5433):1505–1510, 1999.

[94] C. D. Harvell, C. E. Mitchell, J. R. Ward, S. Altizer, A. P. Dobson, R. S. Ostfeld, and M. D. Samuel. Climate warming and disease risks for terrestrial and marine biota. *Science*, 296(5576):2158–2162, 2002.

[95] A. Hastings and T. Powell. Chaos in a three-species food chain. *Ecology*, 72(3): 896–903, 1991.

[96] M. Hayward. *The ecology of the quokka (Setonix brachyurus)(Macropodidae: Marsupialia) in the northern jarrah forest of Australia*. PhD thesis, University of New South Wales, 2002.

[97] M. W. Hayward, J. Paul, M. J. Dillon, and B. J. Fox. Local population structure of a naturally occurring metapopulation of the quokka (setonix brachyurus macropodidae: Marsupialia). *Biological conservation*, 110(3):343–355, 2003.

[98] M. W. Hayward, J. Paul, M. L. Augee, B. J. Fox, and P. B. Banks. Home range and movements of the quokka setonix brachyurus (macropodidae: Marsupialia), and its impact on the viability of the metapopulation on the australian mainland. *Journal of Zoology*, 263(3):219–228, 2004.

[99] M. W. Hayward, P. J. De Tores, and P. B. Banks. Habitat use of the quokka, setonix brachyurus (macropodidae: Marsupialia), in the northern jarrah forest of australia. *Journal of Mammalogy*, 86(4):683–688, 2005.

[100] M. W. Hayward, J. Paul, M. J. Dillon, and P. B. Banks. Predicting the occurrence of the quokka, setonix brachyurus (macropodidae: Marsupialia), in western australia's northern jarrah forest. *Wildlife Research*, 34(3):194–199, 2007.

[101] Ø. Hermansen and B. Dreyer. Challenging spatial and seasonal distribution of fish landings—the experiences from rural community quotas in norway. *Marine Policy*, 34(3):567–574, 2010.

[102] D. J. Higham. An algorithmic introduction to numerical simulation of stochastic differential equations. *SIAM review*, 43(3):525–546, 2001.

[103] R. J. Hobbs. Synergisms among habitat fragmentation, livestock grazing, and biotic invasions in southwestern australia. *Conservation Biology*, 15(6):1522–1528, 2001.

[104] C. S. Holling. Some characteristics of simple types of predation and parasitism. *The Canadian Entomologist*, 91(7):385–398, 1959.

[105] J. C. Holmes. Parasites as threats to biodiversity in shrinking ecosystems. *Biodiversity & Conservation*, 5(8):975–983, 1996.

[106] R. Hopcroft and J. Roff. Zooplankton growth rates: the influence of female size and resources on egg production of tropical marine copepods. *Marine biology*, 132(1): 79–86, 1998.

[107] F. C. Hoppensteadt. *Mathematical methods of population biology*. Number 4. Cambridge University Press, 1982.

[108] T. Huang, H. Zhang, Z. Hu, G. Pan, S. Ma, X. Zhang, and Z. Gao. Predator–prey pattern formation driven by population diffusion based on moore neighborhood structure. *Advances in Difference Equations*, 2019(1):1–20, 2019.

[109] J. M. Hyman and J. Li. An intuitive formulation for the reproductive number for the spread of diseases in heterogeneous populations. *Mathematical biosciences*, 167 (1):65–86, 2000.

[110] R. L. Iman and J. C. Helton. An investigation of uncertainty and sensitivity analysis techniques for computer models. *Risk analysis*, 8(1):71–90, 1988.

[111] R. L. Iman and J. C. Helton. The repeatability of uncertainty and sensitivity analyses for complex probabilistic risk assessments. *Risk Analysis*, 11(4):591–606, 1991.

[112] J. Iveson and R. Hart. Salmonella on rottnest island: implications for public health and wildlife management. *Journal of the Royal Society of Western Australia*, 1983.

[113] V. S. Ivlev. *Experimental ecology of the feeding of fishes*. Yale University Press, 1975.

[114] M. Jackson and B. M. Chen-Charpentier. Modeling plant virus propagation with delays. *Journal of Computational and Applied Mathematics*, 309:611–621, 2017.

[115] S. Jain and P. Roy. Investigating the role of zooplankton in sustaining frog population. *Mathematical Methods in the Applied Sciences*, 45(9):5423–5455, 2022.

[116] S. Jain and P. Roy. Untangling the role of tri-trophic food chain model in sustaining quokka population. *International Journal of Biomathematics*, 15(03):2150053, 2022.

[117] D. M. Johnson, A. M. Liebhold, P. C. Tobin, and O. N. Bjørnstad. Allee effects and pulsed invasion by the gypsy moth. *Nature*, 444(7117):361–363, 2006.

[118] P. T. Johnson, P. J. Lund, R. B. Hartson, and T. P. Yoshino. Community diversity reduces schistosoma mansoni transmission, host pathology and human infection risk. *Proceedings of the Royal Society B: Biological Sciences*, 276(1662):1657–1663, 2009.

[119] S. Jørgensen. Models as instruments for combination of ecological theory and environmental practice. *Ecological Modelling*, 75:5–20, 1994.

[120] S. E. Jorgensen. *Handbook of environmental and ecological modeling*, volume 1. CRC Press, 1995.

[121] S. E. Jørgensen. *Integration of Ecosystem Theories: A Pattern: A Pattern*. Springer Science & Business Media, 2002.

[122] S. E. Jørgensen. Overview of the model types available for development of ecological models. *Ecological Modelling*, 215(1-3):3–9, 2008.

[123] S. E. Jørgensen and B. D. Fath. Spatial modelling. In *Developments in Environmental Modelling*, volume 23, pages 347–368. Elsevier, 2011.

[124] F. Keesing, L. K. Belden, P. Daszak, A. Dobson, C. D. Harvell, R. D. Holt, P. Hudson, A. Jolles, K. E. Jones, C. E. Mitchell, et al. Impacts of biodiversity on the emergence and transmission of infectious diseases. *Nature*, 468(7324):647–652, 2010.

[125] D. G. Kendall. Discussion of 'measles periodicity and community size'by ms bartlett. *J. Roy. Stat. Soc. A*, 120:64–76, 1957.

[126] D. G. Kendall. Mathematical models of the spread of infection. *Mathematics and computer science in biology and medicine*, pages 213–225, 1965.

[127] W. O. Kermack and A. G. McKendrick. A contribution to the mathematical theory of epidemics. *Proceedings of the royal society of london. Series A, Containing papers of a mathematical and physical character*, 115(772):700–721, 1927.

[128] A. Khan, M. Naveed, M. Dur-e Ahmad, and M. Imran. Estimating the basic reproductive ratio for the ebola outbreak in liberia and sierra leone. *Infectious diseases of poverty*, 4(1):1–8, 2015.

[129] D. King and L. Smith. The distribution of the european red fox (vulpes vulpes) in western australia. *Records of the Western Australian Museum*, 12(2):97–205, 1985.

[130] S. E. Kingsland and S. E. Kingsland. *Modeling nature*. University of Chicago Press, 1995.

[131] J. Kinnear, N. Sumner, and M. Onus. The red fox in australia—an exotic predator turned biocontrol agent. *Biological Conservation*, 108(3):335–359, 2002.

[132] D. E. Kirk. optimal control theory: an introduction. printice-hall. *Englewood Cliffs, NJ*, 228, 1970.

[133] D. Kitchener. Quokka (setonix brachyurus). *Mammals of Australia*, pages 401–403, 1995.

[134] C. Kohlmeier and W. Ebenhöh. The stabilizing role of cannibalism in a predator-prey system. *Bulletin of Mathematical Biology*, 57(3):401–411, 1995.

[135] G. Kolosov. Size control of a population described by a stochastic logical model. *Automation and remote control*, 58(4):678–686, 1997.

[136] G. Kolosov and M. Sharov. Approximate synthesis of the optimal control of population size in the'predater-victim'type system (the case of ill adapted predator). , (10):76–86, 1993.

[137] A. M. Kramer, L. Berec, and J. M. Drake. Allee effects in ecology and evolution. *Journal of Animal Ecology*, 87(1):7–10, 2018.

[138] Y. Kuang. *Delay differential equations: with applications in population dynamics*. Academic press, 1993.

[139] R. R. Kuczynski. *Balance of births and deaths. Vol. I: Western and northern Europe*. Macmillan and Company Limited, New York, 1928.

[140] N. Kumari. Pattern formation in spatially extended tritrophic food chain model systems: generalist versus specialist top predator. *International Scholarly Research Notices*, 2013, 2013.

[141] M. Kurlansky and R. M. Davidson. *Cod: a Biography of the Fish that Changed the world*. Phoenix Books, 2006.

[142] M. Lakshmanan and S. Rajaseekar. *Nonlinear dynamics: integrability, chaos and patterns*. Springer Science & Business Media, 2012.

[143] W. F. Laurance, K. R. McDonald, and R. Speare. Epidemic disease and the catastrophic decline of australian rain forest frogs. *Conservation Biology*, 10(2):406–413, 1996.

[144] E. v. Leeuwen, V. Jansen, and P. Bright. How population dynamics shape the functional response in a one-predator–two-prey system. *Ecology*, 88(6):1571–1581, 2007.

[145] E. M. Leroy, P. Rouquet, P. Formenty, S. Souquière, A. Kilbourne, J.-M. Froment, M. Bermejo, S. Smit, W. Karesh, R. Swanepoel, et al. Multiple ebola virus transmission events and rapid decline of central african wildlife. *Science*, 303(5656):387–390, 2004.

[146] M. Lipsitch, T. Cohen, B. Cooper, J. M. Robins, S. Ma, L. James, G. Gopalakrishna, S. K. Chew, C. C. Tan, M. H. Samore, et al. Transmission dynamics and control of severe acute respiratory syndrome. *science*, 300(5627):1966–1970, 2003.

[147] A. L. Lloyd and R. M. May. Spatial heterogeneity in epidemic models. *Journal of theoretical biology*, 179(1):1–11, 1996.

[148] J. O. Lloyd-Smith, A. P. Galvani, and W. M. Getz. Curtailing transmission of severe acute respiratory syndrome within a community and its hospital. *Proceedings of the Royal Society of London. Series B: Biological Sciences*, 270(1528):1979–1989, 2003.

[149] J. E. Longcore, A. P. Pessier, and D. K. Nichols. Batrachochytrium dendrobatidis gen. et sp. nov., a chytrid pathogenic to amphibians. *Mycologia*, 91(2):219–227, 1999.

[150] A. J. Lotka. Analytical note on certain rhythmic relations in organic systems. *Proceedings of the National Academy of Sciences*, 6(7):410–415, 1920.

[151] A. J. Lotka. *Elements of physical biology*. Williams & Wilkins, 1925.

[152] D. Ludwig, S. Carpenter, and W. Brock. Optimal phosphorus loading for a potentially eutrophic lake. *Ecological applications*, 13(4):1135–1152, 2003.

[153] P. M. Luz, C. T. Codeço, E. Massad, and C. J. Struchiner. Uncertainties regarding dengue modeling in rio de janeiro, brazil. *Memórias do Instituto Oswaldo Cruz*, 98 (7):871–878, 2003.

[154] G. Macdonald. The analysis of equilibrium in malaria. *Tropical Disease Bulletin*, 49 (9):813–829, 1952.

[155] N. MacDonald. *Time lags in biological models*, volume 27. Springer Science & Business Media, 2013.

[156] S. Marino, I. B. Hogue, C. J. Ray, and D. E. Kirschner. A methodology for performing global uncertainty and sensitivity analysis in systems biology. *Journal of theoretical biology*, 254(1):178–196, 2008.

[157] R. H. Martin Jr. Logarithmic norms and projections applied to linear differential systems. *Journal of Mathematical Analysis and Applications*, 45(2):432–454, 1974.

[158] L. Matthews, M. Woolhouse, and N. Hunter. The basic reproduction number for scrapie. *Proceedings of the Royal Society of London. Series B: Biological Sciences*, 266(1423):1085–1090, 1999.

[159] L. Matthews, D. Haydon, D. Shaw, M. Chase-Topping, M. Keeling, and M. Woolhouse. Neighbourhood control policies and the spread of infectious diseases. *Proceedings of the Royal Society of London. Series B: Biological Sciences*, 270(1525): 1659–1666, 2003.

[160] S. A. May and T. Norton. Influence of fragmentation and disturbance on the potential impact of feral predators on native fauna in australian forest ecosystems. *Wildlife Research*, 23(4):387–400, 1996.

[161] T. A. McMahon, B. F. Sears, M. D. Venesky, S. M. Bessler, J. M. Brown, K. Deutsch, N. T. Halstead, G. Lentz, N. Tenouri, S. Young, et al. Amphibians acquire resistance to live and dead fungus overcoming fungal immunosuppression. *Nature*, 511(7508): 224–227, 2014.

[162] C. E. Mills, J. M. Robins, and M. Lipsitch. Transmissibility of 1918 pandemic influenza. *Nature*, 432(7019):904–906, 2004.

[163] A. Misra, P. Chandra, and J. Shukla. Mathematical modeling and analysis of the depletion of dissolved oxygen in water bodies. *Nonlinear analysis: real world applications*, 7(5):980–996, 2006.

[164] B. D. Mitchell and P. B. Banks. Do wild dogs exclude foxes? evidence for competition from dietary and spatial overlaps. *Austral Ecology*, 30(5):581–591, 2005.

[165] D. Mollison and M. Denis. *Epidemic models: their structure and relation to data*, volume 5. Cambridge University Press, 1995.

[166] K. E. Moseby, H. Neilly, J. L. Read, and H. A. Crisp. Interactions between a top order predator and exotic mesopredators in the australian rangelands. *International Journal of Ecology*, 2012, 2012.

[167] J. Murray. Mathematical biology springer-verlag. *New York*, 1993.

[168] S. K. Nandi, P. K. Mondal, S. Jana, P. Haldar, and T. Kar. Prey-predator model with two-stage infection in prey: Concerning pest control. *Journal of Nonlinear Dynamics*, 2015, 2015.

[169] I. Nasell. The threshold concept in stochastic epidemic and endemic models. *Epidemic models: their structure and relation to data*, 5:71, 1995.

[170] R. D. Neuenhoff, D. P. Swain, S. P. Cox, M. K. McAllister, A. W. Trites, C. J. Walters, and M. O. Hammill. Continued decline of a collapsed population of atlantic cod (gadus morhua) due to predation-driven allee effects. *Canadian Journal of Fisheries and Aquatic Sciences*, 76(1):168–184, 2019.

[171] D. Nichols and E. Lamirande. Treatment of cutaneous chytridiomycosis in blue-and-yellow poison dart frogs (dendrobates tinctorius). presentation at the conference "getting the jump! on amphibians disease" held august 26-30, 2000. *Cairns, Australia*, 2000.

[172] D. K. Nichols, E. Lamirande, A. Pessier, and J. Longcore. Experimental transmission and treatment of cutaneous chytridiomycosis in poison dart frogs (dendrobates auratus and dendrobates tinctorius). In *ANNUAL CONFERENCE-AMERICAN ASSOCIATION OF ZOO VETERINARIANS*, pages 42–44. American Association of Zoo Veterinarians; 1998, 2000.

[173] A. Nindjin, M. Aziz-Alaoui, and M. Cadivel. Analysis of a predator–prey model with modified leslie–gower and holling-type ii schemes with time delay. *Nonlinear Analysis: Real World Applications*, 7(5):1104–1118, 2006.

[174] B. Novák and J. J. Tyson. A model for restriction point control of the mammalian cell cycle. *Journal of theoretical biology*, 230(4):563–579, 2004.

[175] A. O. of the United Nations. Fisheries Department. *The State of World Fisheries and Aquaculture, 1998*. Food & Agriculture Org., 1999.

[176] A. Okubo and S. A. Levin. The basics of diffusion. In *Diffusion and ecological problems: Modern perspectives*, pages 10–30. Springer, 2001.

[177] C. C. on the Status of Endangered Wildlife in Canada). Cosewic assessment and status report on atlantic cod (gadus morhua) in canada, 2010.

[178] A. O'Neill. *Living with the Dingo*. Annandale, NSW: Envirobook, 2002.

[179] J. M. Parker, I. Mikaelian, N. Hahn, and H. E. Diggs. Clinical diagnosis and treatment of epidermal chytridiomycosis in african clawed frogs (xenopus tropicalis). *Comparative medicine*, 52(3):265–268, 2002.

[180] C. Parmesan and G. Yohe. A globally coherent fingerprint of climate change impacts across natural systems. *nature*, 421(6918):37–42, 2003.

[181] A. Pessier, J. Mendelson, et al. A manual for control of infectious diseases in amphibian survival assurance colonies and reintroduction programs. *IUCN/SSC Conservation Breeding Specialist Group, Apple Valley, MN*, 2010.

[182] R. Peterson. Wolves as interspecific competitors in canid ecology. *Ecology and conservation of wolves in a changing world*, pages 315–324, 1995.

[183] S. V. Petrovskii, A. Y. Morozov, and E. Venturino. Allee effect makes possible patchy invasion in a predator–prey system. *Ecology Letters*, 5(3):345–352, 2002.

[184] J. S. Piotrowski, S. L. Annis, and J. E. Longcore. Physiology of batrachochytrium dendrobatidis, a chytrid pathogen of amphibians. *Mycologia*, 96(1):9–15, 2004.

[185] M. Plehn. Pathogene schimmelpilze in der fischniere. *Z. Fischerei*, 18:51–54, 1916.

[186] L. S. Pontryagin. *Mathematical theory of optimal processes*. Routledge, 2018.

[187] T. C. Porco and S. M. Blower. Hiv vaccines: the effect of the mode of action on the coexistence of hiv subtypes. *Mathematical Population Studies*, 8(2):205–229, 2000.

[188] H. P. Possingham, J. Franklin, K. Wilson, and T. J. Regan. The roles of spatial heterogeneity and ecological processes in conservation planning. In *Ecosystem function in heterogeneous landscapes*, pages 389–406. Springer, 2005.

[189] J. A. Pounds, M. R. Bustamante, L. A. Coloma, J. A. Consuegra, M. P. Fogden, P. N. Foster, E. La Marca, K. L. Masters, A. Merino-Viteri, R. Puschendorf, et al. Widespread amphibian extinctions from epidemic disease driven by global warming. *Nature*, 439(7073):161–167, 2006.

[190] V. Puvanendran, B. J. Laurel, and J. A. Brown. Cannibalism of atlantic cod gadus morhua larvae and juveniles on first-week larvae. *Aquatic Biology*, 2(2):113–118, 2008.

[191] L. A. Real and S. A. Levin. The role of theory in the rise of modern ecology. *Foundations of ecology. University of Chicago Press, Chicago, Illinois, USA*, pages 177–191, 1991.

[192] C. Rebelo, A. Margheri, and N. Bacaër. Persistence in seasonally forced epidemiological models. *Journal of Mathematical Biology*, 64(6):933–949, 2012.

[193] S. A. Richards, H. P. Possingham, and J. Tizard. Optimal fire management for maintaining community diversity. *Ecological Applications*, 9(3):880–892, 1999.

[194] S. Riley, C. Fraser, C. A. Donnelly, A. C. Ghani, L. J. Abu-Raddad, A. J. Hedley, G. M. Leung, L.-M. Ho, T.-H. Lam, T. Q. Thach, et al. Transmission dynamics of the etiological agent of sars in hong kong: impact of public health interventions. *Science*, 300(5627):1961–1966, 2003.

[195] M. E. Roelke-Parker, L. Munson, C. Packer, R. Kock, S. Cleaveland, M. Carpenter, S. J. O'Brien, A. Pospischil, R. Hofmann-Lehmann, H. Lutz, et al. A canine distemper virus epidemic in serengeti lions (panthera leo). *Nature*, 379(6564):441–445, 1996.

[196] G. Rosenlund and Ó. Halldórsson. Cod juvenile production: research and commercial developments. *Aquaculture*, 268(1-4):188–194, 2007.

[197] R. Ross. *The prevention of malaria*. John Murray, 1911.

[198] P. Roy, S. Jain, and M. Maama. Assessing the viability of tri-trophic food chain model in designing a conservation plan: The case of dwindling quokka population. *Ecological Complexity*, 41:100811, 2020.

[199] M. W. Sabelis, A. Janssen, I. Lesna, N. S. Aratchige, M. Nomikou, and P. C. van Rijn. Developments in the use of predatory mites for biological pest control. *IOBC WPRS BULLETIN*, 32:187, 2008.

[200] A. Sadiq. The dynamics and optimal control of a prey–predator system. *Global J. of Pure and Applied Mathematics*, 13:5287–5298, 2017.

[201] B. Sahoo. Effects of additional foods to predators on nutrient-consumer-predator food chain model. *ISRN Biomathematics*, 2012, 2012.

[202] O. B. Samuelsen, A. H. Nerland, T. Jørgensen, M. B. Schrøder, T. Svåsand, and Ø. Bergh. Viral and bacterial diseases of atlantic cod gadus morhua, their prophylaxis and treatment: a review. *Diseases of aquatic organisms*, 71(3):239–254, 2006.

[203] L. Sattenspiel. The geographic spread of infectious diseases. In *The Geographic Spread of Infectious Diseases*. Princeton University Press, 2009.

[204] W. Schäperclaus. *Fish diseases*, volume 1. CRC Press, 1992.

[205] L. M. Schloegel, J.-M. Hero, L. Berger, R. Speare, K. McDonald, and P. Daszak. The decline of the sharp-snouted day frog (taudactylus acutirostris): the first documented case of extinction by infection in a free-ranging wildlife species? *EcoHealth*, 3(1): 35–40, 2006.

[206] T. Schroeder, M. Lewis, A. Kilpatrick, and K. Moseby. Dingo interactions with exotic mesopredators: spatiotemporal dynamics in an australian arid-zone study. *Wildlife Research*, 42(6):529–539, 2015.

[207] L. A. Segel. *Modeling dynamic phenomena in molecular and cellular biology*. Cambridge University Press, 1984.

[208] Y. Sekerci and S. Petrovskii. Mathematical modelling of plankton–oxygen dynamics under the climate change. *Bulletin of mathematical biology*, 77(12):2325–2353, 2015.

[209] L. Semenovich, L. Neustadt, and K. Trirogoff. *The Mathematical Theory of Optimal Processes*. Interscience Publishers, 1962.

[210] Y. Sharma, K. C. Abbott, P. S. Dutta, and A. Gupta. Stochasticity and bistability in insect outbreak dynamics. *Theoretical Ecology*, 8(2):163–174, 2015.

[211] F. R. Sharpe and A. J. Lotka. L. a problem in age-distribution. *The London, Edinburgh, and Dublin Philosophical Magazine and Journal of Science*, 21(124):435–438, 1911.

[212] P. A. Shelton, A. F. Sinclair, G. A. Chouinard, R. Mohn, and D. E. Duplisea. Fishing under low productivity conditions is further delaying recovery of northwest atlantic cod (gadus morhua). *Canadian Journal of fisheries and aquatic sciences*, 63(2): 235–238, 2006.

[213] R. E. Shope and S. C. Oaks. Emerging infections: microbial threats to health in the united states. 1992.

[214] J. Short, J. Kinnear, and A. Robley. Surplus killing by introduced predators in australia—evidence for ineffective anti-predator adaptations in native prey species? *Biological Conservation*, 103(3):283–301, 2002.

[215] W. Silvert and W. R. Smith. Optimal exploitation of a multi-species community. *Mathematical Biosciences*, 33(1-2):121–134, 1977.

[216] E. Sinclair and K. Morris. Where have all the quokkas gone. *Landscope*, 11:49–53, 1996.

[217] L. F. Skerratt, L. Berger, R. Speare, S. Cashins, K. R. McDonald, A. D. Phillott, H. B. Hines, and N. Kenyon. Spread of chytridiomycosis has caused the rapid global decline and extinction of frogs. *EcoHealth*, 4(2):125–134, 2007.

[218] A. Smith and D. Quin. Patterns and causes of extinction and decline in australian conilurine rodents. *Biological Conservation*, 77(2-3):243–267, 1996.

[219] D. L. Smith, F. E. McKenzie, R. W. Snow, and S. I. Hay. Revisiting the basic reproductive number for malaria and its implications for malaria control. *PLoS biology*, 5(3):e42, 2007.

[220] H. L. Smith and H. R. Thieme. *Dynamical systems and population persistence*, volume 118. American Mathematical Soc., 2011.

[221] A. Stegeman, A. Bouma, A. R. Elbers, M. C. de Jong, G. Nodelijk, F. de Klerk, G. Koch, and M. van Boven. Avian influenza a virus (h7n7) epidemic in the netherlands in 2003: course of the epidemic and effectiveness of control measures. *The Journal of Infectious Diseases*, 190(12):2088–2095, 2004.

[222] P. Stephens, W. Sutherland, and R. Freckleton. What is the anee effect? *Oikos*, 50 (186):87, 1999.

[223] P. A. Stephens and W. J. Sutherland. Consequences of the allee effect for behaviour, ecology and conservation. *Trends in ecology & evolution*, 14(10):401–405, 1999.

[224] M. J. Stice and C. J. Briggs. Immunization is ineffective at preventing infection and mortality due to the amphibian chytrid fungus batrachochytrium dendrobatidis. *Journal of Wildlife Diseases*, 46(1):70–77, 2010.

[225] Y. Sun and S. Saker. Existence of positive periodic solutions of nonlinear discrete model exhibiting the allee effect. *Applied mathematics and computation*, 168(2): 1086–1097, 2005.

[226] D. Tilman, P. Kareiva, et al. *Spatial ecology: the role of space in population dynamics and interspecific interactions*. Princeton University Press, 1997.

[227] D. P. Tittensor, M. Walpole, S. L. Hill, D. G. Boyce, G. L. Britten, N. D. Burgess, S. H. Butchart, P. W. Leadley, E. C. Regan, R. Alkemade, et al. A mid-term analysis of progress toward international biodiversity targets. *Science*, 346(6206): 241–244, 2014.

[228] U. Tobler, A. Borgula, and B. R. Schmidt. Populations of a susceptible amphibian species can grow despite the presence of a pathogenic chytrid fungus. *PLoS One*, 7 (4):e34667, 2012.

[229] A. Turing. The chemical basis of morphogenesis (1952). *B Jack Copeland*, 519, 1952.

[230] R. K. Upadhyay, P. Roy, C. Venkataraman, and A. Madzvamuse. Wave of chaos in a spatial eco-epidemiological system: Generating realistic patterns of patchiness in rabbit–lynx dynamics. *Mathematical biosciences*, 281:98–119, 2016.

[231] M. Van Baalen, V. Křivan, P. C. van Rijn, and M. W. Sabelis. Alternative food, switching predators, and the persistence of predator-prey systems. *The American Naturalist*, 157(5):512–524, 2001.

[232] P. Van den Driessche and J. Watmough. Reproduction numbers and sub-threshold endemic equilibria for compartmental models of disease transmission. *Mathematical biosciences*, 180(1-2):29–48, 2002.

[233] A. Veprauskas and J. M. Cushing. A juvenile–adult population model: climate change, cannibalism, reproductive synchrony, and strong allee effects. *Journal of biological dynamics*, 11(sup1):1–24, 2017.

[234] J. Voyles, L. Berger, S. Young, R. Speare, R. Webb, J. Warner, D. Rudd, R. Campbell, and L. F. Skerratt. Electrolyte depletion and osmotic imbalance in amphibians with chytridiomycosis. *Diseases of aquatic organisms*, 77(2):113–118, 2007.

[235] J. Voyles, S. Young, L. Berger, C. Campbell, W. F. Voyles, A. Dinudom, D. Cook, R. Webb, R. A. Alford, L. F. Skerratt, et al. Pathogenesis of chytridiomycosis, a cause of catastrophic amphibian declines. *Science*, 326(5952):582–585, 2009.

[236] V. T. Vredenburg, R. A. Knapp, T. S. Tunstall, and C. J. Briggs. Dynamics of an emerging disease drive large-scale amphibian population extinctions. *Proceedings of the National Academy of Sciences*, 107(21):9689–9694, 2010.

[237] J. Wallinga and P. Teunis. Different epidemic curves for severe acute respiratory syndrome reveal similar impacts of control measures. *American Journal of epidemiology*, 160(6):509–516, 2004.

[238] G.-R. Walther, E. Post, P. Convey, A. Menzel, C. Parmesan, T. J. Beebee, J.-M. Fromentin, O. Hoegh-Guldberg, and F. Bairlein. Ecological responses to recent climate change. *Nature*, 416(6879):389–395, 2002.

[239] J. Wang, J. Shi, and J. Wei. Predator–prey system with strong allee effect in prey. *Journal of Mathematical Biology*, 62(3):291–331, 2011.

[240] W. Wang and X.-Q. Zhao. Threshold dynamics for compartmental epidemic models in periodic environments. *Journal of Dynamics and Differential Equations*, 20(3): 699–717, 2008.

[241] C. R. White, N. G. Schimpf, and P. Cassey. The repeatability of metabolic rate declines with time. *Journal of Experimental Biology*, 216(10):1763–1765, 2013.

[242] S. White. The occurrence of the quokka in the south-west. *Western Australian Naturalist*, 3(5):101–103, 1952.

[243] M. J. Wonham, T. de Camino-Beck, and M. A. Lewis. An epidemiological model for west nile virus: invasion analysis and control applications. *Proceedings of the Royal Society of London. Series B: Biological Sciences*, 271(1538):501–507, 2004.

[244] D. C. Woodhams, R. A. Alford, and G. Marantelli. Emerging disease of amphibians cured by elevated body temperature. *Diseases of aquatic organisms*, 55(1):65–67, 2003.

[245] D. C. Woodhams, J. Bosch, C. J. Briggs, S. Cashins, L. R. Davis, A. Lauer, E. Muths, R. Puschendorf, B. R. Schmidt, B. Sheafor, et al. Mitigating amphibian disease: strategies to maintain wild populations and control chytridiomycosis. *Frontiers in Zoology*, 8(1):1–24, 2011.

[246] R. Woodroffe. Managing disease threats to wild mammals. In *Animal Conservation Forum*, volume 2, pages 185–193. Cambridge University Press, 1999.

[247] M. E. Woolhouse and R. M. Anderson. Understanding the epidemiology of bse. *Trends in microbiology*, 5(11):421–424, 1997.

[248] D. Xiao and S. Ruan. Global dynamics of a ratio-dependent predator-prey system. *Journal of Mathematical Biology*, 43(3):268–290, 2001.

[249] S. Young, L. Berger, and R. Speare. Amphibian chytridiomycosis: strategies for captive management and conservation. *International Zoo Yearbook*, 41(1):85–95, 2007.

[250] X.-B. Zhang, S.-Q. Chang, and H. Huo. Dynamic behavior of a stochastic sir epidemic model with vertical transmission. *Electron. J. Differ. Equat*, 2019:1–20, 2019.

[251] J. Zu and M. Mimura. The impact of allee effect on a predator–prey system with holling type ii functional response. *Applied Mathematics and Computation*, 217(7): 3542–3556, 2010.

Appendix

$$
\begin{aligned}
\rho_1 &= (H_{B_d}+H_{F_I})(H_{B_d}+H_{F_S})(H_{F_I}+H_{F_S})(H_{B_d}+H_Z)(H_{F_I}+H_Z)(H_{F_S}+H_Z)(H_{B_d}\\
&\quad +H_{F_I})(H_{B_d}+H_{F_S})(H_{F_I}+H_{F_S})(H_{B_d}+H_Z)(H_{F_I}+H_Z)(H_{F_S}+H_Z)\\
\rho_2 &= -2A_1H_{B_d}H_{F_I}H_{F_S}H_Z(H_{B_d}+H_{F_I}+H_{F_S}+H_Z)+(H_{B_d}+H_{F_I}+H_{F_S}+H_Z)^2\\
&\quad (b_{44}H_{B_d}H_{F_I}H_{F_S}+b_{22}H_{B_d}H_{F_I}H_Z+b_{33}H_{B_d}H_{F_S}H_Z+b_{11}H_{F_I}H_{F_S}H_Z)\\
&\quad +(H_{B_d}H_{F_I}H_{F_S}+H_{F_I}H_{F_S}H_Z+H_{B_d}(H_{F_I}+H_{F_S})H_Z)(2(b_{22}H_{B_d}H_{F_I}+b_{44}H_{B_d}H_{F_I}\\
&\quad +b_{33}H_{B_d}H_{F_S}+b_{44}H_{B_d}H_{F_S}+b_{11}H_{F_I}H_{F_S}+b_{44}H_{F_I}H_{F_S}+(b_{22}(H_{B_d}+H_{F_I})\\
&\quad +b_{33}(H_{B_d}+H_{F_S})+b_{11}(H_{F_I}+H_{F_S}))H_Z)+(-H_{B_d}-H_{F_I}-H_{F_S}-H_Z)\\
&\quad (b_{44}(H_{B_d}+H_{F_I}+H_{F_S})+b_{22}(H_{B_d}+H_{F_I}+H_Z)+b_{33}(H_{B_d}+H_{F_S}+H_Z)\\
&\quad +b_{11}(H_{F_I}+H_{F_S}+H_Z))+A_1(H_{F_S}H_Z+H_{F_I}(H_{F_S}+H_Z)+H_{B_d}(H_{F_I}+H_{F_S}+H_Z)))\\
&\quad -(H_{B_d}+H_{F_I}+H_{F_S}+H_Z)(b_{22}H_{B_d}H_{F_I}+b_{44}H_{B_d}H_{F_I}+b_{33}H_{B_d}H_{F_S}+b_{44}H_{B_d}H_{F_S}\\
&\quad +b_{11}H_{F_I}H_{F_S}+b_{44}H_{F_I}H_{F_S}+(b_{22}(H_{B_d}+H_{F_I})+b_{33}(H_{B_d}+H_{F_S})\\
&\quad +b_{11}(H_{F_I}+H_{F_S}))H_Z)(H_{F_S}H_Z+H_{F_I}(H_{F_S}+H_Z)+H_{B_d}(H_{F_I}+H_{F_S}+H_Z))\\
\rho_3 &= -A_1^2H_{B_d}H_{F_I}H_{F_S}H_Z+\big(H_{B_d}+H_{F_I}+H_{F_S}+H_Z\big)\big(2A_1b_{44}H_{B_d}H_{F_I}H_{F_S}\\
&\quad +2A_1(b_{22}H_{B_d}H_{F_I}H_Z+b_{33}H_{B_d}H_{F_S}H_Z+b_{11}H_{F_I}H_{F_S}H_Z)+(H_{F_S}H_Z+H_{F_I}(H_{F_S}+H_Z)\\
&\quad +H_{B_d}(H_{F_I}+H_{F_S}+H_Z))(b_{33}b_{44}H_{B_d}-b_{14}b_{41}H_{F_I}+b_{11}b_{44}H_{F_I}+b_{11}b_{33}H_{F_S}-b_{14}b_{41}H_{F_S}\\
&\quad +b_{11}b_{44}H_{F_S}+b_{33}b_{44}H_{F_S}+b_{11}b_{33}H_Z-b_{23}b_{32}(H_{B_d}+H_Z)+b_{22}(b_{44}(H_{B_d}+H_{F_I})\\
&\quad +b_{33}(H_{B_d}+Z)+b_{11}(H_{F_I}+H_Z))))-\big(H_{B_d}+H_{F_I}+H_{F_S}+H_Z\big)^2\big(b_{22}b_{44}H_{B_d}H_{F_I}\\
&\quad -b_{33}b_{44}H_{B_d}H_{F_S}+b_{14}b_{41}H_{F_I}H_{F_S}-b_{11}b_{44}H_{F_I}H_{F_S}+b_{23}b_{32}H_{B_d}H_Z-b_{22}b_{33}H_{B_d}H_Z\\
&\quad -b_{11}b_{22}H_{F_I}H_Z-b_{11}b_{33}H_{F_S}H_Z\big)+\big(H_{B_d}H_{F_I}H_{F_S}+H_{F_I}H_{F_S}H_Z+H_{B_d}(H_{F_I}+H_{F_S})H_Z\big)\\
&\quad \big(A_2(H_{B_d}+H_{F_I}+H_{F_S}+H_Z)-A_1(b_{44}(H_{B_d}+H_{F_I}+H_{F_S})+b_{22}(H_{B_d}+H_{F_I}+H_Z)\\
&\quad +b_{33}(H_{B_d}+H_{F_S}+H_Z)+b_{11}(H_{F_I}+H_{F_S}+Z))-2(b_{33}b_{44}H_{B_d}-b_{14}b_{41}H_{F_I}+b_{11}b_{44}H_{F_I}\\
&\quad +b_{11}b_{33}H_{F_S}-b_{14}b_{41}H_{F_S}+b_{11}b_{44}H_{F_S}+b_{33}b_{44}H_{F_S}+b_{11}b_{33}H_Z-b_{23}b_{32}(H_{B_d}+H_Z)\\
&\quad +b_{22}(b_{44}(H_{B_d}+H_{F_I})+b_{33}(H_{B_d}+H_Z)+b_{11}(H_{F_I}+H_Z))\big)-(b_{22}H_{B_d}H_{F_I}+b_{44}H_{B_d}H_{F_I}\\
&\quad +b_{33}H_{B_d}H_{F_S}+b_{44}H_{B_d}H_{F_S}+b_{11}H_{F_I}H_{F_S}+b_{44}H_{F_I}H_{F_S}+(b_{22}(H_{B_d}+H_{F_I})\\
&\quad +b_{33}(H_{B_d}+H_{F_S})+b_{11}(H_{F_I}+H_{F_S}))H_Z)^2+\big(b_{22}H_{B_d}H_{F_I}+b_{44}H_{B_d}H_{F_I}+b_{33}H_{B_d}H_{F_S}\\
&\quad +b_{44}H_{B_d}H_{F_S}+b_{11}H_{F_I}H_{F_S}+b_{44}H_{F_I}H_{F_S}+(b_{22}(H_{B_d}+H_{F_I})+b_{33}(H_{B_d}+H_{F_S})\\
&\quad +b_{11}(H_{F_I}+H_{F_S}))H_Z\big)\big((H_{B_d}+H_{F_I}+H_{F_S}+H_Z)(b_{44}(H_{B_d}+H_{F_I}+H_{F_S})\\
&\quad +b_{22}(H_{B_d}+H_{F_I}+H_Z)+b_{33}(H_{B_d}+H_{F_S}+H_Z)+b_{11}(H_{F_I}+H_{F_S}+H_Z))\\
&\quad -A_1(H_{F_S}H_Z+H_{F_I}(H_{F_S}+H_Z)+H_{B_d}(H_{F_I}+H_{F_S}+H_Z))\big)
\end{aligned}
$$

$$
\begin{aligned}
\rho_4 \;=\;& A_1^2(b_{44}H_{B_d}H_{F_I}H_{F_S} + b_{22}H_{B_d}H_{F_I}H_Z + b_{33}H_{B_d}H_{F_S}H_Z + b_{11}H_{F_I}H_{F_S}H_Z)\\
&-2A_1\big(H_{B_d} + H_{F_I} + H_{F_S} + Z\big)\big(H_{B_d}H_{F_I}(b_{22}b_{44} - b_{33}b_{44}) + H_{F_I}H_{F_S}(b_{14}b_{41} - b_{11}b_{44})\\
&+H_{B_d}H_Z(b_{23}b_{32} - b_{22}b_{33}) - b_{11}b_{22}H_{F_I}H_Z - b_{11}b_{33}H_{F_S}H_Z\big) - (H_{B_d} + H_{F_I} + H_{F_S} + H_Z)^2\\
&\big(b_{44}H_{B_d}(b_{23}b_{32} + b_{22}b_{33}) - b_{22}H_{F_I}(b_{14}b_{41} + b_{11}b_{44}) - b_{33}H_{F_S}(b_{14}b_{41} + b_{11}b_{44})\\
&-b_{11}H_Z(b_{23}b_{32} + b_{22}b_{33})\big) + (H_{B_d}H_{F_I}H_{F_S} + H_{F_I}H_{F_S}H_Z + H_{B_d}(H_{F_I} + H_{F_S})H_Z)\\
&\big(A_1A_2 - 2A_3\big) - (H_{B_d}H_{F_I}(b_{22} + b_{44}) + H_{B_d}H_{F_S}(b_{33} + b_{44}) + H_{F_I}H_{F_S}(b_{11} + b_{44})\\
&+(b_{22}(H_{B_d} + H_{F_I}) + b_{33}(H_{B_d} + H_{F_S}) + b_{11}(H_{F_I} + H_{F_S}))H_Z)\\
&\big(A_2(H_{B_d} + H_{F_I} + H_{F_S} + H_Z) + A_1(b_{44}(H_{B_d} + H_{F_I} + H_{F_S}) + b_{22}(H_{B_d} + H_{F_I} + H_Z)\\
&+b_{33}(H_{B_d} + H_{F_S} + H_Z) + b_{11}(H_{F_I} + H_{F_S} + H_Z))\\
&+A_3(H_{B_d} + H_{F_I} + H_{F_S} + H_Z)(H_{F_S}H_Z + H_{F_I}(H_{F_S} + H_Z) + H_{B_d}(H_{F_I} + H_{F_S} + H_Z))\big)\\
&+(b_{33}b_{44}H_{B_d} - b_{14}b_{41}H_{F_I} + b_{11}b_{44}H_{F_I} + b_{11}b_{33}H_{F_S} - b_{14}b_{41}H_{F_S} + b_{11}b_{44}H_{F_S} + b_{33}b_{44}H_{F_S}\\
&+b_{11}b_{33}H_Z - b_{23}b_{32}(H_{B_d} + H_Z) + b_{22}(b_{44}(H_{B_d} + H_{F_I}) + b_{33}(H_{B_d} + H_Z)\\
&+b_{11}(H_{F_I} + H_Z)))\big(2 + (-H_{B_d} - H_{F_I} - H_{F_S} - H_Z)(b_{44}(H_{B_d} + H_{F_I} + H_{F_S})\\
&+b_{22}(H_{B_d} + H_{F_I} + H_Z) + b_{33}(H_{B_d} + H_{F_S} + H_Z)\\
&+b_{11}(H_{F_I} + H_{F_S} + H_Z)) + A_1(H_{F_S}H_Z + H_{F_I}(H_{F_S} + H_Z) + H_{B_d}(H_{F_I} + H_{F_S} + H_Z))\big)\\
\rho_5 \;=\;& -A_1^2\big(b_{44}H_{B_d}(b_{22}H_{F_I} + b_{33}H_{F_S}) + b_{11}H_Z(b_{22}H_{F_I} + b_{33}H_{F_S}) - H_{F_I}H_{F_S}(b_{14}b_{41} - b_{11}b_{44})\\
&-H_{B_d}H_Z(b_{23}b_{32} - b_{22}b_{33})\big) - 2A_1(H_{B_d} + H_{F_I} + H_{F_S} + H_Z)\big(b_{44}H_{B_d}(b_{23}b_{32} + b_{22}b_{33})\\
&-b_{22}H_{F_I}(b_{14}b_{41} + b_{11}b_{44}) - b_{33}H_{F_S}(b_{14}b_{41} + b_{11}b_{44}) - b_{11}H_Z(b_{23}b_{32} + b_{22}b_{33})\big)\\
&-A_4(H_{B_d} + H_{F_I} + H_{F_S} + H_Z)^2 - A_1A_2(((b_{22} + b_{44})H_{F_I} + (b_{33} + b_{44})H_{F_S})H_{B_d}\\
&+H_{F_I}H_{F_S}(b_{11} + b_{44}) + (b_{22}(H_{B_d} + H_{F_I}) + b_{33}(H_{B_d} + H_{F_S}) + b_{11}(H_{F_I} + H_{F_S}))H_Z)\\
&+2A_3((b_{22} + b_{44})H_{B_d}H_{F_I} + (b_{33} + b_{44})H_{B_d}H_{F_S} + (b_{11} + b_{44})H_{F_I}H_{F_S}\\
&+(b_{22}(H_{B_d} + H_{F_I}) + b_{33}(H_{B_d} + H_{F_S}) + b_{11}(H_{F_I} + H_{F_S}))H_Z)\\
&-A_3(H_{B_d} + H_{F_I} + H_{F_S} + H_Z)(b_{44}(H_{B_d} + H_{F_I} + H_{F_S}) + b_{22}(H_{B_d} + H_{F_I} + H_Z)\\
&+b_{33}(H_{B_d} + H_{F_S} + Z) + b_{11}(H_{F_I} + H_{F_S} + H_Z)) + A_1A_3(H_{F_S}H_Z + H_{F_I}(H_{F_S} + H_Z)\\
&+H_{B_d}(H_{F_I} + H_{F_S} + H_Z)) - (b_{33}b_{44}H_{B_d} - b_{14}b_{41}H_{F_I} + b_{11}b_{44}H_{F_I} + b_{11}b_{33}H_{F_S}\\
&-b_{14}b_{41}H_{F_S} + b_{11}b_{44}H_{F_S} + b_{33}b_{44}H_{F_S} + b_{11}b_{33}H_Z - b_{23}b_{32}(H_{B_d} + H_Z)\\
&+b_{22}(b_{44}(H_{B_d} + H_{F_I}) + b_{33}(H_{B_d} + H_Z) + b_{11}(H_{F_I} + H_Z)))\\
&\big(A_2(H_{B_d} + H_{F_I} + H_{F_S} + H_Z) - A_1(b_{44}(H_{B_d} + H_{F_I} + H_{F_S}) + b_{22}(H_{B_d} + H_{F_I} + H_Z)\\
&+b_{33}(H_{B_d} + H_{F_S} + H_Z) + b_{11}(H_{F_I} + H_{F_S} + H_Z)) - (b_{33}b_{44}H_{B_d} - b_{14}b_{41}H_{F_I}\\
&+b_{11}b_{44}H_{F_I} + b_{11}b_{33}H_{F_S} - b_{14}b_{41}H_{F_S} + b_{11}b_{44}H_{F_S} + b_{33}b_{44}H_{F_S} + b_{11}b_{33}H_Z\\
&-b_{23}b_{32}(H_{B_d} + H_Z) + b_{22}(b_{44}(H_{B_d} + H_{F_I}) + b_{33}(H_{B_d} + H_Z) + b_{11}(H_{F_I} + H_Z)))\big),
\end{aligned}
$$

$$
\begin{aligned}
\rho_6 \;=\;& A_2A_3(H_{B_d}+H_{F_I}+H_{F_S}+H_Z)+b_{44}H_{B_d}(b_{22}b_{33}-b_{23}b_{32})\\
&+b_{22}H_{F_I}(b_{11}b_{44}-b_{14}b_{41})+b_{33}H_{F_S}(b_{11}b_{44}-b_{14}b_{41})+b_{11}H_Z(b_{22}b_{33}-b_{23}b_{32})\\
&-A_1A_3(b_{44}(H_{B_d}+H_{F_I}+H_{F_S})+b_{22}(H_{B_d}+H_{F_I}+H_Z)+b_{33}(H_{B_d}+H_{F_S}+H_Z)\\
&+b_{11}(H_{F_I}+H_{F_S}+H_Z))+A_1A_2(b_{33}b_{44}H_{B_d}-b_{14}b_{41}H_{F_I}+b_{11}b_{44}H_{F_I}+b_{11}b_{33}H_{F_S}\\
&-b_{14}b_{41}H_{F_S}+b_{11}b_{44}H_{F_S}+b_{33}b_{44}H_{F_S}+b_{11}b_{33}H_Z-b_{23}b_{32}(H_{B_d}+H_Z)\\
&+b_{22}(b_{44}(H_{B_d}+H_{F_I})+b_{33}(H_{B_d}+H_Z)+b_{11}(H_{F_I}+H_Z)))\\
&-2A_3(b_{33}b_{44}(H_{B_d}+H_{F_S})-b_{14}b_{41}(H_{F_I}+H_{F_S})+b_{11}b_{44}(H_{F_I}+H_{F_S})\\
&+b_{11}b_{33}(H_{F_S}+H_Z)-b_{23}b_{32}(H_{B_d}+H_Z)+b_{22}(b_{44}(H_{B_d}+H_{F_I})+b_{33}(H_{B_d}+H_Z)\\
&+b_{11}(H_{F_I}+H_Z))).
\end{aligned}
$$